

ASSESSMENT OF THE IMPACTS OF FUTURE CLIMATIC VARIATIONS
AND ANTHROPOGENIC ACTIVITIES ON BURDUR LAKE LEVELS

A THESIS SUBMITTED TO
THE GRADUATE SCHOOL OF NATURAL AND APPLIED SCIENCES
OF
MIDDLE EAST TECHNICAL UNIVERSITY

BY

HATİCE KILIÇ GERMEÇ

IN PARTIAL FULFILLMENT OF THE REQUIREMENTS
FOR
THE DEGREE OF DOCTOR OF PHILOSOPHY
IN
GEOLOGICAL ENGINEERING

JANUARY 2023

Approval of the thesis:

**ASSESSMENT OF THE IMPACTS OF FUTURE CLIMATIC
VARIATIONS AND ANTHROPOGENIC ACTIVITIES ON BURDUR
LAKE LEVELS**

submitted by **HATİCE KILIÇ GERMEÇ** in partial fulfillment of the requirements
for the degree of **Doctor of Philosophy in Geological Engineering, Middle East
Technical University** by,

Prof. Dr. Halil Kalıpçılar
Dean, Graduate School of **Natural and Applied Sciences** _____

Prof. Dr. Erdin Bozkurt
Head of the Department, **Geological Engineering** _____

Prof. Dr. Hasan Yazıcıgil
Supervisor, **Geological Engineering, METU** _____

Examining Committee Members:

Prof. Dr. İsmail Yücel
Civil Engineering, METU _____

Prof. Dr. Hasan Yazıcıgil
Geological Engineering, METU _____

Prof. Dr. M. Zeki Çamur
Geological Engineering, METU _____

Assoc. Prof. Dr. Şebnem Arslan
Geological Engineering, Ankara University _____

Assist. Prof. Dr. Levent Tezcan
Hydrogeological Engineering, Hacettepe University _____

Date: 24.01.2023

I hereby declare that all information in this document has been obtained and presented in accordance with academic rules and ethical conduct. I also declare that, as required by these rules and conduct, I have fully cited and referenced all material and results that are not original to this work.

Name Last name : Hatice Kılıç Germeç

Signature :

ABSTRACT

ASSESSMENT OF THE IMPACTS OF FUTURE CLIMATIC VARIATIONS AND ANTHROPOGENIC ACTIVITIES ON BURDUR LAKE LEVELS

Kılıç Germeç, Hatice
Doctor of Philosophy, Geological Engineering
Supervisor: Prof. Dr. Hasan Yazıcıgil

January 2023, 172 pages

Lake water levels naturally fluctuate due to imbalances in water inputs and outputs. However, lake hydrologic regimes may be altered by the impacts of climatic factors and human interventions, as in Burdur Lake. The Burdur Lake level has continuously decreased since the beginning of the 1970s. In this study, in order to quantify the loss/gain relationship between the aquifer and the Burdur Lake and specify the potential causes and consequences for the lake level decline, a 3-D numerical groundwater flow model was developed using MODFLOW. Conceptual lake budget components were calculated separately with the analytic methods. Also, a numerical 2-D surface water flow model was developed to calculate the surface water inflow to the lake. Subsequently, a transient calibration was conducted for 1969-1971 and 2014-2016, simulating the lake using the lake package. The model calibrations succeeded within the acceptable error limits with respect to the lake and groundwater levels and conceptual lake budget. The responses of the aquifer and lake to the changes, such as future climatic variations, groundwater pumping, and operation of reservoirs on the streams feeding the lake, were assessed for three scenarios over a period of 46 years. Future climatic data originated from RCP 4.5 and RCP 8.5

scenarios of the CORDEX Regional Climate Models. Burdur Lake level is expected to decline by up to 7 m with the impacts of climate variations and excessive pumping and increase by up to 3 m, despite the effect of climate change with the release of surface water flows within 46 years. The findings suggest that a dynamic lake management plan should be identified to create and maintain desired conditions in Burdur Lake and its watershed.

Keywords: Burdur Lake, Lake Level Variations, MODFLOW, Climate Change, Anthropogenic Activities

ÖZ

GELECEK İKLİM DEĞİŞİMLERİ VE ANTROPOJENİK FAALİYETLERİN BURDUR GÖLÜ SEVİYELERİ ÜZERİNDEKİ ETKİLERİNİN DEĞERLENDİRİLMESİ

Kılıç Germeç, Hatice
Doktora, Jeoloji Mühendisliği
Tez Yöneticisi: Prof. Dr. Hasan Yazıcıgil

Ocak 2023, 172 sayfa

Göl su seviyeleri, göle akış ve gölden akıştaki dengesizlikler nedeniyle doğal olarak dalgalanır. Ancak, göl hidrolojik rejimleri, Burdur Gölü'nde olduğu gibi, iklim değişiklikleri ve insan müdahalelerinin etkisiyle değişebilir. Burdur Gölü seviyesi 1970'li yılların başından beri sürekli olarak düşmektedir. Bu çalışmada, akifer ile Burdur Gölü arasındaki kayıp-kazanç ilişkisini ve göl seviyesindeki düşüşün olası nedenleri ve sonuçlarını belirlemek amacıyla MODFLOW kullanılarak 3 boyutlu sayısal yeraltı suyu akım modeli geliştirilmiştir. Kavramsal göl bütçesi bileşenleri analitik yöntemlerle ayrı ayrı hesaplanmıştır. Ayrıca, göle yüzey suyu girişini hesaplamak için 2 boyutlu sayısal yüzey suyu akış modeli geliştirilmiştir. Akabinde, gölü simüle etmek için göl paketi kullanılarak, 1969-1971 ve 2014-2016 yılları için kararsız akım koşulları altında kalibrasyon yapılmıştır. Model kalibrasyonları, göl ve yeraltı suyu seviyeleri ile kavramsal göl bütçesine göre kabul edilebilir hata limitleri içerisinde başarılı olmuştur. Akifer ve gölün, gelecekteki iklim değişimleri, yeraltı suyu pompajı ve gölü besleyen akarsular üzerindeki rezervuarların işletilmesi gibi değişkenlere verdiği tepkiler, 46 yıllık bir süre için üç senaryo kullanılarak değerlendirilmiştir. Gelecek iklim verileri, CORDEX Bölgesel İklim Modellerinin RCP 4.5 ve RCP 8.5 senaryolarından alınmıştır. Burdur Gölü seviyesinin, 46 yıl

içerisinde, iklim deęişiklięi ve aşırı pompaj etkisiyle 7 m'ye kadar düşmesi ve yüzey sularının salınmasıyla iklim deęişikliğinin etkilerine rağmen 3 m'ye kadar yükselmesi beklenmektedir. Bulgular, Burdur Gölü ve havzasında istenen koşulların oluşturulması ve sürdürülmesi için dinamik bir göl yönetim planının belirlenmesi gerektiğini göstermektedir.

Anahtar Kelimeler: Burdur Gölü, Göl Seviye Deęişimleri, MODFLOW, İklim Deęişikliği, Antropojenik Faaliyetler

To my super mom and beloved husband,

ACKNOWLEDGMENTS

I would like, first, to express my deepest gratitude to my supervisor, Prof. Dr. Hasan Yazıcıgil, for his guidance, criticism, and insight throughout the research. Besides his academic support, I am grateful to him for teaching me not to give up no matter what and to push my limits. Thank you very much for including me in various projects and teaching me work discipline, how valuable keeping promises is, and the importance of timing.

I am also grateful to Prof. Dr. M. Zeki Çamur and Assoc. Prof. Dr. Koray K. Yılmaz for their advice, valuable comments, and kindness from the beginning until the last moment. I would like to thank Assoc. Prof. Dr. Özlem Yağbasan and Assoc. Prof. Şebnem Arslan for their encouragement and motivation throughout the research. I am also very grateful to Assist. Prof. Dr. Levent Tezcan for his constructive comments and suggestions, kindness, and support, and Prof. Dr. İsmail Yücel for their unwavering support on critical parts of the study.

I gratefully acknowledge and appreciate the General Directorate of State Hydraulic Works, especially Mert Toklu, that made my Ph.D. work possible by sharing the required data.

My grateful thanks are to my dearest friends, Dr. Ayşe Peksezer Sayıt and Dr. Çidem Argunhan Atalay. You have always been there with me in times of joy and pain, in tears of happiness and sadness. I feel so lucky to be your friend and colleague. I wish to express my warmest thanks to my dear friends Ecenur Ceyhan and Eda Karakaya, who have provided me with moral and emotional support throughout this study's long and challenging process.

It is a pleasure to thank those who made this thesis possible: my family. My heartfelt thanks are to my mom, Nursel Kılıç, for her endless love, encouragement, and faith in me. I feel so lucky to have a fantastic mother like you. My dearest father, Şenol

Kılıç and sister Dima Kılıç, I am pleased to write your names in this dedication. You will stay in my heart forever. In there, you're still alive. Above all, the person who deserves great thanks and gratitude is the love of my life, Eren Germeç, for his endless love, unwavering support, and unyielding belief in my abilities. He has kept his trust in me even in my most desperate moments. I feel super lucky to have a loving husband and colleague like you.

TABLE OF CONTENTS

ABSTRACT	v
ÖZ.....	vii
ACKNOWLEDGMENTS	x
TABLE OF CONTENTS	xii
LIST OF TABLES	xvi
LIST OF FIGURES	xviii
CHAPTERS	
1 INTRODUCTION	1
1.1 Purpose and Scope	2
1.2 Location of the Study Area	2
1.3 Previous Studies.....	4
2 LITERATURE SURVEY	7
2.1 Analytic Solution Techniques Related to Lake Water Balance.....	8
2.2 Statistical Methods and Soft Computing Techniques Related to Lake Water Balance	8
2.3 Numerical Solution Techniques and Impact Assessment Studies Related to Groundwater-Lake Interactions.....	9
3 DESCRIPTION OF THE STUDY AREA	13
3.1 Topography.....	13
3.2 Climate and Meteorology	13
3.2.1 Precipitation.....	17
3.2.2 Temperature.....	19

3.2.3	Relative Humidity	21
3.2.4	Evaporation	22
3.3	Geology	23
3.3.1	Regional Geology	23
3.3.2	Geology and Stratigraphy of the Study Area	23
4	HYDROGEOLOGY	29
4.1	Water Resources	29
4.1.1	Burdur Lake	29
4.1.2	Streams, Dams, and Ponds	32
4.1.3	Springs	42
4.1.4	Wells	45
4.2	Hydrogeology of the Study Area	47
4.2.1	Groundwater Levels	51
4.2.1.1	Spatial variations in groundwater levels	51
4.2.1.2	Temporal variations in groundwater levels	54
5	CONCEPTUAL MODEL	57
5.1	Conceptual Model of the Study Area	57
5.2	Conceptual Hydrologic Budget	58
5.3	Conceptual Lake Budget	63
5.3.1	Change in Storage	64
5.3.2	Precipitation Over the Lake Surface	64
5.3.3	Evaporation From the Lake Surface	66
5.3.4	Surface Water Inflow	71
5.3.5	Groundwater inflow/outseepage	87

6	GROUNDWATER FLOW MODEL	91
6.1	Computer Code	92
6.2	Model Geometry and Layering	92
6.3	Boundary Conditions	94
6.4	Model Parameters	97
6.4.1	Recharge	97
6.4.2	Hydraulic Parameters	101
6.5	Calibration	106
6.5.1	Steady-State Calibration	106
6.5.2	Transient Calibration	111
6.5.2.1	Lake Levels	112
6.5.2.2	Calibrated Lake Budgets	114
6.5.2.3	Groundwater Levels and Budgets	118
6.6	Sensitivity Analysis	123
7	FUTURE PREDICTIONS OF BURDUR LAKE LEVELS	127
7.1	Climate Models	127
7.2	Scenario No. 1	130
7.3	Scenario No. 2	135
7.4	Scenario No. 3	137
8	DISCUSSIONS	141
9	CONCLUSIONS AND RECOMMENDATIONS	147
	REFERENCES	153
	APPENDICES	
A.	DSI Wells	165

B. DSI water level recorder installed wells	170
CURRICULUM VITAE	171

LIST OF TABLES

TABLES

Table 3.1. Information about meteorological stations	15
Table 4.1. Information about the reservoirs located in the study area.....	35
Table 4.2. Information about the flow gauging stations in and around the study area	37
Table 4.3. Discharge rates for flow gauging stations in and around the study area	38
Table 4.4. Detailed information about the springs	44
Table 5.1. Monthly conceptual water budget results.....	62
Table 5.2 Annual water budget results	63
Table 5.3. HEC-HMS model components.....	77
Table 5.4. Corine land cover classes and appropriate annual crop coefficient (K _c) (Nistor,2020)	79
Table 5.5. Simple Canopy Method Parameters	80
Table 5.6. Standard depression storage from Bennet (1998)	80
Table 5.7. Lag Times for the subbasins.....	81
Table 5.8. Initial and calibrated values of the HEC-HMS model	83
Table 5.9. Performance statistics intervals (Moriassi et al., 2015)	85
Table 5.10. Performance statistics for the calibrated and validated model	85
Table 5.11. Annual lake budget components	90
Table 6.1. Corrected precipitation and temperature data for each recharge zone .	100
Table 6.2. Monthly water budget results for each recharge zone.....	102
Table 6.3. Hydraulic conductivity values assigned to the model	103
Table 6.4. Calculated groundwater budget for the steady state simulations	111
Table 6.5. Calculated monthly lake budget (January 1969-December 1971)	116
Table 6.6. Calculated monthly lake budget (January 2014-December 2016)	117
Table 6.7. Calculated groundwater budget (January 1969-December 1971).....	121
Table 6.8. Calculated groundwater budget (January 2014-December 2016).....	122
Table 7.1. Recharge from precipitation for the RCP 4.5 and 8.5 scenarios	131

Table 7.2. Calculated average monthly lake budget for simulations 1 and 2 of scenario no. 1	134
Table 7.3. Calculated average monthly lake budget for simulations 3 and 4 of scenario no. 2	137
Table 7.4. Calculated average monthly lake budget for simulations 5 and 6 of scenario no. 3	140
Table 9.1. Calculated monthly average lake budget components.....	148
Table 9.2. The predicted lake level, area, and volume changes between December 2018-December 2064.....	150

LIST OF FIGURES

FIGURES

Figure 1.1. Location map of the study area	3
Figure 3.1. Digital elevation model of the study area	14
Figure 3.2. Location of the meteorological stations in the Burdur Lake Basin.....	16
Figure 3.3. Annual precipitation and cumulative deviation from mean annual precipitation graph for the Burdur station	17
Figure 3.4. Annual precipitation and cumulative deviation from mean annual precipitation graph for the Yazıköy station	18
Figure 3.5. Mean monthly precipitation data for the Burdur and Yazıköy stations	19
Figure 3.6. Monthly mean temperature graph of Burdur station.....	19
Figure 3.7. Monthly mean minimum temperature graph of Burdur station	20
Figure 3.8. Monthly mean maximum temperature graph of Burdur station	21
Figure 3.9. Mean monthly relative humidity graph of Burdur station	21
Figure 3.10. Mean monthly evaporation graph for Yazıköy and Burdur stations...	22
Figure 3.11. Regional geological map of the study area (modified from MTA, 2010)	24
Figure 3.12. Generalized columnar section of the study area (modified from MTA,2010).....	25
Figure 3.13. Geological map of the study area (modified from MTA,2010)	26
Figure 3.14. Geological cross-sections.....	27
Figure 4.1. Bathymetric map of the Burdur Lake	30
Figure 4.2. Burdur Lake water level variations (1969-2018) and dry-wet seasons.	31
Figure 4.3. The stage-area and stage-volume curves	32
Figure 4.4. The drainage network of the Burdur Lake basin.....	33
Figure 4.5. Dams and ponds completion years on the water level of Burdur Lake	36
Figure 4.6. The monthly flow rates of the Bozçay stream gauging stations located around Karamanlı Dam (D10A007, D10A035, D10A040, D10A023).....	39

Figure 4.7. The monthly flow rates of the Bozçay stream gauging stations (E10A013, E10A003, D10A013)	41
Figure 4.8. The Monthly flow rates of Büğdüz Stream measured by the station D10A02.....	42
Figure 4.9. Location of the springs on the geological map.....	43
Figure 4.10. Location of the wells drilled within the study area	46
Figure 4.11. Location of the DSI wells drilled within the study area	48
Figure 4.12. Location of the DSI water level recorder installed wells	49
Figure 4.13. Groundwater level map of the area (1969-1971 period)	52
Figure 4.14. Groundwater level map of the area (2014-2016 period)	53
Figure 4.15. Long term continuous groundwater level measurements	55
Figure 4.16. Short term continuous groundwater level measurements.....	56
Figure 5.1. Spatial distribution of curve number in the study area.....	61
Figure 5.2. Burdur Lake volume changes between January 1969-December 2018	65
Figure 5.3. The monthly volume of precipitated water over the Burdur Lake	66
Figure 5.4. The monthly estimated evaporation from Burdur Lake surface.....	70
Figure 5.5. The monthly water volume loss from the evaporation	70
Figure 5.6. The subbasins of the Burdur Lake basin	72
Figure 5.7. The estimated flows of the missing periods and measured flows (D10A013) for the Bozçay Stream	73
Figure 5.8. The estimated flows of the missing periods and measured flows (D10A040) for the Bozçay Stream	74
Figure 5.9. The estimated flows of the missing periods and measured flows (D10A027) for the Büğdüz Stream.....	75
Figure 5.10. Stream networks and subbasins of the study area	76
Figure 5.11. Corine land cover classes of the study area (Corine, 2018)	78
Figure 5.12. Observed and calculated discharge values as a result of calibration performed at Büğdüz station between October 2003-September 2009	84
Figure 5.13. Observed and calculated discharge values as a result of validation performed at Büğdüz station between October 2009-September 2011	84

Figure 5.14. The monthly volume of inflows to the Burdur Lake	86
Figure 5.15. Monthly ET from the old lake bed.....	87
Figure 5.16. Monthly groundwater inflow/outseepage	88
Figure 5.17. Annual lake budget components	89
Figure 6.1. Model domain and grids	93
Figure 6.2. The vertical layout of the model layers for A-A' and B-B' cross-section	94
Figure 6.3. The boundary conditions of the model for 1969 (a), 1969-1971 (b), 2014 (c), 2014-2016 (d).....	96
Figure 6.4. Aerial distribution of recharge in the model domain	98
Figure 6.5. Hypsometric curves for each recharge zone in the model domain	99
Figure 6.6. Hydraulic conductivity distribution within the model domain	104
Figure 6.7. Specific yield distribution within the model domain	105
Figure 6.8. Observed vs. calculated groundwater levels (1969)	107
Figure 6.9. Calculated groundwater levels (1969)	108
Figure 6.10. Observed vs. calculated groundwater levels (2014)	109
Figure 6.11. Calculated groundwater levels (2014)	110
Figure 6.12. Observed and calculated lake levels from January 1969-December 1971 (NRMSE=0.12, RMSE= 0.24, MAE= 0.19, ME= -0.03, R ² =0.63)	113
Figure 6.13. Observed and calculated lake levels from January 2014-December 2016 (NRMSE=0.28, RMSE= 0.28, MAE= 0.21, ME= -0.17, R ² =0.34)	113
Figure 6.14. Burdur Lake level changes according to the satellite image.....	114
Figure 6.15. Observed and calculated lake levels from January 2014-October 2015	115
Figure 6.16. Calculated lake discharge and recharge percentages (January 1969-December 1971)	116
Figure 6.17. Calculated lake discharge and recharge percentages (January 2014-December 2016)	117
Figure 6.18. Observed and calculated head values for Well no 6980-I under transient conditions (R ² =0.44).....	118

Figure 6.19. Observed and calculated head values for Well no 15024 under transient conditions ($R^2=0.07$).....	119
Figure 6.20. Observed and calculated head values for Well no 18705 under transient conditions ($R^2=0.77$).....	119
Figure 6.21. Observed and calculated head values for some DSI water level recorder installed wells.....	120
Figure 6.22. Sensitivity analysis of hydraulic conductivities of lithologies	123
Figure 6.23. Sensitivity analysis of K_x/K_z	124
Figure 6.24. Sensitivity analysis of recharge from precipitation	125
Figure 6.25. Sensitivity analysis of specific yield	125
Figure 6.26. Sensitivity analysis of lakebed leakance	126
Figure 7.1. Annual mean air temperature and annual total precipitation for the period 2006-2021 (Burdur meteorological station), 2006-2098 (RCP 4.5 and RCP 8.5 scenarios), and 2022-2064 (projected bias-corrected).....	129
Figure 7.2. The annual budget components for the lake boundary conditions	132
Figure 7.3. Burdur Lake level change for scenario no.1.....	133
Figure 7.4. The predicted lake surface area in December, 2064 for scenario no.1.....	134
Figure 7.5. Burdur Lake level change for scenario no.2.....	136
Figure 7.6. The predicted lake surface area in December, 2064 for scenario no.2.....	136
Figure 7.7. The annual average streamflows to the lake with and without ponds for RCP 4.5 and RCP 8.5.....	138
Figure 7.8. Burdur Lake level change for scenario no.3.....	139
Figure 7.9. The predicted lake surface area in December 2064 for scenario no.3.....	140
Figure 9.1. The predicted lake surface areas in December 2064	149

CHAPTER 1

INTRODUCTION

Burdur Lake is among the deepest lakes in Turkey, designated as a wetland of international importance under the Ramsar Convention (Ramsar site no. 658). The lake is the stage, winter, and breed of numerous species of waterbirds (Gülle et al., 2008).

The Burdur Lake level has been continuously decreasing since the beginning of 1972. As of 1974, several reservoirs were constructed on the streams feeding the lake in the basin where the licensed and unlicensed groundwater pumpage and surface water usage for irrigation became high. Besides, global warming is predicted to intensify water loss in semi-arid and arid regions, such as Turkey, by changing the precipitation patterns and increasing evaporation (Barcikowska, 2020).

Since water resources management is moving towards a clear understanding of the interaction between the surface water and groundwater flow systems, the groundwater and lake system relationship should be revealed quantitatively to assess the impact of these climatic and human-invented factors on the lake level. Hence, a 3-D groundwater flow model using Visual MODFLOW Flex, incorporating a lake package, was developed in this study. Model calibration was confirmed by the lake and groundwater levels and the conceptual lake budget. The components of this budget were calculated separately using analytic methods. In order to calculate surface water inflow towards the lake, a 2-D surface water model (HEC-HMS) was developed. Impact assessment studies were conducted by considering the originating climate data from RCP 4.5 and RCP 8.5 scenarios of the CORDEX Regional Climate Models, groundwater pumping, and surface water inflow.

Although there are a variety of approaches, such as conceptual, analytic, or remote sensing, simulating the dynamic lake-groundwater relationship with the numerical model is useful in quantifying this relationship and predicting the impacts of different management scenarios. This study provides novel insights into the multifaceted consequences of climatic and anthropogenic pressures imposed on internationally important Burdur Lake.

1.1 Purpose and Scope

The aims of this study are to:

- quantify the loss/gain relationship between the aquifer and the Burdur Lake,
- reveal the potential causes and consequences of the lake level decline,
- assess the impacts of future climate variations and human activities (groundwater pumping and reservoir constructions on the streams feeding the lake) on the Burdur Lake level variations,
- support decision-makers to plan a dynamic lake and watershed management.

In order to achieve these purposes, the hydrogeological characterization of the study area was conducted after all the required meteorological, geological, hydrological, and hydrogeological data were collected and analyzed. Then, a conceptual model, including a lake budget, was developed. Following the conceptualization, the groundwater flow model (MODFLOW), incorporating a lake package, was set up and calibrated. Finally, future climate variations and human activities scenarios were simulated to evaluate their impacts on the Burdur Lake level variations.

1.2 Location of the Study Area

Burdur Lake is located within the provincial borders of Burdur and Isparta in southwestern Turkey. The lake, named after the city of Burdur, is one of the saline and tectonic origin lakes of the Lake District. Although there are many settlements

around the lake, these are generally inland, not at the coastal part of the lake. The closest city center to the lake is Burdur, approximately 4 km east of the lake (Figure 1.1). The catchment area of Burdur Lake is a northeast-southwest trending closed basin with approximately 1630 km² surface area (Figure 1.1). The formation of Burdur Lake Basin is of tectonic origins, such as Burdur Lake.



Figure 1.1. Location map of the study area

1.3 Previous Studies

Burdur Lake has been the focus of the researchers' interest due to its international importance and drastic water level decline. Therefore, several studies have been conducted to investigate geology, hydrology, hydrogeology and hydrochemistry, and limnology and to assess the lake level changes.

One of the earliest geological studies in the Burdur Lake basin was conducted by Price and Scott (1991). The 1/25000 and 1/100000 scaled geological maps of the area were prepared by the General Directorate of Mineral Research and Exploration (MTA). Bozcu et al. (2007) and Özkaptan et al. (2018) studied the Fethiye Burdur Fault Zone.

Initial hydrogeological studies in the Burdur Lake were conducted by DSI (1975) in the southern part of the lake with the title of Erli, Irla, Yazı Plains Hydrogeological Investigation Report. A hydrogeological map of scale 1/100.000 was also included in this study. In 2016, DSI prepared a hydrogeological investigation report (DSI, 2016-a). In this study, hydrogeological characterization of the Burdur Lake basin was conducted, and a conceptual lake budget for the Burdur Lake was developed. Burdur Master Plan report was also prepared in 2016 by DSI (DSI, 2016-b). In addition to these studies, hydrogeological and hydrochemical investigations for the Burdur Lake were also conducted by Davraz et al. (2003) and Şener et al. (2020). The effects of water level changes on water quality and heavy metals in Burdur Lake were investigated by Beyhan et al. (2007). The hydrodynamic relationship between the dry lakes of Insuyu Cave and the Çine aquifer was studied by Taşdelen (2018). The limnology of the Burdur Lake was conducted by Gülle et al. (2008).

In the study area, several studies were conducted to investigate the causes of the lake level change using remote sensing techniques and GIS-based methods (Ataol, 2010; Davraz et al., 2019; Dervişoğlu et al., 2022; Semiz and Akşit, 2013). These studies suggest that changes in Burdur Lake levels depend more on human effects than climatic factors. Çolak et al. (2022) used global circulation models (GCMs) besides

satellite images to analyze the lake level change in Burdur Lake. The study concludes that increased demand for water for irrigation, along with climate change, may accelerate the drying of Burdur Lake.

CHAPTER 2

LITERATURE SURVEY

Lakes are a significant component of the global environment. Because of their environmental significance, lakes and surrounding wetlands have been the subject of studies in hydrology, hydrogeology, water chemistry, and limnology. While previous studies have often focused on the water chemistry and limnology of lakes, hydrological and hydrogeological studies are rarer because of the challenges in data collection and analysis.

The awareness of the environmental fragility of lakes has increased since relating lake ecosystems to climatic and anthropogenic disturbances is useful for impact assessment studies (Adrian et al., 2009; Nilsson et al., 1995; Zhang et al., 2019). The pressure of disturbances on inland lakes is further exacerbated in closed basins, such as the Great Salt Lake in the United States (Meng, 2019), Lake Urmia in Iran (Chaudhari et al., 2018; Khazaei et al., 2019), the lakes on the Mongolian Plateau (Wei et al., 2018), Lake Chad in Africa (Mahmood et al., 2019) and Burdur Lake in Turkey (Çolak et al., 2022). Although saline lakes are of less practical importance to human activities, they are internationally important areas for the continuity of the ecosystems (Williams, 1996).

Since revealing the causes and consequences of the lake level variations is of great research interest, analytical models, statistical methods and soft computing techniques, and numerical models have been widely used based on the scope of the study.

2.1 Analytic Solution Techniques Related to Lake Water Balance

Analytic models are commonly preferred for quantitative evaluation of lake water balance. These models were developed, incorporating measurements or predictions of streamflow inflow, precipitation on the lake surface, evaporation, streamflow outflow, and groundwater inflow and outflow (Gibson et al., 2006; Wu et al., 2014; Yirgalem et al., 2009). The drawback of applying this method is to involve simplifying assumptions, which raises concerns about the validity of the assumptions. Reducing these assumptions is possible for areas with long-term in situ measurements. Remote Sensing Techniques are preferred in areas where there is a lack of traditional meteorological and hydrological observations to quantify lake budget components. Nourani et al. (2021) and Song et al. (2014) assessed applications of remote sensing techniques on changes in the lake area, water level, and water budget components in Tibetan Plateau, Central Asia, and Urmia Lake in Iran, respectively. Remotely sensed imagery is also used in Lake Kyoga, Uganda (Nsubuga et al., 2017), Lake Victoria in East Africa (Swenson and Wahr, 2009), and Lake Seyfe, Turkey (Reis and Yilmaz, 2008) to detect changes in the lake surface area. Although remote sensing studies are helpful where hydroclimatic data are challenging to obtain, extracting data depends on human experience and the accuracy of image classifications. Besides, there is also a requirement for continuous monitoring data to accurate simulation and prediction and evaluate the performance of image extraction.

2.2 Statistical Methods and Soft Computing Techniques Related to Lake Water Balance

Statistical methods and soft computing models are commonly employed to improve the understanding of drivers behind changes in lake levels. Trend analyses may be applied to determine potential trends in lake levels, meteorological variables, and their dominant periods by the Mann-Kendall, Modified Mann-Kendall, Sen Trend,

and Linear trend methods (Dai et al., 2020; Nourani et al., 2018; Sattari et al., 2020; Yağbasan et al., 2020; Yücel et al., 2022). Since the classical regression approaches include some drawbacks due to the basic assumption requirements, fuzzy and artificial neural network (ANN) modeling are efficient alternatives to traditional statistical methods for estimating changes in the water level (Chen et al., 2017; Deng et al., 2021; Yazar et al., 2009). The main disadvantage of soft computer models is the difficulty of tuning model parameters for the optimal learning process since it affects the prediction performance of the models.

2.3 Numerical Solution Techniques and Impact Assessment Studies Related to Groundwater-Lake Interactions

The hydraulic interaction between lakes and groundwater is essential for effective water resources management since a change in water quantity and/or quality in one system will impact the other (Dimova et al., 2013; Kidmose et al., 2015; Rossman et al., 2019; Zhou et al., 2013). Observation of lake–groundwater interactions can be provided by field measurements using seepage meters, stable isotope sampling, and hydraulic gradient measurements based on piezometers or potentiometers (Campodonico et al., 2019; Kidmose et al., 2011; Lu et al., 2020; Schneider et al., 2005). However, these methods are mainly based on point data of local fluxes, which, in many cases, are challenging to upscale to the entire lake basin due to spatial heterogeneity (Lu et al., 2022). Therefore, in the lake water balance studies, groundwater inflow and outflow to the lake are commonly based on a residual in the hydrologic budget of the lake. Instead, numerical models that integrate information across different temporal and spatial scales are commonly used for estimating lake–groundwater interactions (Abbo et al., 2003; Ala-Aho et al., 2015; Smerdon et al., 2007).

The selection of the modeling technique depends on the modeling objective, available data, and the scale of the model. Numerical modeling techniques for simulating lake-groundwater interaction can be categorized as the fixed stage

approach, the high conductivity zone, and sophisticated lake packages (Hunt et al., 2003). In order to apply the fixed lake stages approach, fixed lake levels are specified as constant-head or head-dependent conditions (Ayenew and Tilahun, 2018; Candela, 2014; Chebud and Melesse, 2009; El-Zehairy et al., 2017; Mylopoulos, 2007). Since the lake levels do not change unless the user has specified the time-dependent lake stages as input, the true nature of the interaction between the lake and groundwater can not be simulated with this condition properly. Another approach for simulating lake levels is specifying lake areas as high conductivity zone (Hunt et al., 2000; Wollschläger et al., Yihdego and Becht, 2013). However, this approach may require a long computational time to converge if it is necessary to use a large contrast between the hydraulic conductivity of the lake nodes and the surrounding aquifer (Anderson et al., 2002). The sophisticated lake packages are the last and most widely used approach for simulating lake-groundwater interaction (Hunt, 2005; Viridi et al., 2013; Yağbasan and Yazıcıgil, 2009). These provide a separate water budget for the lake to simulate the dynamic relationship between groundwater and lake by computing volumetric water exchange between the lake and aquifer. LAK1 (Cheng and Anderson 1993), LAK2 (Council, 1998), and LAK3 (Merritt and Konikow, 2000) are the sophisticated lake packages in the MODFLOW. LAK2 was developed to handle the limitations of LAK1, and the lake package, LAK3, was improved over earlier packages. These lake packages are capable of simulating lake budget components, including groundwater flow, stream flow, precipitation into the lake, and evaporation from the lake by calculating changes in lake level and can thus be used to assess the impact of climate and/or anthropogenic activities (Yağbasan and Yazıcıgil, 2012; Yihdego et al., 2016).

Climate change and anthropogenic activities are major threats to the water balance of lakes. The lakes may dry out temporarily or permanently, starting from the particularly vulnerable shallower areas. Although climate change is commonly considered a dominant environmental disturbance, direct anthropogenic pressures such as dam construction, groundwater-surface water usage, and poor irrigation

systems compound and sometimes supersede climatic factors in many regions (Yapiyev et al. 2017; ModaresiRad et al. 2022; Saini et al. 2022).

General Circulation Models (GCMs) are commonly coupled with groundwater-lake models considering all hydrological cycle components to generate climate change scenarios (Lin et al., 2007). However, basin-scale climate change impact assessments require high spatial resolution data, hence imposing regional climate models (RCMs). CORDEX is the initiative of the World Climate Research Program (WCRP), which aims to create high-resolution downscaled climate projections for different identified domains worldwide (Aziz et al., 2020). Voulanas et al. (2021) is one of the preliminary studies using CORDEX to predict the discharge of the Kastoria aquifer towards the lake under different climate change scenarios.

This study assessed the impacts of future climatic variations and anthropogenic activities in the internationally important Burdur Lake wildlife protection area (Ramsar site no. 658). Since Burdur Lake is a salt lake in a closed basin, it is highly sensitive to climatic and anthropogenic changes. The response of the lake levels to CORDEX RCMs was predicted using a 3-D numerical groundwater-lake model. In the lake water budget studies, a 2-D surface water model was developed for calculating surface water inflow towards the lake, besides analytic methods for calculating budget components. Since understanding the response of the lake levels to future climatic variations and anthropogenic activities is of great practical importance for water resources management, this is a novel study.

CHAPTER 3

DESCRIPTION OF THE STUDY AREA

3.1 Topography

The study area is located on different types of topographic forms, mainly related to tectonic movement. The topography is flat in the Burdur Lake Plain, steeping towards the basin boundaries. The digital elevation model (DEM) of the study area was created by 1/25.000 scaled topographical maps, where 5 m interval contours were used (Figure 3.1). The altitude of the study area ranges between 780 – 2030 m based on the DEM of the study area. The alluvium plain around the lake has the lowest ground elevations between 780 – 1000 m. In the west and eastern parts of the basin, mountainous regions have the highest peaks, over 2000 m. Between these lowest and highest elevations, relatively lower hills with 1000 – 2030 m are located in the study area dispersedly.

3.2 Climate and Meteorology

Burdur Lake Basin is geographically located in the Mediterranean Region. This area is under the influence of a transitional climate between the continental climate of Central Anatolia and the Mediterranean climate due to its altitude of 1100 m above sea level and the location of the Western Taurus Mountains. Summers are hot and dry in the region, and winters are cool and snowy. According to the Turkish State Meteorological Service (MGM) Thornthwaite Climate Classification, the study area is a semi-dry and low humid (2nd-degree mesothermal) climate class.

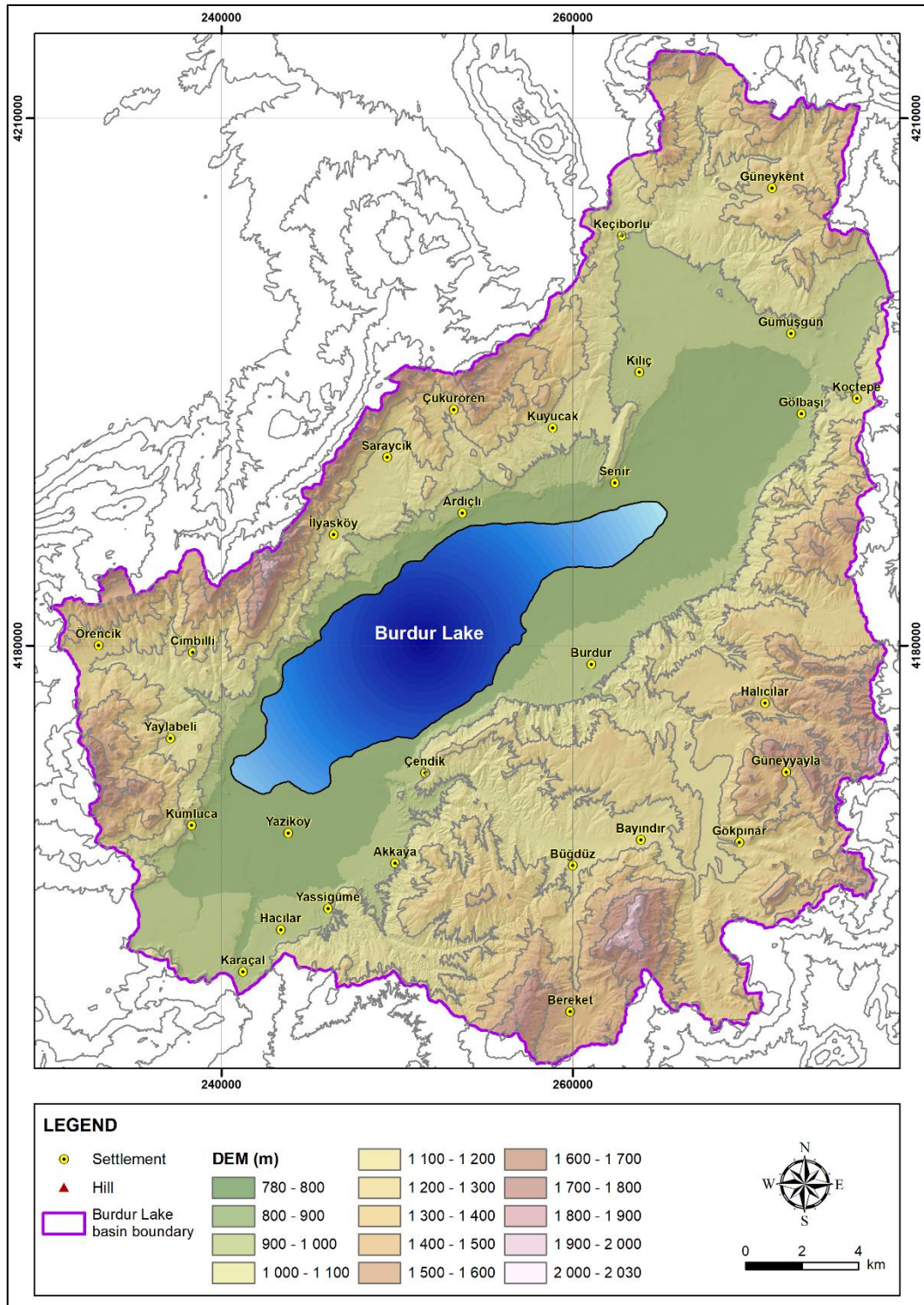


Figure 3.1. Digital elevation model of the study area

Meteorological stations located in the Burdur Lake Basin were investigated to determine the meteorological characteristics of the study area. Detailed information about these stations is given in Table 3.1. Among the meteorological stations operated by the Turkish State Meteorological Service, Burdur meteorological station (station no: 17238) is the closest to the lake with long-term measurements (Figure 3.2). This station is representative of the Burdur Lake Basin. In addition, Yazıköy station (station no: D10M007), operated by the General Directorate of State Hydraulic Works (DSI), is located near the lake at the average lake level and is representative of the lake plain area. However, this station has long-term data only for precipitation and evaporation measurements. Therefore, to analyze the long-term meteorological characteristics of the study area, both Burdur and Yazıköy stations were used. Since the Burdur Lake level change was analyzed for the time interval between January 1969 and December 2018, meteorological analysis was also conducted for the same time interval.

Table 3.1. Information about meteorological stations

Station No.	Station Name	Operator	Coordinate (UTM)		Elevation (m)	Operational Period
			Easting	Northing		
17238	Burdur	MGM	261537	4178594	957	1969 - 2019
17241	Isparta Süleyman Demirel Airport	MGM	268504	4193212	869	2007 - 2019
18314	Mehmet Akif Ersoy University	MGM	265394	4174318	1230	2015 - 2019
18316	Keçiborlu	MGM	262169	4201647	1030	2015 - 2019
18622	Burdur/Yaylabeli Village	MGM	236677	4174929	1235	2015 - 2019
18995	Burdur Lake	MGM	251271	4174632	867	2019
6676	Keçiborlu	MGM	262797	4203885	990	1972 - 1989
D10M007	Yazıköy	DSI	242659	4169312	865	1969 - 2019

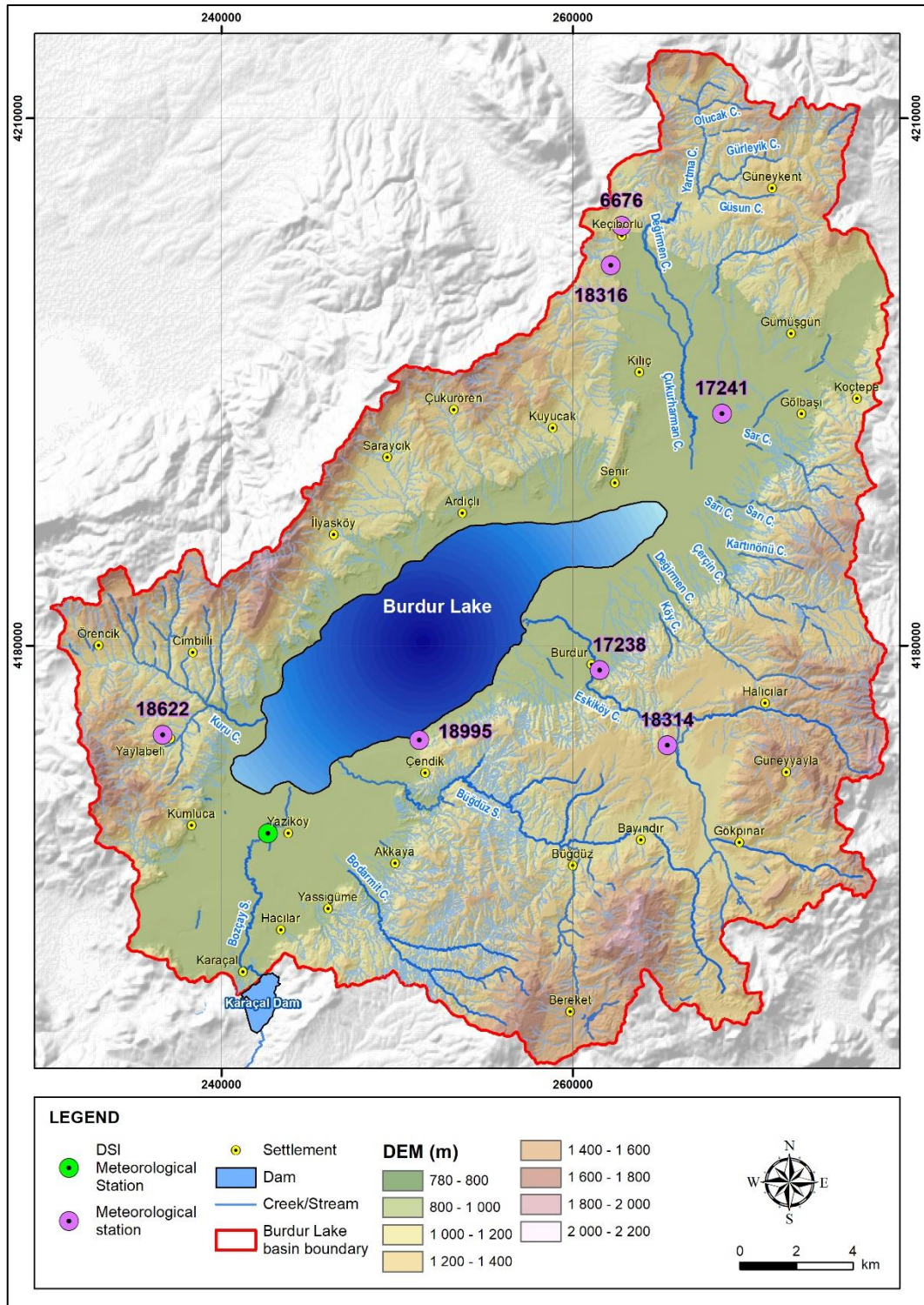


Figure 3.2. Location of the meteorological stations in the Burdur Lake Basin

3.2.1 Precipitation

Burdur meteorological station was used to determine the long-term precipitation trend of the basin. Annual total precipitation and cumulative deviation from mean annual precipitation graphs are shown in Figure 3.3 for the 1969-2018 period. The driest year is 1973 (270 mm), and the wettest is 1969 (615 mm) within the operational period. The long-term average annual precipitation is calculated as 418.6 mm. The cumulative deviation from the mean annual precipitation graph (Figure 3.3) shows that 1977-1985 and 1995-2006 correspond to main wet periods, whereas major dry periods are observed between 1969-1977 and 1985-1995 with several other short wet and dry periods.

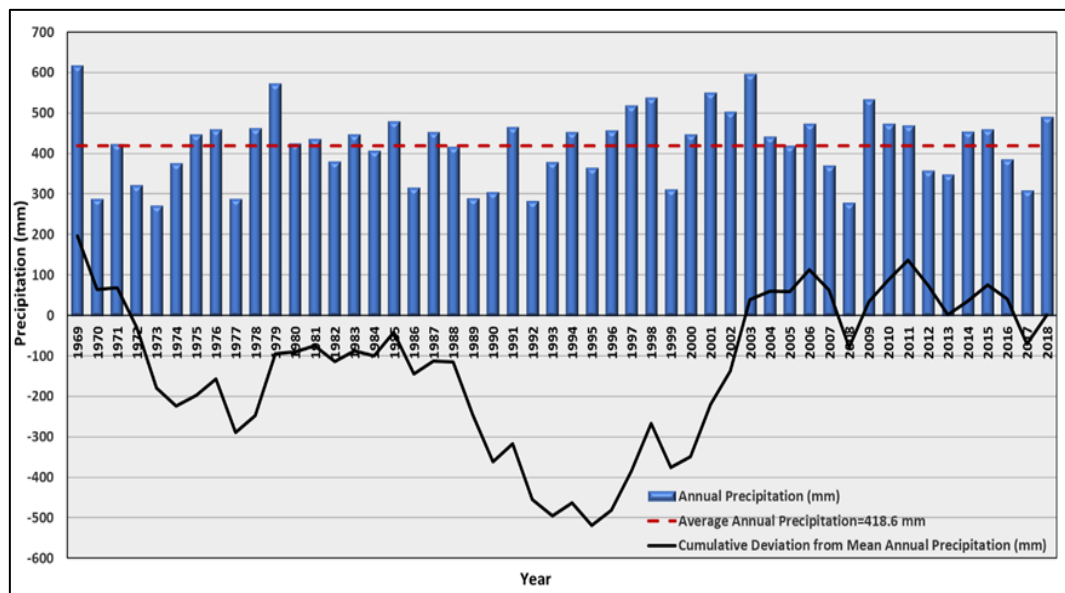


Figure 3.3. Annual precipitation and cumulative deviation from mean annual precipitation graph for the Burdur station

Annual total precipitation and cumulative deviation from mean annual precipitation graphs are also drawn for the Yazıköy station to understand the precipitation trend of the lake plain (Figure 3.4). For the 1969-2018 period, 2013 is the driest (166 mm),

and 1969 (557 mm) is the wettest year. The mean annual precipitation of the station, which is located at a lower elevation, is calculated as 361.7 mm, 14 % lower than the Burdur station. Cumulative deviation from the mean annual precipitation graph indicates that 1969-1977, 1983-1993, 2003-2008, and 2011-2018 correspond to dry periods, whereas wet periods are observed between 1977-1983, 1993-2003, and 2008-2011. The wet and dry periods in Burdur and Yazıköy stations are similar to each other.

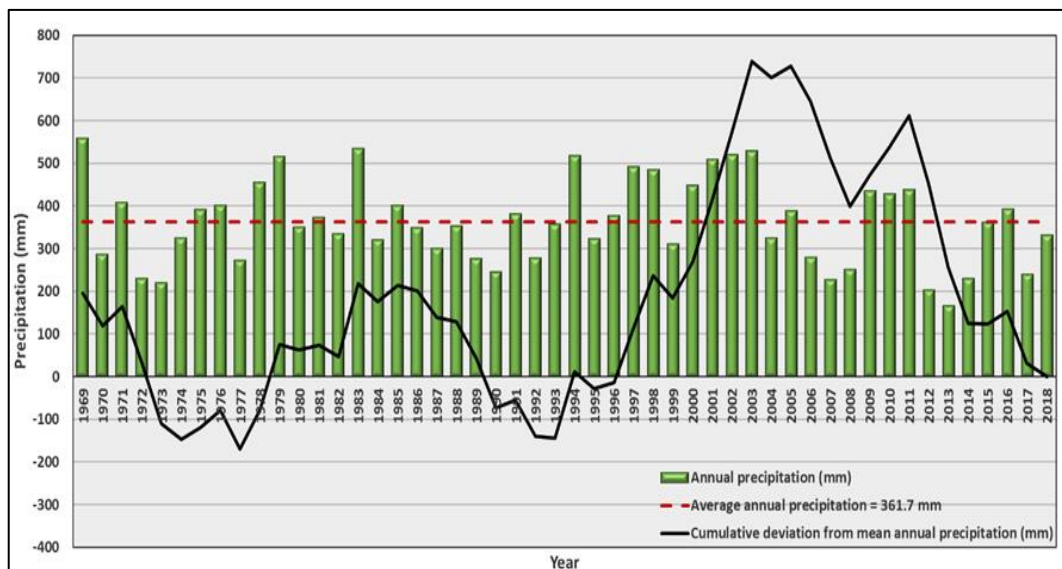


Figure 3.4. Annual precipitation and cumulative deviation from mean annual precipitation graph for the Yazıköy station

The average monthly precipitations measured in Burdur and Yazıköy stations for the 1969-2018 period are given in Figure 3.5. Both stations show similar precipitation trends. Precipitation generally falls in winter and spring (between December and May) for the given period. In both stations, December is the wettest month, whereas July and August are the driest. Except for August, precipitation in Burdur station is higher than in Yazıköy station since it is located at a higher elevation.

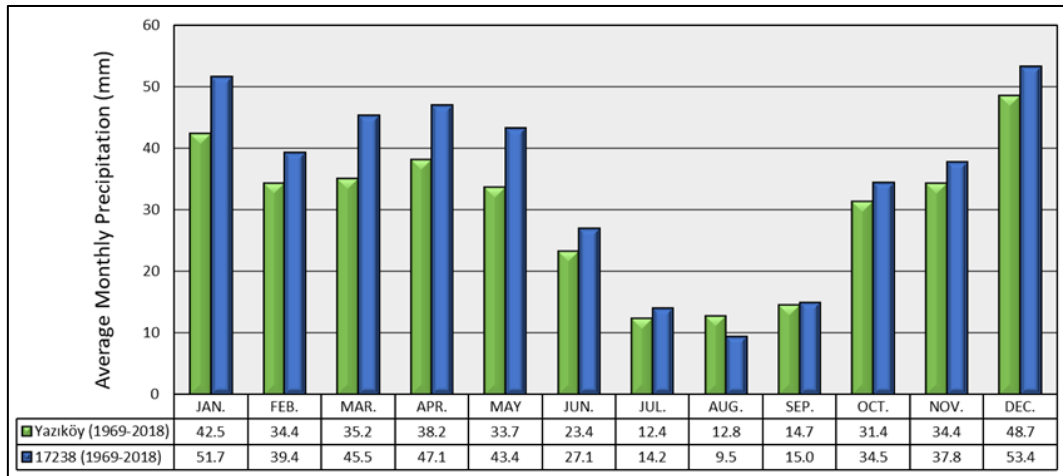


Figure 3.5. Mean monthly precipitation data for the Burdur and Yazıköy stations

3.2.2 Temperature

The mean monthly temperature values measured in the Burdur station are given in Figure 3.6 for the 1969-2018 period. Seasonality can be seen in the mean monthly temperature values. July and August are the hottest months, with mean temperatures exceeding 24°C.

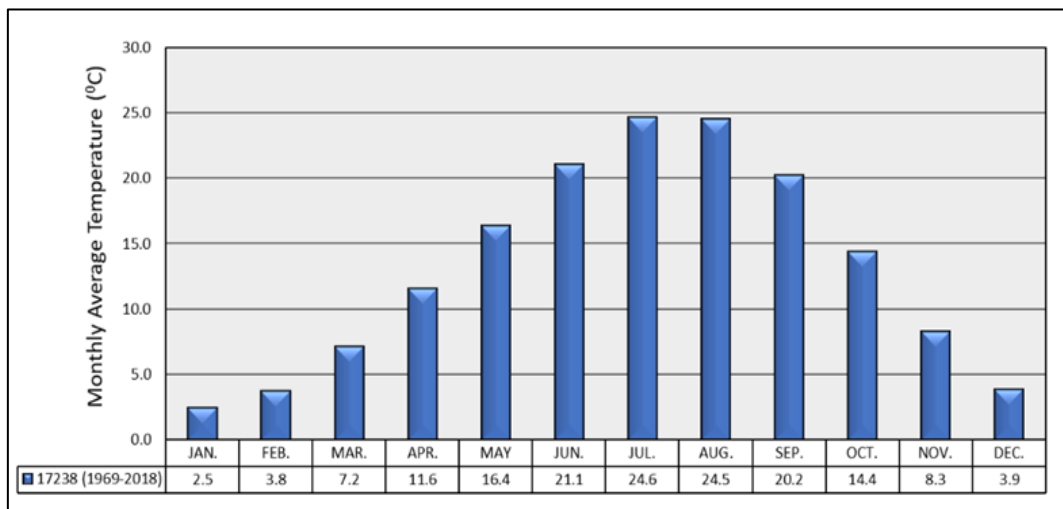


Figure 3.6. Monthly mean temperature graph of Burdur station

In the winter months, the mean monthly temperatures drop minimum values. January is the coldest month, with a 2.5°C mean monthly temperature value. The long term (1969-2018) mean annual temperature is 13.2 °C.

The minimum monthly temperature values in Figure 3.7 indicate that the study area is experiencing icing events in November-March. Especially in January and February, temperature values could lie below -7°C.

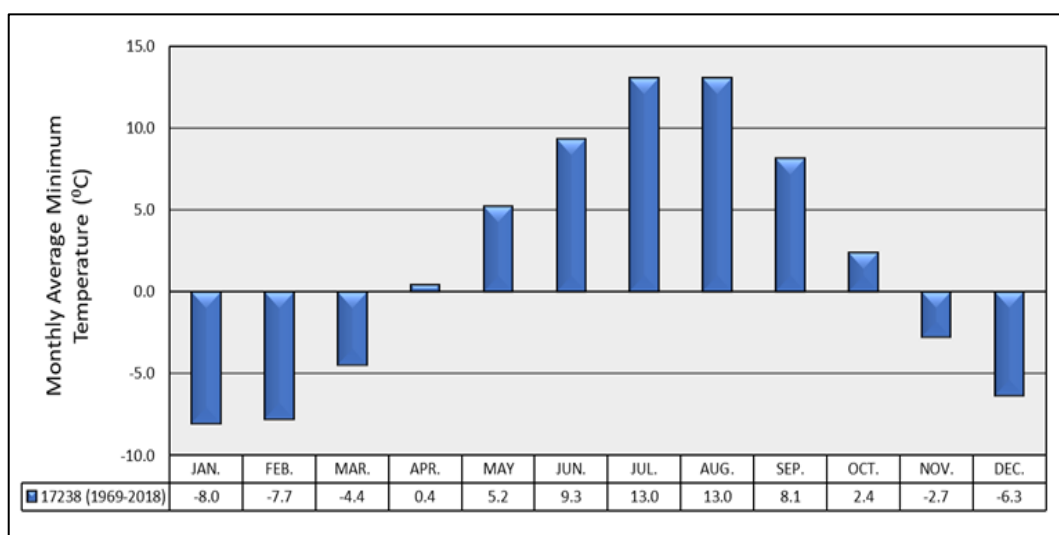


Figure 3.7. Monthly mean minimum temperature graph of Burdur station

According to the monthly average maximum temperature values in Figure 3.8, similar to the average temperature values, July and August are the hottest months. The average maximum temperature values reach over 36°C for these summer months, which could drop below 13°C in January.

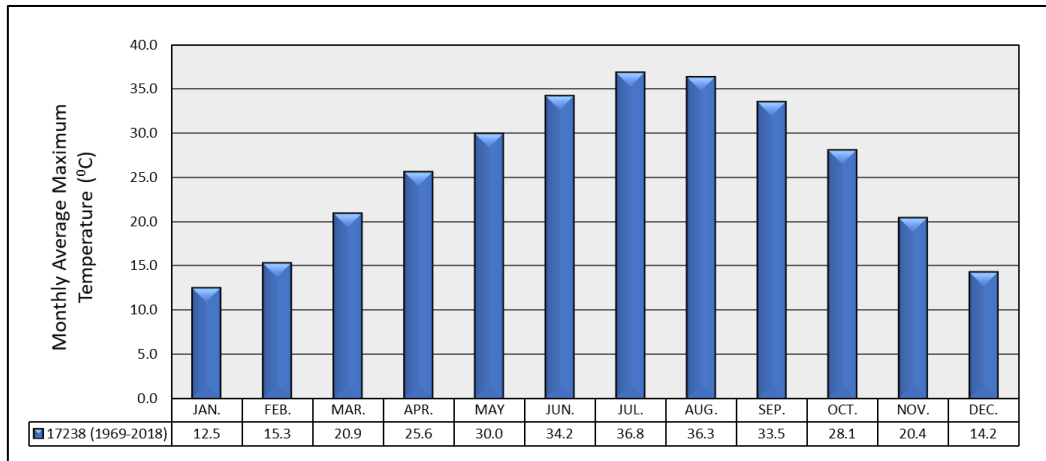


Figure 3.8. Monthly mean maximum temperature graph of Burdur station

3.2.3 Relative Humidity

Monthly average relative humidity values measured in the Burdur station for the 1969-2018 period are given in Figure 3.9.

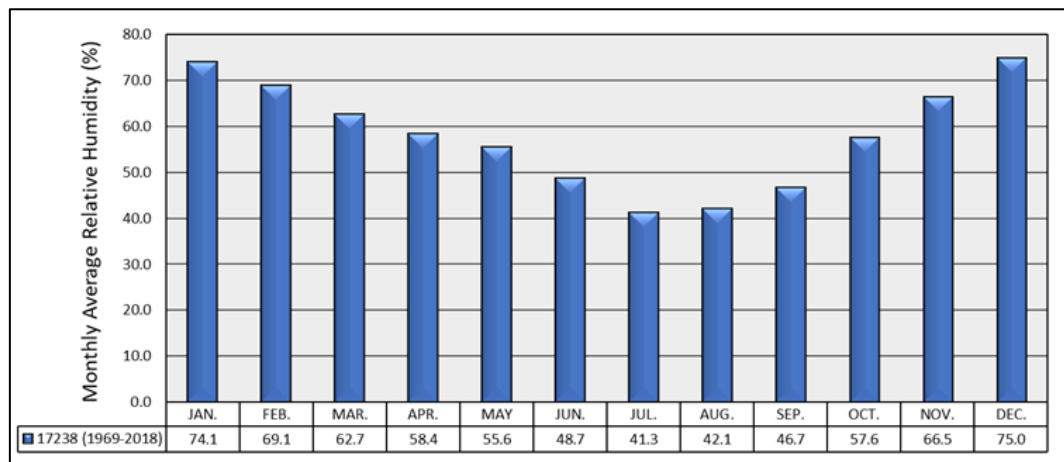


Figure 3.9. Mean monthly relative humidity graph of Burdur station

As shown in Figure 3.9, relative humidity shows an inversely proportional distribution to the air temperature. The highest monthly average relative humidity value is observed in December (75 %), and the lowest is in July (41.3 %).

3.2.4 Evaporation

Monthly total open surface evaporation was measured only for the April-October period between 1971-2018 at Burdur station and the same period between 1970-2005 at Yazıköy station (Figure 3.10).

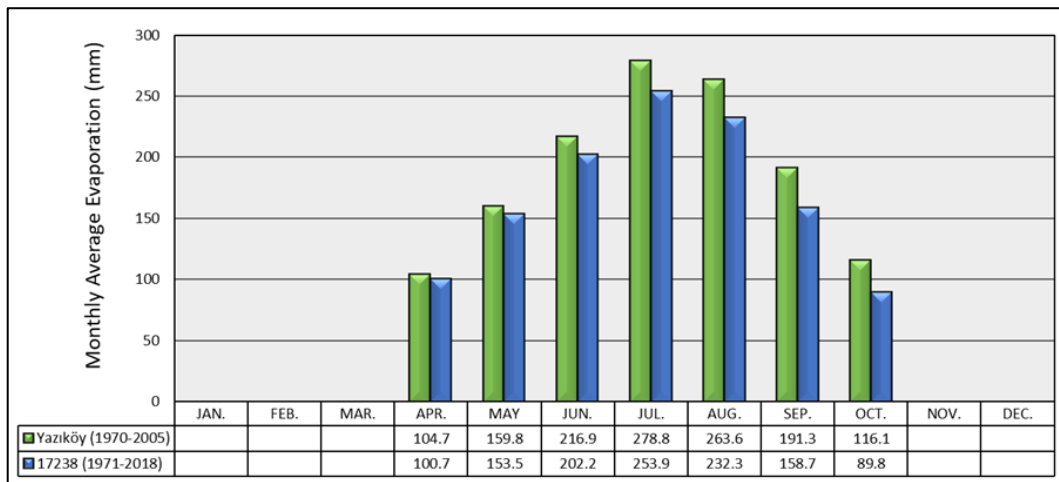


Figure 3.10. Mean monthly evaporation graph for Yazıköy and Burdur stations

The mean monthly maximum evaporation value is 278.8 mm and 253.9 mm in July, whereas the minimum is in April (104.7 mm) and in October (89.8 mm) at the Yazıköy and Burdur stations, respectively. No measurements were taken during the winter months (November-March). Although these two stations show a similar evaporation trend, the annual evaporation (1331.2 mm) at Yazıköy station is 12 % higher than Burdur station (1191.2 mm).

3.3 Geology

3.3.1 Regional Geology

Around Burdur Lake, the Beydağları autochthon, Yeşilbarak nappe, and Lycian nappes are exposed. The Beydağları autochthon is represented by the Beydağları formation, composed of Jurassic-Cretaceous, neritic limestones, while the Lycian nappes are composed of tectonostratigraphic units, representing different environmental conditions. The Yeşilbarak nappe lies between the Beydağları autochthon and Lycian nappes and extends laterally in all directions. In the region, this nappe is represented by the Elmalı Formation, composed of the Early Miocene-aged clastic rocks. Paleocene-Oligocene paraallochthonous and neoautochthonous Pliocene-Quaternary units are the cover units. Major fractures developed during and after the Pliocene in the region (MTA, 2010). The regional geological map is presented in Figure 3.11.

3.3.2 Geology and Stratigraphy of the Study Area

In the study area, the basement rock units are the components of Yeşilbarak and Lycian nappes. The Elmalı Formation (Te), one of the units of Yeşilbarak nappe, consists of Eocene-aged flysch, turbiditic sandstone, and shale. Cretaceous peridotite (Kmo) and ophiolitic mélange (Kkzm) are the units of the Lycian nappes. Ophiolitic mélange is comprised of limestone and dolomitic limestone (Kst), cherty micrite, calciturbidite (Jko), Jurassic-Triassic limestone and recrystallized limestone (TRjd), Jurassic-Cretaceous micrite and volcanic radiolarite, chert, shale units (Jko) and limestone units.

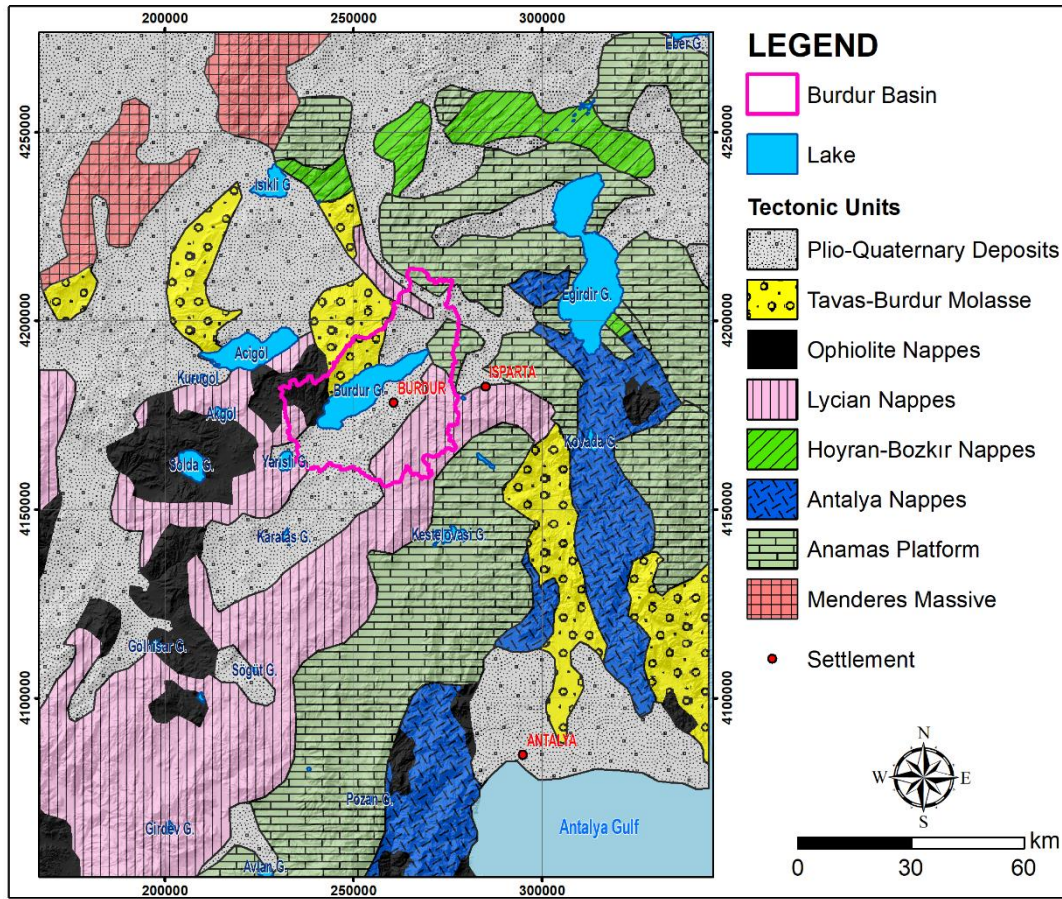


Figure 3.11. Regional geological map of the study area (modified from MTA, 2010)

On the Lycian nappes, transgressions occurred four times in the Paleocene, Middle Eocene, and Oligocene. As a result of these transgressions, para-allochthonous Paleocene reefal limestone (Tpm) and Oligocene thick-layered polygenic gravel and conglomerate (Toa) formations were developed.

The upper neo-autochthonous sedimentary unit unconformably overlies para-allochthonous units in the study area. These sedimentary units include Pliocene-Plio-Quaternary and Quaternary-aged terrestrial rock units. Pliocene unit (plç) includes conglomerate, sandstone, claystone, siltstone, marl, and limestone. Plio-Quaternary plQg and plQt units are usually represented by lacustrine sediments. The dominant lithologies of these sediments are claystone, sandstone, conglomerate, and siltstone.

There are also Plio-Quaternary aged tuff, tuffite, and travertine units. Old fluvial terrace deposits (Qt), alluvium (Qal)), recent alluvial fans (Qay), and slope debris and cone of dejection (Qym) comprise the Quaternary units. This unit is mainly located around the Burdur Lake area and overlies all the units in the study area.

The generalized columnar section and geological map of the study area are given in Figure 3.12 and Figure 3.13, respectively. The cross-sections are shown in Figure 3.14. The geological data for the study area was obtained from 1/100000 scaled geological maps of Isparta- M24 (MTA, 2010).

AGE	SYMBOL	LITHOLOGY
Quaternary	Qt, Qal, Qay, Qym	Slope debris and cone of dejection (Qym), Alluvial fans (Qay), Alluvium (Qal), Old fluvial terrace fills (Qt)
Plio-Quaternary	plQt, plQg	Conglomerate, Sandstone, Mudstone and Travertine (plQt) Tuff, Tuffite, Pumice, Sandstone, Claystone, Siltstone (plQg)
Pliocene	plç	Conglomerate, Sandstone, Claystone, Siltstone, Marl, Limestone (plç)
Oligocene	Toa	Conglomerate, thick layered polygenic gravel (Toa)
Paleocene	Tpm	Reefel limestone (Tpm)
Cretaceous	Kkzm	Ophiolitic melange, Olistostrome (Kkzm)
	TRjd	Jurassic-Triassic Limestone with megalodont, Recrystallized limestone (TRjd)
	Jko	Jurassic-Cretaceous Micrite, cherty micrite, calciturbidite (Jko)
	Kst	Limestone, Dolomitic limestone (Kst)
Eocene	Kmo, Te	Peridotite: Harzburgite, Serpentinite, Dunite (Kmo) Eocene Flysch: Sandstone, shale (Te)

Figure 3.12. Generalized columnar section of the study area (modified from MTA, 2010)

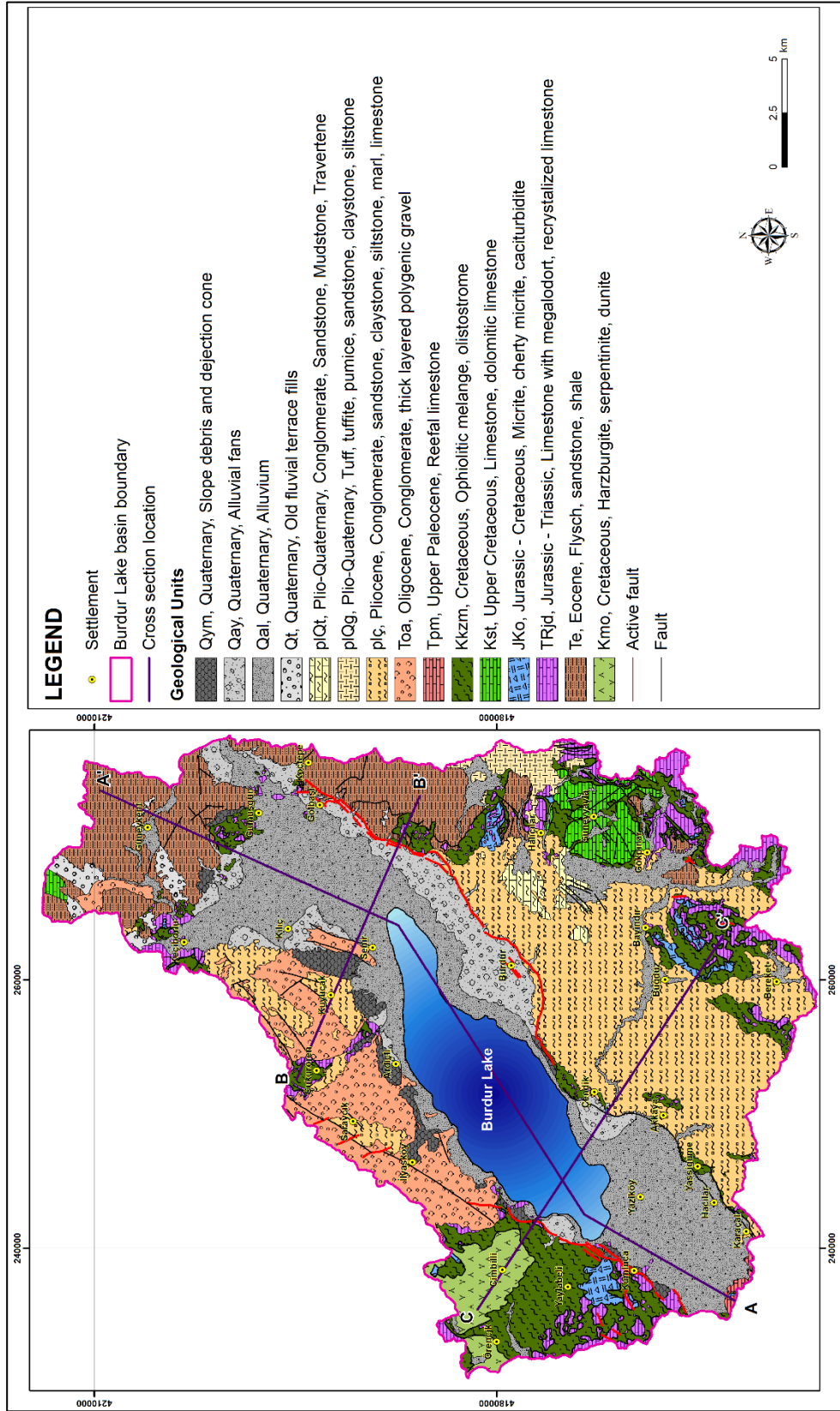


Figure 3.13. Geological map of the study area (modified from MTA, 2010)

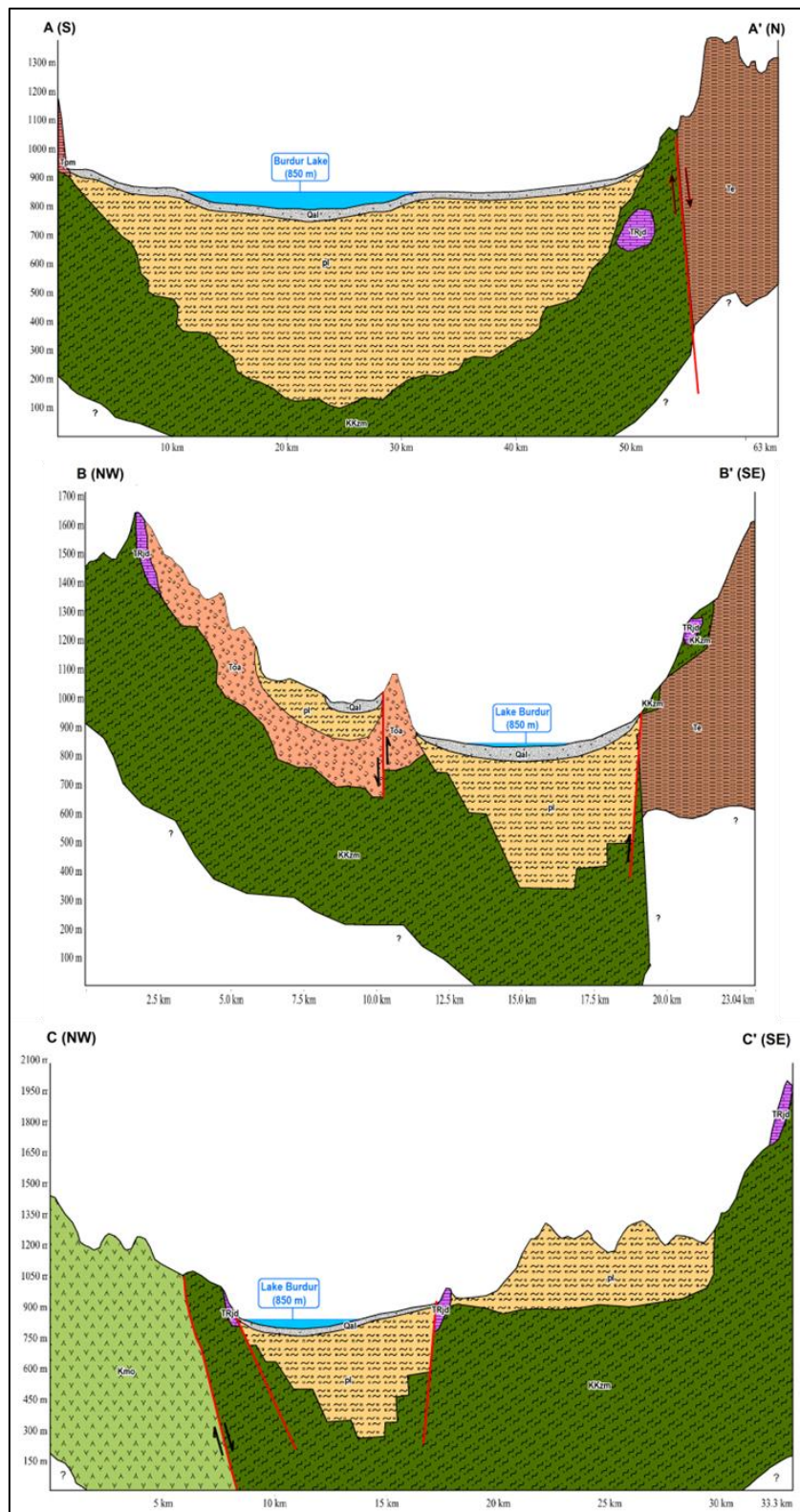


Figure 3.14. Geological cross-sections

CHAPTER 4

HYDROGEOLOGY

4.1 Water Resources

4.1.1 Burdur Lake

Burdur Lake is one of the saline, highly alkaline, and tectonic-origin lakes in Lakes District, southwest Turkey (Şener et al., 2020). The lake is an important area for numerous species of waterbirds during breeding and wintering periods and endemic fish species that have adapted to the lake's salty water. It was designated as a Ramsar site (no. 658) of international importance in 1994 and gained a Wildlife Protection Area status.

Based on the bathymetry prepared by DSI in 2015 (Figure 4.1), the lake area is about 133 km² with an average depth of 47 m. The maximum depth is around 61 m.

Burdur Lake levels during dry-wet periods (Burdur meteorological station no:17238) are shown in Figure 4.2. The lake level measurements were taken for a long period from 1969 to 2018. The lake did not show a sudden decrease in lake levels until 1971. After this year, the lake levels declined over the time period between 1971 and 1977, in parallel to the dry period observed in those years. During the wet period between 1977-1985, firstly, lake levels increased and then fluctuated seasonally. After 1985, the lake level decreased drastically independent from the dry-wet seasons except for short-term increases in wet seasons. The difference between the maximum (May 1970) and minimum (September 2018) water levels of the lake is approximately 17 m.

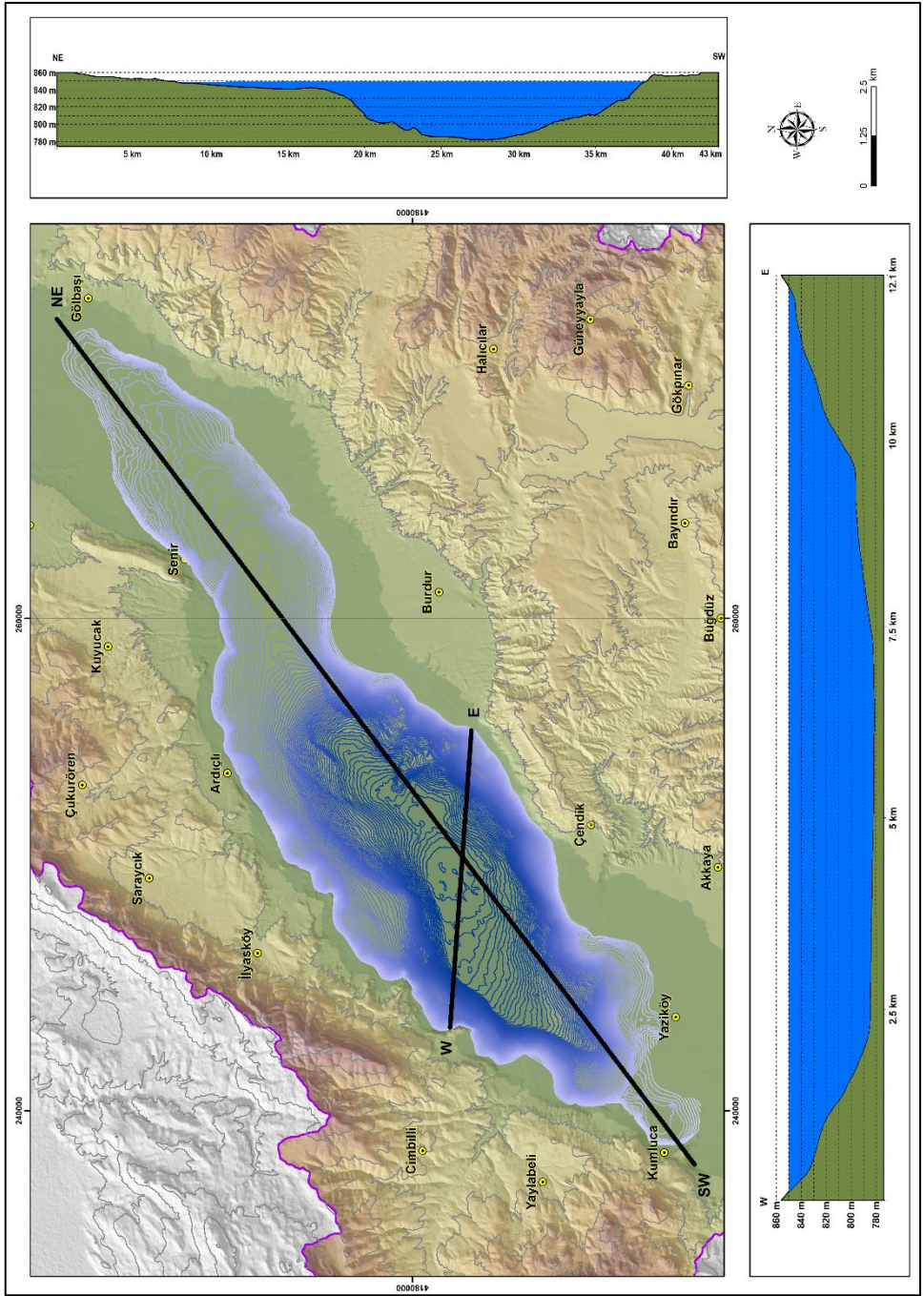


Figure 4.1. Bathymetric map of the Burdur Lake

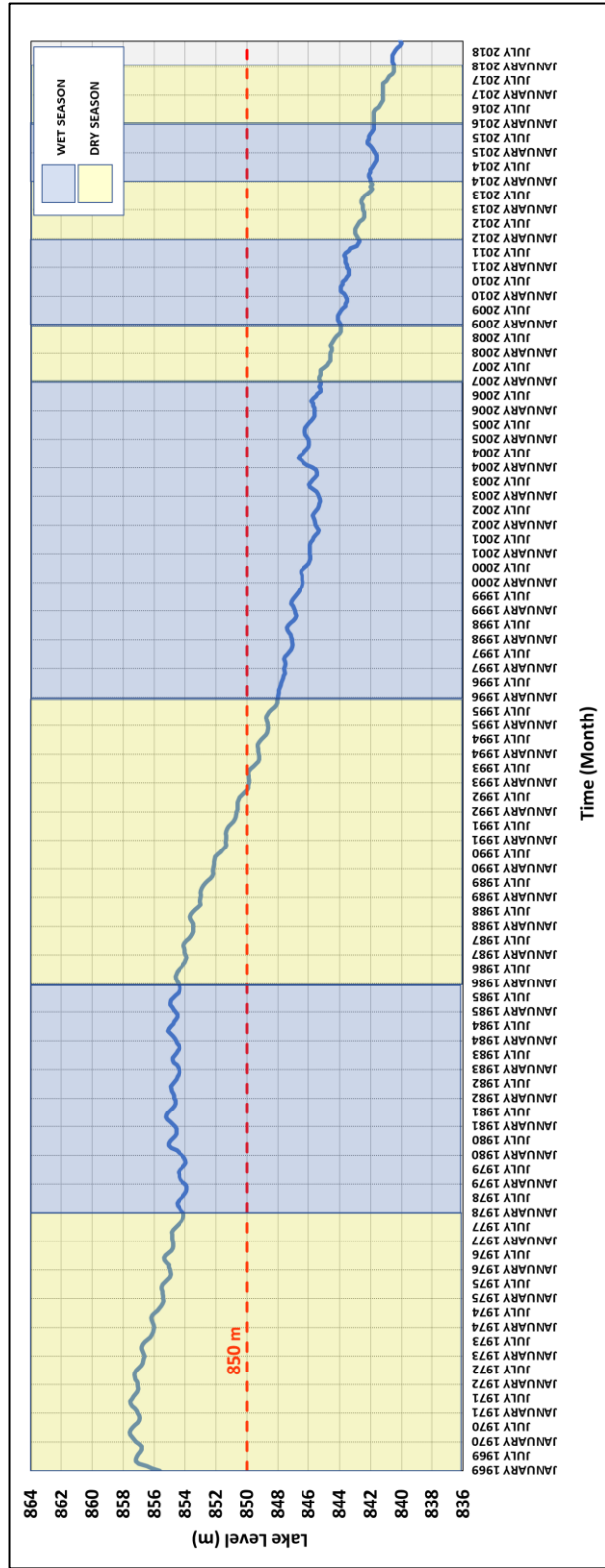


Figure 4.2. Burdur Lake water level variations (1969-2018) and dry-wet seasons

The stage-area and stage-volume curves of the lake are given in Figure 4.3 (DSI, 2016-b). 17 m water loss corresponds to a 95 km² area and 2989 hm³ volume loss of the lake.

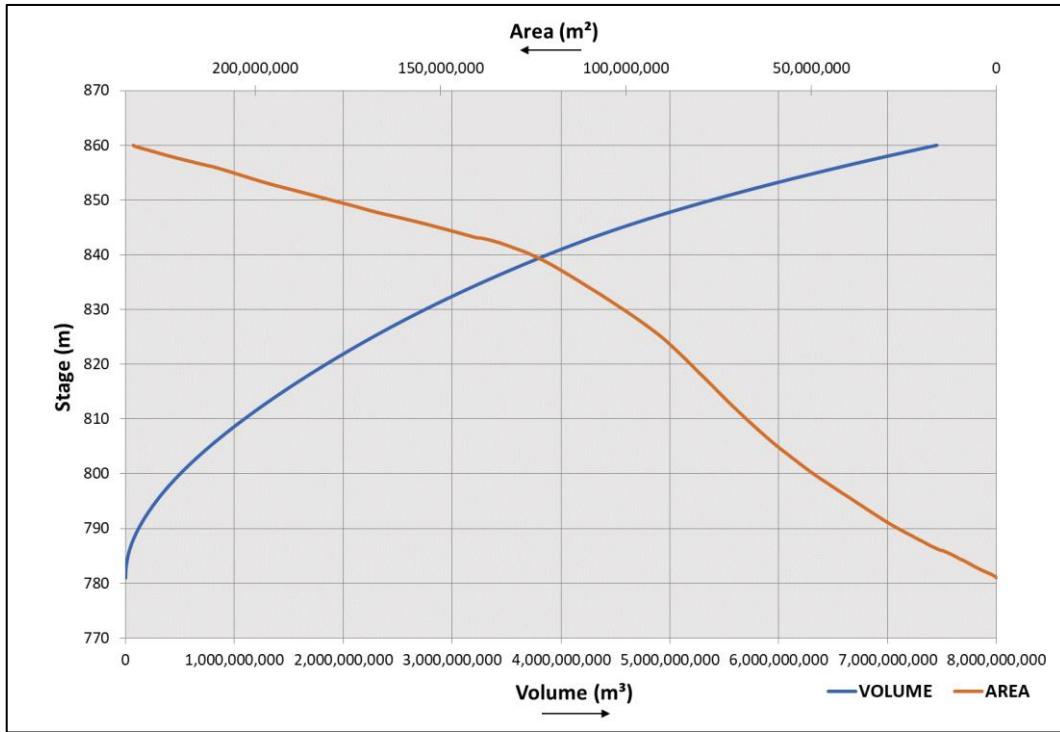


Figure 4.3. The stage-area and stage-volume curves

4.1.2 Streams, Dams, and Ponds

The drainage network of the Burdur Lake basin is shown in Figure 4.4. The lake is fed by several ephemeral and perennial streams and creeks from all directions, namely Bozcay and Bügdüz streams and, Bodarmit, Eskiköy, Değirmen, Çerçin, Sarı, Sar, Keçiborlu, Çukurharman, and Kuru creeks. These main streams and creeks are located in the south, east, and northern part of the lake (Figure 4.4). Because of the steep slope and low permeable geological units, there is no perennial stream in the western part of the lake.

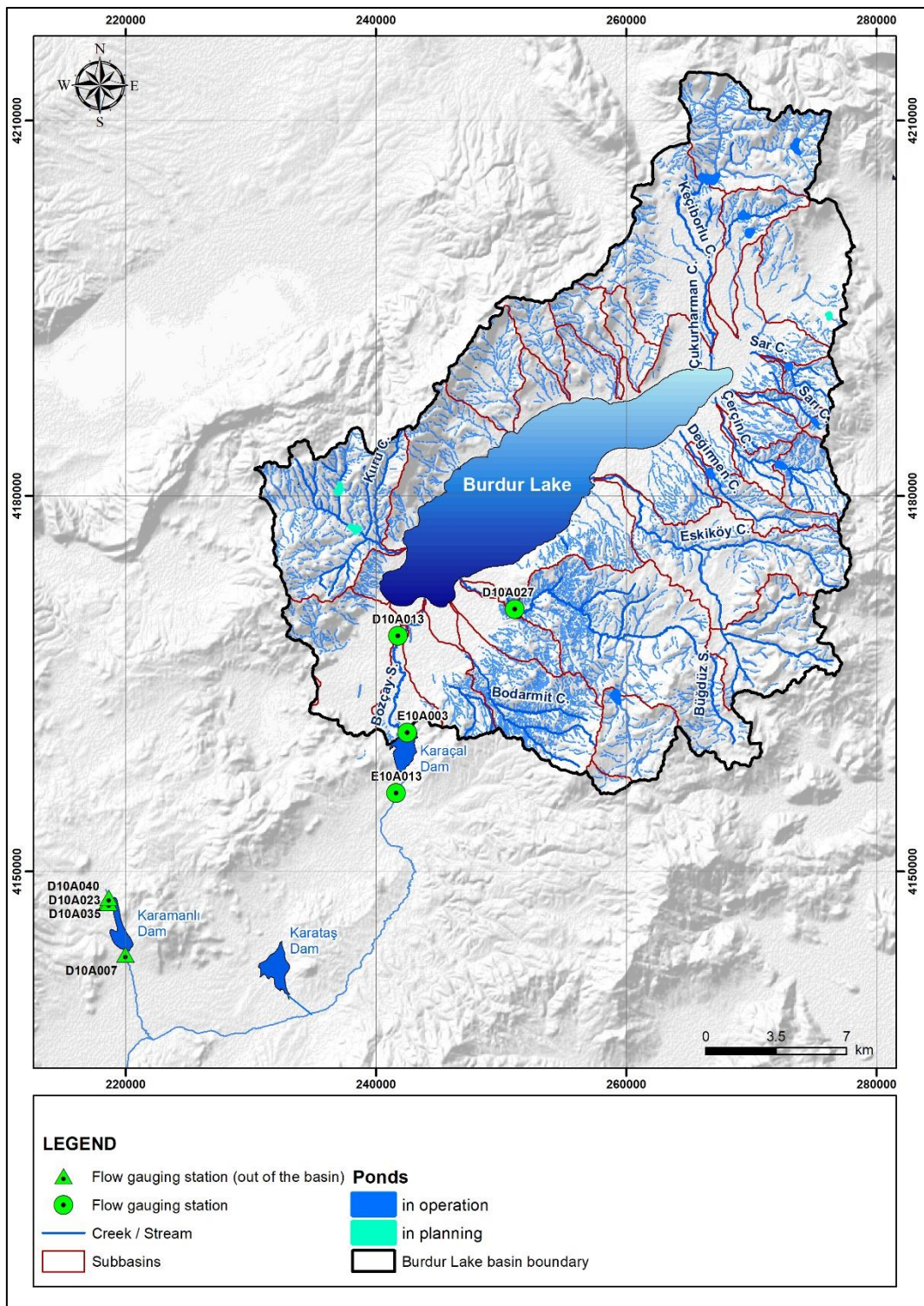


Figure 4.4. The drainage network of the Burdur Lake basin

The dams located around the study area are the Karamanlı, Karataş, and Karaçal dams. These dams control the flow of the Bozçay Stream in the southern part of the basin and are used for irrigation and flood protection purposes. The Karamanlı and Karataş dams are located upstream of the Karaçal Dam which is located at the southern lake basin boundary. Detailed information about the dams is given in Table 4.1. In addition to dams, nine ponds are in operation for irrigational purposes on several streams and creeks in the study area (Table 4.1). The completion years of these dams and ponds are plotted on the Burdur Lake level-time graph to show the changes in the lake level during dry and wet periods after the reservoir construction (Figure 4.5). The lake levels fluctuated seasonally between 1969 and 1971 despite the dry period observed in those years. However, the lake levels declined rapidly over the time period between 1971 and 1977 as a result of the constructions of the Karataş Dam in 1974 and the Karamanlı Dam in 1975. In the wet period observed between 1977 and 1985, the lake levels reached a new equilibrium condition with seasonal fluctuations after a drop of about 2 meters compared to the initial unaffected dry conditions between 1969-1971. Over the dry period observed between 1985 and 1995, the lake levels decreased an additional 7 meters in conjunction with the construction of several reservoirs since the beginning of 1989 and the drier climatic conditions. Over the long wet period between 1995 and 2006, the total drop in lake levels was less (only about 2.5 m) due to the wetter conditions, in spite of the storage of surface waters in the reservoirs. Over the several short dry and wet periods observed between 2007 and 2018, the lake levels dropped further by 5.5 m as a consequence of the construction of the Karaçal Dam in 2010 and several others afterward.

The locations of the streamflow gauging stations in and around the study area are given in Figure 4.4. The discharge rates monitored at these flow gauging stations were investigated to determine surface water potential and the discharge from streams to the lake. DSI and Electrical Power Resources Survey and Development Administration (EIEI) established seven flow gauging stations on the Bozçay Stream and its tributaries.

Table 4.1. Information about the reservoirs located in the study area

Name	Completion Year	Stream Name	Purpose	Lake Volume (hm ³)	Irrigation Area (ha)
Merkez Gökçebağ P.	1989	Boğaz	Irrigation	1.19	168
Merkez Askeriye P.	1994	Değirmendere	Irrigation	1.09	132
Keçiborlu Güneykent Uzundere P.	1991	Keçiborlu	Irrigation	1.43	380
Keçiborlu Güneykent Uludere P.	1996	Keçiborlu	Irrigation	0.74	209
Keçiborlu Merkez P.	1990	Keçiborlu	Irrigation	4.72	803
Yakaören P.	2011	Saman	Irrigation	-	88
Güneykent P.	2016	Karagöz	Irrigation	0.46	96
Bügdüz P.	2016	Bügdüz	Irrigation	2.07	328
Gölbaşı P.	2017	Sar	Irrigation	0.63	68
Karaçal D.	2010	Bozçay	Irrigation & Flood protection	63.50	5006
Karataş D.	1974	Bozçay	Irrigation	65.30	6490
Karamanlı D.	1975	Bozçay	Irrigation & Flood protection	24.60	3747

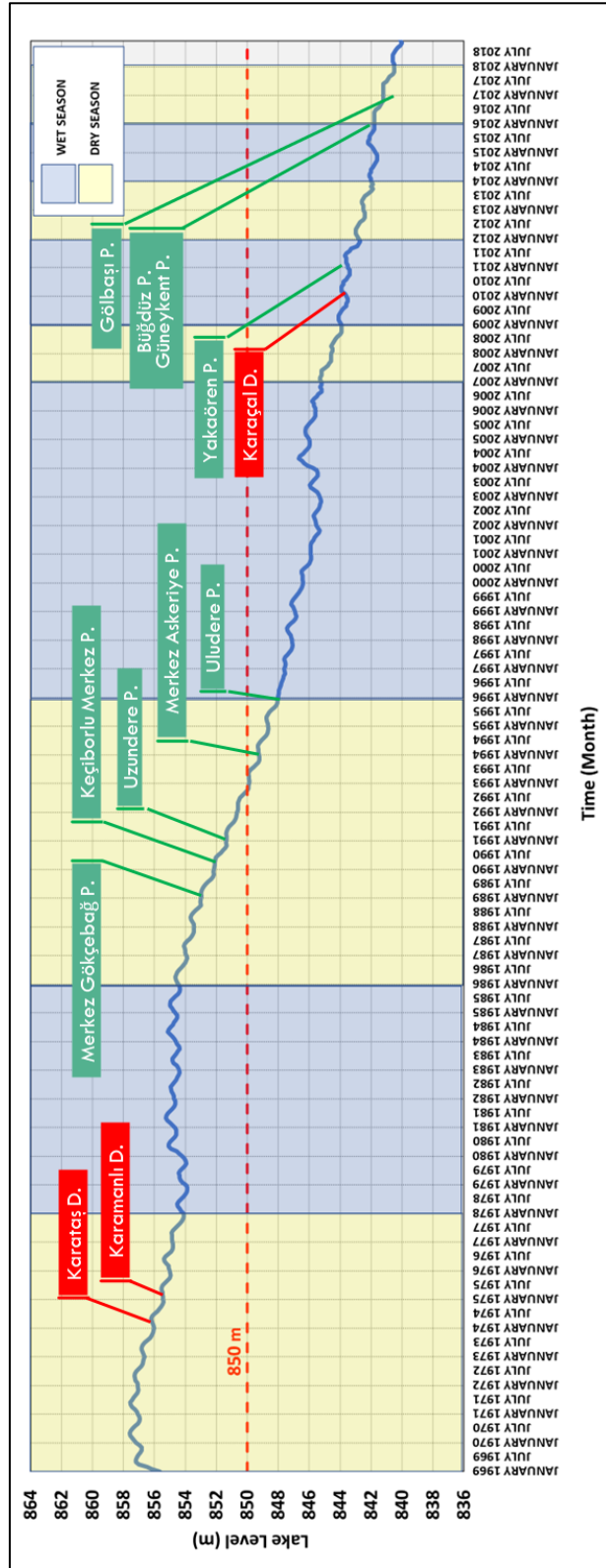


Figure 4.5. Dams and ponds completion years on the water level of Burdur Lake

Four of them are located around the Karamanlı Dam, while three are around the Karaçal Dam (Figure 4.4). In the study area, there is also a flow gauging station on the Bügdüz Stream, as seen in Figure 4.4.

Detailed information about the flow gauging stations in the study area is presented in Table 4.2. The operational periods of these stations change from 4 to 50 years. However, since the Burdur Lake level change was analyzed for the time interval between January 1969 and December 2018, the measurements of the flow gauging stations corresponding to this period were included in the analysis.

Table 4.2. Information about the flow gauging stations in and around the study area

Station No.	Station Name	Operator	Coordinates		Elevation	Watershed Area (km ²)	Data Period
			Latitude	Longitude			
D10A013	Bozçay Yazıköy	DSI	37.63	30.07	865	1571	1969-1988 1991-1992 1995-2009 2012-2018
D10A027	Bügdüz Suludere	DSI	37.65	30.18	920	214	1979-2018
E10A013	Bozçay Boğaziçi	EIE / DSI	37.52	30.08	961	1337	2004-2015 2017-2018
E10A003	Bozçay Karaçal	EIE	37.56	30.08	910	1542	1969-1994
D10A007	Karamanlı Değirmenler C.	DSI	37.39	29.84	1145	171	1969-1974
D10A023	Upstream Karamanlı Dam	DSI	37.43	29.82	1191	114	1974-2007
D10A035	Karamanlı Dam. Upstream Değirmen C.	DSI	37.43	29.82	1191	84	2007-2012
D10A040	Karamanlı Dam Upstream Değirmen C.	DSI	37.43	29.82	1191	110	2012-2018

The measured minimum, maximum and average flow rates of the flow gauging stations are summarized in Table 4.3. The monthly flow rates of the Bozçay stream around the Karamanlı Dam (D10A007, D10A023, D10A035, D10A040) were taken in consecutive periods (Table 4.3 and Figure 4.6). The monthly average flow rates

for the years between 1969-1974, 1974-2007, 2007-2012, and 2012-2018 are 0.416 m³/s, 0.30 m³/s, 0.23 m³/s, and 0.326 m³/s, respectively. There is no flow in October 1997 and 1998, September 2000, and August-September 2001. The maximum flow rate was measured as 3.037 m³/s in April 1971 (D10A007). Since the flow gauging stations D10A023, D10A035, and D10A040 are located upstream of the Karamanlı Dam, the construction of the Karamanlı and Karataş dams had no impact on the measurements of these stations. Although station D10A007 is located downstream of Karamanlı Dam, the data period of the station (1969-1974) covers the years before the construction. Thus, flow measurements were not affected by the dam storage.

Table 4.3. Discharge rates for flow gauging stations in and around the study area

Station No.	Stream and Location	Coordinates		Data Period	Discharge Rate (m ³ /s)		
		Latitude	Longitude		Min.	Max.	Ave.
E10A013	Bozçay Stream (Karaçal Dam)	37.52	30.08	2004-2015 2017-2018	0.017	6.840	0.947
E10A003		37.56	30.08	1969-1994	DRY	15.400	1.654
D10A013		37.63	30.07	1969-1988 1991-1992 1995-2009 2012-2018	DRY	15.530	1.060
D10A027	Bügdüz	37.65	30.18	1979-2018	0.003	9.028	0.880
D10A007	Bozçay Stream (Karamanlı Dam)	37.39	29.84	1969-1974	0.009	3.037	0.416
D10A023		37.43	29.82	1974-2007	DRY	1.897	0.300
D10A035		37.43	29.82	2007-2012	0.002	0.967	0.230
D10A040		37.43	29.82	2012-2018	0.065	2.110	0.326

According to the flow measurements taken from the stream gauging stations located around Karamanlı Dam (D10A007, D10A023, D10A035, D10A040), there were seasonal fluctuations until 2015. However, flow amounts decreased after this year under the dry season condition, and no seasonal variation for the flows could be detected (Figure 4.6).

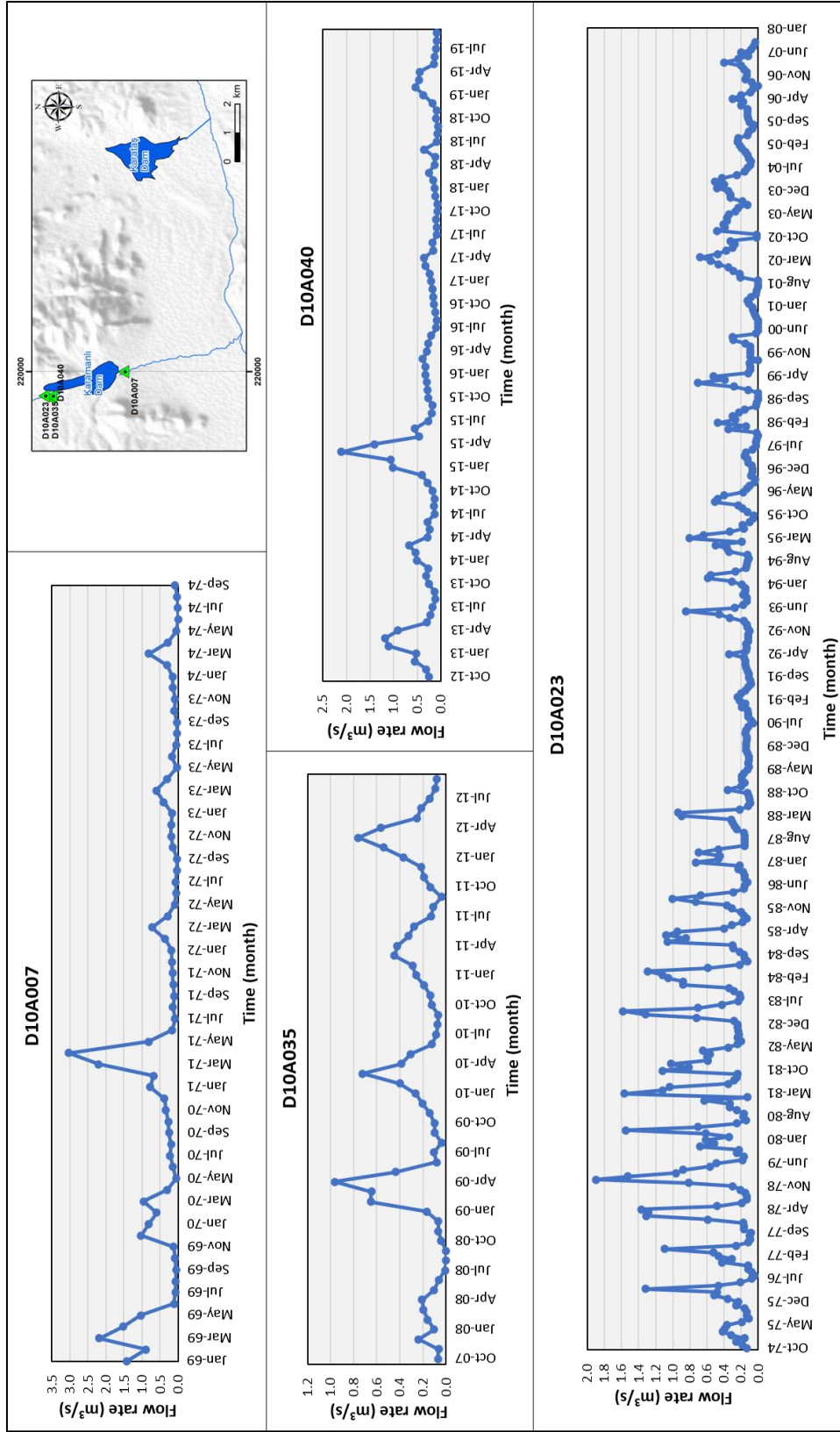


Figure 4.6. The monthly flow rates of the Bozçay stream gauging stations located around Karamanlı Dam (D10A007, D10A035, D10A040, D10A023)

The monthly flow rates of the Bozçay stream were also measured by the stations located around the Karaçal Dam (D10A013, E10A003, E10A013). Average flow rates for D10A013, E10A003, and E10A013 stations are 1.06 m³/s (1969-2018), 1.654 m³/s (1969-1994), and 0.947 m³/s (2004-2018), respectively (Table 4.3). The minimum flow rates (sometimes even dry) were measured in July-August based on D10A013 and E10A003, whereas the maximum flow rate was 15.53 m³/s in March 1969 (D10A013). The maximum discharge rates were measured in spring due to the snow melting, whereas the minimum values were recorded in summer.

The monthly flow rates of the Bozçay stream gauging stations around Karaçal Dam (D10A013, E10A003, E10A013) are shown in Figure 4.7. When Figure 4.7 is examined, it can be seen that before the constructions of the Karataş and Karamanlı dams in 1974, the measured flow rates showed seasonal variations (E10A003 and D10A013). After the construction of these dams in 1975, flow rates of the Bozçay Stream decreased significantly until 1977, according to measurements of stations E10A003 and D10A013. Since the wet period started after 1977, flow rates increased but could not reach the values before 1974. When the wet season ended in 1985, the flow rates began to decrease again. Finally, with the construction of the Karaçal Dam in 2010, the flow regime of the Bozçay Stream was taken entirely under control by the dams, as seen from the downstream stations (E10A003 and D10A013).

The average flow rates after 2010 decreased to 0.25 m³/s according to measurements of station D10A013. Station E10A013 is located at the downstream part of the Karataş and Karamanlı dams but the upstream part of the Karaçal Dam. Thus, the flow rates of the station were only under the control of the Karataş and Karamanlı dams. Since the data period of the station is between 2003-2018 (nearly 30 years after the Karamanlı Dam), only seasonal changes can be seen during the data period.

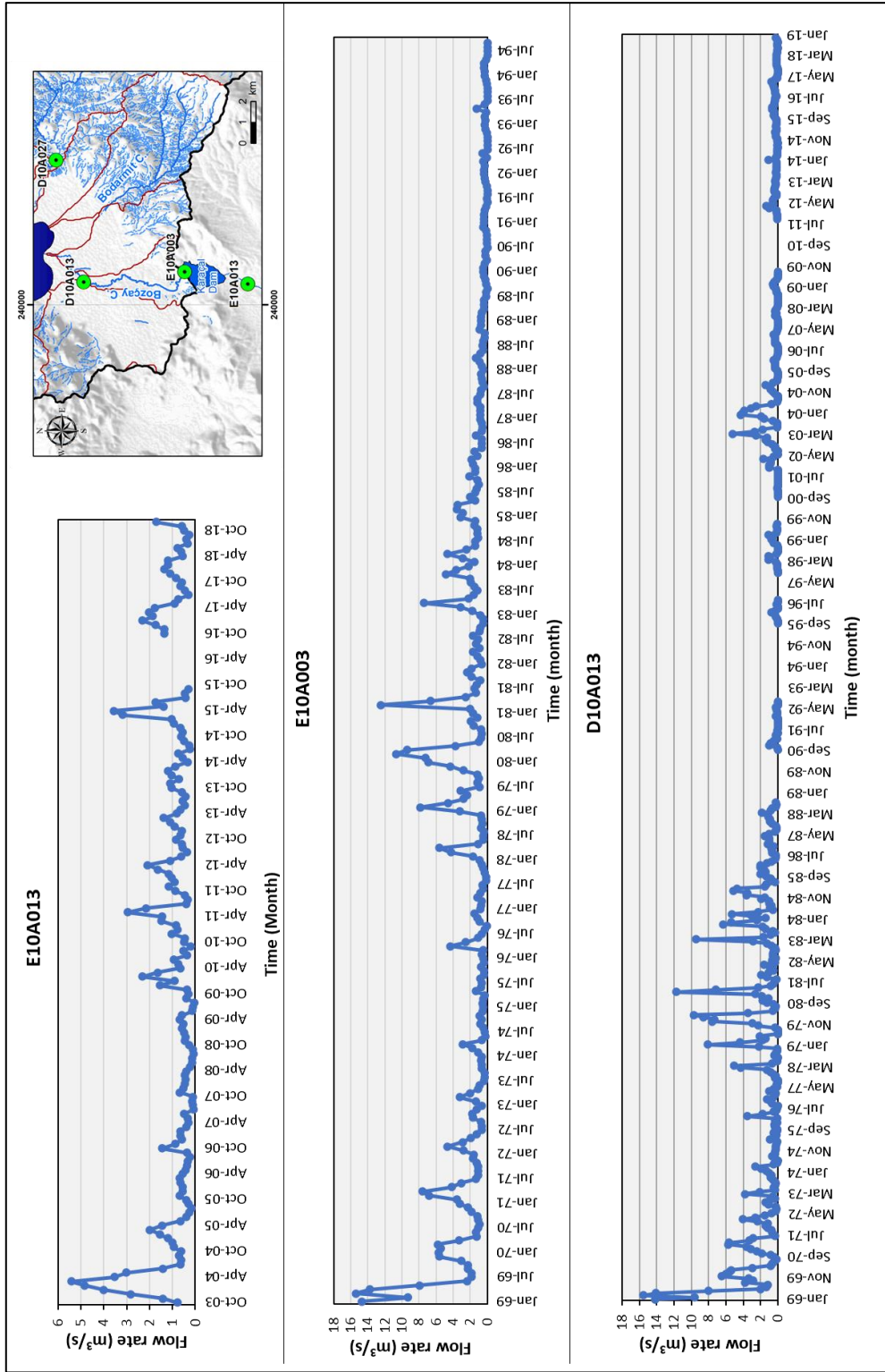


Figure 4.7. The monthly flow rates of the Bozçay stream gauging stations (E10A013, E10A003, D10A013)

In addition to the flow measurement of Bozçay Stream, monthly flow rates of Büğdüz Stream were also recorded at the station D10A027 during 1978-2018 in the basin (Figure 4.8).

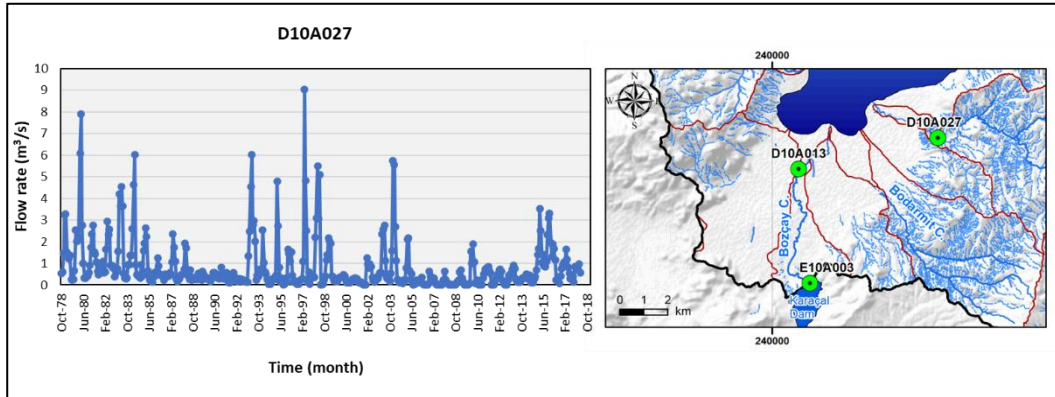


Figure 4.8. The Monthly flow rates of Büğdüz Stream measured by the station D10A02

The average flow rate measured in this station is $0.88 \text{ m}^3/\text{s}$, whereas the maximum flow rate was $9.028 \text{ m}^3/\text{s}$ in April 1997 (Table 4.3). Between 2006 and 2013, no flow could usually be recorded for the summer and October-November months. In 2016, the Büğdüz Pond construction was completed on the Büğdüz Stream. However, the effect of the pond on the streamflow could not be determined explicitly since the measurements can be taken only for a short period after the construction of the pond (only two years).

4.1.3 Springs

During the hydrogeological investigation studies of the Burdur Lake basin (DSİ, 2016-a), six important springs were identified within the boundaries of the study area. The locations of the springs are shown on the geological map (Figure 4.9).

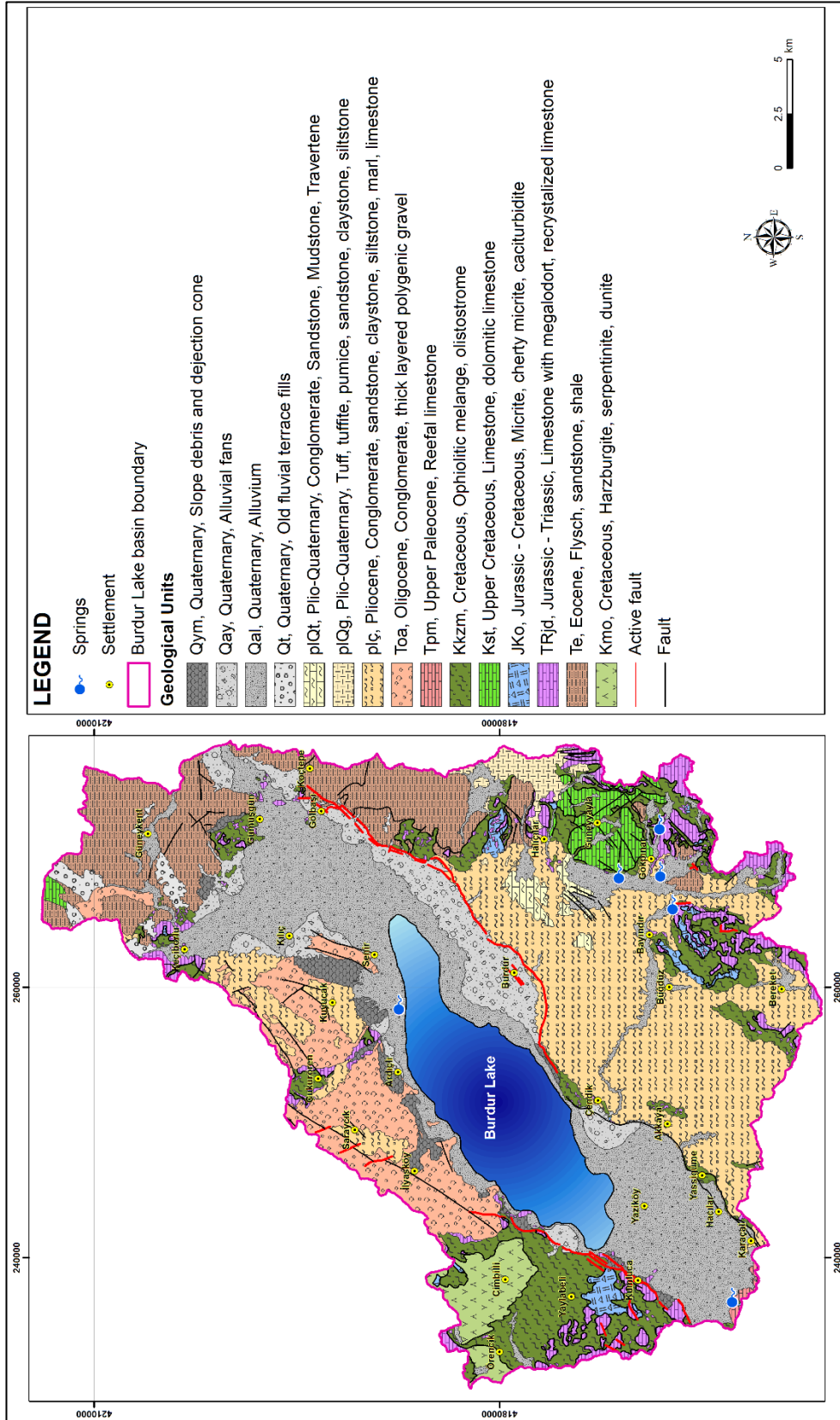


Figure 4.9. Location of the springs on the geological map

İnsuyu Cave spring, Taşkapı, Kocapınar-Kayaaltı, and Gökpınar springs are located in the eastern part of the study area around Çine, which is the important karst region in Turkey. These springs discharge from the karstic dolomitic limestone. Although these springs had higher discharge rates in the early 1970s, they completely dried up after 1986 (Taşdelen, 2018). In addition to karstic springs in the Çine region, there are also two important springs called Pınargözü in Düger Village of Yazı Plain and Senir on the coast of the Senir. Pınargözü spring discharges from Upper Paleocene reefal limestone located in the southern boundary of the study area with limited extent. According to DSİ (2016-a), significant decreases have occurred in the discharge amount of Pınargözü spring after the 2010s. The Senir spring discharges to Burdur Lake. It emerged on the Senir coast after 2000 due to the decrease in the water levels of Burdur Lake. As in Pınargözü, the discharge of the Senir spring has also dramatically decreased after 2004 and completely dried after 2012 (DSİ, 2016-a).

Detailed information about the coordinates, elevation, average discharge rates, and measurement periods of the aforementioned springs is provided in Table 4.4. Continuous measurements were not taken from the springs in the study area. However, the average discharge rates were calculated using monthly average discharge rates taken from DSI for the measurement periods in Table 4.4.

Table 4.4. Detailed information about the springs

Name	Coordinate (UTM)		Elevation	Discharge Rate (L/s)	Measurement Period
	Easting	Northing			
İnsuyu Cave	268427	4171185	1209	57	1980-1981
Taşkapı	272054	4168167	1219	64	1990-1991
Gökpınar	268556	4168108	1192	180	1979-1981
Kocapınar - Kayaaltı	266127	4167201	1265	167	1979-1981
Düger - Pınargözü	237075	4162810	918	240	1975
Senir	258721	4187450	858	226	2000-2012

4.1.4 Wells

According to DSI Hydrogeological Investigation Report (2016-a), the wells in the study area can be categorized as private, DSI, municipal, and institutional wells. The locations of these wells are shown in Figure 4.10.

Most of the wells in the study area are private wells drilled for the irrigation of the agricultural areas around Burdur Lake. There are 3110 private wells within the basin, 891 of which are licensed, and 2219 are unlicensed (Figure 4.10). According to DSI, in the Burdur Lake basin, an average of 5000 m³ of water is pumped per hectare yearly (DSI, 2016-a). Therefore, 16.9 hm³ of water is pumped to irrigate 3390 ha of the agricultural area in the basin in a year. The only recorded information for private wells is the locations and depths if they can be measured.

For irrigation, drinking, and domestic purposes, a total of 429 wells were drilled by municipalities and other institutions in the basin. For irrigational purposes, 2.8 hm³ of water is pumped yearly from 30 wells with 3 L/s per well. In order to supply domestic water, 342 wells are used to pump 15.7 hm³/year of water (DSI, 2016-a). 1 L/s of water per well is pumped from 30 wells in the Çine region, while 1.5 L/s per well from the remaining 312 wells. There are also 57 wells drilled to supply water to Burdur Province and the other settlements within the Burdur Lake basin. Bank of Provinces and DSI drilled seven wells around Çine region between 1967 and 1993 and pumped 300 L/s (9.5 hm³/year) of water to supply the drinking water needs of the Burdur Province in 2015. For the other settlements, from 50 wells, total water consumption of 1.9 hm³/year was calculated according to their population, assuming the 250 L/day water requirement per person at that time. In 1969, 125 L/s water was pumped from the five DSI wells drilled in 1967-1968 to supply drinking water to the Burdur Province according to the calculation of the population rate.

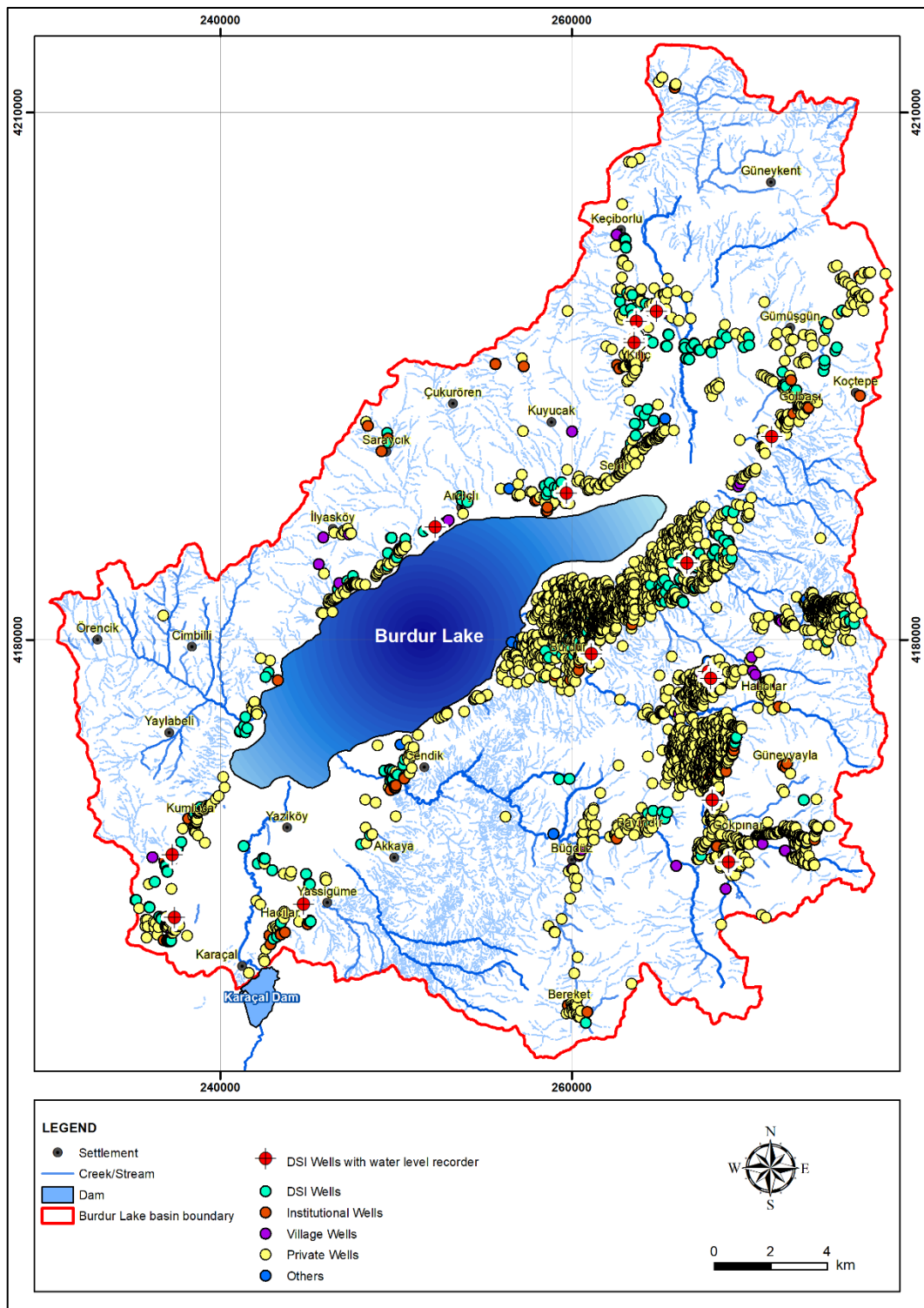


Figure 4.10. Location of the wells drilled within the study area

Between 1963 and 2015, 282 wells were drilled by DSI for exploration and operation purposes in the basin. 17.8 hm³/year of water is pumped from 249 wells to irrigate the 3552-ha cooperative site in the basin. The locations of these wells are shown on the geological map in Figure 4.11. The 184 well logs were taken from DSI. Detailed information about these wells is provided in Appendix A. To take continuous measurements, DSI installed water level recorders in 16 wells, the locations of which are shown in Figure 4.12. Groundwater elevation levels were measured at these wells monthly, varying from July 1974 to December 2018. Detailed information about the wells with a water level recorder is given in Appendix B.

According to the calculations, in 2015, 64.6 hm³ of water was pumped yearly from 3821 wells in the Burdur Lake basin. In 1969, a total amount of 3.95 hm³/year of water was pumped to supply drinking water to the Burdur Province.

4.2 Hydrogeology of the Study Area

The hydrogeology of the study area was conceptualized using the information gathered from literature, the wells, Burdur Lake, streams, and springs in the basin. Hydrogeological properties of the geological units within the Burdur Lake basin were explained from the basement to the top.

The Eocene aged Elmalı Formation (Te), Cretaceous peridotite (Kmo), and ophiolitic mélangé (Kkzm), outcropping mainly at the north, east and southwestern part of the study area, are the basement rock units. This Elmalı Formation (Te) consists of Eocene aged flysch, clastic sedimentary rocks, and local limestone levels. Although these rock units are generally impervious or semi-pervious, limestone levels may bear groundwater. With the effect of tectonism, these young deposits are overlain by the other basement rock units, which are Cretaceous peridotite (Kmo) and ophiolitic mélangé (Kkzm). These basement rock units show impervious or semi-pervious character, as in Elmalı Formation. However, the discontinuities that result from tectonism may transmit water.

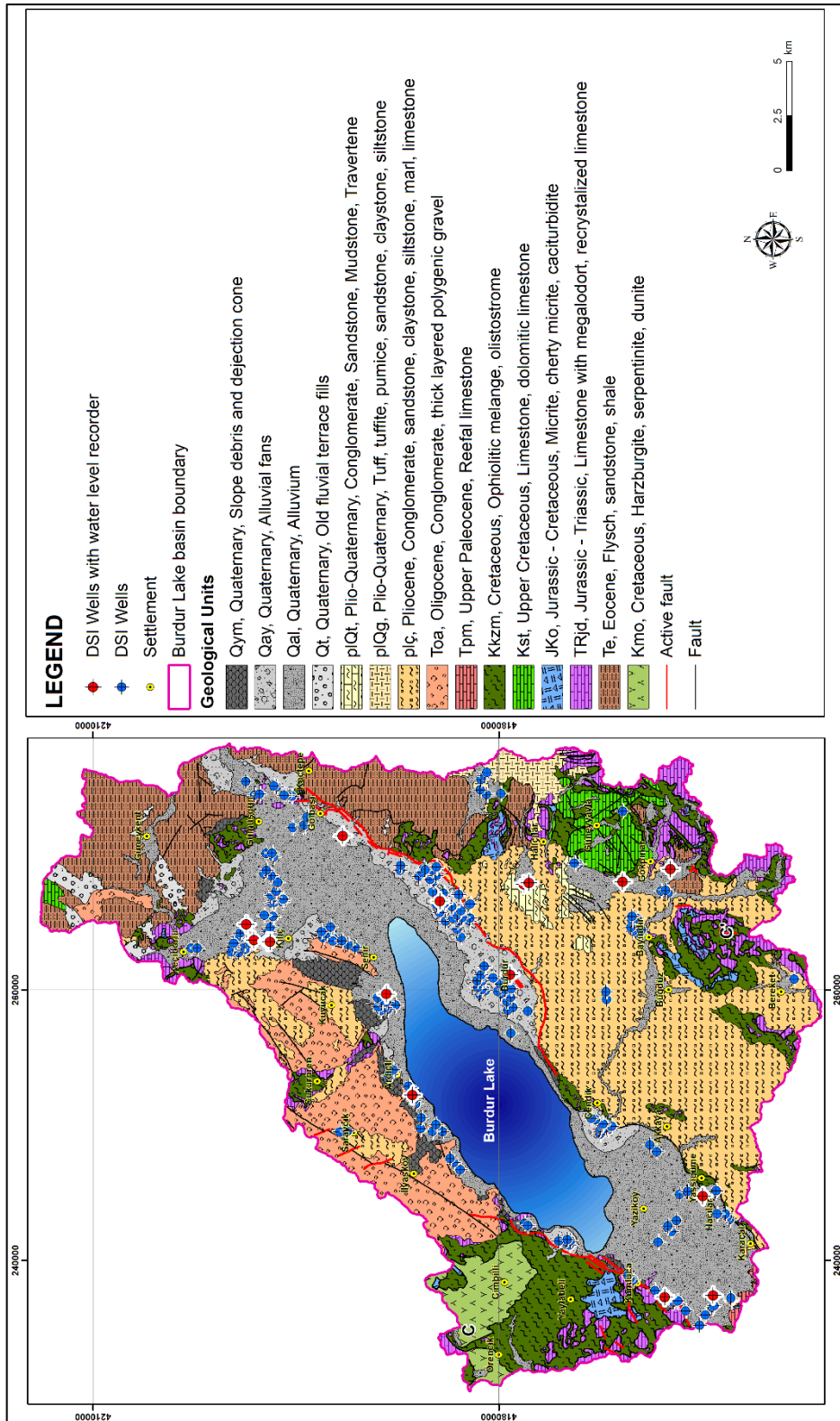


Figure 4.11. Location of the DSI wells drilled within the study area

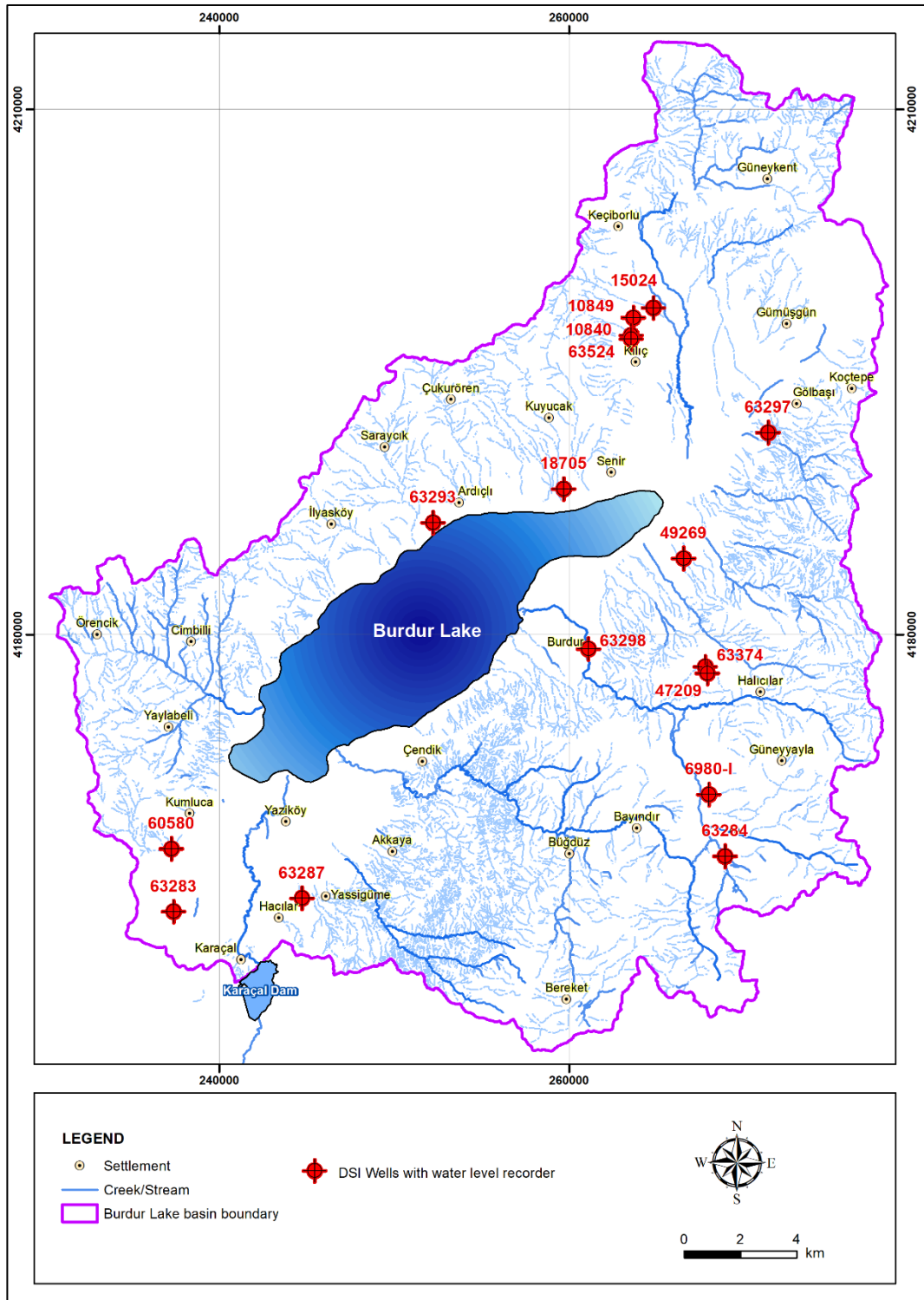


Figure 4.12. Location of the DSI water level recorder installed wells

Karstic Jurassic-Triassic limestone and Upper Cretaceous dolomitic limestone units may also bear groundwater. The average hydraulic conductivity of Cretaceous units is 2.18×10^{-5} m/s (DSI, 2016-a).

Paleocene aged reefal limestone exposes along the southern boundary of the basin. According to the pumping tests conducted in this unit (DSI, 2016-a), limestone is pervious with relatively high conductivity ($K=1 \times 10^{-3}$ m/s). The Oligocene conglomerate (Toa), outcropping at the northwestern part of the study area, overlies Paleocene limestone. According to Price (1991), it has an average thickness of 70 m in the basin. Since this unit is consolidated, poorly sorted, and indurated, it behaves like a semi-pervious unit ($K=2.6 \times 10^{-5}$ m/s)

Pliocene aged plç and Plio-Quaternary aged plQg, plQt units have an approximate thickness of 650 m in the basin that overlies the Oligocene conglomerates (Toa). These units are composed of fine to medium-grained clastic sedimentary rocks. Pliocene plç unit outcrops in the east and western part of the basin, including conglomerate, sandstone, claystone, siltstone, marl, and limestone, whereas Plio-Quaternary units are in the eastern region with the dominant lithologies of tuff-tuffite (plQg), and travertine (plQt). The conglomerate, sandstone, limestone, travertine, and tuff layers may contain groundwater depending on their thickness (Şener et al., 2015). Since distinguishing Pliocene and Plio-Quaternary aged units is difficult in the basin, the hydraulic conductivity was calculated as 1.17×10^{-5} average for these units (DSI, 2016-a).

The Quaternary alluvium consisting of clay, silt, sand, and gravel encompasses the Burdur Lake and reaches 50 m thickness under the lake bottom. The alluvium in the northern part of the lake forms an unconfined aquifer. Because of the clay content, it has low to average hydraulic conductivity values ($K=4 \times 10^{-5}$ m/s) in the southern part of the study area (DSI, 1975).

4.2.1 Groundwater Levels

4.2.1.1 Spatial variations in groundwater levels

In the study area, the static groundwater levels of the wells detected in the field were measured four times in two dry (October 2014 and October 2015) and two wet (April 2015 and April 2016) seasons during the preparation of the DSI Hydrogeological Investigation Report (DSI, 2016-a). In addition to these measurements, the static groundwater levels of DSI wells were measured following the well drilling completion. There are also 16 DSI wells with water level recorders that measure groundwater levels. In the study area, groundwater elevation maps were prepared separately for the periods 1969-1971 and 2014-2016 (Figures 4.13-4.14). The groundwater level measurements in the existing monitoring wells and the elevations of the springs and streams were used to prepare the groundwater elevation maps. Additionally, lake levels of two periods were used to draw the maps. The lake levels were approximately 857 m and 842 m in 1969-1971 and 2014-2016, respectively.

In the groundwater level maps, the groundwater elevations vary from the lake area to the basin boundary as 857 m to 1750 m for 1969-1971 (Figure 4.13), whereas they vary from 842 m to 1750 m for 2014-2016 (Figure 4.14). Since it is a closed basin, the direction of the groundwater flow is towards the Burdur Lake.

When the groundwater level maps of the two periods given in Figures 4.13 and 4.14 are compared, it can be understood that the hydraulic gradients around the lake are increased from 1969 to 2016. Especially in the eastern part of the study area, hydraulic gradients increased in the range of 10-20 times by the effect of the excessive pumping within the same time interval. The groundwater elevation difference between the periods of 1969-1971 and 2014-2016 reaches to about 50 m towards the northwestern part of the study area.

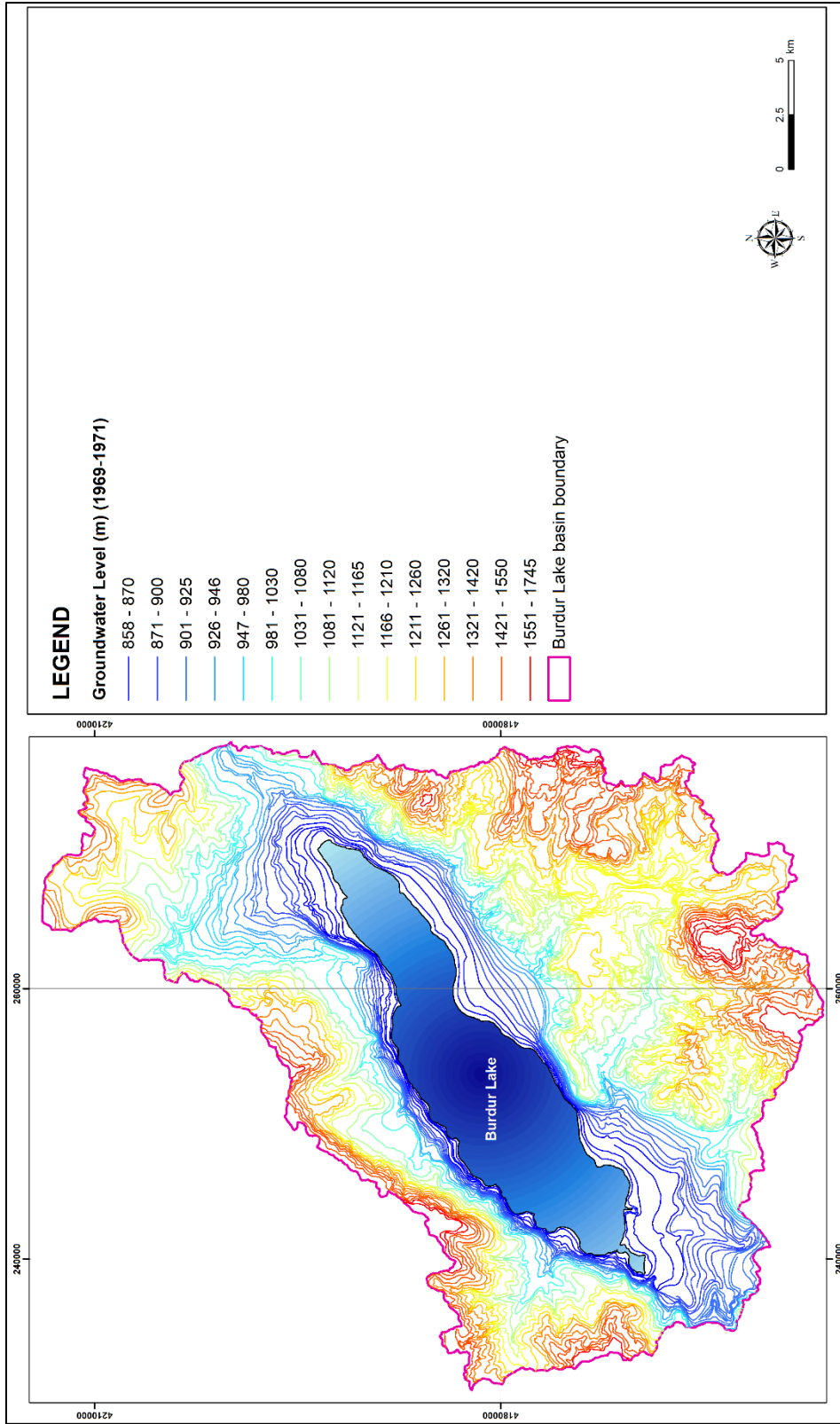


Figure 4.13. Groundwater level map of the area (1969-1971 period)

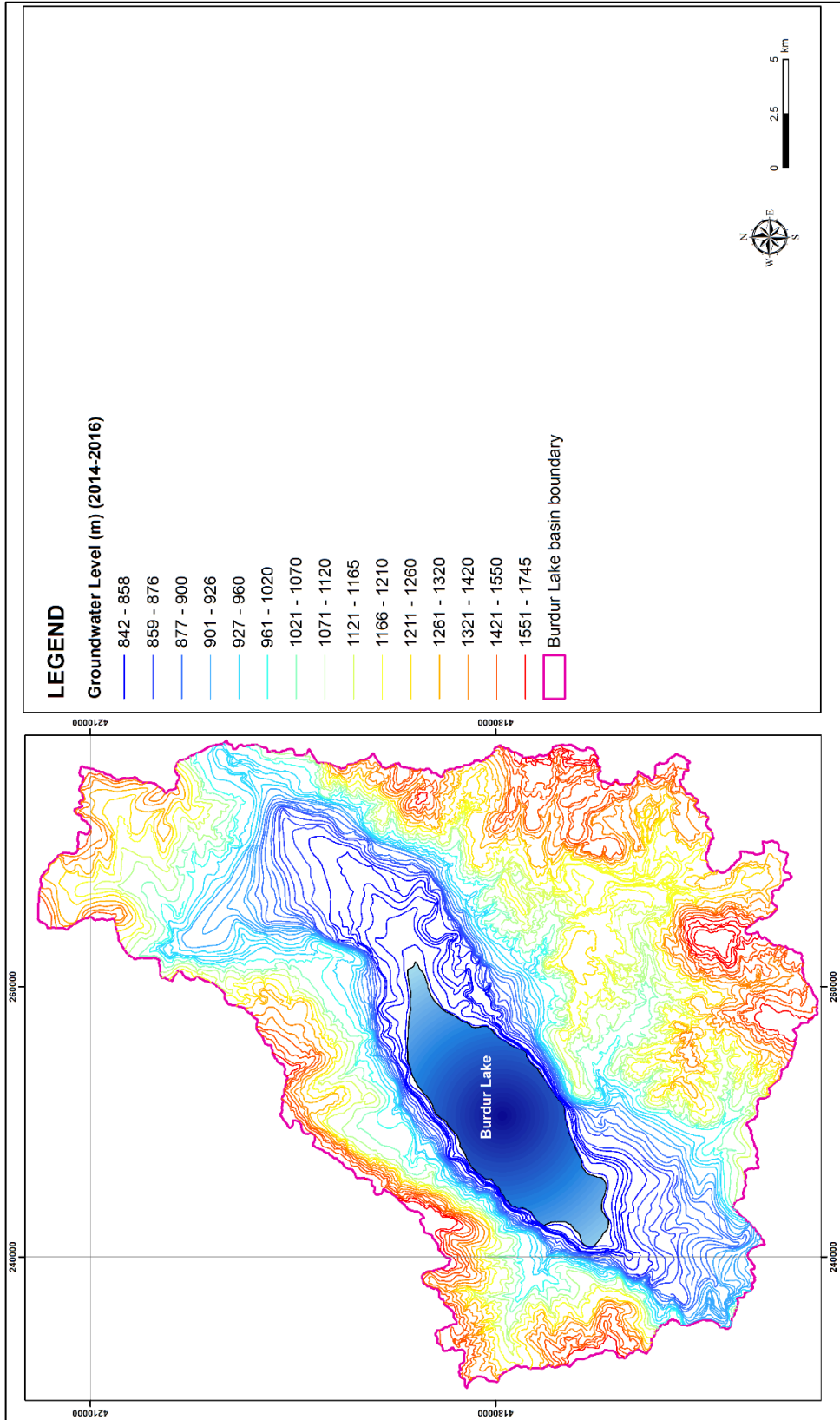


Figure 4.14. Groundwater level map of the area (2014-2016 period)

4.2.1.2 Temporal variations in groundwater levels

DSI installed water level recorders in 16 wells in the study area to take continuous measurements. The locations of these wells are shown in Figure 4.12. Groundwater levels were measured from these wells monthly in varying periods from July 1974 to December 2018. The groundwater levels are always higher than the lake level during the measurement period of these wells.

The wells 6980-I, 15024, 10840, and 18705 have long-term continuous data (Figure 4.15). Among those, 18705, with a data period from March 1976 to December 2018, is the closest well to the lake. According to Figure 4.15, groundwater levels in this well are not conformed with the lake level changes. This situation proves that no lake water outflow to the groundwater from this location takes place during the measurement period (Figure 4.15).

The fluctuations in the groundwater levels in wells 15024 and 10840 are usually caused by seasonal changes. Groundwater levels have decreased in recent years due to the effects of excessive pumping from well 6980-I in İnsuyu and 18705 in the Senir region (Figure 4.15).

Groundwater levels were measured only for a short period of time (usually after October 2015) from the wells given in Figure 4.16. Although the effect of the lake level decrease on the groundwater levels can not be determined reliably from the measurement of these wells, seasonal changes are generally observed. The groundwater level measurements at wells 60580, 63297, 63374, 63524, and 63293 also reflect the effect of increasing pumping in the basin in recent years (Figure 4.16).

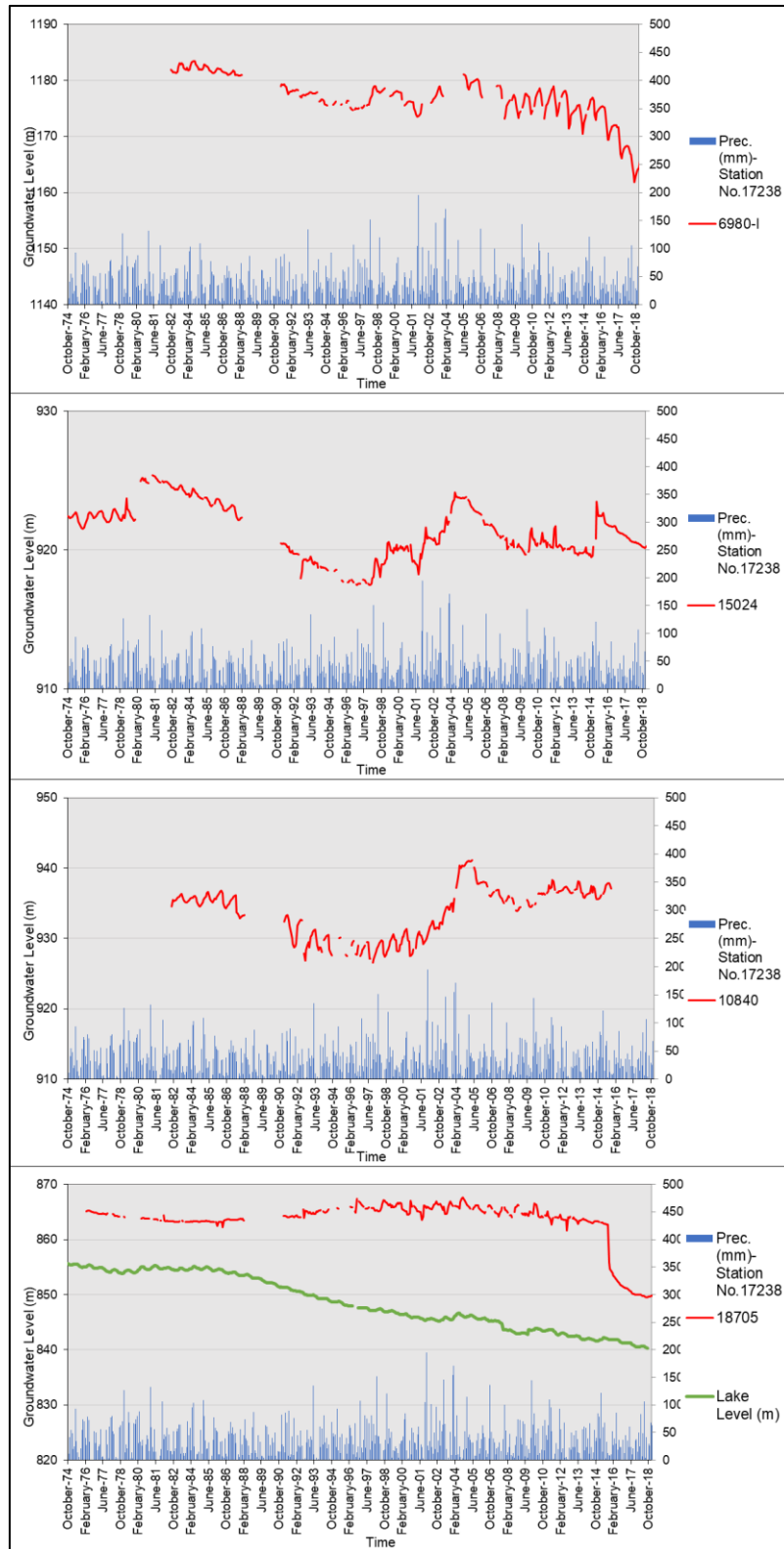


Figure 4.15. Long term continuous groundwater level measurements

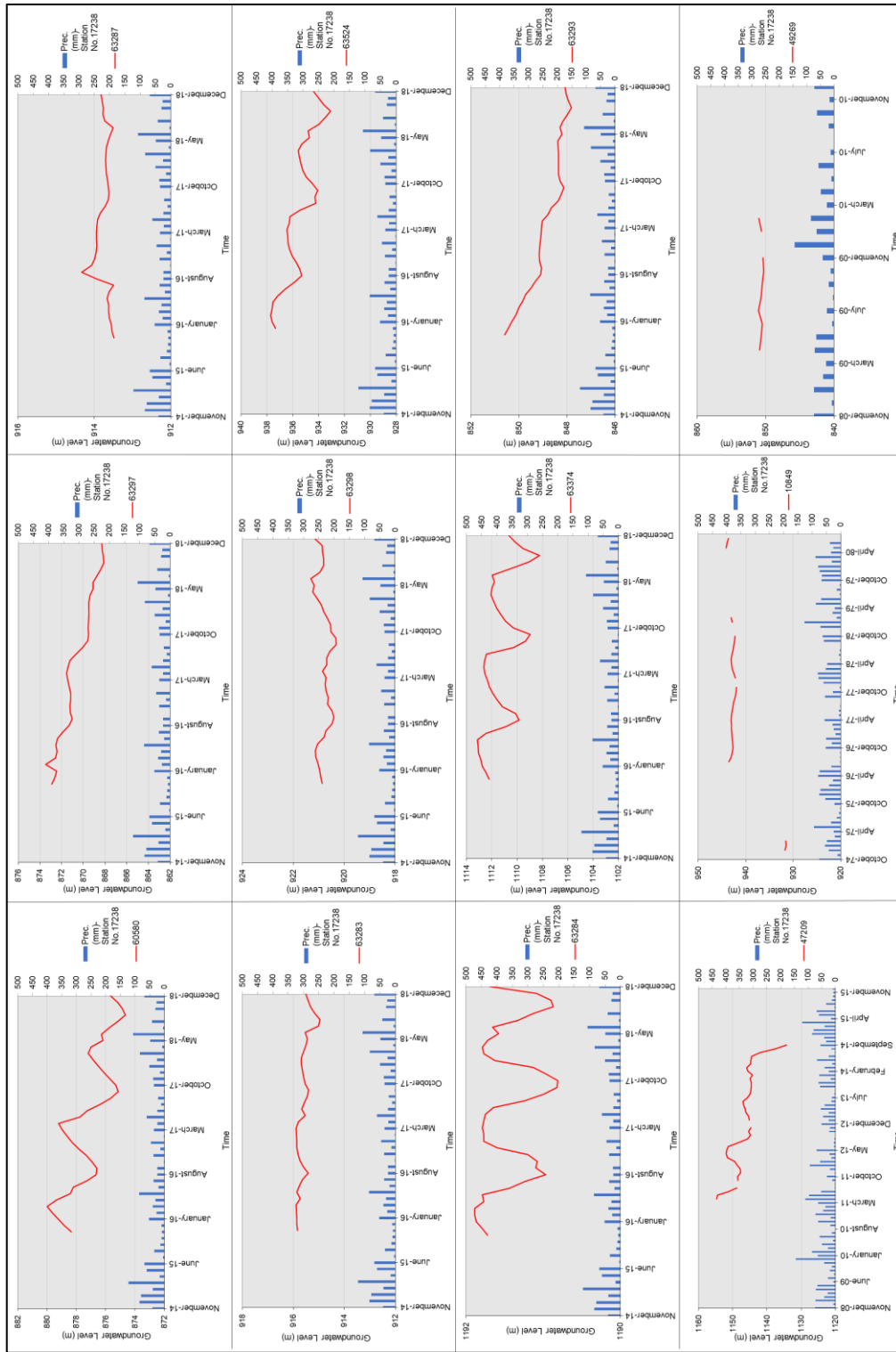


Figure 4.16. Short term continuous groundwater level measurements

CHAPTER 5

CONCEPTUAL MODEL

The conceptual model, the precise consolidation of all goal-relevant information, provides the foundation for the development of numerical models. It involves the identification of the geological units and their hydrogeological characters, deciding the flow system with appropriate boundary conditions, and estimating sources and sinks.

The main concern in the Burdur Lake basin is quantifying the relationship between groundwater and lake water. Therefore, the conceptual model of the study area is developed with a conceptual lake budget considering this relationship. The development of the conceptual groundwater budget can not be realized due to the lack of data about groundwater usage. However, the conceptual hydrologic budget of the study area is explained below in detail.

5.1 Conceptual Model of the Study Area

The Quaternary alluvium unit consists of clay, silt, sand, and gravel and can be defined as the main aquifer in the study area. This unconfined character unit has a limited extent and thickness around and bottom of the lake area. It is surrounded by basement rock units in the basin and overlies the low-permeable Pliocene units (Figure 3.14). Although basement rock units show impervious character in the study area, the Jurassic-Triassic limestone, which has outcrops in the southeastern and southwestern parts of the study area, can be defined as an unconfined aquifer. Upper Cretaceous dolomitic limestone, exposed in the eastern part of the study area, also has an unconfined karstic character.

In the basin, the alluvium aquifer is recharged from direct precipitation and lateral groundwater inflow across the southern boundary of the study area. It discharges to the streams and Burdur Lake. The groundwater flow from the alluvium to Pliocene units is another discharge component of the alluvium aquifer.

Karstic limestone and dolomitic limestone units are recharged directly from precipitation and discharged by the springs. Dolomitic limestone is also discharged to the İnsuyu Cave spring. Since this unit extends out of the basin in the east, there is a lateral groundwater flow from this part of the study area.

In the study area, groundwater level maps were prepared separately for 1969-1971 and 2014-2016, showing that the groundwater flow is towards the lake for both periods. (Figure 4.13-4.14).

5.2 Conceptual Hydrologic Budget

Precipitation reaching the basin is transformed into runoff, infiltration, and evapotranspiration components. The ratio of these components to precipitation is calculated using long-term monthly average meteorological data in water budget calculations. The Thornthwaite method was used to calculate potential evapotranspiration, while the Curve Number method was used to calculate surface runoff. The remaining portion of precipitation was assumed to infiltrate into groundwater.

The latitude of the basin, long-term monthly mean temperature, and total precipitation values of the Burdur Meteorological station were used in the Thornthwaite method (1948). The monthly uncorrected potential evaporation (UPET) was calculated by Thornthwaite methods using the formulas given below:

$$UPET_m = 16x \left(\frac{10t_m}{I} \right)^a \quad (Eq. 5.1)$$

$$a = (675x10^{-9})I^3 - (771x10^{-7})I^2 + (179x10^{-4})I + 0.492 \quad (Eq. 5.2)$$

$$i = \sum_{i=1}^{12} \left(\frac{t_i}{5} \right)^{1.514} \quad (Eq. 5.3)$$

where:

m: month index

t: mean monthly temperature ($^{\circ}C$)

I: annual heat index (equals to the sum of monthly heat indices(*i*))

a: coefficient that depends on the heat index

The surface runoff values were calculated using the Curve Number (CN) method developed by U.S. Soil Conservation Service (SCS, 1964). This calculation was conducted based on: (i) direct runoff (or excess rainfall), P_e , is less than or equal to total precipitation (P); (ii) soil moisture retention occurring after runoff begins (F_a) is less than or equal to the potential soil moisture retention (S). Runoff is not observed until precipitation reaches a specific value (I_a , initial abstraction). Thus, potential runoff is equal to $P - I_a$. The ratio of two real and two potential values mentioned above are equal in the CN method. Direct runoff (or excess rainfall, P_e) can be calculated by applying the continuity principle ($P = P_e + I_a + F_a$):

$$P_e = \frac{(P-I_a)^2}{P-I_a+S} \quad (Eq. 5.4)$$

For small watersheds, since $I_a = 0.2xS$, the generalized form of the CN method is calculated as:

$$P_e = \frac{(P-0.2S)^2}{P+0.8S} \quad (Eq. 5.5)$$

The Curve number is derived from curves drawn based on the P and P_e relationship obtained from many basins. CN is related to potential soil moisture retention by $CN=1000/(S+10)$ or $S(in)=1000/(CN-10)$. Hence, runoff curve numbers represent

the runoff potential from a hydrologic soil-cover complex during periods when the soil is not frozen. A higher CN corresponds to a higher runoff potential.

In the Burdur Lake Basin, the Curve Number (CN) was calculated from the 250 m grid size GCN250 dataset (Jaafar et al., 2019). The CN of the study area ranges between 72 and 94, excluding Burdur Lake (Figure 5.1). The area-weighted average CN is 76.

For each month, the long-term conceptual hydrologic water budget components were calculated using the CN of the study area, potential evapotranspiration was calculated using the Thornthwaite method, and the long-term mean monthly precipitation (Table 5.1).

The monthly potential evapotranspiration values were calculated by correcting the UPET value with coefficient r , obtained from the basin latitude (38°). Surface runoff was calculated using monthly precipitation and the CN (CN=76). Infiltration equals the difference between monthly precipitation and runoff. The soil moisture capacity was assumed to be 100 mm, and a change in soil moisture was calculated for each month. Actual evapotranspiration, surface runoff, and groundwater recharge values were estimated based on these calculations.

According to water budget calculations, the average annual groundwater recharge from direct precipitation is 25.7 mm, corresponding to 6% of total annual precipitation (Table 5.2).

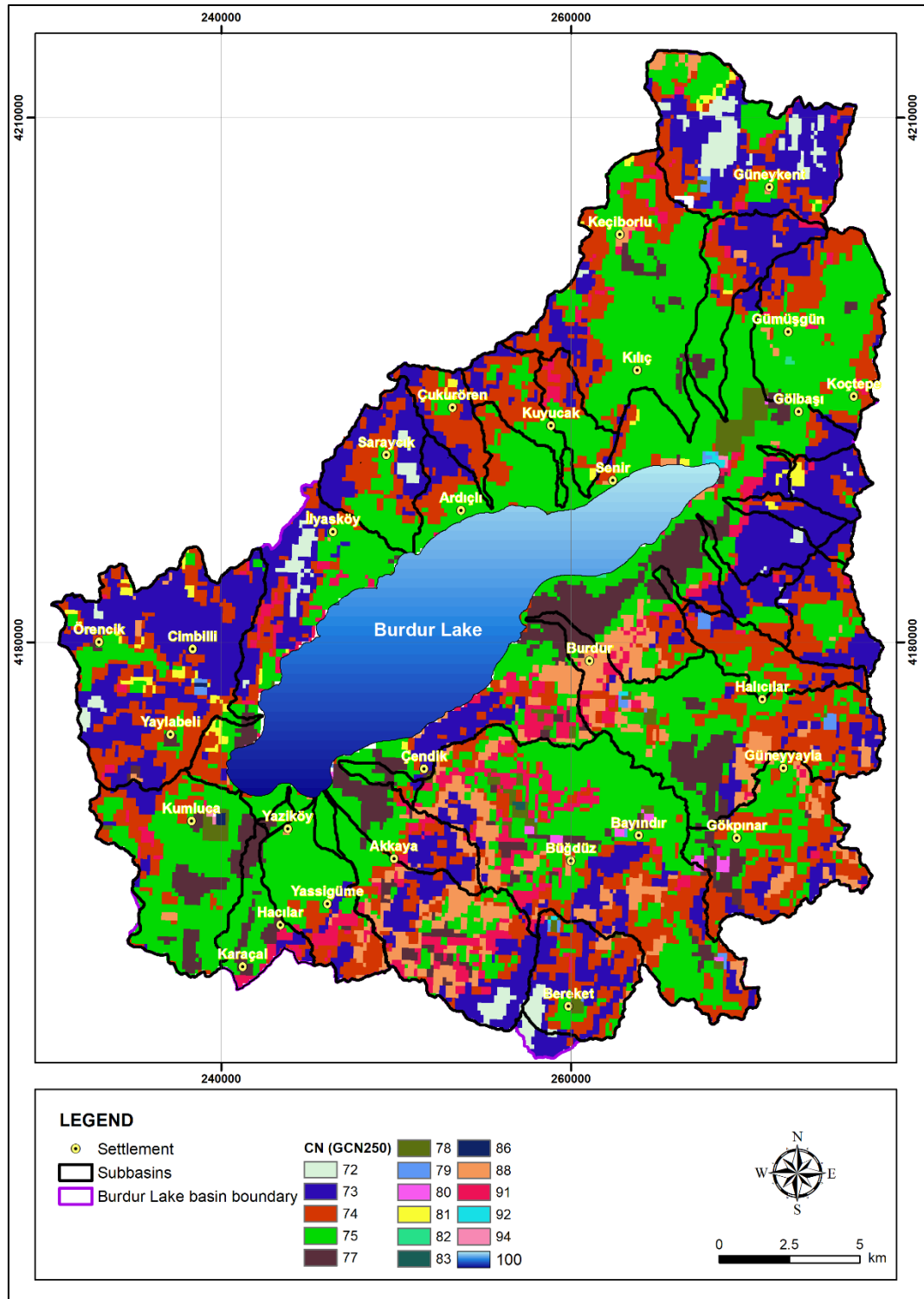


Figure 5.1. Spatial distribution of curve number in the study area

Table 5.1.1. Monthly conceptual water budget results

Parameter	Jan	Feb	Mar	Apr	May	Jun	Jul	Aug	Sep	Oct	Nov	Dec	TOTAL	Ratio to prec.(%)
Mean Monthly Temperature (°C)	2.5	3.8	7.2	11.6	16.4	21.1	24.6	24.5	20.2	14.4	8.3	3.9		
i	0.35	0.66	1.73	3.55	6.02	8.82	11.19	11.06	8.27	4.94	2.17	0.69	59.4	
a:	1.4	1.4	1.4	1.4	1.4	1.4	1.4	1.4	1.4	1.4	1.4	1.4	17.1	
UPET	4.60	8.44	20.98	41.24	67.81	97.06	121.42	120.13	91.42	56.23	25.93	8.81	664.1	
PET	3.95	7.09	21.61	45.36	82.72	119.38	151.78	140.55	94.16	54.55	22.04	7.31	750.5	
r	0.86	0.84	1.03	1.10	1.22	1.23	1.25	1.17	1.03	0.97	0.85	0.83		
Precipitation (mm)	51.7	39.4	45.5	47.1	43.4	27.1	15.1	10.1	15.9	35.2	37.8	53.4	421.8	
Surface runoff coefficient	1	1	1	1	1	1	0	0	0	1	1	1		
Surface runoff (mm)	11.00	5.28	7.89	8.68	6.94	1.34	0.00	0.00	0.00	3.70	4.64	11.86		
Infiltration (l)	40.75	34.15	37.56	38.44	36.42	25.77	15.07	10.14	15.95	31.51	33.15	41.52		
I-PET	36.79	27.06	15.95	-6.92	-46.30	-93.61	-136.71	-130.41	-78.21	-23.04	11.11	34.21		
TOTAL (P-PET)	0.00	0.00	0.00	-6.92	-53.22	-146.83	-283.54	-413.95	-492.16	-515.20	0.00	0.00		
Soil moisture	100.00	100.00	100.00	93.31	58.73	23.03	5.87	1.59	0.73	0.58	11.69	45.90		
Change in soil moisture	36.79	17.31	0.00	-6.69	-34.58	-35.70	-17.16	-4.28	-0.86	-0.15	11.11	34.21		
AET	3.95	7.09	21.61	45.13	71.00	61.47	32.23	14.42	16.81	31.66	22.04	7.31	334.7	79%
Excess precipitation (I-AET)	11.00	15.03	23.84	8.68	6.94	1.34	0.00	0.00	0.00	3.70	4.64	11.86	87.0	
Surface runoff	11.00	5.28	7.89	8.68	6.94	1.34	0.00	0.00	0.00	3.70	4.64	11.86	61.3	15%
Groundwater recharge	0.00	9.75	15.95	0.00	0.00	0.00	0.00	0.00	0.00	0.00	0.00	0.00	25.7	6%
												TOTAL	421.8	100%

Table 5.2 Annual water budget results

Hydrologic Component	Amount (mm/year)	Ratio to Precipitation (%)
Precipitation	421.8	100
Evapotranspiration	334.7	79
Surface Runoff	61.3	15
Groundwater Recharge	25.7	6

5.3 Conceptual Lake Budget

The development of the conceptual lake budget is necessary to determine the interaction between hydrological system components and the lake. The fluxes of water to and from lakes with regard to each of these components represent the water budget of a lake:

$$\text{Inflow} - \text{Outflow} = \pm \Delta S \quad (\text{Eq. 5.6})$$

According to Eq. 5.6, the difference between the inflow and outflow components is a function of the changes in storage (ΔS). The lake gains water from: (1) the atmosphere by precipitation directly on the surface of the lake, (2) surface water by streamflow to the lake, and (3) groundwater by seepage into the lake, and it loses water to: (1) the atmosphere, by evaporation directly from the surface, (2) surface water, by streamflow from the lake, and (3) groundwater, by seepage from the lake. For any given time period, the imbalance between these gains and losses results in a change in storage reflected by the change in lake level (Lerman et al., 1995).

Mathematically, the calculation of the lake budget is straightforward, as in Eq. 5.6. but, in practice, measuring the water fluxes to and from lakes is not simple since the ability to measure the various hydrological components are limited. In this study, Burdur Lake budget components were determined monthly and yearly within the

period of January 1969 to December 2018 by available data and several approaches for the ungauged components. Storage changes in the lake were estimated from the stage-volume curve, while precipitation on the lake surface and evaporation from the lake surface were determined using available climate data. In the study area, there is no streamflow from the lake. Although there is streamflow into the lake, their flow rates are either ungauged or measured for a certain period of time. Thus, this component was estimated for the ungauged periods and basins by the drainage area ratio method and a 2-D surface water model. Finally, since there is no measurement for the groundwater fluxes, this component was calculated from the imbalance between the change in storage and inflows-outflows.

5.3.1 Change in Storage

The Burdur Lake levels were measured monthly by DSI between January 1969 and December 2018 (Figure 5.2). For each month, the lake volume corresponding to the lake level was estimated from the stage volume curve in Figure 4.3. Then, the lake volumes in the consecutive months were subtracted from each other to calculate the monthly change in storage values. The results are provided in Figure 5.2. The change in lake storage is also high when the monthly lake level changes are high in consecutive months, such as March-April 1980, January-February 2004, and September-October 2011 (Figure 5.2).

5.3.2 Precipitation Over the Lake Surface

Precipitation is one of the significant inflow components of the lake budget. Since the DSI Yazıköy meteorological station is located in the southern part of the Burdur Lake (~2.5 km) at an elevation of 865 m, nearly the same as the average lake level (average 850 m), monthly precipitation measurements of this station were used to determine the precipitation over the lake surface.

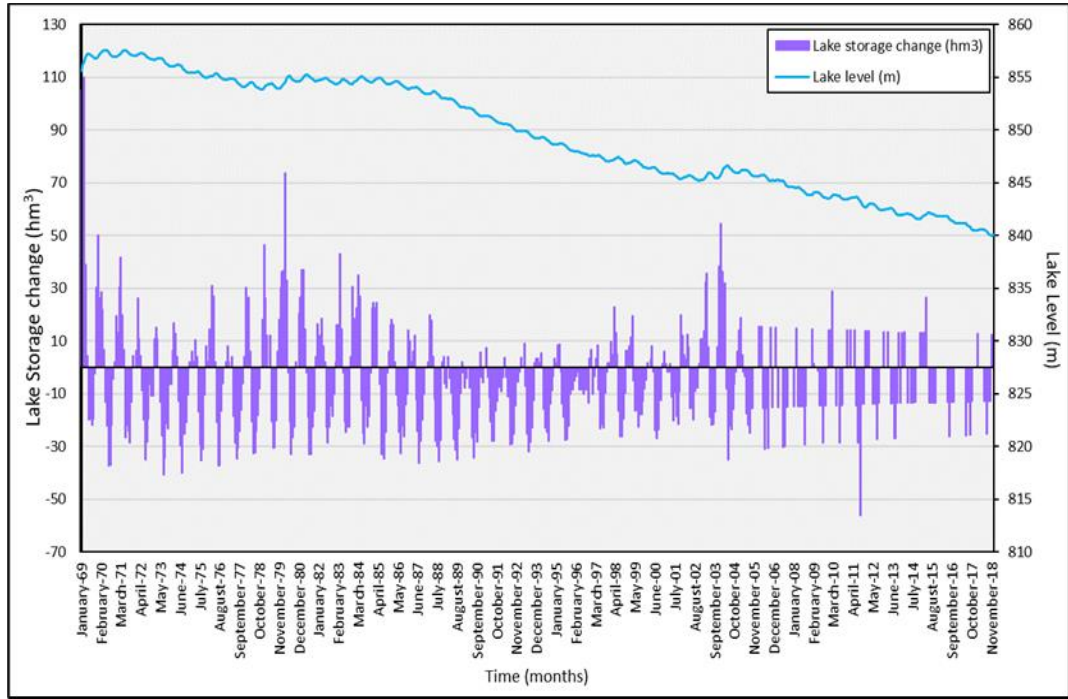


Figure 5.2. Burdur Lake volume changes between January 1969-December 2018

For each month between January 1969 and December 2018, the water volume due to precipitation (V_P) was calculated by:

$$V_P = A P \quad (\text{Eq. 5.7})$$

where:

A : average lake area during the month

P : precipitation in mm/month

The calculated volumes of precipitated water over the lake surface and dry-wet seasons based on the Yazıköy station are shown in Figure 5.3. The average water volume from the mean annual 361.7 mm precipitation was calculated as 5.3 hm³ and this volume decreased drastically after 2011 with decreasing lake surface area in the dry season.

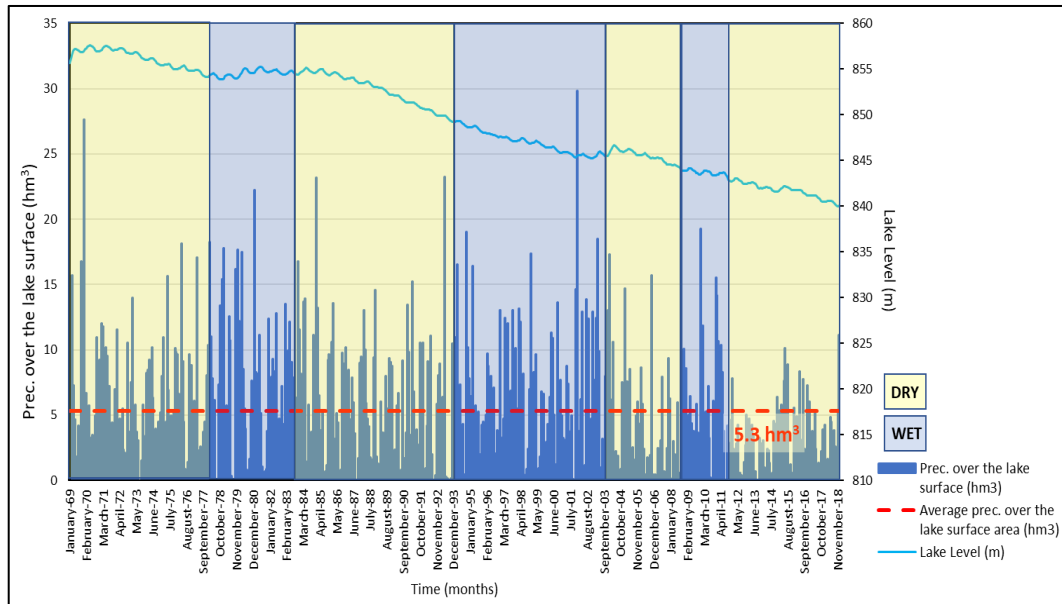


Figure 5.3. The monthly volume of precipitated water over the Burdur Lake

5.3.3 Evaporation From the Lake Surface

Evaporation is one of the primary water loss components of the lake budget. In the study area, this component was not directly measured. Therefore, climatic variables such as air temperature and evaporation, water temperature, wind velocity, and absolute humidity of the air above the lake surface were used to determine evaporation as accurately as possible. The pan evaporation method in the months with air evaporation measured and the Meyer empirical formula approach in the non-measured months were used to estimate evaporation from the lake surface.

In the Burdur Lake basin, air evaporation measurements were taken at DSI Yazıköy stations only in the months covered from April to October between 1970-2005 (Figure 3.10). For this season, the evaporation from the lake surface was calculated by:

$$E = E_{pm} C_p \quad (\text{Eq. 5.8})$$

where:

E_{pm} : pan evaporation

C_p : pan coefficient

The General Directorate of State Hydraulic Works (DSI) suggests an annual pan factor (C_p) between 0.6-0.8 for Turkey. Since the evaporation pan approach was applied when evaporation is maximum for the Burdur Lake basin, the pan coefficient (C_p) between April and October was taken as 0.8.

Although evaporation from the lake surfaces decreases between November-March, it also occurs. However, no measurement was taken for this period. Therefore, Meyer's formula was used in this study to estimate the evaporation from the lake surface for the months without measurement. Evaporation rates were calculated daily between November-March 1969 and 2018. According to Meyer's formula (Meyer,1915), lake evaporation in mm/day is:

$$E = K_M(e_w - e_a)\left(1 + \frac{u_9}{16}\right) \quad (\text{Eq. 5.9})$$

where:

K_M : coefficient accounting for various other factors with a value of 0.36 for lakes

e_w : saturated vapor pressure at the water surface temperature

e_a : actual vapor pressure of overlying air at a specified height

u_9 : wind velocity at about 9 m above the water surface

Daily temperature, wind velocity, and relative humidity data of the Burdur station (station no: 17238) were taken from MGM to apply Meyer's formula for a period between 1969-2018. Since the elevation of this station (960 m) is higher than the average lake level (850 m), the temperature was assumed to decrease linearly with elevation, using the free-air moist adiabatic lapse rate of 0.0065 °C/m. Hence, the

daily mean temperature (T_p) measurements of Burdur station were corrected based on the elevation by using the given equation:

$$T_p = T - T_i x (H_i - H_0) \quad (\text{Eq. 5.10})$$

where:

T : daily average temperature of the station

H_i : the average elevation of the lake

H_0 : the height of the meteorological station

T_i : lapse rate ($0.0065 \text{ } ^\circ\text{C/m}$)

In Meyer's formula, u_9 is the wind velocity 9 m above the water surface. However, daily wind velocity measurements of the Burdur station were taken 10 m above the ground surface. Therefore, the equation given below was used to estimate daily wind velocity 9 m above the lake area:

$$u_9 = u \left[\frac{z_9}{z} \right]^{1/7} \quad (\text{Eq. 5.11})$$

where:

u : wind velocity at about 10 m above the ground surface that the station located

z : the height of the meteorological station

z_9 : the average elevation of the lake

The saturation vapor pressure at the water surface temperature (e_w) is another parameter in Meyer's formula. It depends on temperature and can be calculated using daily corrected temperature values of Burdur station by:

$$e_w = 4.584 \exp \left(\frac{17.27t}{237.3+t} \right) \quad (\text{Eq. 5.12})$$

where:

e_w : saturation vapor pressure at the water surface temperature in mm of Hg

t : temperature in $^\circ\text{C}$

The actual vapor pressure of air at a specified height (e_a) has a relation with e_w depending on the relative humidity:

$$e_a = R_h e_w \quad (\text{Eq. 5.13})$$

where:

R_h : Relative humidity

The daily actual vapor pressure (e_a) values were calculated using the daily relative humidity measurements of the Burdur station by Eq. 5.13. After all the parameters in Eq. 5.9 were calculated separately, the Meyer formula was applied to estimate the daily evaporation rates from the lake. Finally, results were converted to a monthly basis.

The estimated monthly evaporation values using the pan evaporation method (April-October 1970-2005) and the Meyer empirical formula (November-March 1969, 2006-2018) were provided in Figure 5.4. The annual mean evaporation is 1278 mm for the whole period. Although between 2006-2018, higher evaporation rates of the summer months can be considered an overestimation, it can be the effect of the increasing temperatures. The annual mean temperature of Burdur station is 12.9 °C between 1969-2005, while it is 14 °C for 2006-2018. Besides, since the evaporation estimation for 1969 with the Meyer formula is conformable with the pan evaporation method results around this year, the estimation was assumed successful.

After the monthly evaporation rates were estimated for the period between January 1969 and December 2018, the monthly volume of water lost from the evaporation (V_E) was calculated by:

$$V_E = AE \quad (\text{Eq. 5.14})$$

where:

A : average lake area during the month

E : evaporation in mm/month

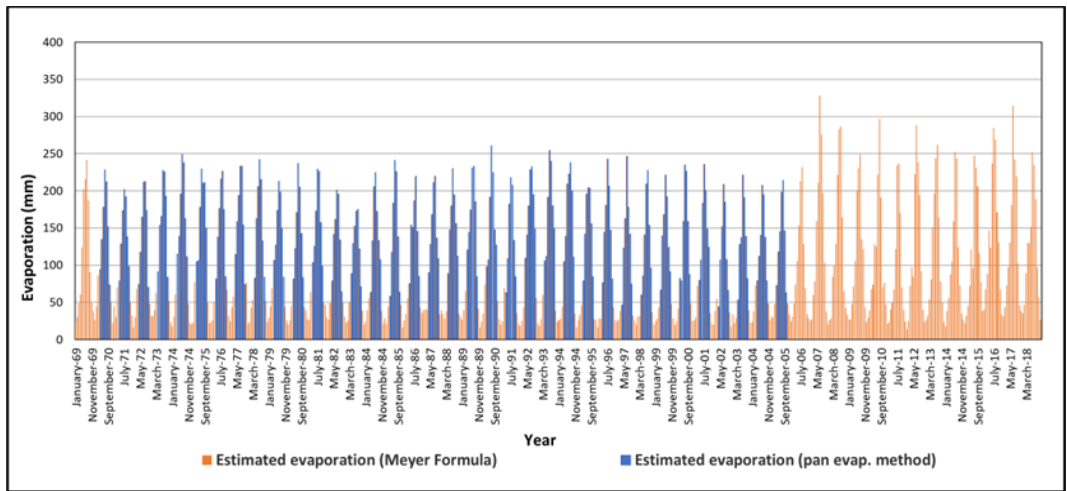


Figure 5.4. The monthly estimated evaporation from Burdur Lake surface

The results are shown in Figure 5.5. The average water volume loss from the mean annual 1278 mm evaporation was estimated 18.8 hm³ for Burdur Lake. Although evaporation rates were estimated higher for the years after 2005, the volume of water lost by evaporation decreases over time due to decreasing lake surface area.

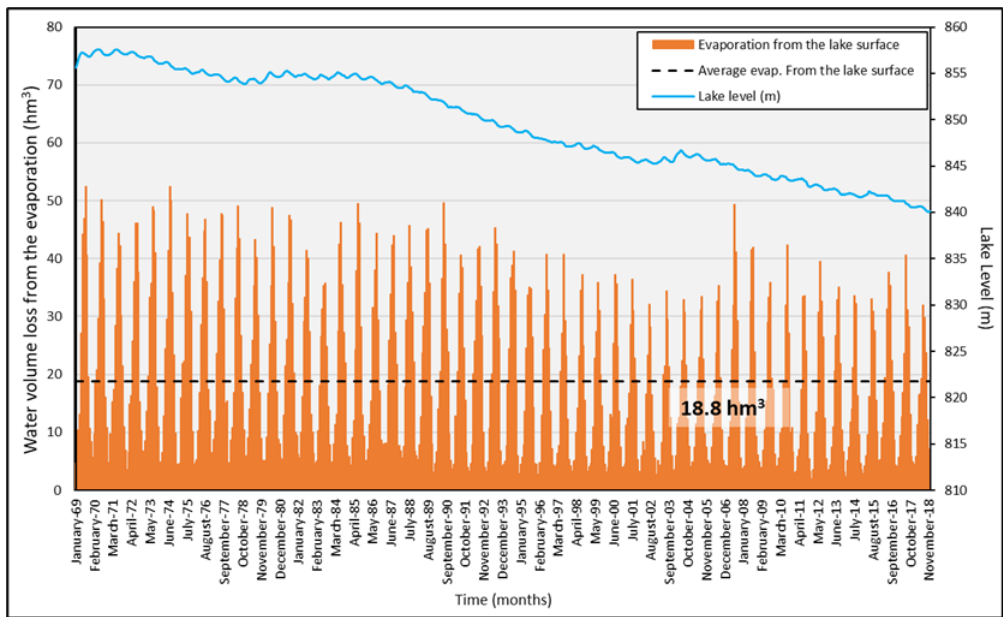


Figure 5.5. The monthly water volume loss from the evaporation

5.3.4 Surface Water Inflow

Surface water inflow, characterized by perennial and ephemeral stream flows, is another lake inflow component of the Burdur Lake budget. In this study, quantifying this component is challenging due to the lack of continuously measured data.

The surface water inflow in the Burdur Lake basin was calculated for the subbasins given in Figure 5.6. In the study area, there are only two gauged basins. Flow measurements were taken only for two main streams, Bozçay and Büğdüz, while the other basins were ungauged. The measurements of these streams were not taken for the whole study period from January 1969 to December 2018. Therefore, the flows to the lake from Bozçay and Büğdüz streams were estimated from January 1969 to December 2018 by applying the drainage area ratio method for the missing periods.

A 2-D surface flow model was developed for the Burdur Lake basin using HEC-HMS (The Hydrologic Modeling System) to predict surface water inflows from all the ungauged basins to the lake between January 1969-December 2018 (Figure 5.6). However, in addition to the lack of measurement, cutting streamflow to the lake by human activities is another constraint while estimating the surface water inflow component. The flow of the streams in the eastern and western parts of the lake was cut by roads, and there is no flow to the lake from the regions of Burdur city settlement, and airport (white colored basins in Figure 5.6). Moreover, nine ponds are in operation on streams and creeks in the study area (Figure 5.6). For each pond basin (green-colored basin in Figure 5.6), inflows were estimated with the HEC-HMS model. However, it is assumed that there is no flow from these basins to the lake after the construction year of each pond. The inflows from the northern subbasins (shown in pink in Figure 5.6) were cut after the construction of Isparta Süleyman Demirel Airport in 1993. Although Çukurharman was a significant stream feeding the lake from the northern part of the basin, it could not reach the Burdur Lake after it was drained into a canal to dewater the airport area. This shallow part of the lake dried up after dewatering, and the northern basins could not reach the lake.

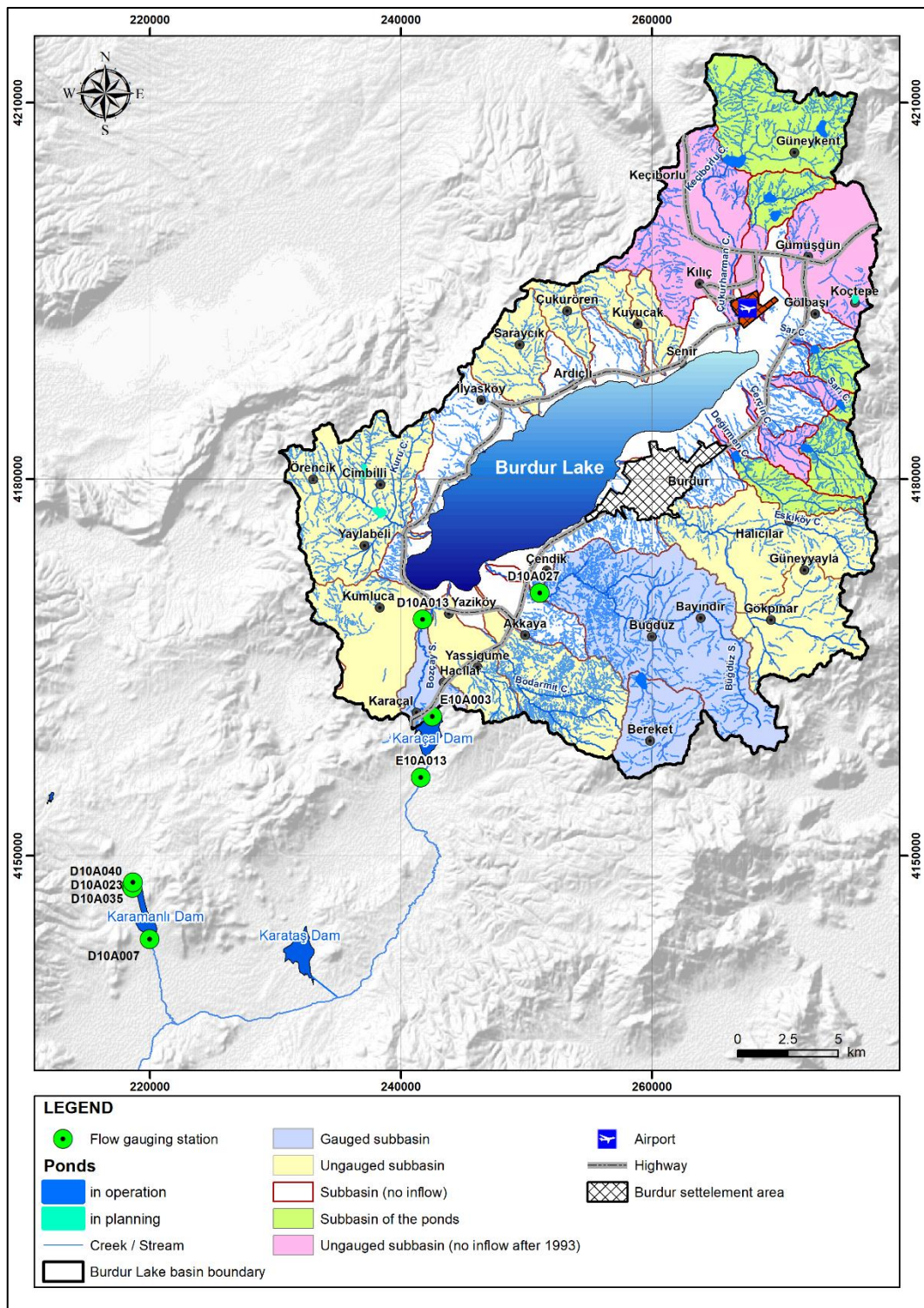


Figure 5.6. The subbasins of the Burdur Lake basin

Thus, it is assumed that there was no inflow to the lake from these northern basins after 1993 (Figure 5.6). After calculating the predicted inflows from the ungauged basins by HEC-HMS models, these corrections were conducted manually.

In order to estimate inflows from the Bozçay Stream to the lake, flow measurements of station D10A013 were used (Figure 5.6). The data period of the station is between 1969-1988, 1991-1992, 1995-2009, and 2012-2018. The missing data of station D10A013 (drainage area:1571.3 km²) between 1988-1990 and 1992-1994 were completed by the drainage area ratio method using station E10A003 (drainage area:1541.6 km²), whereas, for 2009-2011, station E10A013 (drainage area of 1336.9 km²) was used. The estimated flows of the missing periods and measured flows for the Bozçay Stream are presented in Figure 5.7.

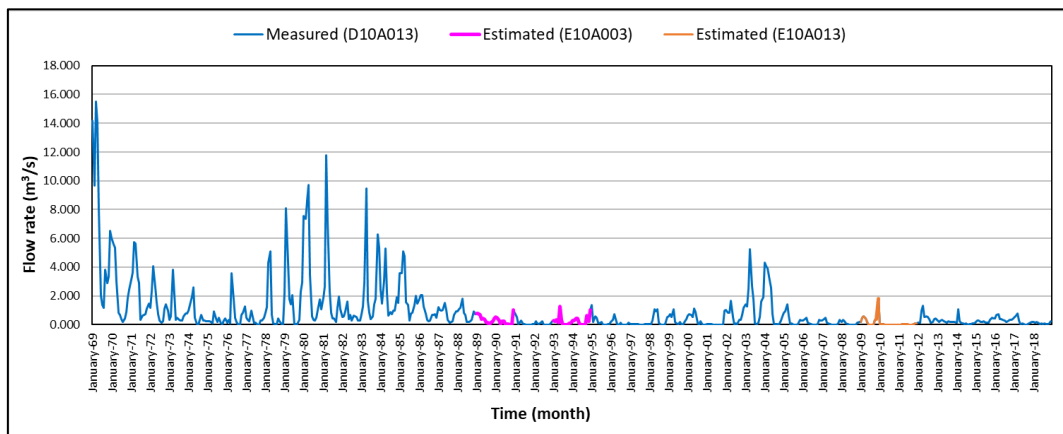


Figure 5.7. The estimated flows of the missing periods and measured flows (D10A013) for the Bozçay Stream

In addition to Bozçay Stream, the inflows from the Büğdüz Stream to the lake were estimated by the flow measurements of station D10A027 (Figure 5.6). However, this station has measurements from 1979 to 2018. Since the flow gauging stations around Karaçal Dam are located downstream of the Karamanlı and Karataş dams, the measurements between 1974-1978 were under the effect of dam storage. Therefore,

to estimate the missing data of the first ten years of the study period, 1969-1979, flow gauging stations around Karamanlı Dam were used to apply the drainage area ratio method (Figure 5.6). For this purpose, this method was first applied for stations D10A007 (drainage area:163.4 km²), D10A023 (drainage area:114.17 km²), D10A035 (drainage area:83.6 km²), and D10A040 (drainage area:110.36 km²). After the operational periods of the other stations were completed, only D10A040 continued to take measurements. Since the stations D10A023, D10A035 and D10A040 are located upstream of the Karamanlı Dam and the data period of downstream station (D10A007) is between 1969-1974 (before the construction of Karamanlı Dam), a complete flow dataset representing the natural flow conditions, were created from 1969 to 2018 at the location of station D10A040 (Figure 5.8). Subsequently, the drainage area ratio method was applied between D10040 and D10A027 (drainage area:214.3 km²) to predict the flow amounts of Büğdüz Stream for 1969-1979. The estimated flows of the missing periods and measured flows for the Büğdüz Stream are presented in Figure 5.9.

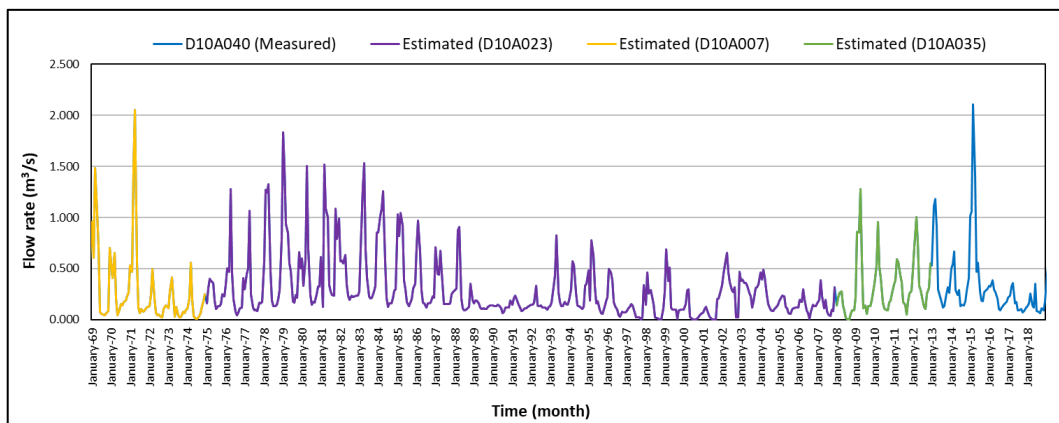


Figure 5.8. The estimated flows of the missing periods and measured flows (D10A040) for the Bozçay Stream

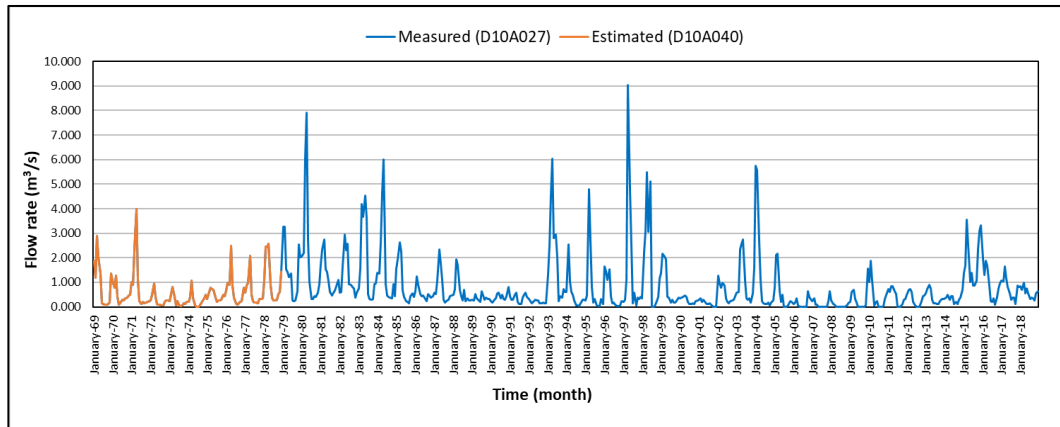


Figure 5.9. The estimated flows of the missing periods and measured flows (D10A027) for the Büğdüz Stream

After calculating the inflows from the Bozçay, and Büğdüz streams by using the drainage area ratio method, inflows from ungauged basins were calculated by the HEC-HMS model. HEC-HMS is a physically-based semi-distributed 2-D model created by the U.S. Army Corps of Engineers in 1998 to simulate rainfall-runoff processes of watershed systems (USACE, 2018). This software is used as a decision support tool in event-based short-term and continuous long-term hydrological processes analysis. In this study, a continuous model was developed to estimate the streamflow inflows from the ungauged watersheds for daily time steps.

HEC-HMS model development can be simplified into four main components: basin model, meteorological model, data input, and control specifications (USACE, 2018). The basin model describes physical basin characteristics and represents rainfall-runoff processes such as loss, transform, baseflow, and routing methods. The meteorological model simulates precipitation, evapotranspiration, and snowmelt events. The third component is data input which includes required time series and gridded or paired data. The control specification is the last component used to control simulations for the given time interval.

In this study, spatial data of the model were prepared using the preprocessing HEC-GeoHMS tool. HEC-GeoHMS, an extension of Arc GIS software, was developed by

the United States Army Corps of Engineers (USACE) in partnership with the Environmental System Research Institute (USACE, 2013). Stream networks and interconnected subbasins were derived with the help of this tool only for watersheds of streams that can reach Burdur Lake (Figure 5.10). The total model area covers 1123 km² and includes 26 subbasins.

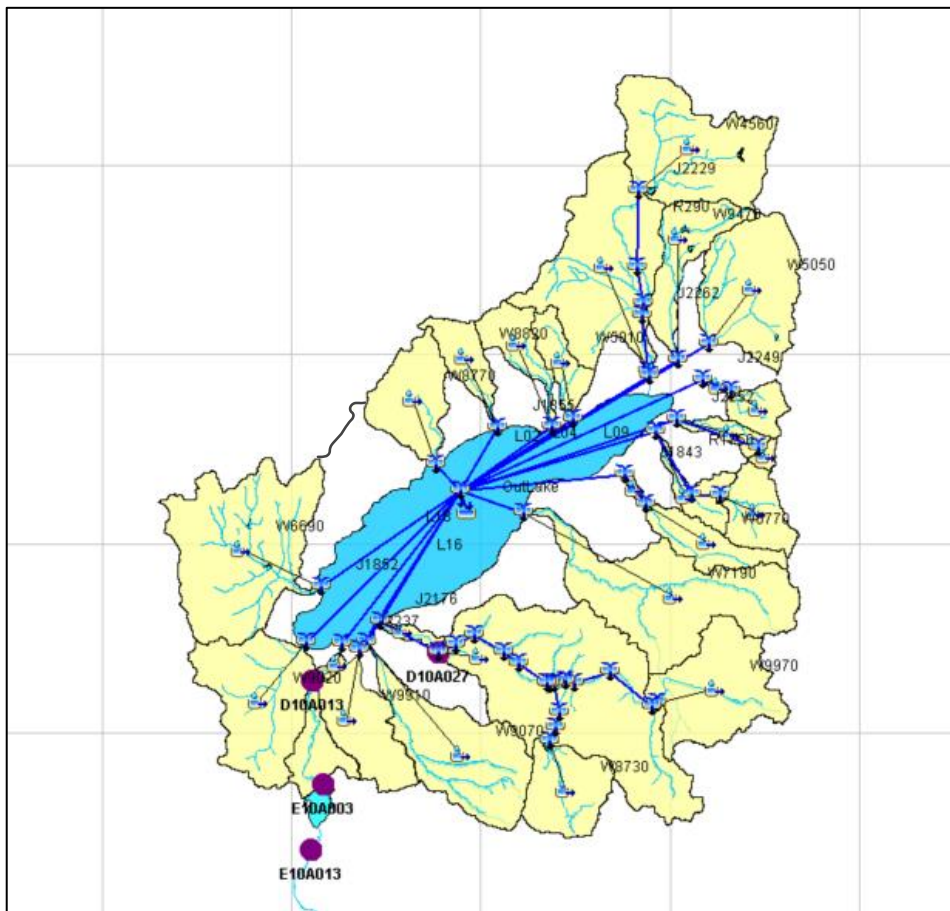


Figure 5.10. Stream networks and subbasins of the study area

The HEC-HMS model has six model components with two to eleven different methods to simulate hydrologic processes (Table 5.3). The methods marked in Table 5.3 were chosen for the simulations of the hydrologic system of the Burdur Lake.

Table 5.3. HEC-HMS model components

Components	Methods
Canopy	Dynamic Canopy Gridded Simple Canopy Simple Canopy*
Surface	Gridded Simple Surface Simple Surface*
Loss	Deficit and Constant* Exponential Loss Green and Ampt Gridded Deficit Constant Gridded Green Ampt Gridded SCS Curve Number Gridded Soil Moisture Accounting Initial and Constant SCS Curve Number Smith Parlange Soil Moisture Accounting
Transform	Clark Unit Hydrograph Kinematic Wave ModClark Synder Unit Hydrograph SCS Unit Hydrograph* User-Specified S-Graph User-Specified Unit Hydrograph
Baseflow	Bounded Recession Constant Monthly Linear Reservoir Nonlinear Boussinesq Recession*
Routing	Kinematic Wave Lag Lag & K Modified Puls Muskingum* Muskingum-Cunge Normal Depth Straddle Stagger
*Selected methods in this study	

In this study, the simple canopy method was chosen (Table 5.3). This method uses initial storage, maximum storage, and crop coefficient parameters. Initial and maximum storage parameters were determined during calibration. However, crop coefficients (K_c) were estimated according to the Corine land cover classes (Corine, 2018) of the study area (Figure 5.11). For each Corine class, corresponding crop coefficient values were determined from Table 5.4 (Nistor, 2020). Then, K_c was calculated using the area-weighted average method for each subbasin (Table 5.5).

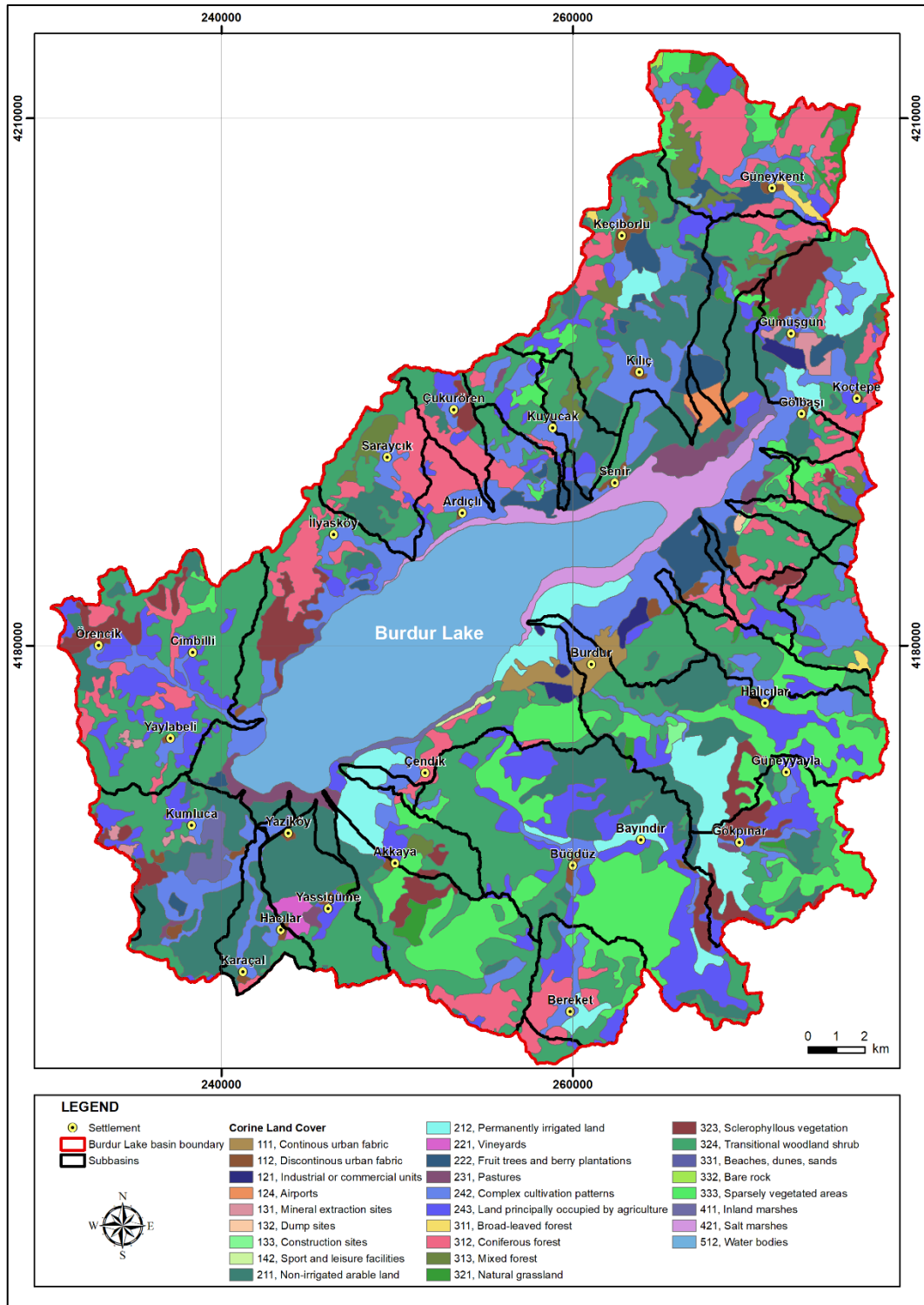


Figure 5.11. Corine land cover classes of the study area (Corine, 2018)

Table 5.4. Corine land cover classes and appropriate annual crop coefficient (Kc)
(Nistor,2020)

CLC code 2012	Corine Land Cover CLC Description	Kc annual				
		Kc	Ks	Ku	Kw	Kclc
111	Continuous urban fabric	-	-	0.3	-	0.29
112	Discontinuous urban fabric	-	-	0.2	-	0.21
121	Industrial or commercial units	-	-	0.3	-	0.3
122	Road and rail networks and associated land	-	-	0.3	-	0.25
123	Port areas	-	-	0.4	-	0.39
124	Airports	-	-	0.3	-	0.3
131	Mineral extraction sites	-	-	0.3	-	0.26
132	Dump sites	-	-	0.3	-	0.26
133	Construction sites	-	-	0.3	-	0.26
141	Green urban areas	-	-	0.2	-	0.21
142	Sport and leisure facilities	-	-	0.2	-	0.21
211	Non-irrigated arable land	1.14	-	-	-	1.14
212	Permanently irrigated land	1.25	-	-	-	1.25
213	Rice fields	0.94	-	-	-	0.94
221	Vineyards	0.5	-	-	-	0.5
222	Fruit trees and berry plantations	0.68	-	-	-	0.68
223	Olive groves	0.66	-	-	-	0.66
231	Pastures	0.7	-	-	-	0.7
241	Annual crops associated with permanent crops	0.67	-	-	-	0.67
242	Complex cultivation patterns	1.16	-	-	-	1.16
243	Land principally occupied by agriculture, with significant areas of natural vegetation	0.92	-	-	-	0.92
244	Agro-forestry areas	0.92	-	-	-	0.92
311	Broad-leaved forest	1.42	-	-	-	1.42
312	Coniferous forest	1	-	-	-	1
313	Mixed forest	1.33	-	-	-	1.33
321	Natural grasslands	0.97	-	-	-	0.97
322	Moors and heathland	0.92	-	-	-	0.92
323	Sclerophyllous vegetation	0.62	-	-	-	0.62
324	Transitional woodland-shrub	0.83	-	-	-	0.83
331	Beaches, dunes, sands	-	0.23	-	-	0.23
332	Bare rocks	-	0.15	-	-	0.15
333	Sparsely vegetated areas	0.48	-	-	-	0.48
334	Burnt area	-	0.1	-	-	0.1
335	Glaciers and perpetual snow	-	-	-	0.51	0.51
411	Inland marshes	-	-	-	0.45	0.45
412	Peat bogs	-	-	-	0.37	0.37
421	Salt marshes	-	-	-	0.32	0.32
422	Salines	-	0.1	-	-	0.1
423	Intertidal flats	-	-	-	0.64	0.64
511	Water courses	-	-	-	0.63	0.63
512	Water bodies	-	-	-	0.64	0.64
521	Coastal lagoons	-	-	-	0.68	0.68
522	Estuaries	-	-	-	0.62	0.62
523	Sea and ocean	-	-	-	0.74	0.74

Table 5.5. Simple Canopy Method Parameters

Subbasin	Crop Coefficient (Kc)	Initial Storage (%)	Max. Storage (mm)
W4560	0.93	1	2.2
W5010	0.83		
W5050	0.82		
W6330	0.89		
W6690	0.88		
W6770	0.85		
W7190	0.85		
W8730	0.89		
W8770	0.93		
W8820	0.90		
W8910	1.11		
W9020	0.85		
W9070	0.79		
W9160	1.11		
W9220	0.82		
W9270	0.89		
W9360	1.02		
W9370	0.94		
W9470	0.88		
W9620	0.92		
W9660	0.98		
W9820	0.79		
W9910	0.98		
W9920	0.93		
W9960	0.85		
W9970	0.82		

As a surface component, the simple surface method was chosen. The input values for these components were determined from Table 5.6 (Bennet, 1998) and modified during the calibration.

Table 5.6. Standard depression storage from Bennet (1998)

Description	Slope (%)	Surface Storage (mm)
Paved impervious areas	NA	3.2-6.4
Steep, smooth slopes	>30	1
Moderate to gentle slopes	5-30	12.7-6.4
Flat, furrowed land	0-5	50.8

The deficit and constant method, which needs minimum information about the soil, was chosen for the loss parameter due to the lack of data. Initial and maximum deficits and constant rate parameters were determined during the calibration process.

The SCS Unit Hydrograph method was used to simulate the transform component of the model. In this method, basin lag time (Lag) was calculated by the HEC-GeoHMS tool during the preprocessing step according to the NRSC lag method (NRSC, 1997):

$$Lag = \frac{L^{0.8}(S+1)^{0.7}}{1900Y^{0.5}} \quad (Eq. 5.15)$$

where:

L: Hydraulic length of the watershed (feet)

S: (100/CN)-10

Y: Basin slope (%)

CN: Curve Number

Eq. 5.15 used the area-weighted average CN, calculated as 76 for the basin (Figure 5.1). The lag time results for each subbasin are given in Table 5.7.

Table 5.7. Lag Times for the subbasins

Subbasin	Lag Time (min)	Subbasin	Lag Time (min)
W4560	100.41	W9160	78.835
W5010	47.328	W9220	136.19
W5050	127.04	W9270	56.954
W6330	68.053	W9360	27.085
W6690	109.17	W9370	27.279
W6770	83.386	W9470	136.28
W7190	177.77	W9620	83.805
W8730	93.245	W9660	194.95
W8770	91.525	W9820	37.729
W8820	85.022	W9910	131.86
W8910	89.488	W9920	93.381
W9020	122.62	W9960	189.68
W9070	111.35	W9970	86.261

Baseflow parameter simulation was conducted by the recession method. Initial discharge, recession constant, and ratio to peak values were determined during the calibration process to apply this method.

The last component of the HEC-HMS model is routing. The Muskingum method was chosen to simulate this component. The parameters of Muskingum K, X, and the number of subreaches were decided during the calibration.

The meteorological model simulates daily precipitation measurements and calculated evapotranspiration (ET) values of Burdur station (station no: 17238). For the calculation of ET, the Food and Agriculture Organization (FAO) of the United Nations recommends the Penman-Monteith method in FAO-56 Paper (Allen et al., 1998). Daily radiation, air temperature, humidity, and wind speed data were required to apply this method. Therefore, these data were taken for the Burdur station, and daily ET_0 values were calculated by:

$$ET_0 = \frac{0.408\Delta(R_n - G) + \gamma \frac{900}{T + 273} u_2 (e_s - e_a)}{\Delta + \gamma(1 + 0.34u_2)} \quad (Eq. 5.16)$$

where:

ET_0 : reference evapotranspiration ($mm \text{ day}^{-1}$)

R_n : net radiation at the crop surface ($MJ \text{ m}^{-2} \text{ day}^{-1}$)

G : soil heat flux density ($MJ \text{ m}^{-2} \text{ day}^{-1}$)

T : mean daily air temperature at 2 m height ($^{\circ}C$)

u_2 : wind speed at 2 m height ($m \text{ s}^{-1}$)

e_s : saturation vapor pressure (kPa)

e_a : actual vapor pressure (kPa)

$e_s - e_a$: saturation vapor pressure deficit (kPa)

Δ : slope vapor pressure curve ($kPa \text{ }^{\circ}C^{-1}$)

γ : psychrometric constant ($kPa \text{ }^{\circ}C^{-1}$)

The model was calibrated between October 2003-September 2009 and validated between October 2009-September 2011 using daily streamflow measurements of the Büğdüz flow gauging station (D10A027). These periods were chosen since the station had continuous measurements before the construction of Büğdüz pond at that time interval.

In Table 5.8, the initial values and calibration values of each parameter are provided. The graphs of observed and calculated discharge values at the end of the calibration and validation periods are shown in Figures 5.12 and 5.13, respectively.

Table 5.8. Initial and calibrated values of the HEC-HMS model

METHODS	PARAMETERS	INITIAL VALUE	CALIBRATED VALUE
Simple canopy	Initial storage (%)	1	1
	Max. storage (mm)	1.6	2.2
	Crop coefficient	given in Table 5.5	given in Table 5.5
Simple surface	Initial storage (%)	2	20
	Maximum storage (mm)	20	60
Deficit and constant	Initial Deficit (mm)	10	1
	Maximum storage (mm)	60	60
	Constant rate (mm/hr)	1	1
	Impervious (%)	5	3
SCS Unit hydrograph	Lag time (min)	given in Table 5.7	given in Table 5.7
Recession	Initial discharge (m ³ /sec)	0.1	0.01
	Recession constant	0.7	0.95
	Threshold type	Ratio to Peak	Ratio to Peak
	Ratio to peak value	0.2	0.62
Muskingum	Muskingum K (hr)	50	12
	Muskingum X	0.2	0.1
	Number of subreaches	1	1

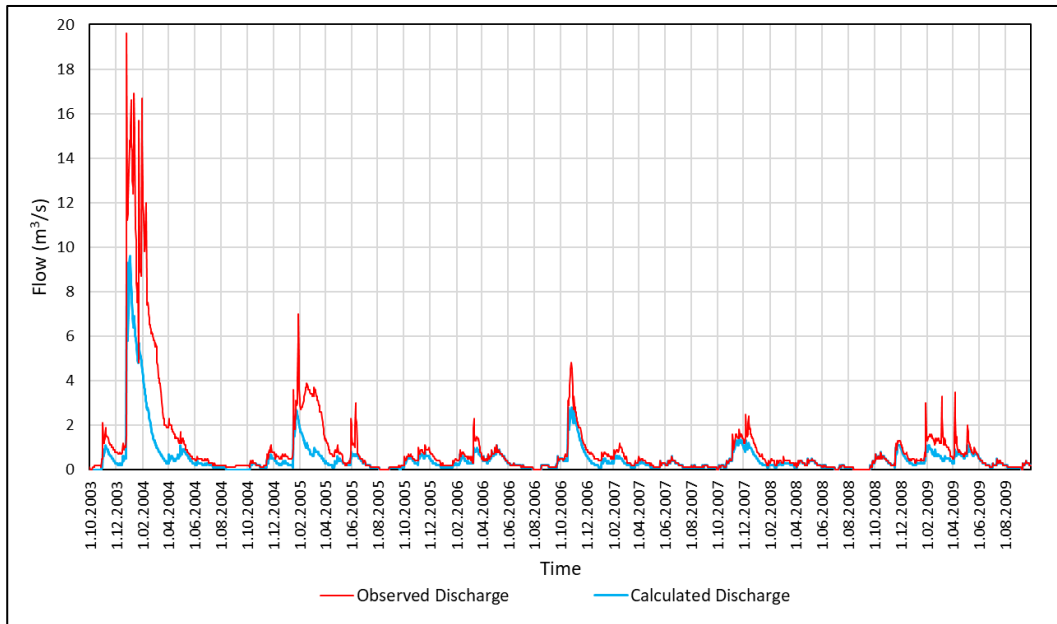


Figure 5.12. Observed and calculated discharge values as a result of calibration performed at Büğdüz station between October 2003-September 2009

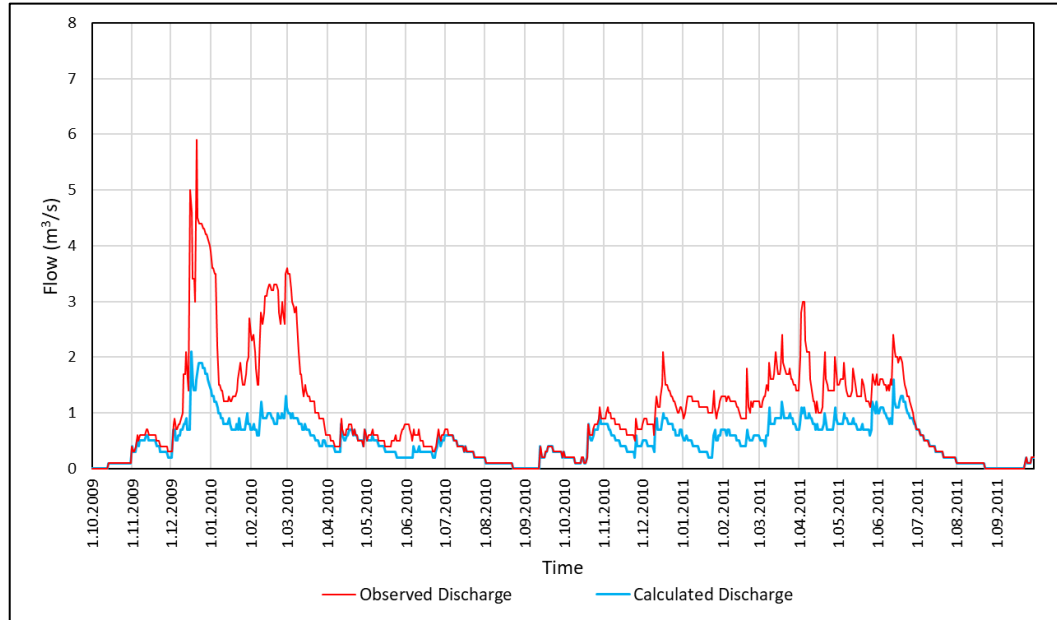


Figure 5.13. Observed and calculated discharge values as a result of validation performed at Büğdüz station between October 2009-September 2011

HEC-HMS model performance was evaluated using statistical measures such as Nash-Sutcliffe (NSE):

$$NSE = 1 - \frac{\sum_{t=1}^T (Q_t^{obs} - Q_t^{calc})^2}{\sum_{t=1}^T (Q_t^{obs} - \bar{Q}^{obs})^2} \quad (Eq. 5.17)$$

Percent Bias (PBIAS):

$$PBIAS = \frac{\sum_{t=1}^T Q_t^{obs} - Q_t^{calc}}{\sum_{t=1}^T Q_t^{obs}} \times 100 \quad (Eq. 5.18)$$

and Coefficient of Determination (R^2):

$$R^2 = \left[\frac{\sum_{t=1}^T (Q_t^{obs} - \bar{Q}^{obs}) \times (Q_t^{calc} - \bar{Q}^{calc})}{\sqrt{\sum_{t=1}^T (Q_t^{obs} - \bar{Q}^{obs})^2 \times \sum_{t=1}^T (Q_t^{calc} - \bar{Q}^{calc})^2}} \right] \quad (Eq. 5.19)$$

In Table 5.9, performance statistics intervals for a satisfactory model are given (Moriassi et al., 2015). In this study, calculated model performance statistics are given in Table 5.10. According to the intervals given in Table 5.9, the model calibration and validation can be defined as satisfactory.

Table 5.9. Performance statistics intervals (Moriassi et al., 2015)

Performance Evaluation	PBIAS	NSE	R²
Very good	PBIAS < ±10	0.75 < NSE ≤ 1.00	R ² > 0.85
Good	±10 ≤ PBIAS < ±15	0.65 < NSE ≤ 0.75	0.70 < R ² ≤ 0.85
Satisfactory	±15 ≤ PBIAS < ±25	0.50 < NSE ≤ 0.65	0.50 < R ² ≤ 0.70
Unsatisfactory	PBIAS ≥ ±25	NSE ≤ 0.50	R ² ≤ 0.50

Table 5.10. Performance statistics for the calibrated and validated model

Performance Evaluation	PBIAS	NSE	R²
Calibrated Model	16.97	0.61	0.61
Validated Model	12.99	0.50	0.52

The HEC-HMS model was simulated between January 1969 and December 2018 by assigning the calibrated parameters to calculate surface water inflow from all the ungauged basins to the Burdur Lake. Because of the assumptions of no flow from subbasins of ponds after the construction years and no flow from northern subbasins (pink colored in Figure 5.6) after the airport construction in 1993, the inflows were corrected manually. The inflows from the Büğdüz and Bozçay streams calculated by the drainage area ratio method were added to inflows calculated by the HEC-HMS model. According to DSI (2016-b), the total amount of irrigation from the surface waters of the Burdur Lake basin has been 0.46-1.97 hm³ between May and September since 1975. Hence, water usage was subtracted from the inflows. As a result, the estimated surface water inflows to Burdur Lake during the dry-wet seasons are given in Figure 5.14.

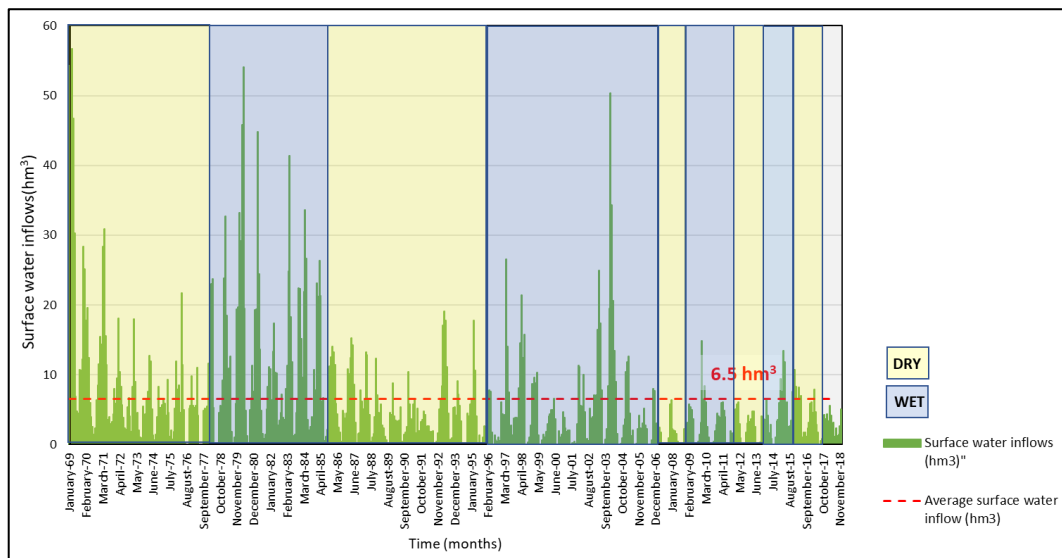


Figure 5.14. The monthly volume of inflows to the Burdur Lake

The long-term average inflow was calculated as 6.5 hm³. Although the inflows are conformable with the dry-wet seasons of the Burdur meteorological station (no:17238), they decrease significantly after 2003 regardless of seasons.

5.3.5 Groundwater inflow/outseepage

The groundwater inflow/outseepage is considered the most difficult component of the water budget to measure or estimate. The continuity equation was used to calculate this parameter. However, another mechanism was taken into consideration before the calculation. Burdur Lake has lost 95 km² area or 2989 hm³ volume from January 1969 to December 2018. The area lost is considerable and is equal to approximately 13000 soccer fields. In the study area, the old lake bed has high groundwater levels with a depth of 2-3 m below the ground. Thus, there is evapotranspiration from this area during the year, which causes a decrease in groundwater inflows to the lake. In order to quantify this loss, ET values corresponding to this area were calculated between January 1969 and December 2018. For this purpose, the maximum area that the lake reached was specified as 220.7 km² in May 1970. The ET values were then calculated for the area between this maximum area and the current size of the lake at each month. The results are provided in Figure 5.15. The resulting monthly groundwater inflow/outseepage rates after subtracting evaporation rates are given in Figure 5.16.

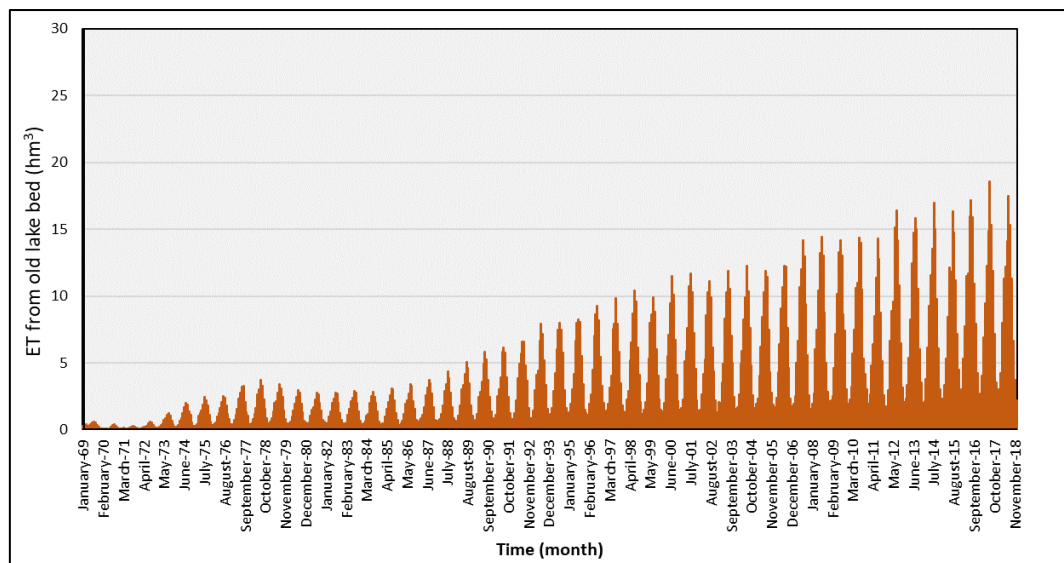


Figure 5.15. Monthly ET from the old lake bed

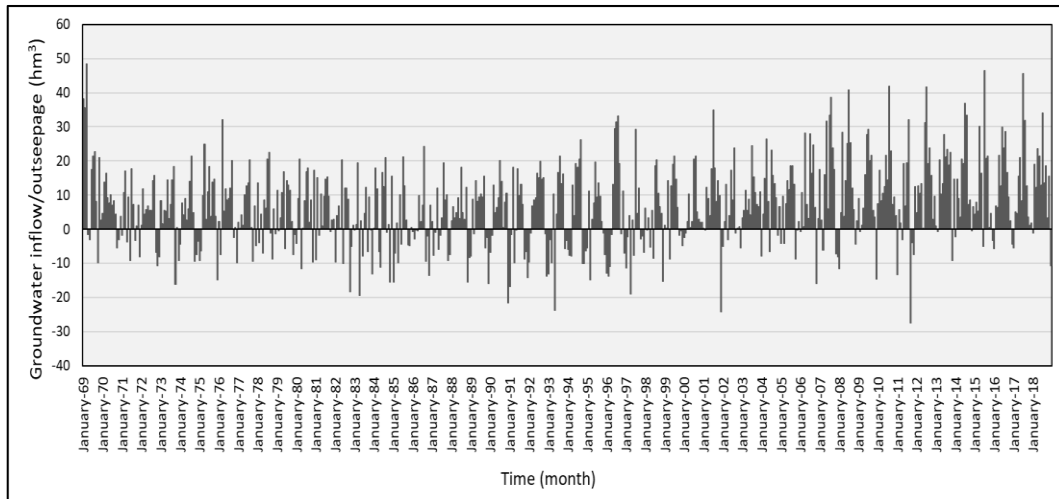


Figure 5.16. Monthly groundwater inflow/outseepage

In the study area, groundwater inflow to the lake usually occurs in the summer, and outflow from the lake is in the winter. The reason is supplying water loss of the lake from evaporation in summer by groundwater inflow. In order to minimize the seasonal impact on the water budget, all components were also evaluated annually. The results are given in Figure 5.17 and Table 5.11.

The precipitation over the lake surface, surface water inflow, and evaporation from the lake surfaces decreased with the lake area decrease. Evaporation is the main outflow component of the lake, whereas the surface water and groundwater inflows to the lake are the dominant inflow components. Although the contribution of surface water was higher until 2005, groundwater inflow replaced this contribution between 2005 and 2018. Although this shift may be due to the reduction of the surface water reaching the lake following the construction of several dams and ponds after the 2000s, it will be confirmed by the numerical lake groundwater model in the following chapters.

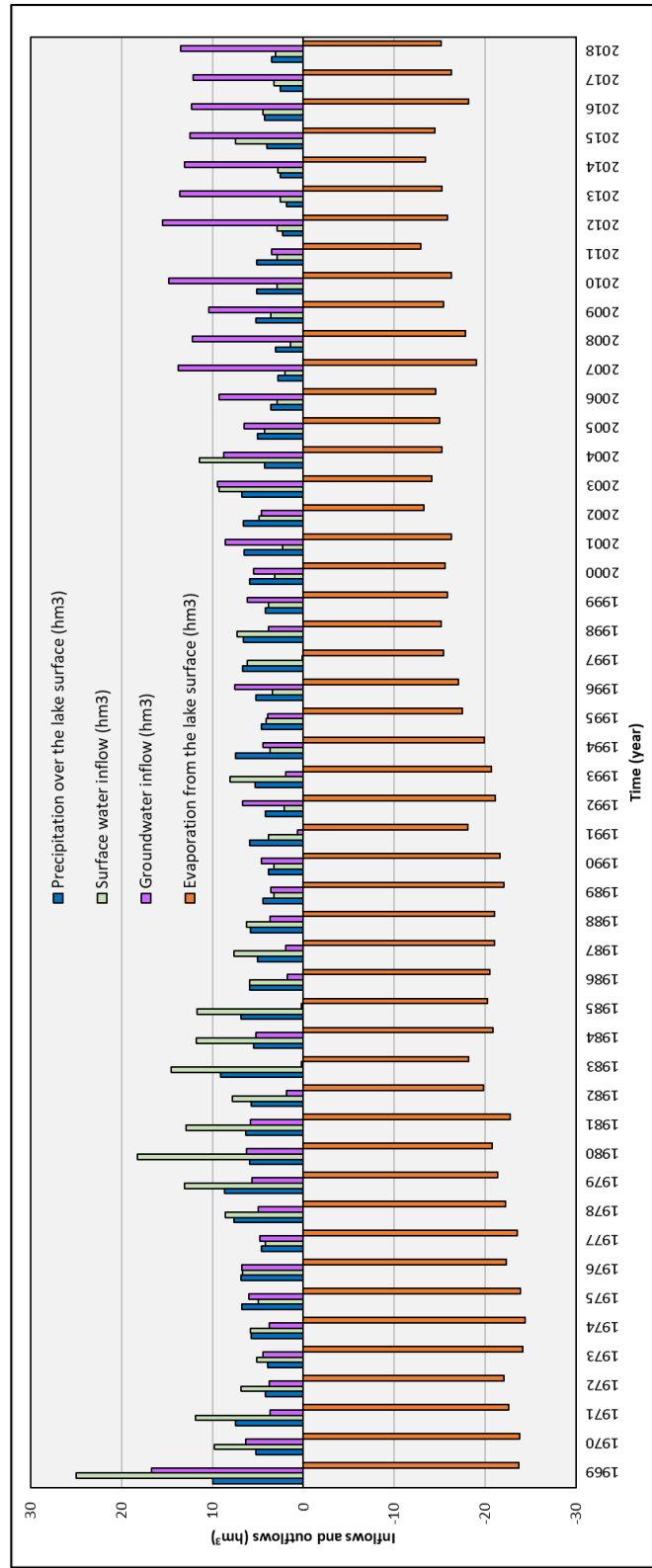


Figure 5.17. Annual lake budget components

Table 5.11. Annual lake budget components

Year	Lake level (m)	ΔS (hm ³)	Prec. over the lake sur. (hm ³)	Evap. from the lake sur. (hm ³)	Surface water inflow (hm ³)	Gw. inflow (hm ³)
1969	856.79	27.60	9.97	23.68	24.95	16.72
1970	857.27	-2.54	5.20	23.75	9.80	6.36
1971	857.27	0.18	7.42	22.63	11.84	3.68
1972	857.04	-7.57	4.16	22.08	6.87	3.76
1973	856.52	-11.19	3.92	24.12	5.17	4.46
1974	855.90	-10.13	5.71	24.38	5.83	3.72
1975	855.32	-7.42	6.75	23.88	4.93	6.01
1976	855.08	-3.26	6.90	22.29	6.66	6.81
1977	854.59	-11.71	4.62	23.55	4.16	4.76
1978	854.19	-2.86	7.65	22.25	8.60	4.98
1979	854.18	4.20	8.66	21.35	13.04	5.64
1980	854.71	8.14	5.94	20.78	18.23	6.26
1981	854.93	0.85	6.38	22.76	12.90	5.79
1982	854.71	-5.95	5.70	19.86	7.83	1.86
1983	854.58	4.07	9.06	18.17	14.52	0.18
1984	854.80	0.17	5.45	20.84	11.80	5.23
1985	854.69	-3.06	6.83	20.23	11.67	0.24
1986	854.33	-8.60	5.88	20.49	5.95	1.80
1987	853.82	-8.33	5.00	20.99	7.66	1.92
1988	853.36	-7.41	5.83	21.06	6.24	3.66
1989	852.65	-13.43	4.44	22.08	3.21	3.56
1990	851.83	-12.79	3.86	21.63	3.27	4.65
1991	851.11	-10.80	5.89	18.07	3.84	0.66
1992	850.37	-11.77	4.20	21.15	2.07	6.68
1993	849.66	-9.30	5.30	20.73	8.06	1.96
1994	849.04	-8.54	7.49	19.91	3.64	4.41
1995	848.48	-9.23	4.61	17.46	4.09	3.94
1996	847.81	-5.44	5.25	17.03	3.41	7.53
1997	847.38	-7.14	6.73	15.40	6.20	0.04
1998	847.15	-2.44	6.58	15.16	7.33	3.85
1999	846.85	-6.81	4.17	15.83	3.83	6.13
2000	846.24	-6.55	5.87	15.58	3.16	5.44
2001	845.71	-4.77	6.51	16.27	2.28	8.61
2002	845.48	-2.80	6.62	13.25	4.86	4.61
2003	845.61	5.63	6.76	14.12	9.30	9.49
2004	846.22	3.11	4.24	15.26	11.42	8.77
2005	845.98	-5.17	5.06	14.95	4.29	6.51
2006	845.49	-5.09	3.56	14.55	2.87	9.30
2007	844.98	-7.50	2.84	19.07	2.02	13.80
2008	844.28	-8.54	3.04	17.86	1.39	12.22
2009	843.84	-3.59	5.20	15.40	3.57	10.39
2010	843.66	-1.19	5.09	16.29	2.88	14.77
2011	843.35	-8.17	5.16	12.95	2.85	3.51
2012	842.73	-3.41	2.31	15.88	2.87	15.45
2013	842.30	-5.60	1.87	15.28	2.54	13.57
2014	841.87	-3.32	2.53	13.45	2.81	13.10
2015	841.96	1.10	4.01	14.47	7.43	12.45
2016	841.59	-6.56	4.29	18.17	4.47	12.33
2017	840.96	-7.50	2.58	16.32	3.24	12.12
2018	840.39	-4.22	3.49	15.16	3.10	13.50

CHAPTER 6

GROUNDWATER FLOW MODEL

Groundwater models have been driven to understand the groundwater flow systems at basin scales by integrating the geological features of the hydrogeological system. Although it was not until the 1960s that researchers started to view lakes from the perspective of groundwater flow systems, these are the interconnected components of one single resource, and any changes in either of these components will have an impact on the quantity or quality of the other (Toth, 1999). Therefore, groundwater and lake need to be incorporated into the numerical models to represent groundwater flow systems better. These groundwater-lake models have key aims, such as understanding the reliability of the conceptual model and groundwater flow systems budgets and ensuring the development and management of water resources. They also play an essential role in predicting management measures' effects on integrated water resources systems.

This study covers the period between January 1969 to December 2018, which coincides with the period when the Burdur Lake level change can be observed. In order to develop a groundwater-lake model between these periods, groundwater usage must be known for all years. However, annual groundwater consumption is known only for 2015 (DSI, 2016-a). It is also known that groundwater usage reached critical levels after 1975 in the basin (DSI, 1975 & 2016-b). Although some wells were drilled for drinking purposes between 1967-1975, no excess water was pumped. Since there is no groundwater usage measurement during all study periods, the groundwater and lake models were developed for two different years, 1969 and 2014, under steady-state conditions and for two three-year periods, 1969-1971 and 2014-2016, under transient conditions. The 1969-1971 period represents the natural

conditions in which the lake level was affected only by climatic conditions. In contrast, the 2014-2016 period represents the human intervention period, including 2015, when the annual groundwater pumping rates were known.

6.1 Computer Code

The regional groundwater numeric model for the Burdur Lake basin area was developed using the Visual MODFLOW Flex Software. Visual MODFLOW Flex is developed by HydroGeologic Inc. (2018) as a newer and later version after the retirement of Visual MODFLOW Classic. It is a graphical user interface for the modular finite-difference flow model (MODFLOW) introduced by USGS (Harbaugh, 2005).

In this study, Visual MODFLOW Flex is used to solve the flow equation by finite difference approach governing 3-D saturated fluxes in constant density saturated porous media. In order to simulate the lake-groundwater relationship, the lake boundary condition, which is one of the head-dependent flux boundary conditions of Visual MODFLOW Flex, was used.

6.2 Model Geometry and Layering

The model domain covers an area of 1630 km². It is bounded by the Karaçal Dam Reservoir in the south, and the watershed divides in all other directions. The extent of the model domain in N-S and E-W directions are approximately 62 and 46 km, respectively (Figure 6.1).

The study area was discretized into variable cell sizes. Since the lake area has more interest, it was surrounded by a 100 m x 100 m grid size, and the dimensions of the grids got coarser towards the basin boundary as 150 m x 150 m, 200 m x 200 m, 300 m x 300 m, and finally 400 m x 400 m. These grid sizes resulted in 115654 active cells in a single layer. The resulting grid is rotated 30°.

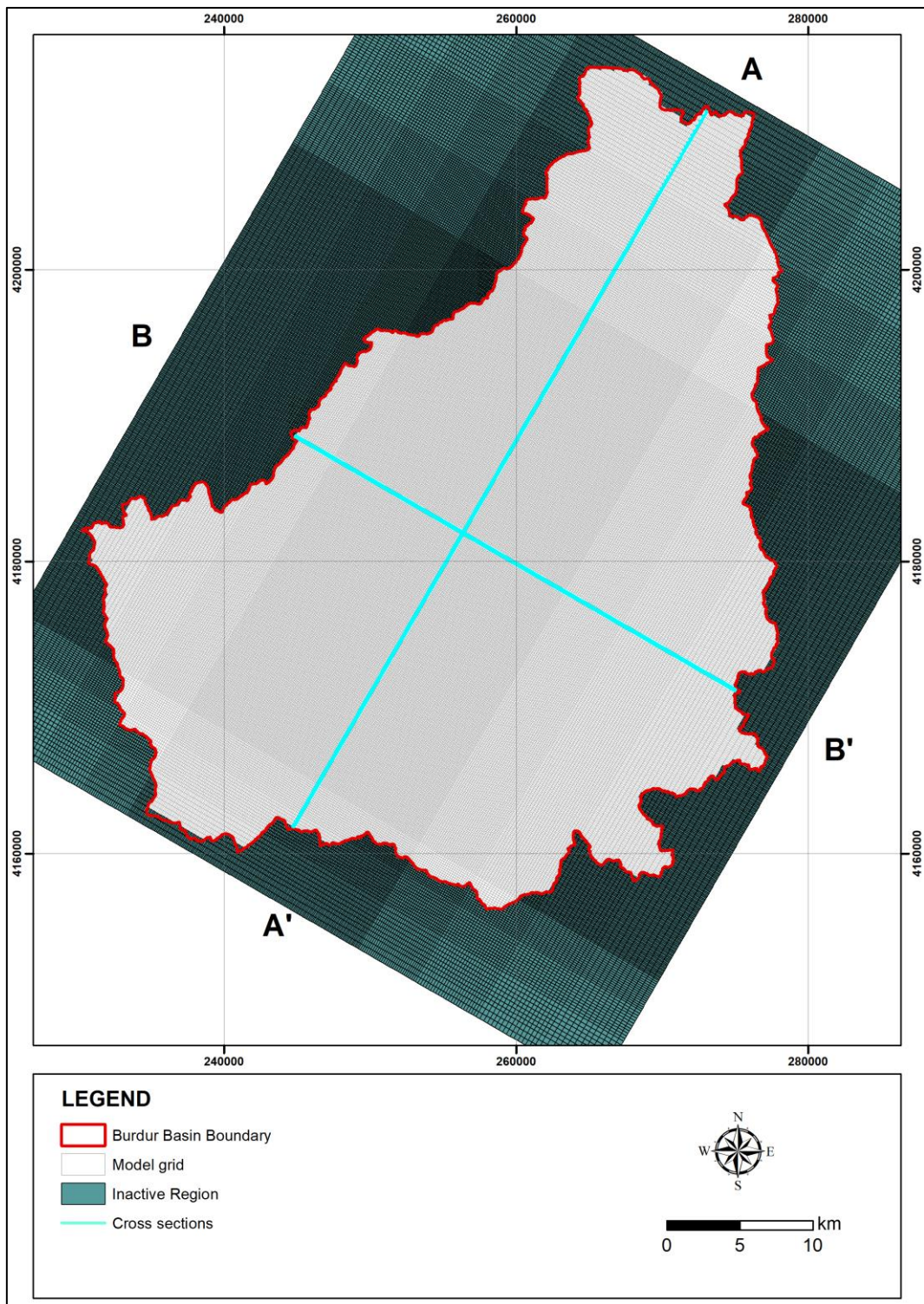


Figure 6.1. Model domain and grids

The model area was subdivided into seven layers to simulate the vertical hydrogeological properties (Figure 6.2). The top of the uppermost layer is the topographical surface with a 781 m-2028 m elevation range within the model domain. The bottom of the first layer was specified as uniformly 780 m according to lake bottom elevation and alluvium thickness. Then, the thickness of the second layer was determined as 30 m for the domain of interest at the lake bottom. Finally, all the other layers were divided with a 50 m uniform thickness until the 500 m elevation since the elevation lower than 500 m is represented with impermeable units.

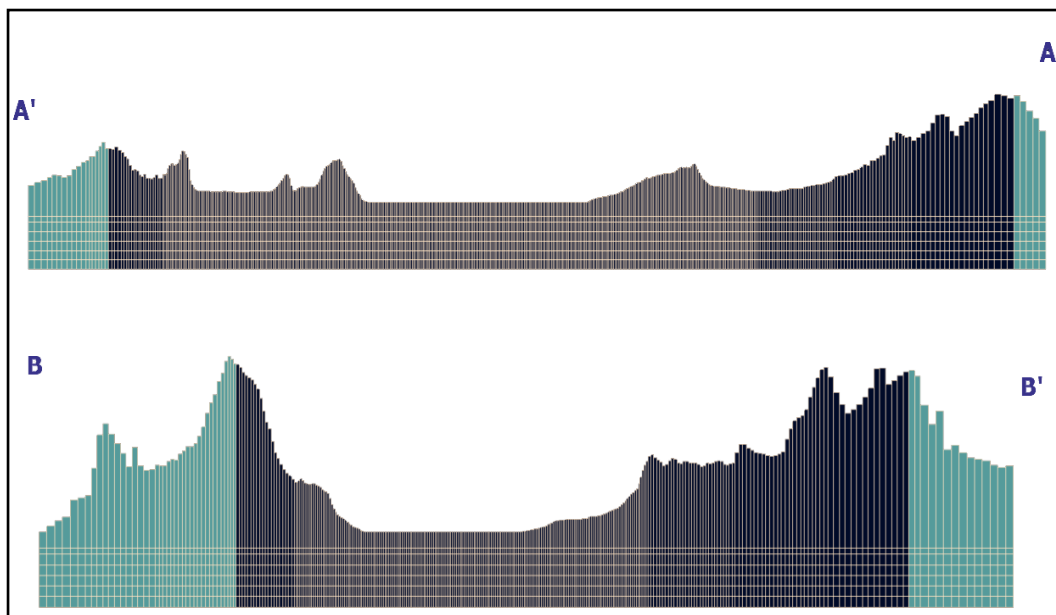


Figure 6.2. The vertical layout of the model layers for A-A' and B-B' cross-section

6.3 Boundary Conditions

In groundwater modeling, appropriate boundary conditions are required to represent the relationship of the groundwater to the surrounding systems. In MODFLOW, there are three types of boundary conditions; specified heads, specified fluxes, and head-dependent fluxes. The default boundary condition is the no-flow boundary. Appropriate boundary conditions were chosen in the model to simulate steady-state

conditions in 1969 and 2014 and transient conditions in the 1969-1971 and 2014-2016 periods. The boundary conditions assigned to the model domain are shown in Figure 6.3.

The lateral groundwater flow from the karstic dolomitic limestone, which has an outcrop at the eastern part of the study area, was represented by the general head boundary condition (Figure 6.3). For this boundary, horizontal hydraulic conductivity and head values were assigned as 8×10^{-6} m/s (same as dolomitic limestone) and 1600 m, respectively.

The Bozçay stream, which enters the study area from the southern boundary, was also represented by the general head boundary condition. However, this boundary condition was not included in the models for the 2014-2016 period since the flow amount of the stream became negligible after the construction of the Karamanlı (1975), Karataş (1974), and Karaçal (2010) dams. A no-flow boundary condition represents the basin boundary for the rest of the study area.

Under steady-state conditions, Burdur Lake was described by a constant head boundary condition. The hydraulic heads of the lake are set equal to 857 m and 842 m, respectively, in the models developed for 1969 and 2014. In order to simulate lake and groundwater interaction under transient conditions, the lake boundary condition was used. The lake bottom was assigned to the model using the bathymetry map prepared by DSI in 2015. Due to the lack of detailed hydrological data, lakebed hydraulic conductivity and thickness are estimated to be 1×10^{-5} m/s and 1 m, respectively, during the calibration. The leakance is calculated as 0.864 1/day along the lake boundary by the ratio of lakebed hydraulic conductivity to lakebed thickness. As input, DSI lake stage measurements and lake budget parameters such as precipitation, evaporation, and runoff are assigned to lake boundary conditions.

In the model domain, the springs in the karstic dolomitic limestone are represented by the drain boundary condition. Due to the lack of detailed hydrological data, spring elevations and conductance values are estimated during the model calibration according to the springs' flow rates.

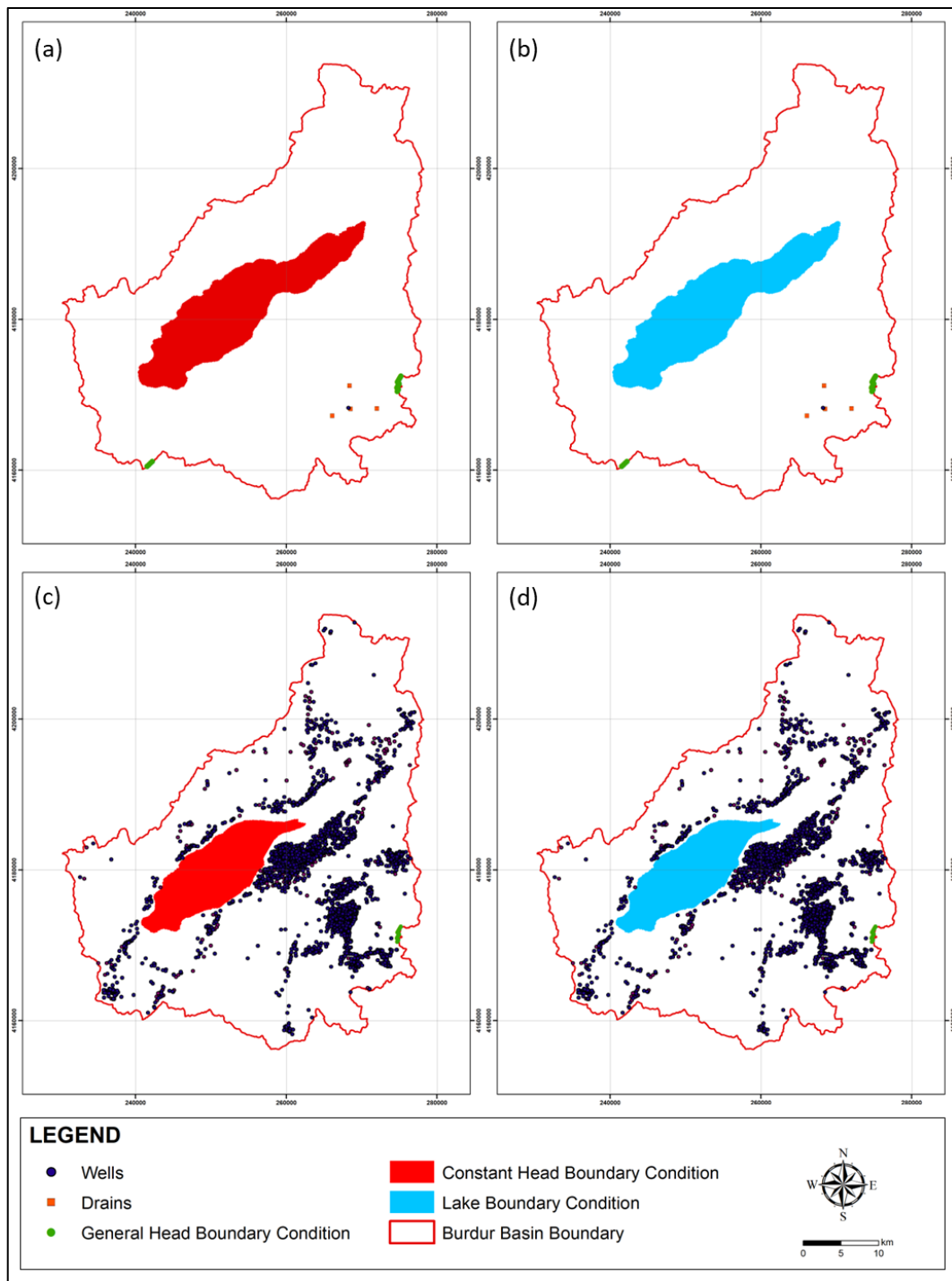


Figure 6.3. The boundary conditions of the model for 1969 (a), 1969-1971 (b), 2014 (c), 2014-2016 (d)

The groundwater pumping is represented by the well boundary condition. According to hydrogeological studies, 3788 wells are used for irrigation, drinking, and domestic purposes within the model domain. According to their drilling purposes, the assigned pumping rates for these wells change between 0.02 L/s to 50 L/s. For the 1969-1971 period, the drinking water supply for the Burdur Province was simulated by pumping from 5 DSI wells with a flow rate of 25 L/s each.

6.4 Model Parameters

Groundwater models require quantitative parameters such as recharge, hydraulic conductivity, and storage coefficient to describe the properties of the porous media. These input parameters can be modified during calibration to obtain a good match between the observed and simulated lake and groundwater levels.

6.4.1 Recharge

The mean annual precipitation of the Burdur Lake basin was calculated as 421.8 mm from Burdur meteorological station 1969-2018 precipitation data. In the hydrologic budget calculations, the Thornthwaite method and SCS curve number were used to calculate potential evapotranspiration and surface runoff. The average annual groundwater recharge from direct precipitation in the basin is 25.7 mm, comprising 6 % of the annual precipitation (Table 5.2).

The elevation distribution dramatically changes in the study area because of the steep and undulating topography around the gentle lake basin. There is a direct relationship between precipitation and elevation; as the elevation increases, more precipitation is observed. Also, at higher altitudes, the precipitation may occur as snow, resulting in more recharge in these regions. Therefore, according to elevation intervals, the study area was divided into four zones (Figure 6.4).

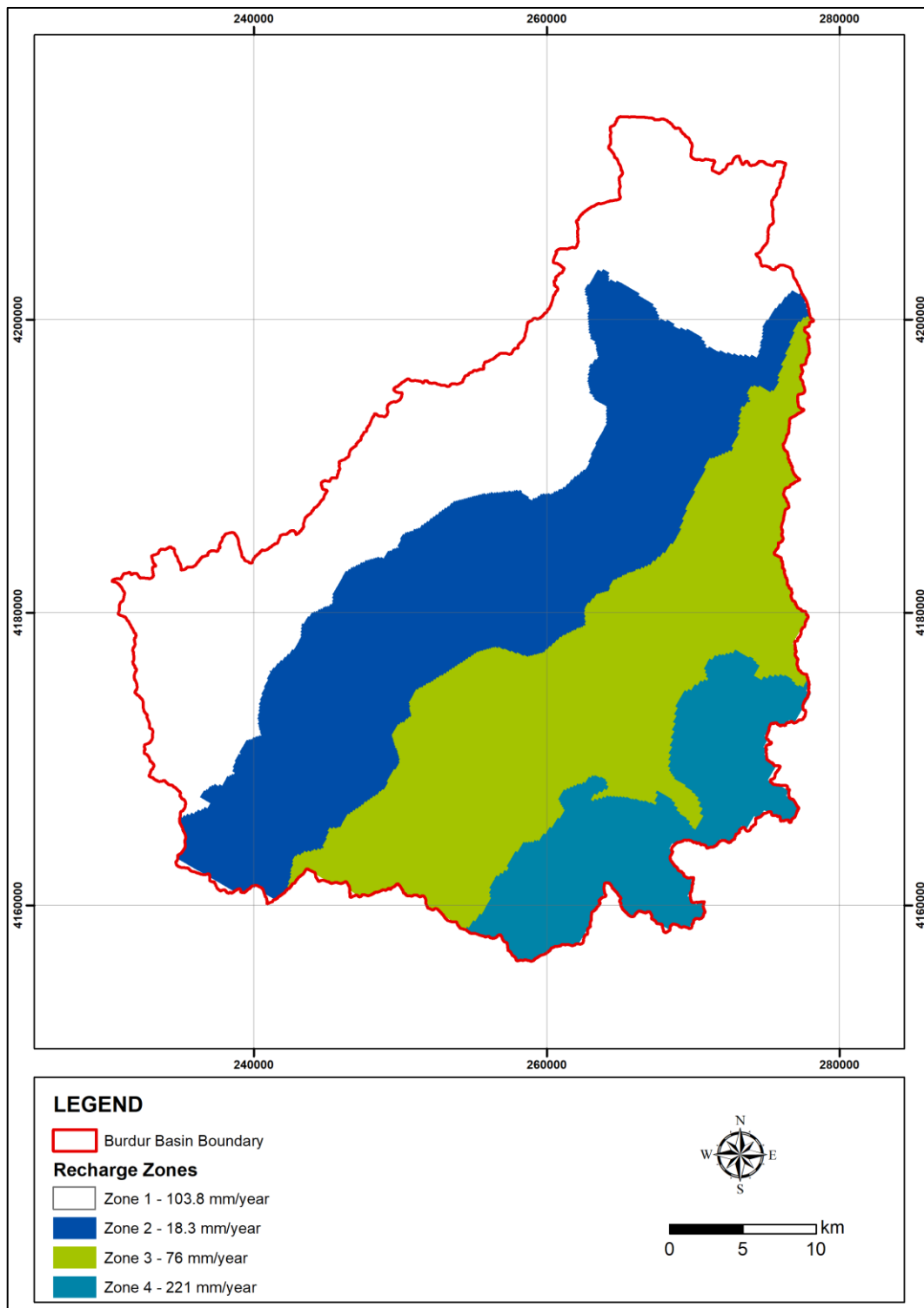


Figure 6.4. Aerial distribution of recharge in the model domain

For each zone, the median elevations were determined following the hypsometric curves in Figure 6.5.

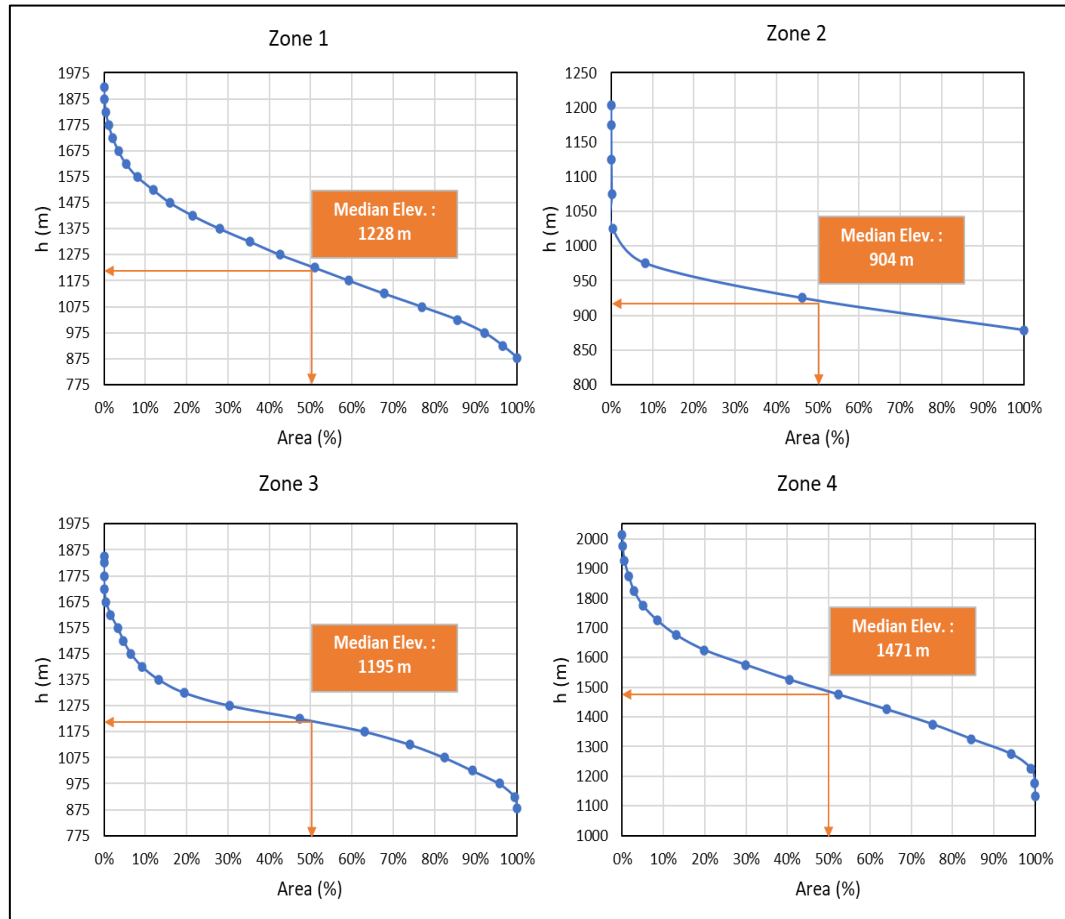


Figure 6.5. Hypsometric curves for each recharge zone in the model domain

Then, the long-term precipitation and temperature measured at the Burdur Meteorological station are correlated according to elevation differences between the station and the median elevation of each zone (Table 6.1). The temperature was assumed to decrease linearly with elevation, using the free-air moist adiabatic lapse rate of $0.0065 \text{ }^{\circ}\text{C/m}$.

Table 6.1. Corrected precipitation and temperature data for each recharge zone

Corrected Meteorological Parameters	Recharge Zones	Jan.	Feb.	Mar.	Apr.	May.	Jun.	Jul.	Aug.	Sep.	Oct.	Nov.	Dec.	Annual
Corrected monthly average temperature (°C)	Zone 1	2.6	2.9	5.7	8.5	14.1	19.0	21.4	21.9	18.4	11.1	7.2	2.0	11.2
	Zone 2	4.7	5.0	7.8	10.6	16.2	21.1	23.5	24.0	20.5	13.2	9.3	4.1	13.3
	Zone 3	2.8	3.2	6.0	8.7	14.4	19.3	21.6	22.1	18.6	11.4	7.4	2.2	11.5
	Zone 4	1.0	1.4	4.2	6.9	12.6	17.5	19.8	20.3	16.8	9.6	5.6	0.4	9.7
Corrected monthly total precipitation (mm)	Zone 1	94.9	62.0	67.8	72.2	48.2	21.0	25.3	10.3	9.9	42.1	46.5	87.6	587.7
	Zone 2	66.7	43.5	47.7	50.7	33.9	14.7	17.7	7.2	7.0	29.6	32.7	61.6	413.0
	Zone 3	92.0	60.1	65.8	70.0	46.7	20.3	24.5	10.0	9.6	40.8	45.1	85.0	569.9
	Zone 4	116.0	75.8	83.0	88.3	59.0	25.6	30.9	12.6	12.2	51.5	56.8	107.2	718.9

The monthly mean temperature (T_P) is estimated by using the given equation:

$$T_P = T - T_i \times (H_i - H_0) \quad (\text{Eq. 6.1})$$

where:

T : monthly average temperature of the station

H_i : the median elevation of the basin zone

H_0 : the height of the meteorological station

T_i : lapse rate (0.0065 °C/m)

The Schreiber formula determines the changes in precipitation based on elevation (Erinç, 1969). The monthly average precipitation (P_h) increases by 54 mm for every 100 meters according to the given formula:

$$P_h = P_0 \pm (54 \times h) \quad (\text{Eq. 6.2})$$

where:

P_0 : monthly total precipitation of the station (mm)

h : the height difference between the meteorological station and the median elevation of the basin zone (hm)

Then, the Thornthwaite method and SCS curve number were used for each zone to calculate potential evapotranspiration and surface runoff values. Curve number values were calculated as 75, 76, 77, and 76 from zones 1 to 4, respectively, using the GCN250 dataset in Figure 5.1 (Jaafar et al., 2019). The monthly water budget results for each recharge zones are given in Table 6.2. The recharge rate was assigned 18.3 mm/year in the Burdur Lake plain, 103.8 mm/year for the western part, and 76 mm/year for the eastern part of the plain. This rate was calculated as 147.3 mm/year for the east karstic limestone region. However, the recharge rate for the karstic areas can be assumed to be higher since the precipitation infiltrates rapidly with low evaporation amounts (Milanović, 1981). Therefore, during calibration, the recharge from precipitation was estimated as 221 mm/year (fifty percent more than the calculated value) for the eastern part of the study area.

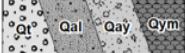
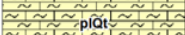
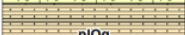



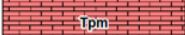



6.4.2 Hydraulic Parameters

The hydraulic conductivities of the geological units outcropping in the study area were determined by the pumping tests conducted by DSI. Since a pumping test was not conducted in the Eocene unit, and distinguishing Plio-Quaternary, Pliocene, and Cretaceous units is difficult, the hydraulic conductivities of those units were specified during the calibration period. Plio-Quaternary and Pliocene units are continuous through the seven layers, so the hydraulic conductivity values of the unit along these layers were also decided during calibration. The hydraulic conductivity values obtained from the pumping test results were assigned to the model within the minimum and maximum limits (Table 6.3). The layers were assumed to be anisotropic with $K_x=K_y$ and $K_z=K_x/10$.

Table 6.2. Monthly water budget results for each recharge zone

Recharge Zones	Parameter	Jan	Feb	Mar	Apr	May	Jun	Jul	Aug	Sep	Oct	Nov	Dec	TOTAL	Ratio to prec.(%)	
Zone 1	Mean Monthly Temperature (°C)	2.6	2.9	5.7	8.5	14.1	19.0	21.4	21.9	18.4	11.1	7.2	2.0			
	i	0.37	0.45	1.23	2.22	4.82	7.57	9.02	9.34	7.19	3.36	1.73	0.25	47.6		
	a:	1.2	1.2	1.3	1.2	1.2	1.2	1.2	1.2	1.2	1.2	1.2	1.2	1.2	14.9	
	UPET	7.46	8.80	20.20	32.77	61.89	89.54	103.36	106.37	85.85	46.03	26.65	3.48	594.4		
	PET	6.42	7.39	20.81	36.05	75.50	110.14	129.20	124.46	88.44	44.65	22.65	4.55	670.2		
	r	0.86	0.84	1.03	1.10	1.22	1.23	1.25	1.17	1.03	0.97	0.85	0.83			
	Precipitation (mm)	94.9	62.0	67.8	72.2	48.2	21.0	25.3	10.3	9.9	42.1	46.5	87.6	587.7		
	Surface runoff coefficient	1	1	1	1	1	1	1	0	0	1	1	1			
	Surface runoff (mm)	36.63	15.19	18.61	21.28	8.12	0.15	0.67	0.00	0.00	5.53	7.35	31.51			
	Infiltration (I)	58.22	46.77	49.21	50.89	40.08	20.80	24.59	10.30	9.94	36.60	39.13	56.11			
	I-PET	51.80	39.38	28.40	14.85	-35.42	-89.33	-104.61	-114.16	-78.49	-8.05	16.48	51.57			
	TOTAL (P-PET)	0.00	0.00	0.00	0.00	-35.42	-124.78	-229.37	-343.53	-422.02	-430.07	0.00	0.00			
	Soil moisture	100.00	100.00	100.00	100.00	100.00	70.17	28.72	10.09	3.22	1.47	1.36	17.83	69.40		
	Change in soil moisture	30.80	0.00	0.00	0.00	-29.83	-41.45	-18.63	-6.87	-1.75	-0.11	16.48	51.57			
	AET	6.42	7.39	20.81	36.05	69.91	62.26	43.22	17.17	11.69	36.71	22.65	4.55	338.8	58%	
	Excess precipitation (HAET)	57.84	54.57	47.01	36.13	8.12	0.15	0.67	0.00	0.00	5.53	7.35	31.51	248.9		
	Surface runoff	36.63	15.19	18.61	21.28	8.12	0.15	0.67	0.00	0.00	5.53	7.35	31.51	145.0	25%	
Groundwater recharge	21.20	39.38	28.40	14.85	0.00	0.00	0.00	0.00	0.00	0.00	0.00	0.00	103.8	18%		
													TOTAL	587.7	100%	
Zone 2	Parameter	Jan	Feb	Mar	Apr	May	Jun	Jul	Aug	Sep	Oct	Nov	Dec	TOTAL	Ratio to prec.(%)	
	Mean Monthly Temperature (°C)	4.7	5.0	7.8	10.6	16.2	21.1	23.5	24.0	20.5	13.2	9.3	4.1			
	i	0.90	1.01	1.98	3.11	5.95	8.87	10.40	10.73	8.47	4.37	2.55	0.74	59.1		
	a:	1.4	1.4	1.4	1.4	1.4	1.4	1.4	1.4	1.4	1.4	1.4	1.4	17.0		
	UPET	11.47	12.77	23.91	36.56	67.23	97.76	113.42	116.87	93.63	50.31	30.35	9.55	663.8		
	PET	8.87	10.73	24.63	40.22	82.02	120.24	141.78	136.73	96.43	48.80	25.80	7.93	745.2		
	r	0.86	0.84	1.03	1.10	1.22	1.23	1.25	1.17	1.03	0.97	0.85	0.83			
	Precipitation (mm)	66.7	43.5	47.7	50.7	33.9	14.7	17.7	7.2	7.0	29.6	32.7	61.6	413.0		
	Surface runoff coefficient	1	1	1	1	1	0	1	0	0	1	1	1			
	Surface runoff (mm)	19.74	7.11	9.04	10.58	3.30	0.00	0.04	0.00	0.00	2.00	2.90	16.63			
	Infiltration (I)	46.92	36.43	38.62	40.14	30.57	14.72	17.71	7.24	6.99	27.60	29.75	44.94			
	I-PET	37.05	25.70	13.99	-0.08	-51.45	-105.52	-124.07	-129.50	-89.45	-21.21	3.96	37.01			
	TOTAL (P-PET)	0.00	0.00	0.00	-0.08	-51.53	-157.05	-281.12	-410.61	-500.06	-521.27	0.00	0.00			
	Soil moisture	100.00	100.00	100.00	99.92	59.73	20.79	6.01	1.65	0.67	0.54	4.50	41.52			
	Change in soil moisture	37.05	21.44	0.00	-0.08	-40.19	-38.94	-14.78	-4.37	-0.97	-0.13	3.96	37.01			
	AET	8.87	10.73	24.63	40.22	70.76	53.66	32.49	11.60	7.96	27.73	25.80	7.93	323.4	78%	
	Excess precipitation (HAET)	19.74	11.38	23.03	10.58	3.30	0.00	0.04	0.00	0.00	2.00	2.90	16.63	89.6		
Surface runoff	19.74	7.11	9.04	10.58	3.30	0.00	0.04	0.00	0.00	2.00	2.90	16.63	71.3	17%		
Groundwater recharge	0.00	4.27	13.99	0.00	0.00	0.00	0.00	0.00	0.00	0.00	0.00	0.00	18.3	4%		
													TOTAL	413.0	100%	
Zone 3	Parameter	Jan	Feb	Mar	Apr	May	Jun	Jul	Aug	Sep	Oct	Nov	Dec	TOTAL	Ratio to prec.(%)	
	Mean Monthly Temperature (°C)	2.8	3.2	6.0	8.7	14.4	19.3	21.6	22.1	18.6	11.4	7.4	2.2			
	i	0.41	0.50	1.30	2.31	4.94	7.70	9.16	9.48	7.32	3.46	1.81	0.29	48.7		
	a:	1.3	1.3	1.3	1.3	1.3	1.3	1.3	1.3	1.3	1.3	1.3	1.3	15.1		
	UPET	7.93	9.27	20.62	33.17	62.40	90.30	104.28	107.33	86.58	46.45	27.05	5.96	601.3		
	PET	6.82	7.78	21.23	36.48	76.12	111.07	130.35	125.57	89.17	45.06	22.99	4.94	677.6		
	r	0.86	0.84	1.03	1.10	1.22	1.23	1.25	1.17	1.03	0.97	0.85	0.83			
	Precipitation (mm)	92.0	60.1	65.8	70.0	46.7	20.3	24.5	10.0	9.6	40.8	45.1	85.0	569.9		
	Surface runoff coefficient	1	1	1	1	1	1	1	0	0	1	1	1			
	Surface runoff (mm)	39.16	17.03	20.61	23.39	9.52	0.36	1.09	0.00	0.00	6.69	8.68	33.92			
	Infiltration (I)	52.82	43.05	45.15	46.60	37.22	19.95	23.40	9.99	9.64	34.16	36.39	51.04			
	I-PET	46.00	35.27	23.92	10.11	-38.90	-91.11	-106.95	-115.59	-79.53	-10.90	13.40	46.10			
	TOTAL (P-PET)	0.00	0.00	0.00	0.00	-38.90	-130.01	-238.96	-352.54	-432.08	-442.98	0.00	0.00			
	Soil moisture	100.00	100.00	100.00	100.00	67.77	27.25	9.35	2.94	1.33	1.19	14.59	60.69			
	Change in soil moisture	39.21	0.00	0.00	0.00	-32.23	-40.52	-17.90	-6.41	-1.61	-0.14	13.40	46.10			
	AET	6.82	7.78	21.23	36.48	69.45	60.48	41.30	16.39	11.26	34.29	22.99	4.94	333.4	59%	
	Excess precipitation (HAET)	45.84	52.30	44.53	33.50	9.52	0.36	1.09	0.00	0.00	6.69	8.68	33.92	236.4		
Surface runoff	39.16	17.03	20.61	23.39	9.52	0.36	1.09	0.00	0.00	6.69	8.68	33.92	160.4	28%		
Groundwater recharge	6.69	35.27	23.92	10.11	0.00	0.00	0.00	0.00	0.00	0.00	0.00	0.00	76.0	13%		
													TOTAL	569.9	100%	
Zone 4	Parameter	Jan	Feb	Mar	Apr	May	Jun	Jul	Aug	Sep	Oct	Nov	Dec	TOTAL	Ratio to prec.(%)	
	Mean Monthly Temperature (°C)	1.0	1.4	4.2	6.9	12.6	17.5	19.8	20.3	16.8	9.6	5.6	0.4			
	i	0.09	0.14	0.76	1.63	4.03	6.64	8.03	8.34	6.28	2.67	1.18	0.02	39.8		
	a:	1.1	1.1	1.1	1.1	1.1	1.1	1.1	1.1	1.1	1.1	1.1	1.1	13.5		
	UPET	3.35	4.78	16.81	29.67	58.28	84.41	97.21	99.97	80.98	42.87	23.46	1.29	543.1		
	PET	2.88	4.01	17.31	32.64	71.10	103.83	121.51	116.97	83.41	41.58	19.94	1.07	616.3		
	r	0.86	0.84	1.03	1.10	1.22	1.23	1.25	1.17	1.03	0.97	0.85	0.83			
	Precipitation (mm)	116.0	75.8	83.0	88.3	59.0	25.6	30.9	12.6	12.2	51.5	56.8	107.2	718.9		
	Surface runoff coefficient	1	1	1	1	1	1	1	0	0	1	1	1			
	Surface runoff (mm)	54.70	24.99	29.86	33.62	14.57	0.94	2.19	0.00	0.00	10.56	13.39	47.75			
	Infiltration (I)	61.33	50.81	53.10	54.67	44.40	24.69	28.71	12.60	12.16	40.97	43.46	59.44			
	I-PET	58.45	46.80	35.79	22.03	-26.70	-79.14	-92.80	-104.37	-71.24	-0.61	23.53	58.36			
	TOTAL (P-PET)	0.00	0.00	0.00	0.00	-26.70	-105.84	-198.84	-303.01	-374.26	-374.87	0.00	0.00			
	Soil moisture	100.00	100.00	100.00	100.00	76.57	34.70	13.72	4.83	2.37	2.35	25.88	84.24			
	Change in soil moisture	15.76	0.00	0.00	0.00	-23.43	-41.87	-20.98	-8.89	-2.46	-0.01	23.53	58.36			
	AET	2.88	4.01	17.31	32.64	67.83	66.56	49.69	21.48	14.62	40.99	19.94	1.07	339.0	47%	
	Excess precipitation (HAET)	97.39	71.79	65.65	55.65	14.57	0.94	2.19	0.00	0.00	10.56	13.39	47.75	379.9		
Surface runoff	54.70	24.99	29.86	33.62	14.57	0.94	2.19	0.00	0.00	10.56	13.39	47.75	232.6	32%		
Groundwater recharge	42.69	46.80	35.79	22.03	0.00	0.00	0.00	0.00	0.00	0.00	0.00	0.00	147.3	20%		
													TOTAL	718.9	100%	

Table 6.3. Hydraulic conductivity values assigned to the model

AGE	SYMBOL	Hydraulic Conductivity of units, K (m/s)				Assigned value
		Minimum	Maximum	Average		
				Aritmetic	Geometric	
Quaternary		4×10^{-5}				Qt, Qal, Qym: 4.7×10^{-5} , Qay: 9×10^{-4}
Plio-Quaternary		1.73×10^{-6}	6.45×10^{-5}	1.67×10^{-5}	1.17×10^{-5}	9×10^{-6} (Layer 1-2-3), plQt: 1×10^{-7}
						8×10^{-6} (Layer 4)
						6×10^{-6} (Layer 5)
Pliocene						3×10^{-6} (Layer 6-7)
Oligocene		9.10×10^{-6}	7.26×10^{-5}	3.95×10^{-5}	2.96×10^{-5}	2.6×10^{-5}
Paleocene		1.06×10^{-3}				1×10^{-3}
Cretaceous		1.53×10^{-5}	4.92×10^{-5}	2.42×10^{-5}	2.18×10^{-5}	Kkzm-Jko-Kmo: 7×10^{-7} , TRjd: 7×10^{-6} , Kst: 8×10^{-6}
						
Eocene		No pumping test result				1×10^{-6}

Within the model domain, the lateral and vertical hydraulic conductivity distributions along the cross-sections C-C' and D-D' are given in Figure 6.6.

The specific yield and specific storage values in the model domain were determined during simulations under transient conditions. The initial value of the specific yield was 0.2 in the model. During calibration, it is assumed to be 0.15 and 0.05 for the alluvium and the other units, respectively.

The specific storage parameter is determined as $1 \times 10^{-5} \text{ m}^{-1}$ for the units within the study area. The distribution of storage parameters within the model domain is given in Figure 6.7.

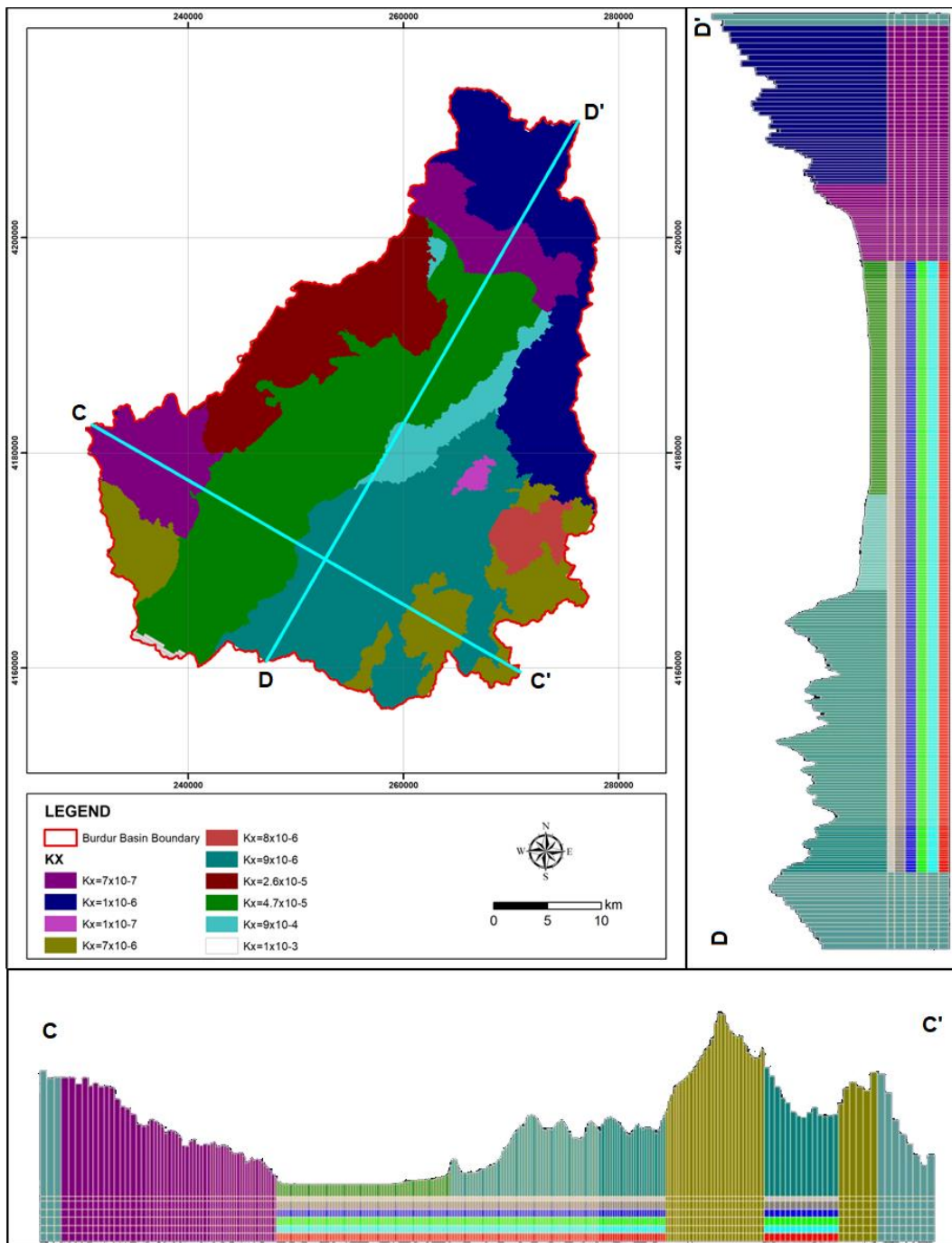


Figure 6.6. Hydraulic conductivity distribution within the model domain

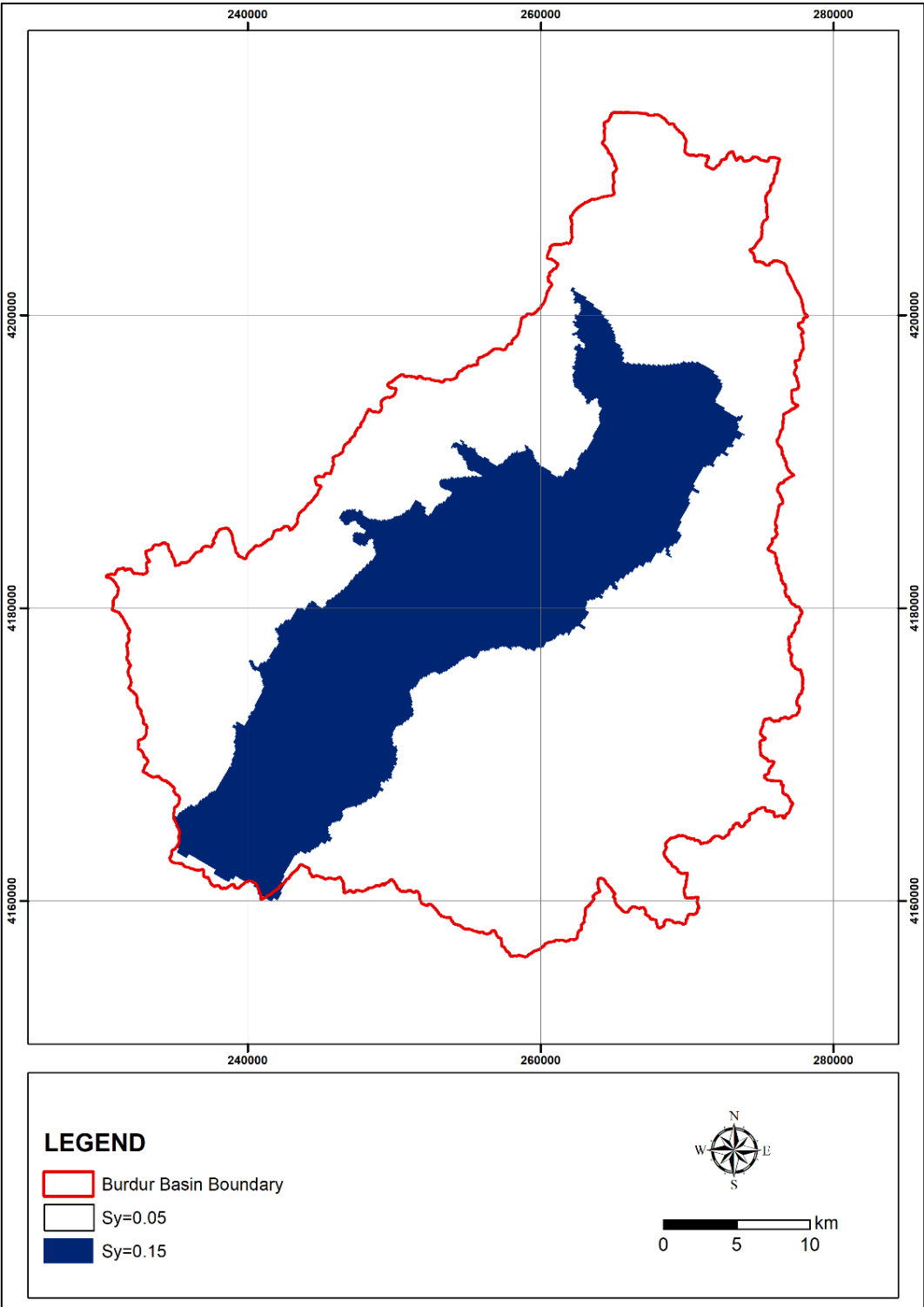


Figure 6.7. Specific yield distribution within the model domain

6.5 Calibration

Model calibration is the process of establishing a set of parameters, boundary conditions, and stresses that produce simulated heads that match the measured values within acceptable error limits (Anderson & Woessner, 1991). In this study, the trial-and-error adjustment was used to estimate calibrated geological, hydrological, and hydrogeological model parameters for both steady-state and transient simulations. In addition to groundwater levels, Burdur Lake levels and calculated groundwater and lake budgets were compared with the measurements to test the success of the calibrated models.

6.5.1 Steady-State Calibration

In the Burdur Lake basin, steady-state models were developed simulating the years 1969 and 2014 to obtain the initial head values of the transient models by using the calibrated hydraulic conductivity values and boundary conditions except for the lake boundary. Since the simulation of the interaction between the lake and groundwater is meaningful only under the transient conditions, Burdur Lake was represented with a constant head boundary condition in these models.

The root mean square error (RMSE) and normalized RMSE (NRMSE) were used as a measure of the success of the match between observed and calculated groundwater levels.

$$RMS = \left[\frac{1}{n} \sum_{i=1}^n (h_m - h_s)_i^2 \right]^{0.5} \quad (Eq. 6.3)$$

$$NRMS(\%) = \frac{RMS}{(h_m)_{max} - (h_m)_{min}} \quad (Eq. 6.4)$$

where:

n : total number of observation points

h_m : measured hydraulic head

h_s : simulated hydraulic head

$(h_m)_{max}$: maximum value of observed hydraulic head

$(h_m)_{min}$: minimum value of observed hydraulic head

For the calibration of the steady-state model simulating the natural conditions of the basin in 1969, 24 observation wells were used. The model was calibrated with an RMSE of 13.52 m and NRMSE of 4.03 %, indicating that the model can successfully simulate the actual field conditions (Figure 6.8). The areal distributions of the calculated groundwater levels are shown in Figure 6.9. The observed and calculated groundwater levels are consistent, as seen in Figures 4.13 and 6.9.

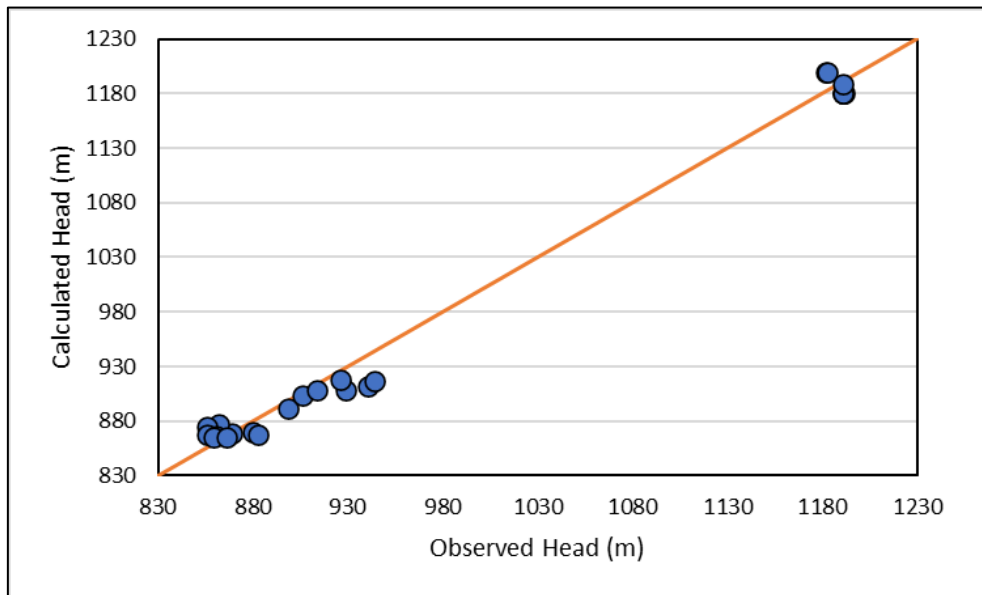


Figure 6.8. Observed vs. calculated groundwater levels (1969)

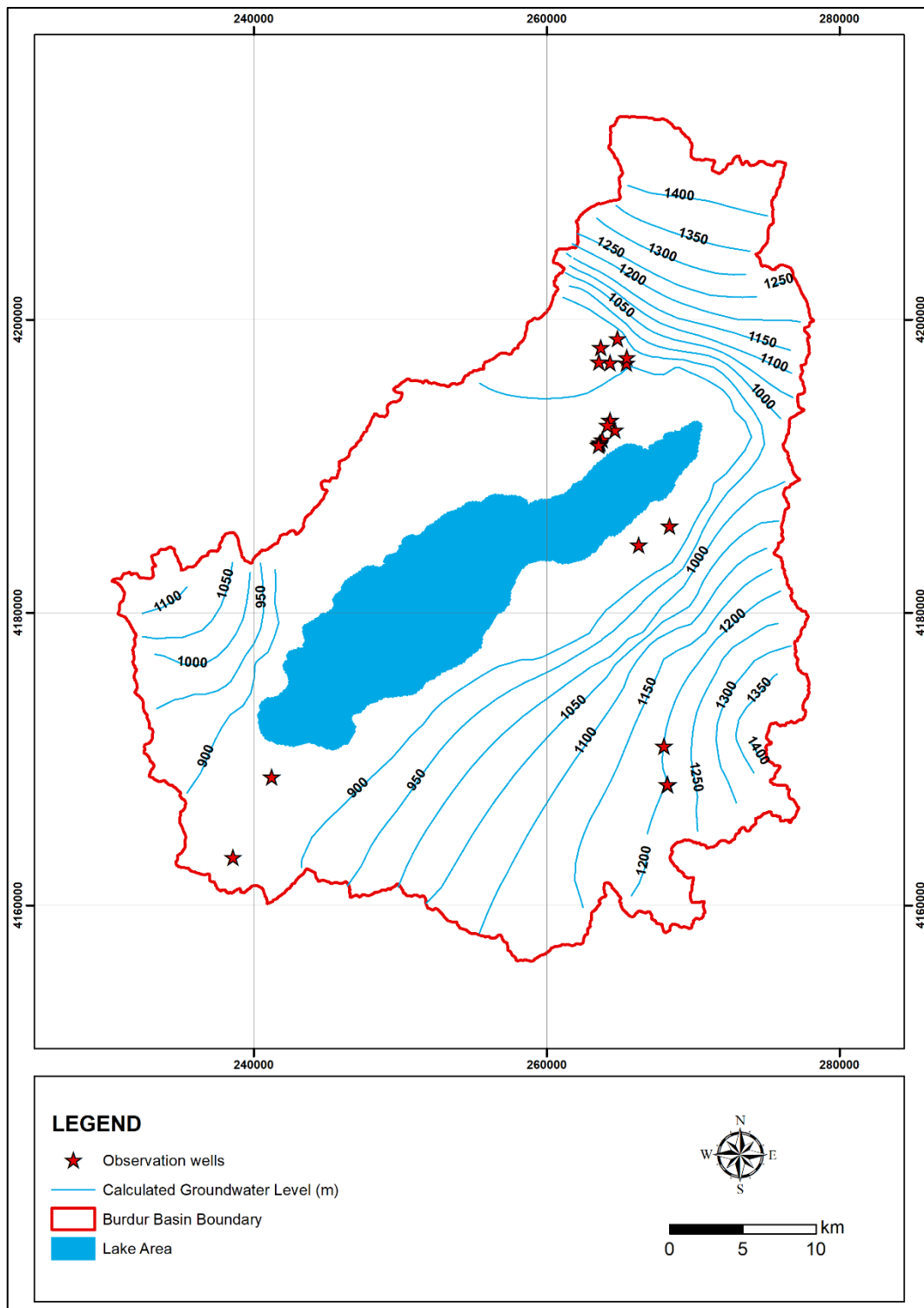


Figure 6.9. Calculated groundwater levels (1969)

The steady-state model, which represents the higher groundwater discharge rates in 2014, is calibrated using 39 observation wells. At the end of the calibration, RMSE and NRMSE were calculated as 17.26 m and 3.49 %, respectively (Figure 6.10). The groundwater levels of calibrated model show consistency with the groundwater level map generated in the conceptual model (Figures 4.14 and 6.11).

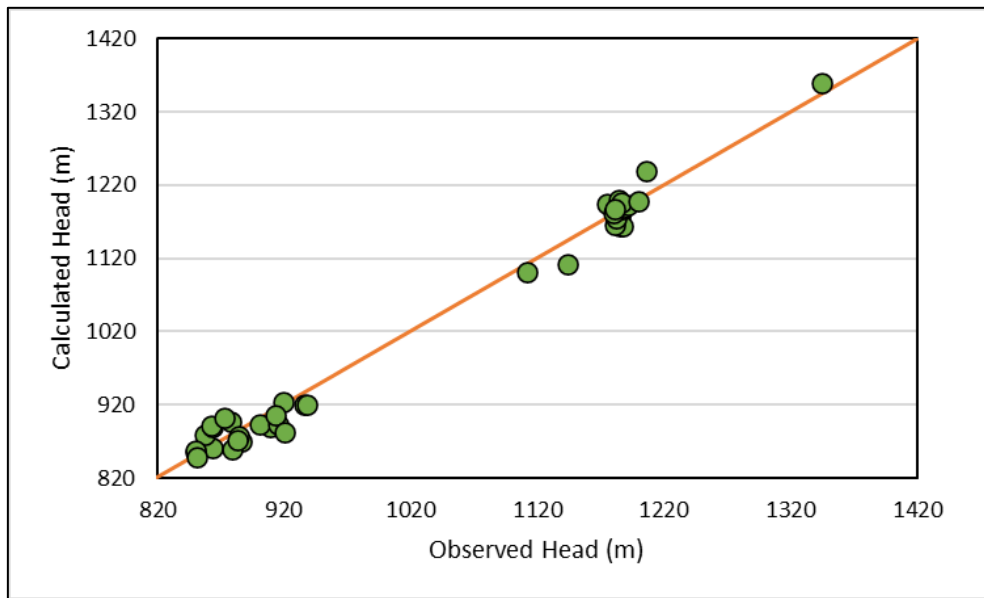


Figure 6.10. Observed vs. calculated groundwater levels (2014)

Calculating the groundwater budget is challenging at the basin scale because of the uncertainties of groundwater usage. Although the groundwater budget could not be used as a calibration parameter, the calculated groundwater budgets for 1969 and 2014 by the MODFLOW models are given in Table 6.4.

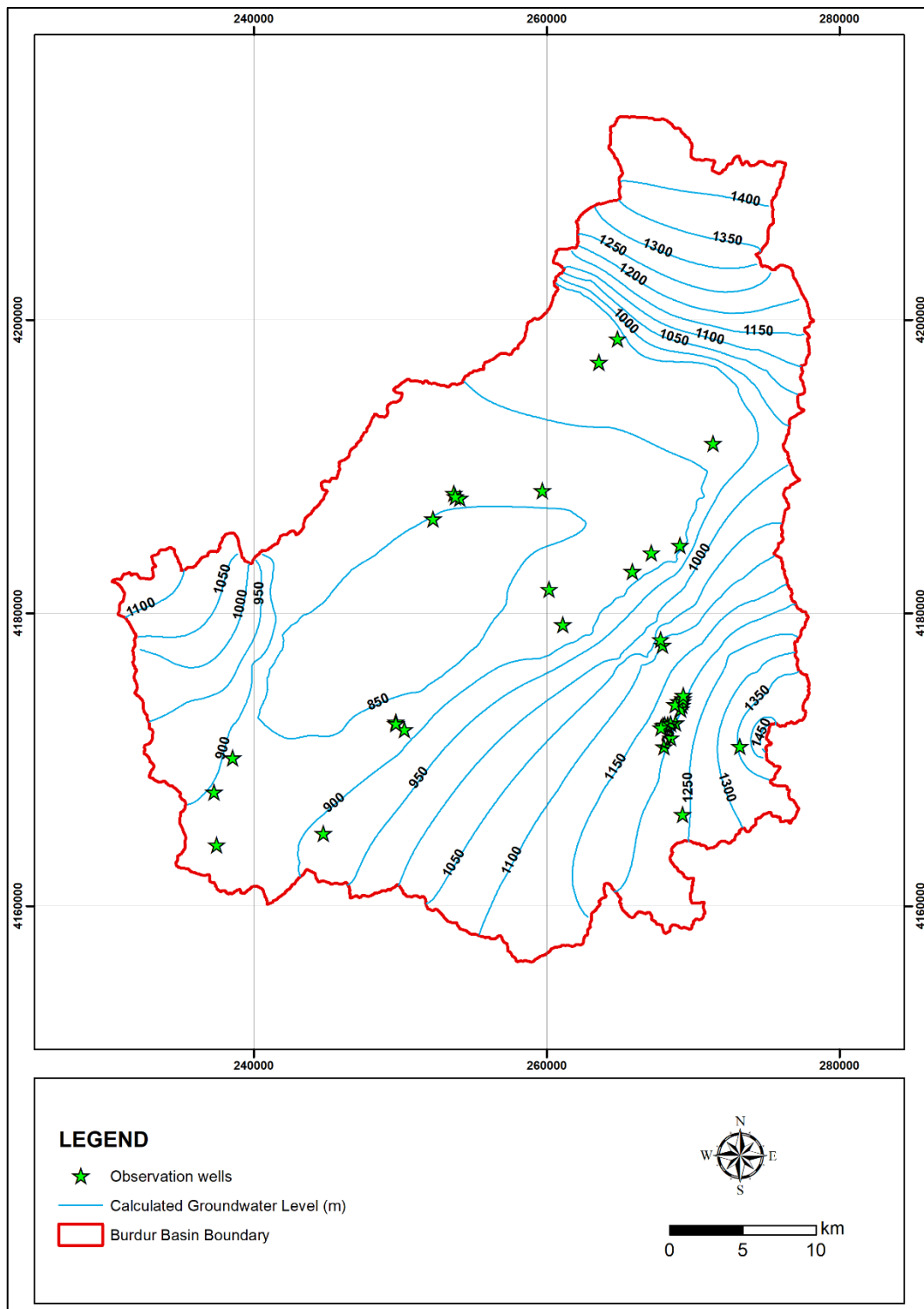


Figure 6.11. Calculated groundwater levels (2014)

Table 6.4. Calculated groundwater budget for the steady state simulations

1969			
RECHARGE (hm ³ /year)		DISCHARGE (hm ³ /year)	
Recharge	132	Constant head (lake)	167
GHB (East)	52	Pumping wells	4
GHB (South)	0.17	Drains (Springs)	13
TOTAL	184	TOTAL	184
2014			
Recharge	133.46	Constant head (lake)	121.41
GHB (East)	52.28	Pumping wells	64.33
GHB (South)	-	Drains (Springs)	-
TOTAL	186	TOTAL	186

6.5.2 Transient Calibration

Steady-state calibrated groundwater models were also simulated under transient conditions to assess the temporal aspects of the aquifer-lake responses to the changes. The transient simulation periods are from January 1969 to December 1971 and from January 2014 to December 2016. These periods were divided into 36 monthly stress periods separately to represent variations in recharge, discharge, storage, and lake levels.

Agricultural groundwater pumpages were apportioned between May and September, and a lake boundary condition represented Burdur Lake. To achieve transient calibration, measured and observed lake and groundwater levels and conceptual and calculated lake budgets are compared.

6.5.2.1 Lake Levels

Lake level calibration was conducted based on measurements of Burdur Lake level and the corresponding model lake stage values. In order to check the validity of calibrations and the goodness of the matches between observed and calculated lake levels, in addition to R^2 , RMSE, and NRMSE, ME (Mean Error) and MAE (Mean Absolute Error) parameters were also calculated.

$$ME = \frac{1}{n} \sum_{i=1}^n (h_m - h_s)_i \quad (\text{Eq. 6.5})$$

$$MAE = \frac{1}{n} \sum_{i=1}^n |(h_m - h_s)_i| \quad (\text{Eq. 6.6})$$

where:

n : total number of observation points

h_m : measured lake level

h_s : simulated lake level

The observed and calculated lake levels were compared to check the consistency of the model results. Although observed and calculated lake levels are coherent between 1969 and 1971 and 2014-2015, these are incompatible between November 2015 and June 2016 (Figures 6.12 and 6.13). However, when the lake level measurements are examined in detail during this period, it is seen that the lake levels were measured at the same level for eight consecutive months in different seasons (Figure 6.13), which most likely represents data errors. Hence, Burdur lake levels were also analyzed by extracting volume for the same period from the satellite images (Figure 6.14).

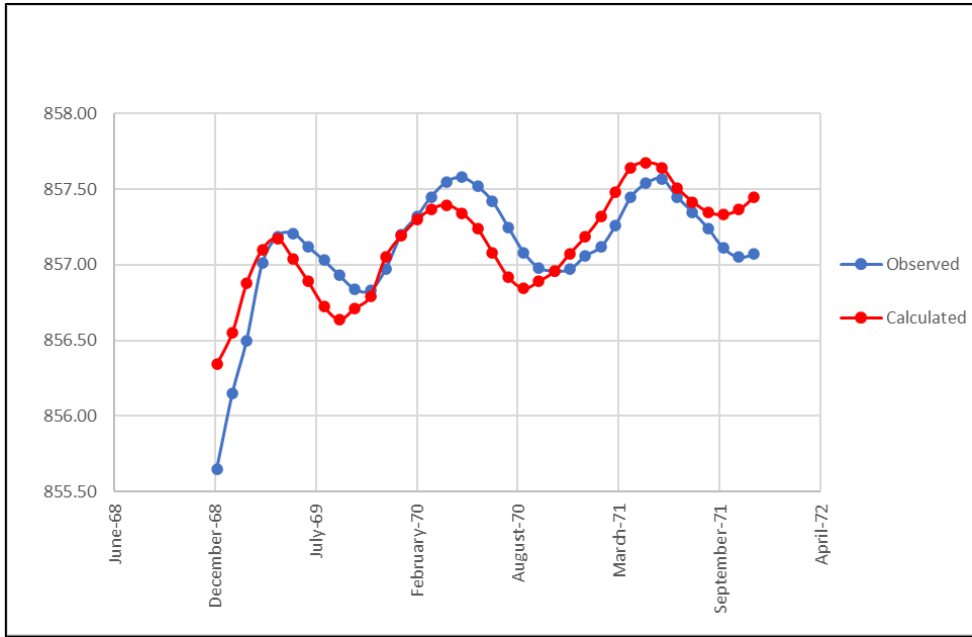


Figure 6.12. Observed and calculated lake levels from January 1969-December 1971 (NRMSE=0.12, RMSE= 0.24, MAE= 0.19, ME= -0.03, R²=0.63)

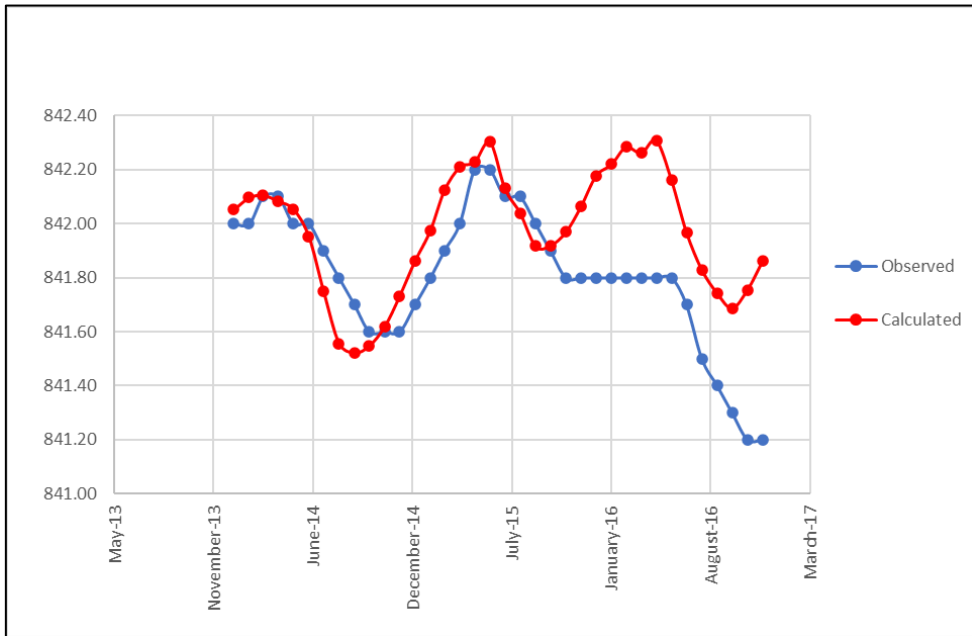


Figure 6.13. Observed and calculated lake levels from January 2014-December 2016 (NRMSE=0.28, RMSE= 0.28, MAE= 0.21, ME= -0.17, R²=0.34)

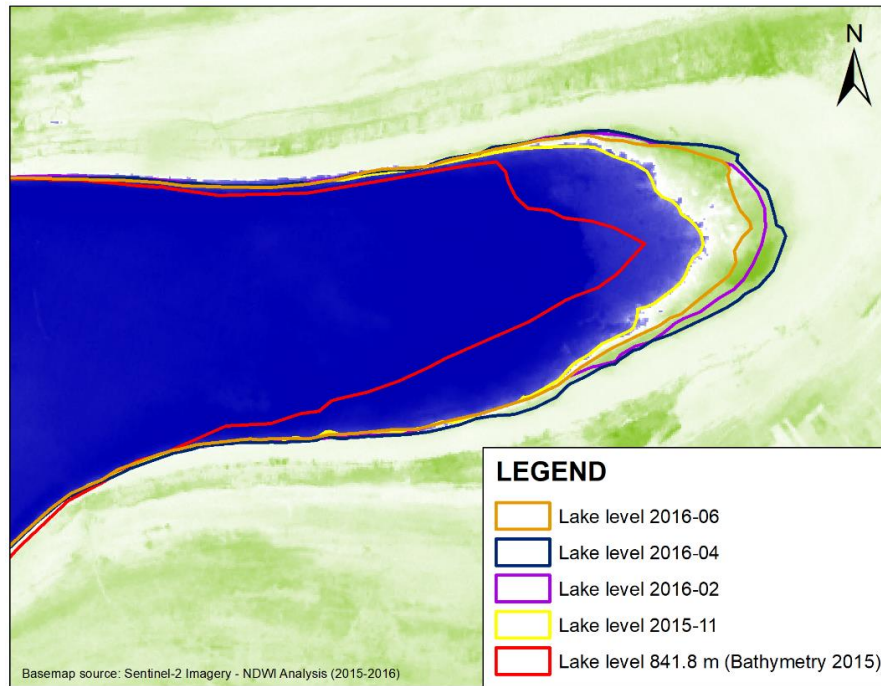


Figure 6.14. Burdur Lake level changes according to the satellite image

Although the lake area and the lake level change can be seen based on this analysis, the absence of any difference in the lake level measurements indicates a measurement error. Therefore, the models, calibrating with error values in Figures 6.12 and 6.13, show that the model could simulate lake level change successfully for the years between January 1969 - December 1971 and January 2014 – December 2016. In order to check the model performance simulating the years 2014-2016, the measured and observed lake levels were redrawn by excluding the year considered to have been incorrectly measured. Calculated error parameters are shown in Figure 6.15.

6.5.2.2 Calibrated Lake Budgets

The conceptual lake budget was simulated using the lake boundary condition to obtain calculated lake stages and calculate the groundwater inflow and outflow from the lake.

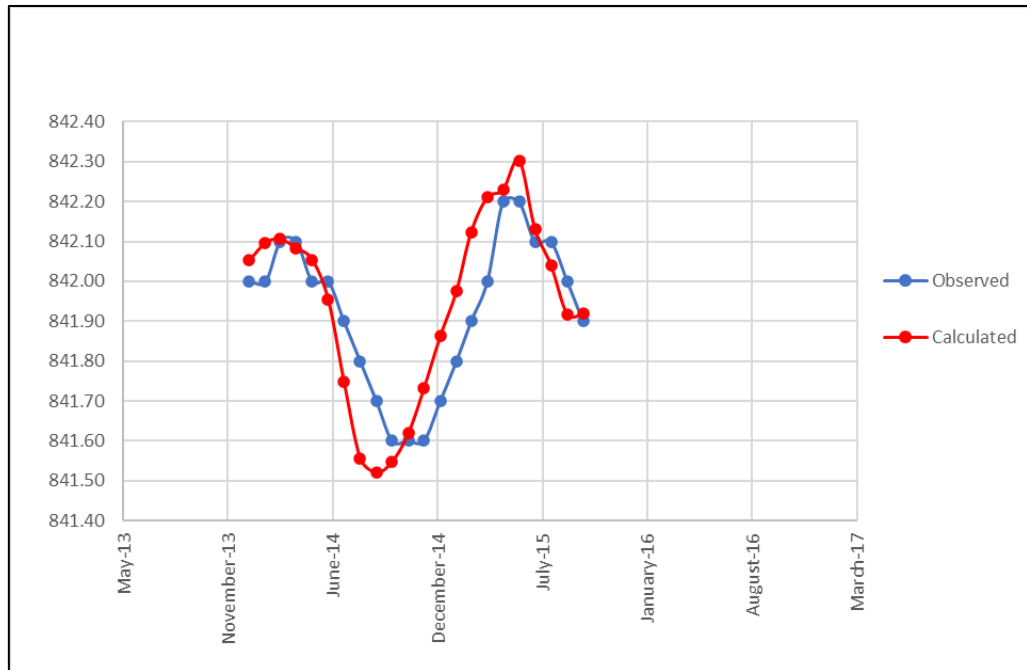


Figure 6.15. Observed and calculated lake levels from January 2014-October 2015 (NRMSE=0.20, RMSE= 0.12, MAE= 0.10, ME= -0.02, R²=0.72)

The results are given in Table 6.5, Figure 6.16, and Table 6.6, Figure 6.17 for January 1969 – December 1971 and January 2014 – December 2016, respectively. As seen from these tables and pie charts, groundwater inflow has the highest contribution to the lake, while evaporation is the main reason for the lake water discharge for both periods. These major components are followed by runoff and precipitation as recharge and groundwater outflow as discharge. Although the ratio of the groundwater inflow to the lake relative to precipitation and runoff increases, the total amount decreases with time with the effect of excessive pumping and the decrease in the precipitation and runoff. Lake water outflow to the groundwater does not show a significant difference over the years since the evaporation rate does not change dramatically (Tables 6.5-6.6 and Figures 6.16-6.17).

Table 6.5. Calculated monthly lake budget (January 1969-December 1971)

(hm ³ /month)	Precipitation	Runoff	GW inflow	Total lake recharge	Evaporation	GW outflow	Total lake discharge	Reserve Change
January-69	17.70	54.31	4.63	76.64	4.72	0.05	4.76	71.87
February-69	12.01	33.22	5.34	50.57	6.11	0.03	6.15	44.43
March-69	15.14	56.71	5.81	77.66	9.94	0.05	9.99	67.67
April-69	6.93	46.71	5.90	59.55	12.40	0.03	12.43	47.11
May-69	4.39	30.25	6.16	40.80	25.61	0.01	25.62	15.19
June-69	0.45	6.94	6.56	13.94	41.73	0.00	41.73	-27.78
July-69	1.73	4.74	6.83	13.30	44.45	0.00	44.45	-31.15
August-69	3.98	4.49	7.08	15.55	49.79	0.00	49.79	-34.24
September-69	2.66	10.74	7.21	20.62	38.57	0.00	38.57	-17.96
October-69	16.03	10.62	7.21	33.85	18.66	0.01	18.66	15.19
November-69	7.61	12.27	7.27	27.16	10.12	0.01	10.13	17.03
December-69	26.29	28.38	7.17	61.83	7.95	0.03	7.99	53.84
January-70	2.23	25.13	7.28	34.64	5.37	0.02	5.39	29.25
February-70	6.31	17.75	7.51	31.57	9.11	0.01	9.12	22.45
March-70	4.77	19.60	7.91	32.27	17.73	0.01	17.74	14.54
April-70	5.38	12.47	7.85	25.71	19.43	0.00	19.43	6.28
May-70	2.72	5.95	7.99	16.67	27.76	0.00	27.76	-11.10
June-70	3.12	3.99	8.15	15.26	36.77	0.00	36.77	-21.52
July-70	3.28	2.54	8.33	14.15	47.04	0.00	47.04	-32.89
August-70	0.00	1.40	8.48	9.88	43.79	0.00	43.79	-33.91
September-70	4.70	2.39	8.53	15.62	31.36	0.00	31.36	-15.74
October-70	10.40	6.34	8.48	25.22	15.22	0.00	15.22	10.00
November-70	7.24	8.51	8.49	24.25	10.20	0.00	10.21	14.04
December-70	8.79	11.51	8.46	28.76	4.50	0.01	4.51	24.25
January-71	8.56	15.43	8.49	32.48	9.16	0.01	9.17	23.32
February-71	11.41	14.35	8.65	34.40	6.14	0.01	6.15	28.25
March-71	11.14	28.34	8.93	48.41	14.42	0.02	14.44	33.97
April-71	9.45	30.92	8.74	49.11	16.26	0.02	16.27	32.84
May-71	9.51	15.57	8.81	33.89	26.57	0.00	26.58	7.31
June-71	8.91	11.39	8.91	29.21	35.82	0.00	35.82	-6.60
July-71	1.26	3.58	9.08	13.92	41.61	0.00	41.61	-27.69
August-71	6.79	3.94	9.15	19.88	39.68	0.00	39.68	-19.80
September-71	2.27	3.00	9.21	14.48	28.55	0.00	28.55	-14.08
October-71	4.21	3.21	9.22	16.64	20.30	0.00	20.30	-3.66
November-71	3.84	4.33	9.20	17.37	10.36	0.00	10.36	7.01
December-71	6.62	8.00	9.17	23.80	6.58	0.01	6.59	17.21
AVERAGE	7.16	15.53	7.84	30.53	22.05	0.01	22.06	8.47

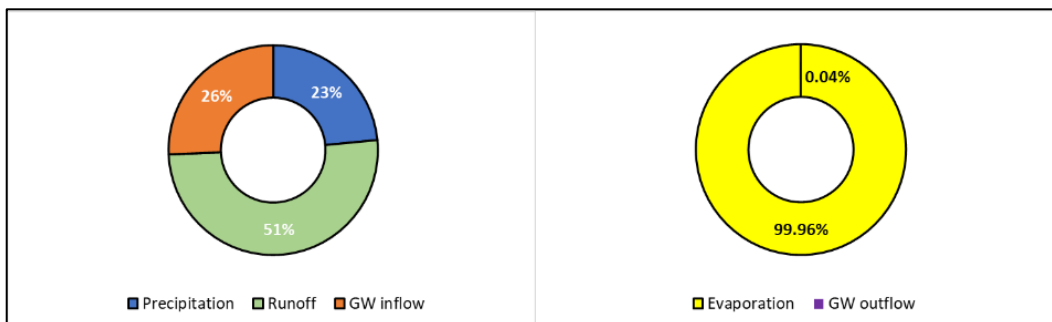


Figure 6.16. Calculated lake discharge and recharge percentages (January 1969-December 1971)

Table 6.6. Calculated monthly lake budget (January 2014-December 2016)

(hm ³ /month)	Precipitation	Runoff	GW inflow	Total lake recharge	Evaporation	GW outflow	Total lake discharge	Reserve Change
January-14	3.02	3.54	3.12	9.67	2.33	0.00	2.33	7.34
February-14	1.01	6.56	3.69	11.25	5.04	0.00	5.04	6.22
March-14	0.37	4.17	4.25	8.79	7.36	0.00	7.36	1.43
April-14	2.38	1.67	4.69	8.74	11.55	0.00	11.55	-2.81
May-14	2.28	2.84	5.06	10.18	13.93	0.00	13.93	-3.75
June-14	1.32	0.89	5.39	7.61	21.03	0.00	21.03	-13.42
July-14	0.29	0.00	5.71	6.00	33.40	0.00	33.40	-27.40
August-14	0.56	0.00	5.93	6.49	32.21	0.00	32.21	-25.72
September-14	4.58	1.08	6.01	11.67	16.40	0.00	16.40	-4.74
October-14	3.68	3.41	6.12	13.22	9.59	0.00	9.59	3.63
November-14	4.42	3.59	6.21	14.22	4.60	0.00	4.61	9.61
December-14	6.44	6.03	6.26	18.72	3.50	0.01	3.51	15.22
January-15	4.71	9.40	6.30	20.41	2.88	0.01	2.89	17.52
February-15	5.38	7.62	6.44	19.44	4.18	0.01	4.19	15.25
March-15	5.80	13.44	6.66	25.89	5.94	0.01	5.95	19.95
April-15	2.75	11.82	6.60	21.17	9.51	0.00	9.51	11.66
May-15	7.52	4.37	6.61	18.50	15.97	0.00	15.97	2.53
June-15	10.01	6.05	6.58	22.64	12.65	0.00	12.65	9.98
July-15	0.50	2.51	6.75	9.76	32.74	0.00	32.74	-22.97
August-15	8.79	2.70	6.78	18.27	30.61	0.00	30.61	-12.34
September-15	0.50	3.42	6.85	10.77	27.27	0.00	27.27	-16.50
October-15	1.19	7.64	6.88	15.70	15.39	0.00	15.39	0.31
November-15	0.56	9.46	6.89	16.91	10.14	0.00	10.14	6.77
December-15	0.08	10.68	6.89	17.65	5.11	0.00	5.11	12.54
January-16	5.54	8.34	6.89	20.76	5.21	0.01	5.22	15.55
February-16	1.30	6.33	7.04	14.66	8.98	0.00	8.99	5.68
March-16	4.93	8.17	7.27	20.37	11.64	0.00	11.64	8.72
April-16	2.57	6.73	7.22	16.52	19.41	0.00	19.41	-2.89
May-16	8.37	6.97	7.13	22.47	16.30	0.00	16.30	6.18
June-16	3.10	1.02	7.25	11.36	31.30	0.00	31.30	-19.94
July-16	2.89	1.70	7.33	11.92	37.67	0.00	37.67	-25.75
August-16	7.84	1.71	7.35	16.90	35.60	0.00	35.60	-18.70
September-16	2.44	1.19	7.35	10.98	22.64	0.00	22.64	-11.66
October-16	0.05	2.40	7.41	9.86	17.24	0.00	17.24	-7.38
November-16	7.42	3.17	7.37	17.96	8.85	0.00	8.86	9.10
December-16	5.40	5.86	7.35	18.60	4.44	0.00	4.45	14.16
AVERAGE	3.61	4.90	6.38	14.89	15.35	0.002	15.35	-0.46

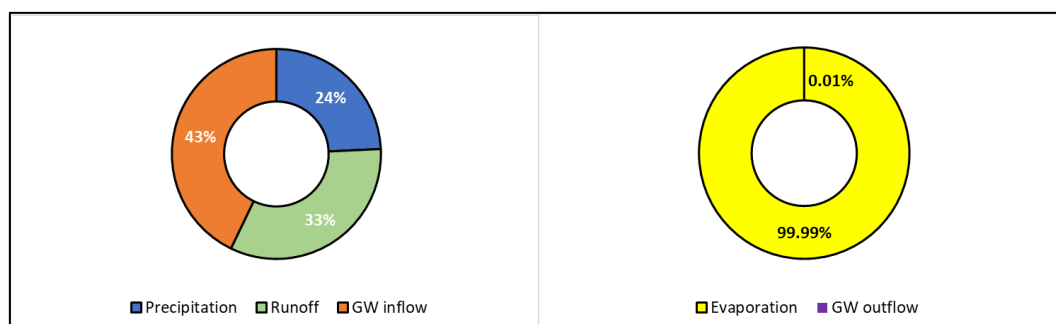


Figure 6.17. Calculated lake discharge and recharge percentages (January 2014-December 2016)

6.5.2.3 Groundwater Levels and Budgets

Groundwater level changes could not be used in the performance evaluation of the transient model simulating 1969-1971 since no continuous groundwater level measurement exists. However, the model simulating the groundwater level changes in 2014-2016 was evaluated using continuous measurements of DSI water level recorder installed wells (Figure 4.12). For this purpose, three observation wells (6980-I, 15024, 18705) with measurements for the model period were chosen to analyze transient calibration reliability (Figures 6.18-6.19-6.20). Other DSI wells with one-year measurements were also used to compare calibrated levels (Figure 6.21).

Although the observed and calculated groundwater level fluctuations are consistent, their correlation can not be considered successful. It is because getting a good correlation with the observed and calculated heads is challenging at the basin scale, as in the Burdur Lake basin with uncertainties associated with groundwater usage. However, since the fluctuations in the calculated and observed heads are similar, it can be considered that the models give proper responses to the seasonal changes.

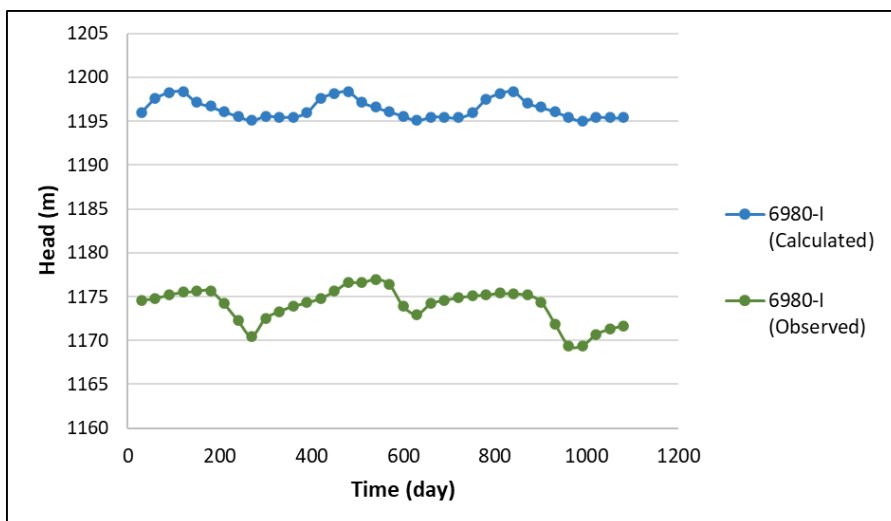


Figure 6.18. Observed and calculated head values for Well no 6980-I under transient conditions ($R^2=0.44$)

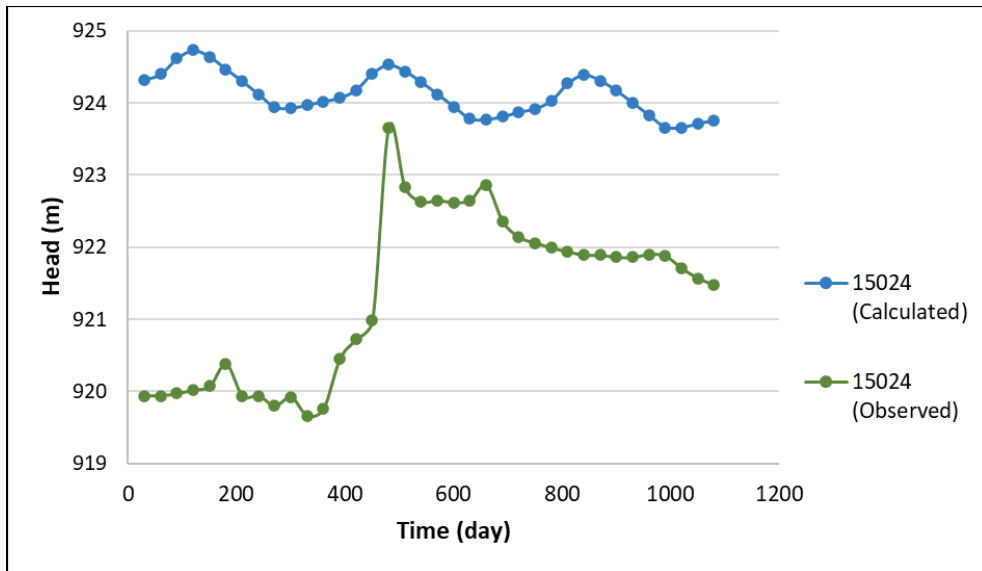


Figure 6.19. Observed and calculated head values for Well no 15024 under transient conditions ($R^2=0.07$)

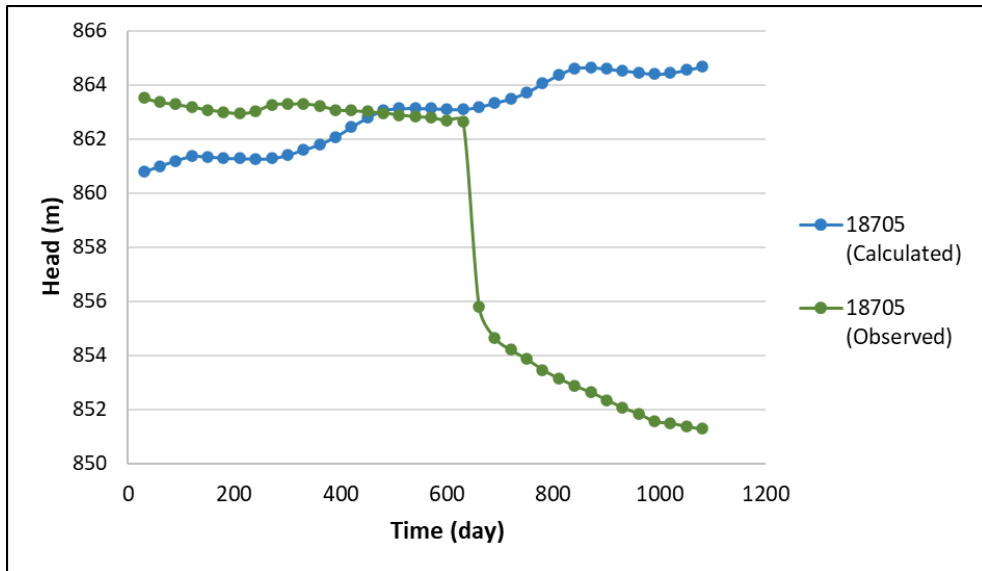


Figure 6.20. Observed and calculated head values for Well no 18705 under transient conditions ($R^2=0.77$)

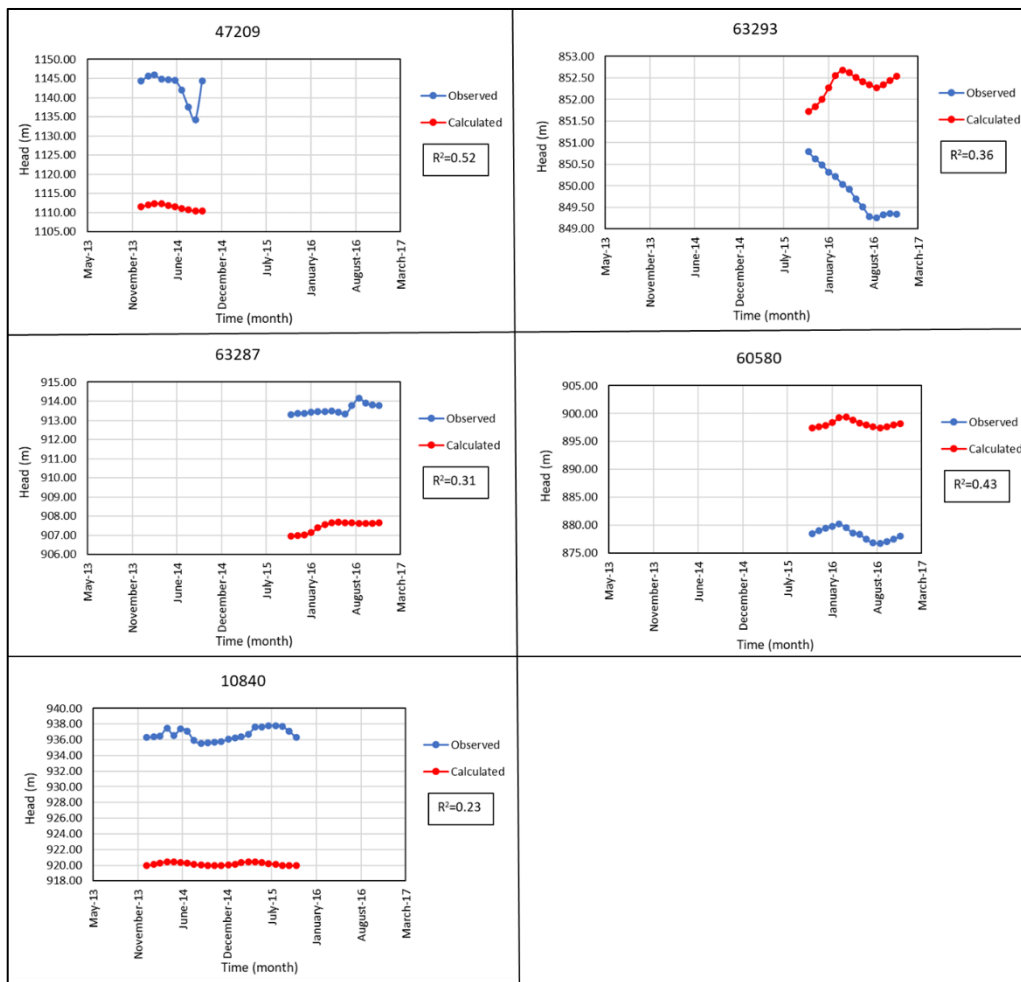


Figure 6.21. Observed and calculated head values for some DSI water level recorder installed wells

The transient calibration results were also used to specify the recharge and discharge components of the model domain (Tables 6.7 and 6.8). According to the results from January 1969 to December 1971 (Table 6.7), the recharge components include (i) recharge from precipitation (71.76 %), (ii) lateral inflow (28.18 %), and (iii) lake seepage in (0.06 %). On the other hand, the discharge components can be summarized as (i) lake seepage out (84.85 %), (ii) springs (11.64 %), and (ii) wells (3.52 %).

According to the results from January 2014 to December 2016 (Table 6.8), the recharge components include (i) recharge from precipitation (71.85 %), (ii) lateral inflow (28.14 %), and (iii) lake seepage in (0.01 %). On the other hand, the discharge components can be summarized as (i) lake seepage out (54.68 %) and (ii) wells (45.32 %).

Table 6.7. Calculated groundwater budget (January 1969-December 1971)

(hm ³ /month)	Recharge from precipitation	Lateral inflow	Lake seepage in	Total recharge	Lake seepage out	Wells	Spring	Total discharge
January-69	25.18	4.26	0.05	29.49	4.63	0.32	1.07	6.02
February-69	48.96	4.24	0.03	53.23	5.34	0.32	1.14	6.80
March-69	38.25	4.23	0.05	42.53	5.81	0.32	1.17	7.30
April-69	17.83	4.23	0.03	22.09	5.90	0.32	1.16	7.38
May-69	0.00	4.24	0.01	4.25	6.16	0.32	1.13	7.61
June-69	0.00	4.25	0.00	4.25	6.55	0.32	1.10	7.98
July-69	0.00	4.26	0.00	4.26	6.82	0.32	1.08	8.23
August-69	0.00	4.27	0.00	4.27	7.07	0.32	1.06	8.46
September-69	0.00	4.27	0.00	4.27	7.21	0.32	1.05	8.58
October-69	0.00	4.28	0.01	4.29	7.20	0.32	1.03	8.55
November-69	0.00	4.29	0.01	4.29	7.27	0.32	1.01	8.60
December-69	0.00	4.29	0.03	4.33	7.16	0.32	1.00	8.49
January-70	25.18	4.27	0.02	29.47	7.27	0.32	1.05	8.64
February-70	48.96	4.25	0.01	53.22	7.51	0.32	1.13	8.96
March-70	38.25	4.24	0.01	42.49	7.90	0.32	1.16	9.38
April-70	17.83	4.23	0.00	22.07	7.85	0.32	1.15	9.32
May-70	0.00	4.25	0.00	4.25	7.99	0.32	1.11	9.42
June-70	0.00	4.25	0.00	4.25	8.14	0.32	1.09	9.56
July-70	0.00	4.26	0.00	4.26	8.32	0.32	1.07	9.72
August-70	0.00	4.27	0.00	4.27	8.48	0.32	1.05	9.85
September-70	0.00	4.28	0.00	4.28	8.52	0.32	1.04	9.88
October-70	0.00	4.28	0.00	4.29	8.48	0.32	1.02	9.82
November-70	0.00	4.29	0.00	4.29	8.48	0.32	1.01	9.82
December-70	0.00	4.30	0.01	4.31	8.45	0.32	0.99	9.77
January-71	25.18	4.27	0.01	29.47	8.48	0.32	1.04	9.85
February-71	48.96	4.25	0.01	53.23	8.64	0.32	1.12	10.09
March-71	38.25	4.24	0.02	42.51	8.92	0.32	1.15	10.40
April-71	17.83	4.24	0.02	22.09	8.74	0.32	1.15	10.21
May-71	0.00	4.25	0.00	4.25	8.80	0.32	1.11	10.24
June-71	0.00	4.26	0.00	4.26	8.90	0.32	1.09	10.31
July-71	0.00	4.26	0.00	4.26	9.08	0.32	1.07	10.47
August-71	0.00	4.27	0.00	4.27	9.14	0.32	1.05	10.52
September-71	0.00	4.28	0.00	4.28	9.20	0.32	1.03	10.56
October-71	0.00	4.28	0.00	4.28	9.21	0.32	1.02	10.55
November-71	0.00	4.29	0.00	4.29	9.20	0.32	1.00	10.53
December-71	0.00	4.30	0.01	4.30	9.16	0.32	0.99	10.48
AVERAGE	10.85	4.26	0.01	15.12	7.83	0.32	1.07	9.23

Table 6.8. Calculated groundwater budget (January 2014-December 2016)

(hm ³ /month)	Recharge from precipitation	Lateral inflow	Lake seepage in	Total recharge	Lake seepage out	Wells	Total discharge
January-14	25.19	4.29	0.00	29.48	3.12	2.23	5.35
February-14	49.29	4.27	0.00	53.56	3.69	2.23	5.92
March-14	39.29	4.26	0.00	43.55	4.25	2.23	6.48
April-14	17.84	4.26	0.00	22.10	4.69	2.23	6.92
May-14	0.00	4.27	0.00	4.27	5.06	9.57	14.63
June-14	0.00	4.28	0.00	4.28	5.39	9.57	14.97
July-14	0.00	4.29	0.00	4.29	5.71	9.57	15.28
August-14	0.00	4.30	0.00	4.30	5.93	9.57	15.50
September-14	0.00	4.31	0.00	4.31	6.01	9.57	15.58
October-14	0.00	4.31	0.00	4.31	6.12	2.23	8.35
November-14	0.00	4.32	0.00	4.32	6.21	2.23	8.44
December-14	0.00	4.33	0.01	4.33	6.26	2.23	8.49
January-15	25.19	4.30	0.01	29.50	6.30	2.23	8.53
February-15	49.29	4.28	0.01	53.57	6.44	2.23	8.67
March-15	39.29	4.27	0.01	43.57	6.66	2.23	8.89
April-15	17.84	4.27	0.00	22.11	6.60	2.23	8.83
May-15	0.00	4.28	0.00	4.28	6.61	9.57	16.18
June-15	0.00	4.29	0.00	4.29	6.58	9.57	16.15
July-15	0.00	4.29	0.00	4.29	6.75	9.57	16.32
August-15	0.00	4.30	0.00	4.30	6.78	9.57	16.35
September-15	0.00	4.31	0.00	4.31	6.85	9.57	16.42
October-15	0.00	4.32	0.00	4.32	6.88	2.23	9.10
November-15	0.00	4.32	0.00	4.32	6.89	2.23	9.12
December-15	0.00	4.33	0.00	4.33	6.89	2.23	9.12
January-16	25.19	4.30	0.01	29.50	6.89	2.23	9.12
February-16	49.29	4.28	0.00	53.57	7.04	2.23	9.27
March-16	39.29	4.27	0.00	43.56	7.27	2.23	9.50
April-16	17.84	4.27	0.00	22.10	7.22	2.23	9.45
May-16	0.00	4.28	0.00	4.28	7.13	9.57	16.70
June-16	0.00	4.29	0.00	4.29	7.25	9.57	16.82
July-16	0.00	4.30	0.00	4.30	7.33	9.57	16.90
August-16	0.00	4.30	0.00	4.30	7.35	9.57	16.92
September-16	0.00	4.31	0.00	4.31	7.35	9.57	16.92
October-16	0.00	4.32	0.00	4.32	7.41	2.23	9.64
November-16	0.00	4.32	0.00	4.33	7.37	2.23	9.60
December-16	0.00	4.33	0.00	4.33	7.35	2.23	9.57
AVERAGE	10.97	4.29	0.00	15.26	6.38	5.29	11.67

6.6 Sensitivity Analysis

Sensitivity analysis quantifies how model results are sensitive to changes in the model parameters. This analysis is useful for estimating variances and confidence intervals for the aquifer and lake parameters to minimize model errors. In this study, simulations were conducted on the models calibrated for the years 1969, 1971, 1969-1971, and 2014-2016. In order to analyze the sensitivity of the model parameters, hydraulic conductivity values of the lithologies, the ratio of horizontal to vertical hydraulic conductivity (K_x/K_z), recharge from precipitation, the specific yield of the aquifer, and lakebed leakance values were changed by multiplying the appropriate factors (equals 1 for calibrated models). The results were evaluated by comparing the RMSE, NRMSE, MAE, and ME parameters.

The model is sensitive to changes in the hydraulic conductivity of the lithologies (Figure 6.22). It shows high sensitivity to both increase or decrease in hydraulic conductivity. Although the model is sensitive to horizontal hydraulic conductivity changes, it is insensitive to K_x/K_z (Figure 6.23).

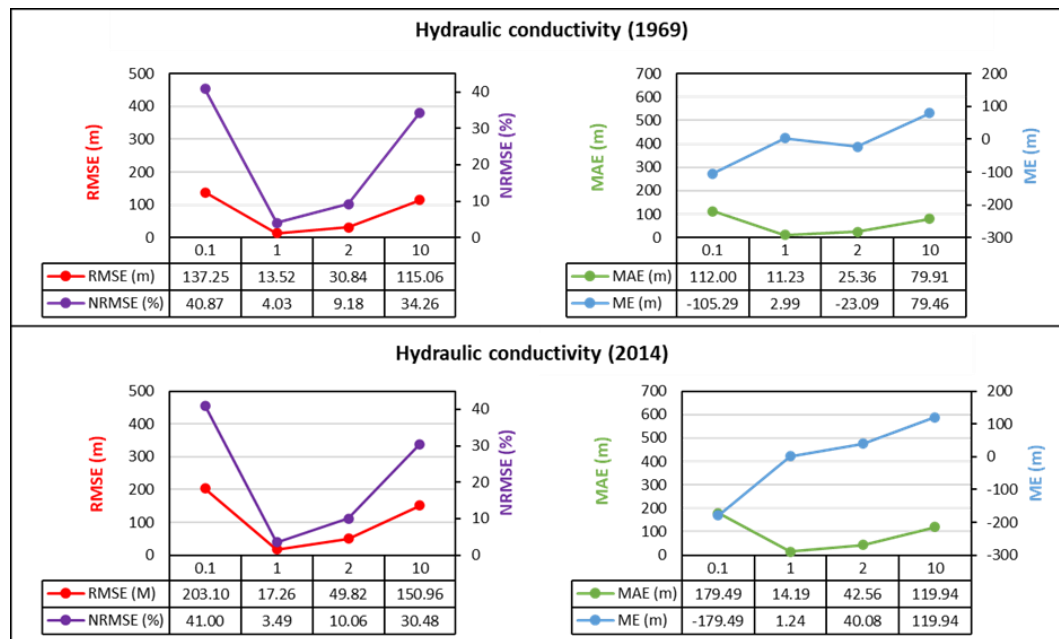


Figure 6.22. Sensitivity analysis of hydraulic conductivities of lithologies

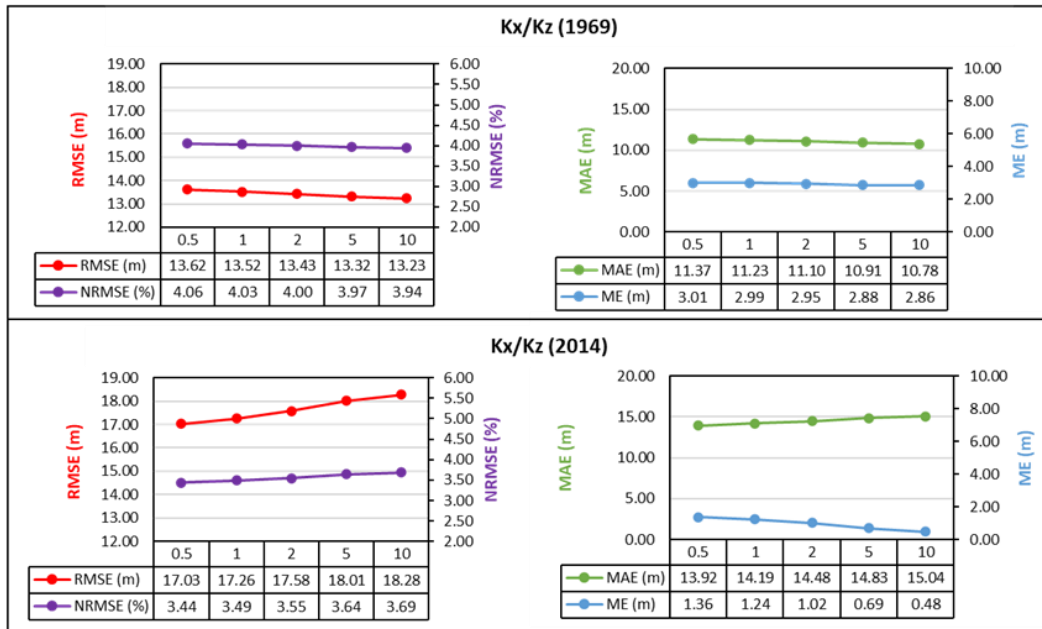


Figure 6.23. Sensitivity analysis of K_x/K_z

The recharges from precipitation assigned in the calibrated model are 18.3 mm/year, 76 mm/year, 103.8 mm/year, and 221 mm/year (Figure 6.4). In order to determine the sensitivity of this parameter, the recharge values were multiplied by the values 0.5, 2, and 4. According to the results shown in Figure 6.24, the model is more sensitive to increasing recharge rates than decreasing. Until that point, the sensitivity of hydraulic conductivity and recharge were determined by comparing the error values calculated from the differences between observed and calculated groundwater levels. In order to determine the sensitivities of specific yield and lakebed leakance, error rates calculated for the lake levels were used. The specific yield values were assigned 0.15 around the lake and 0.05 for the other regions within the model domain (Figure 6.7). When the following multipliers 0.5, 2, and 4 have been used, the calculated error values remained almost the same (Figure 6.25). It proves that the model is insensitive to the changes in the specific yield. Lakebed leakance is another parameter that the model is not sensitive to its variability (Figure 6.26). As can be seen in Figure 6.26, error rates of the lake levels did not respond to lakebed leakance changes until two digits.

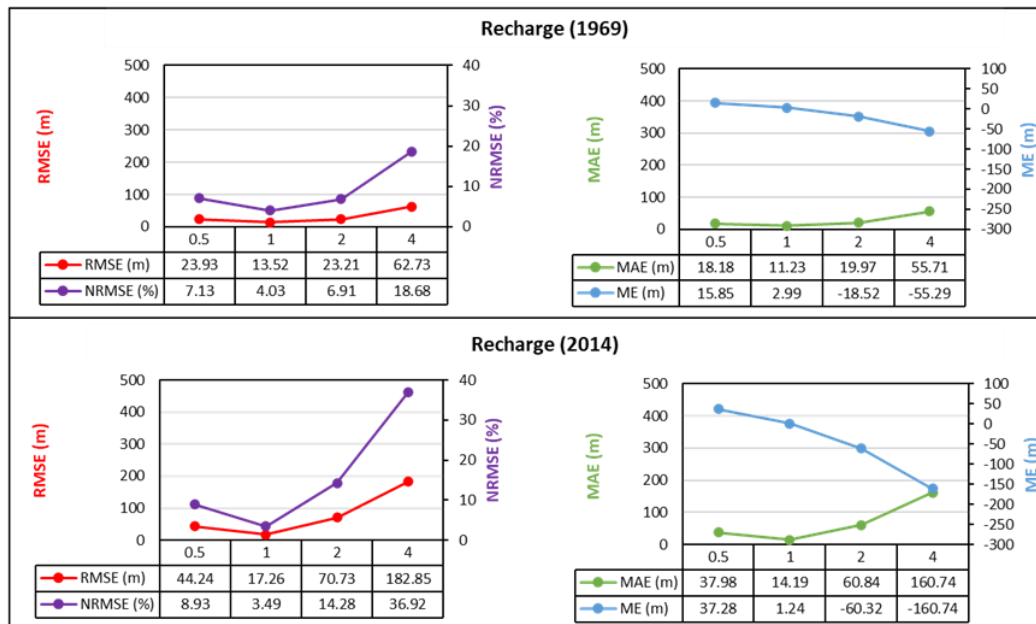


Figure 6.24. Sensitivity analysis of recharge from precipitation

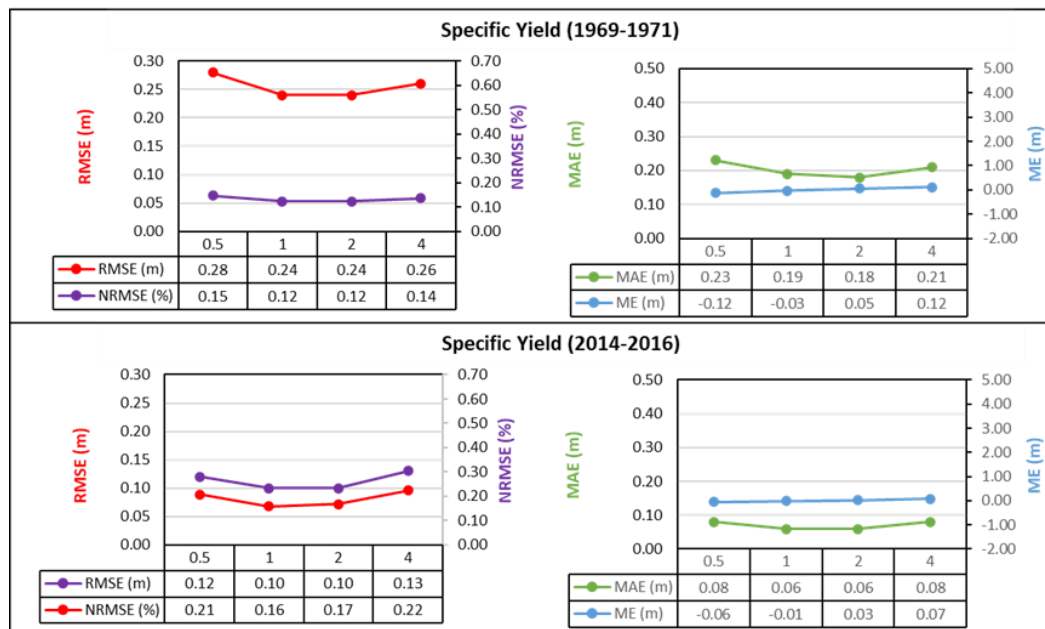


Figure 6.25. Sensitivity analysis of specific yield

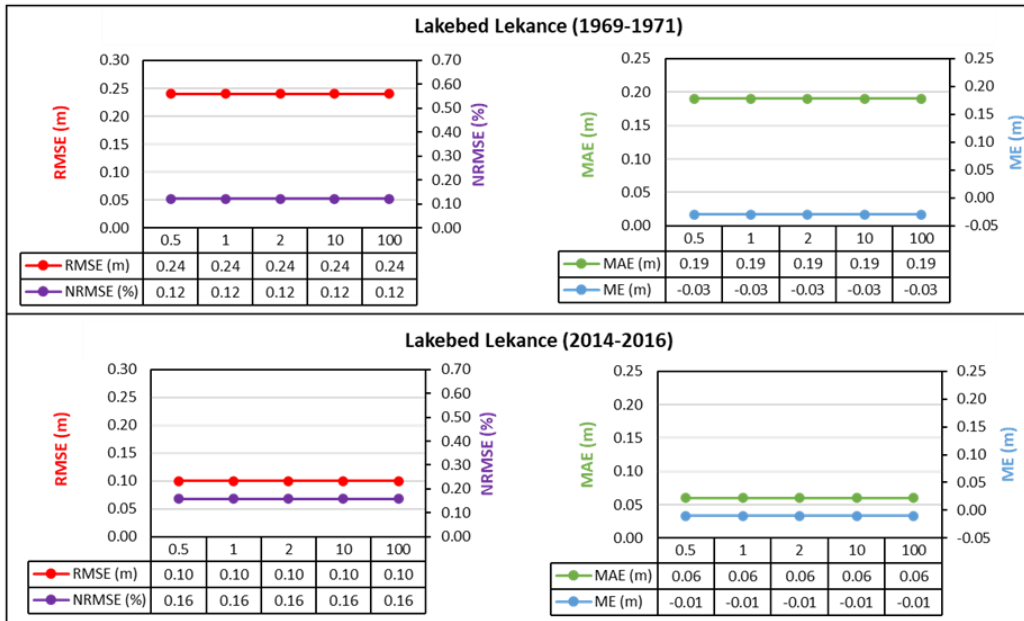


Figure 6.26. Sensitivity analysis of lakebed leakance

According to sensitivity analysis, the parameters used in the calibrated models give the lowest error rates except for K_x/K_z . The multiplication factor of 10 for the model calibrated in 1969 and 0.5 for the model calibrated in 2014 reveals the best error rates for the simulations of K_x/K_z . However, since the model is not highly sensitive to change in this parameter and provides different results for these two periods, the original values considering the optimum value were used for model calibration.

CHAPTER 7

FUTURE PREDICTIONS OF BURDUR LAKE LEVELS

Burdur Lake level was measured monthly by DSI from 1969 to 2018 (Figure 4.2). However, since the groundwater withdrawals were not recorded during all this time, a continuous model simulation could not be conducted from 1969 to 2018. Therefore, future scenarios can be utilized to investigate the causes of lake level declines in the past by estimating the sensitivity of the lake levels to future changes. These scenario simulations are also useful in developing the protection and management plan for Burdur Lake by predicting the future lake levels.

Three case scenarios were considered to estimate possible future levels of Burdur Lake due to climate change and anthropogenic activities. The simulations were conducted quarterly for a period of 46 years between January 2019 and December 2064.

7.1 Climate Models

The regional-scale climate projections were generated from the Coordinated Regional Downscaling Experiment (CORDEX) regional climate models (RCMs) with a grid resolution of 0.11° (~12.5 km) based on the worst greenhouse gas (GHG) emission scenario (RCP 8.5) and intermediate GHG emission scenario (RCP 4.5).

The daily projected precipitation and temperature data were obtained for Turkey by using a 12-member ensemble of CORDEX RCMs based on the worst GHG emission scenario (RCP8.5) in the studies conducted by Aziz and Yücel (2021) and Aziz et al. (2020). In these studies, for each of the seven geographical regions of Turkey, the performances of the CORDEX RCMs were evaluated by calculating statistics of root

mean square error (RMSE), mean absolute error (MAE), mean bias error (MBE), and correlation coefficient (CORR). Based on these statistical calculations, each model was ranked (with a rank value of 1 being the best) for each region. MOHC-HadGEM2-ES GCM, RACMO22E RCM for daily precipitation, and MOHC-HadGEM2-ES GCM, CCLM 4-8-17 RCM for daily temperature show the most skillful performances (with mean rank values smaller than 4) in Mediterranean region (Aziz and Yücel, 2020 & Aziz et al., 2020). In order to create a long-term future climate dataset to investigate the impacts of climate variabilities on Burdur Lake levels, daily precipitation and temperature data were extracted from these best top GCMs for their model periods 2006 to 2098. Then, these daily climate data were converted to the mean monthly temperature and precipitation values for the Burdur Lake basin. The annual mean air temperature and total precipitation for the period of 2006-2098 are presented in Figure 7.1.

The climate model (MOHC-HadGEM2-ES) indicates that long term (2006-2098) average annual mean temperature will be 14.3 °C and 15.3 °C, whereas long term (2006-2098) total annual precipitation is predicted as 596.5 mm and 582.6 mm, for the RCP 4.5 and RCP 8.5 scenarios, respectively. Although the data period of the climate models covers 94 years between 2006 and 2098, the data of the years between 2022-2064, representing the prediction period for the lake level change, was used in the 46-years simulations. The average annual precipitations and mean temperature values for the RCP 4.5 and RCP 8.5 were calculated as 603.6 and 603.9 mm, and 14.1 °C and 14.6 °C, respectively, for the prediction period (2022-2064).

In order to improve the reliability of the simulations, bias corrections were applied for the climate data prediction period (2022-2064) by using the Burdur meteorological station (17238) measured data between 2006-2021 (Figure 7.1).

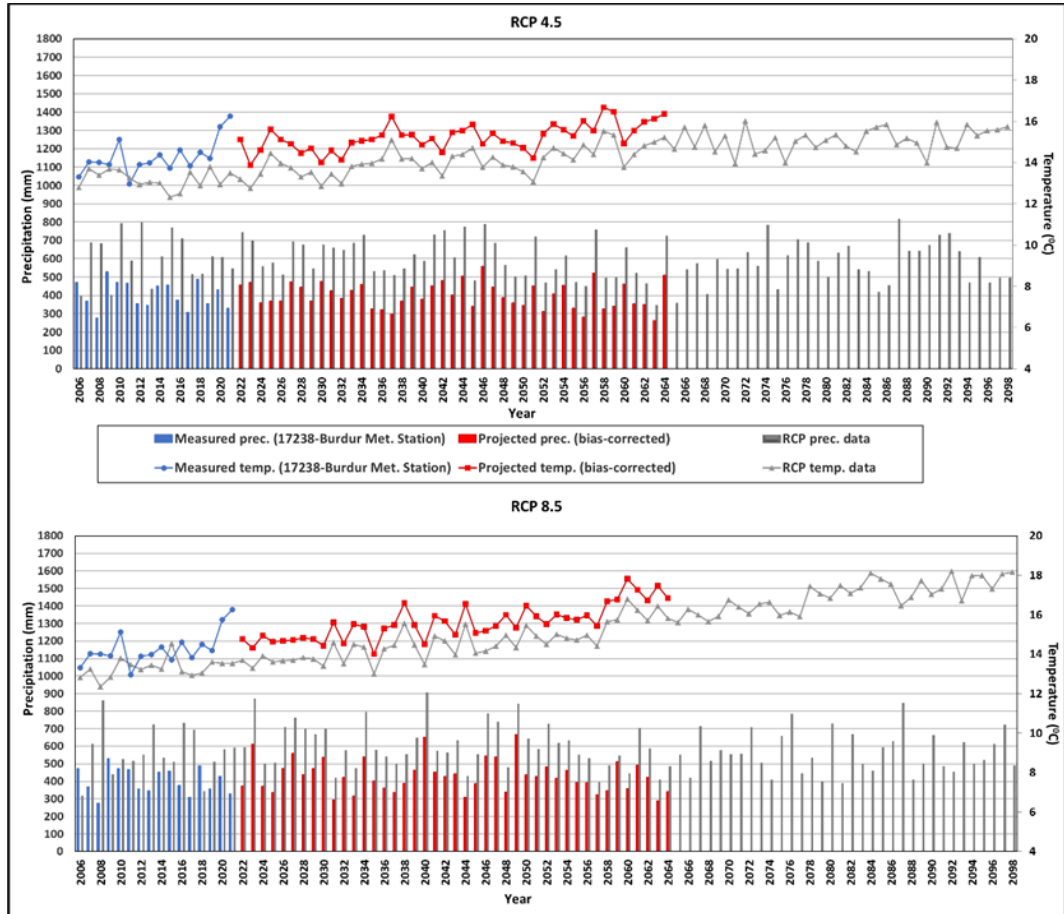


Figure 7.1. Annual mean air temperature and annual total precipitation for the period 2006-2021 (Burdur meteorological station), 2006-2098 (RCP 4.5 and RCP 8.5 scenarios), and 2022-2064 (projected bias-corrected)

Biases in the precipitation data were corrected by using the linear scaling method (Ines and Hansen, 2006):

$$P_{Bias\ Corrected(model)} = P_{Model} \chi \left(\frac{\bar{P}_{Observation}}{\bar{P}_{Model}} \right) \quad (Eq. 7.1)$$

where:

$P_{Bias\ Corrected(model)}$: bias-corrected monthly precipitation

P_{Model} : monthly precipitation model value

$\bar{P}_{Observation}$: observation value for the corresponding month

\bar{P}_{Model} : model value for the corresponding month

Temperature data were corrected for bias using a simple seasonal bias correction method (Soriano et al., 2019):

$$T_{Bias\ Corrected(model)} = T_{Model} - \Delta T \quad (Eq. 7.2)$$

where:

$T_{Bias\ Corrected(model)}$: bias-corrected monthly temperature

T_{Model} : monthly temperature model value

ΔT : difference between the mean temperature of the climate model and the observations in the corresponding month

The annual mean temperature and precipitation values between 2022-2064 after bias correction are shown in Figure 7.1. The bias-corrected annual mean temperatures are 15.2 °C and 15.6 °C for the RCP 4.5 and RCP 8.5. These are 2-2.4 °C warmer compared to the long-term average mean annual temperature of Burdur meteorological station (17238) for 1969-2018 of 13.2 °C. After the bias correction, the total annual precipitations were calculated as 401.8 mm and 431 mm for the RCP 4.5 and RCP 8.5, respectively. The annual precipitation is predicted to decrease by 4 % (RCP 4.5) and increase by 3 % (RCP 8.5) from the long-term annual mean precipitation of Burdur meteorological station (17238) of 418.6 mm (1969-2018).

7.2 Scenario No. 1

The possible future levels of Burdur Lake due to the impact of climate change were estimated quarterly with respect to the output of 2 model simulations over a period of 2019-2064. RCP 4.5 and RCP 8.5 emission scenarios were considered for simulations 1 and 2, respectively. From January 2019 to November 2022, observed climate data of the Yazıköy meteorological station was used for both simulations as

in the conceptual lake budget, whereas between November 2022 and December 2064, bias-corrected climate data of the RCP 4.5 and RCP 8.5 scenarios were used.

In the calibrated model domain, there are four recharge zones (Figure 6.4). For each of these zones, the calculated recharges from precipitation were modified by the Thornwaite and SCS curve number method using the 10-year average temperature and average total precipitation values obtained from climate models. The resulting recharges from precipitation values are presented in Table 7.1.

Table 7.1. Recharge from precipitation for the RCP 4.5 and 8.5 scenarios

Years	Zone 1		Zone 2		Zone 3		Zone 4	
	RCP 4.5	RCP 8.5	RCP 4.5	RCP 8.5	RCP 4.5	RCP 8.5	RCP 4.5	RCP 8.5
2019-2025	71.8	69.8	5.6	3.0	52.59	51.2	114.8	109.8
2026-2035	88.8	107.3	18.4	26.2	68.16	82.0	139.1	148.3
2036-2045	88.6	80.1	10.7	12.0	64.62	58.2	131.3	120.9
2046-2055	83.4	104.3	5.6	39.0	61.78	81.2	126.8	142.1
2056-2064	75.5	52.2	0.8	0.4	53.81	34.6	119.4	94.9

Another model boundary condition that is affected by climatic variabilities is the lake boundary. Monthly precipitation, evaporation, and runoff values are the inputs of this boundary condition to calculate the lake budget components. Monthly average precipitation values were taken directly from the Yazıköy meteorological station measurements for 2019-2021 as in the conceptual lake budget, and RCP 4.5 and RCP 8.5 climate scenarios for 2022-2064. The monthly evaporation values for the scenarios were calculated by correlation method using the equation of the relationship between the monthly temperatures and evaporations of the Burdur meteorological station for 1969-2019 ($R^2=0.78$). To calculate the monthly runoff series, the HEC-HMS model was rerun with the climate data of RCP scenarios. It is assumed that surface water usage will be the same as during 1969-2018 throughout the simulation process (0.46-1.97 hm³ between May and September). The resulting

annual budget components for the lake boundary conditions are presented in Figure 7.2.

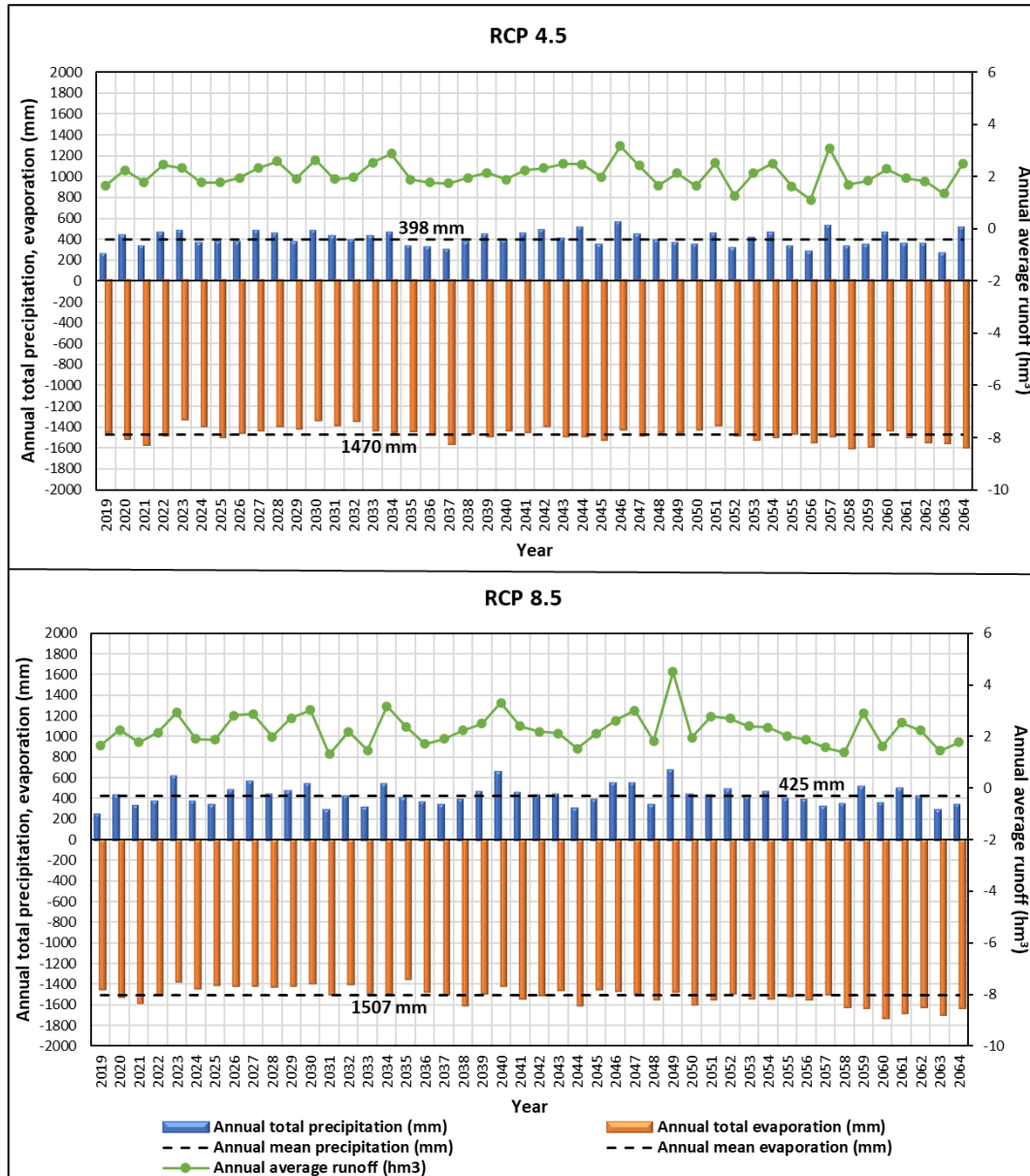


Figure 7.2. The annual budget components for the lake boundary conditions

After modifying the recharge and lake boundary conditions, the simulations were conducted for simulations 1, and 2 of scenario no. 1. The Burdur Lake level changes for these simulations are presented in Figure 7.3, and the predicted lake surface areas in December 2064 are given in Figure 7.4.

The predicted lake levels in December 2064 are 834.9 m (RCP 4.5) and 836 m (RCP 8.5), which are 5-6 m lower than the lake level in December 2018 (840.1). At the beginning of the simulation period, a rapid decrease in lake level was observed in both simulations. The reason for this decline is the low precipitation measurements and high evaporation calculations of the Yazıköy meteorological station. Although these data do not represent climate change, they were considered the data of the warm-up period of the model. The other drastic decreases are seen after 2056 for RCP 8.5 and 2045 for RCP 4.5, with the impacts of higher evaporation and lower precipitation values of the RCPs (Figure 7.2).

The monthly average lake budget components calculated for the first and second simulations of scenario no. 1 are given in Table 7.2. As in the calibrated lake budgets (Tables 5.5 and 5.6), the most important input parameter to the lake is groundwater inflow and the output parameter is evaporation. The decrease in the reserve change also verifies the decline of the lake level.

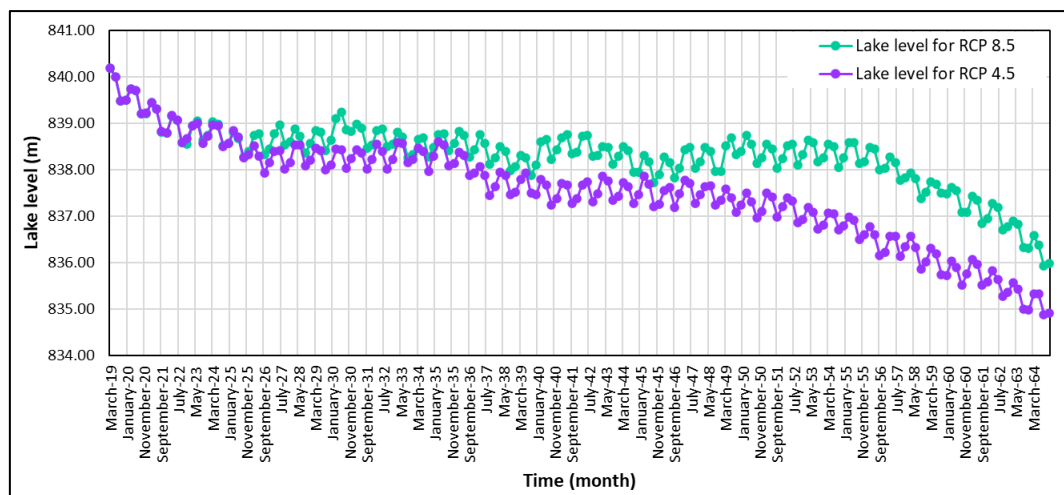


Figure 7.3. Burdur Lake level change for scenario no.1

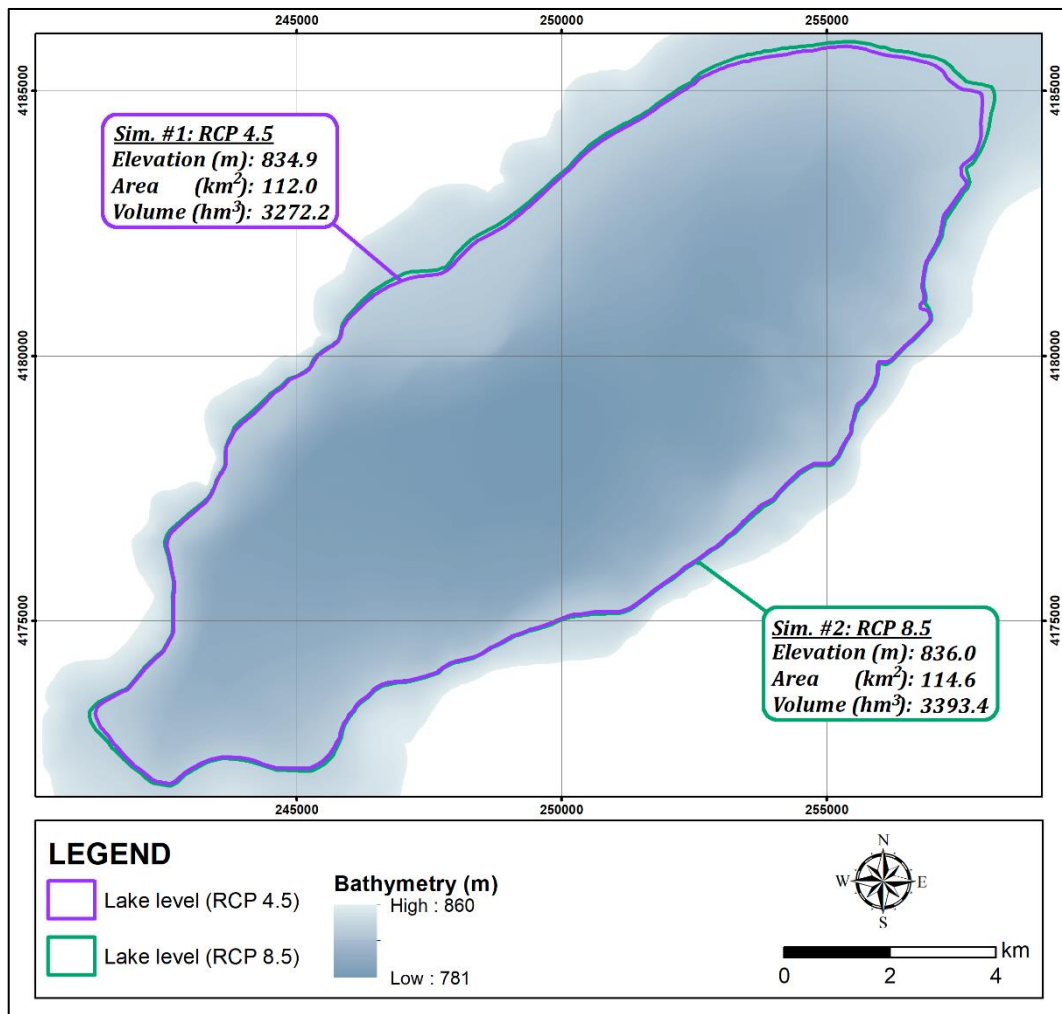


Figure 7.4. The predicted lake surface area in December, 2064 for scenario no.1

Table 7.2. Calculated average monthly lake budget for simulations 1 and 2 of scenario no. 1

(hm ³ /month)		Prec.	Runoff	GW inflow	Total lake recharge	Evap.	GW outflow	Total lake discharge	Reserve Change
Scenario 1	Sim. # 1 (RCP 4.5)	4.11	2.09	7.82	14.02	15.19	0.001	15.20	-1.17
	Sim. # 2 (RCP 8.5)	4.39	2.26	8.00	14.66	15.58	0.001	15.58	-0.93

7.3 Scenario No. 2

Burdur Lake cannot be used for domestic and agricultural purposes due to its salty, brackish, and arsenic-containing water characteristics (Dervişoğlu et al., 2022). Therefore, groundwater is abstracted from aquifers for irrigation, drinking, and domestic purposes. In 2015, 64.6 hm³/year of groundwater was pumped in the Burdur Lake basin (DSI, 2016-a). The pumping rates for the other years are uncertain. Therefore, two simulations were conducted using the population increase amount to understand the impact of groundwater pumpage on the Burdur Lake level. The population of Burdur was 78331 in 2015 and is estimated to reach 113962 in 2050, with an approximate increase of 46 %, according to the population projection applied in the DSI Master Plan Report (DSI, 2016-b). The same increase rate was used to increase the pumping amounts of the wells linearly in the simulation period between 2019-2064. As a result of this approach, the pumping rate is predicted to increase by 70 % in 2064 compared to 2015.

In order to conduct simulations of this scenario, a climate series representing future conditions is also needed. Therefore, the impacts of the increase in pumping rates were evaluated with the climate series taken from RCP 4.5 (simulation 3) and RCP 8.5 (simulation 4). The pumping rates of the wells are identical in both simulations. Burdur Lake level change for scenario no. 2 is given Figure 7.5 and the predicted lake surface areas in December 2064 are shown in Figure 7.6.

In December 2064, the lake levels are estimated to be 832.8 m for RCP 4.5 and 833.9 m for RCP 8.5. These values are 6-7 m lower than the lake level, measured at 840.1 m in December 2018. Although the periods of increase-decrease in the lake level are the same as in scenario no.1, the lake level decrease is predicted to be 1 m more than the first scenario due to higher groundwater pumpage.

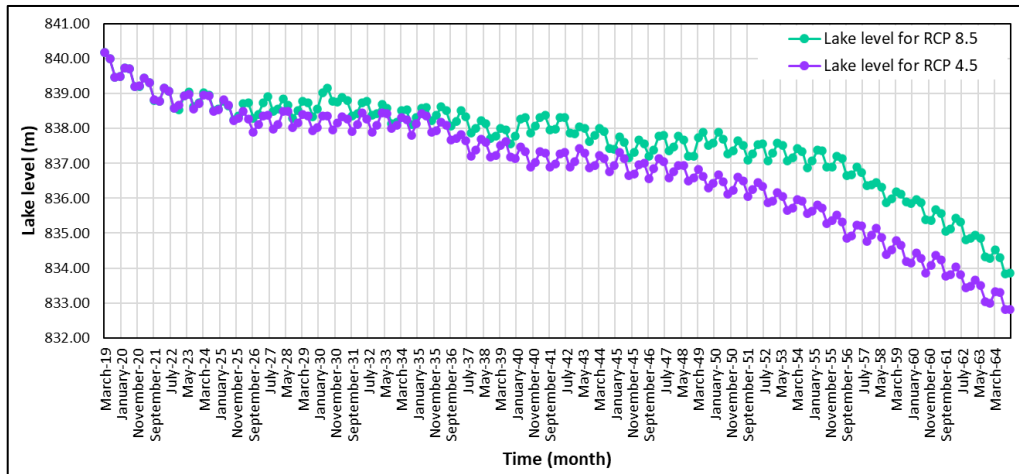


Figure 7.5. Burdur Lake level change for scenario no.2

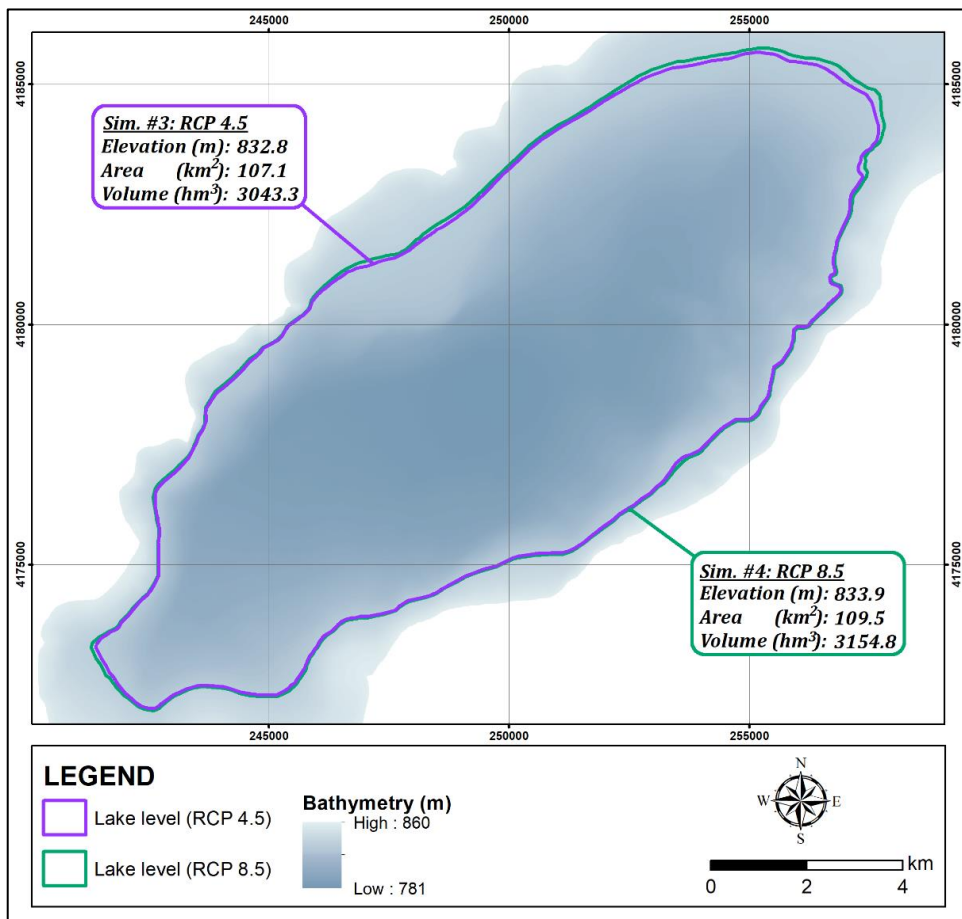


Figure 7.6. The predicted lake surface area in December, 2064 for scenario no.2

The monthly average lake budget components calculated for the first and second simulations of scenario no. 2 show the reserve change decrease, which corresponds to the lake level decrease (Table 7.3). As in the case of scenario no. 1, although the most important input parameter to the lake is groundwater inflow, the amount of inflow decreases with the increasing amount of pumping. The dominant output parameter is evaporation also for this scenario.

Table 7.3. Calculated average monthly lake budget for simulations 3 and 4 of scenario no. 2

(hm ³ /month)		Prec.	Runoff	GW inflow	Total lake recharge	Evap.	GW outflow	Total lake discharge	Reserve Change
Scenario 2	Sim. # 3 (RCP 4.5)	4.11	2.09	7.34	13.55	15.19	0.001	15.20	-1.65
	Sim. # 4 (RCP 8.5)	4.39	2.26	7.51	14.17	15.58	0.001	15.58	-1.41

7.4 Scenario No. 3

In the Burdur Lake basin, from 1989 to 2017, 9 reservoirs in various volumes (> 460000 m³) were constructed for irrigation purposes (Table 4.1 and Figure 4.4). These reservoirs cut the natural flow of the streams feeding the lake. However, since there is no gauging station on all these streams, the effect of the ponds on the stream flows could not be specified with measurements. In the conceptual lake budget calculations, The HEC-HMS model was developed to calculate the streamflow inflow to the lake, and it was considered that there was no flow from the subbasins of ponds to the lake during the operation years.

In this scenario, it was assumed that there were no ponds and surface water usage in the basin. For this purpose, the HEC-HMS model was rerun with the climate data of RCP 4.5 and RCP 8.5 over a period of 2019-2064 to calculate the streamflows from

all the subbasins. For both RCPs, the annual average inflows to the lake with and without ponds are given in Figure 7.7 in the simulation period.

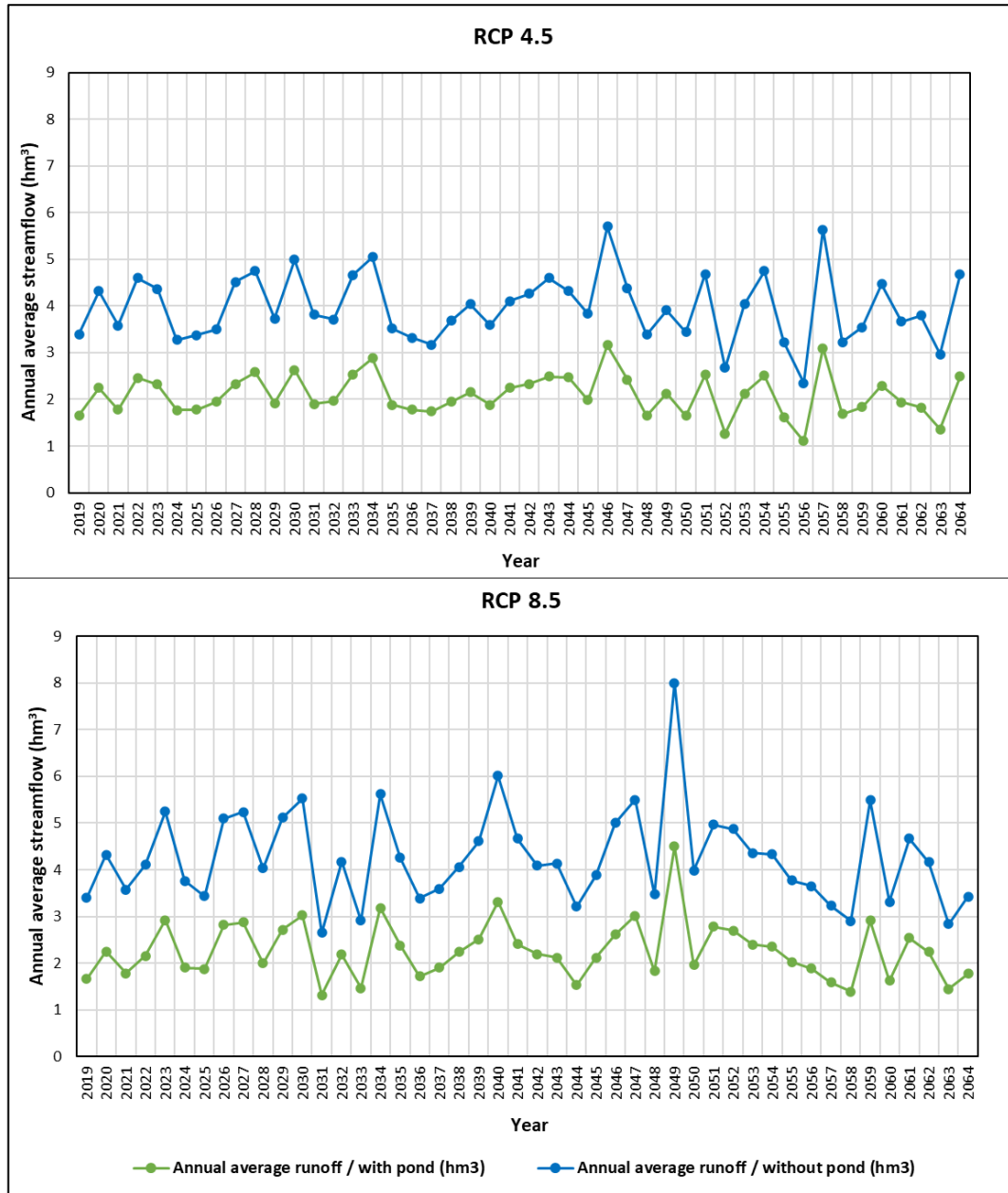


Figure 7.7. The annual average streamflows to the lake with and without ponds for RCP 4.5 and RCP 8.5

After the runoff series for the lake boundary condition was changed, there is also a need to represent future climatic conditions using RCPs, as in the other scenarios. Therefore, lake and recharge boundary conditions were modified using RCP 4.5 (simulation 5) and RCP 8.5 (simulation 6) to assess the impacts of the constructed reservoirs in the basin. The lake level change for scenario no.3 is shown in Figure 7.8 and the estimated lake surface areas in December 2064 as a result of the simulations are shown in Figure 7.9.

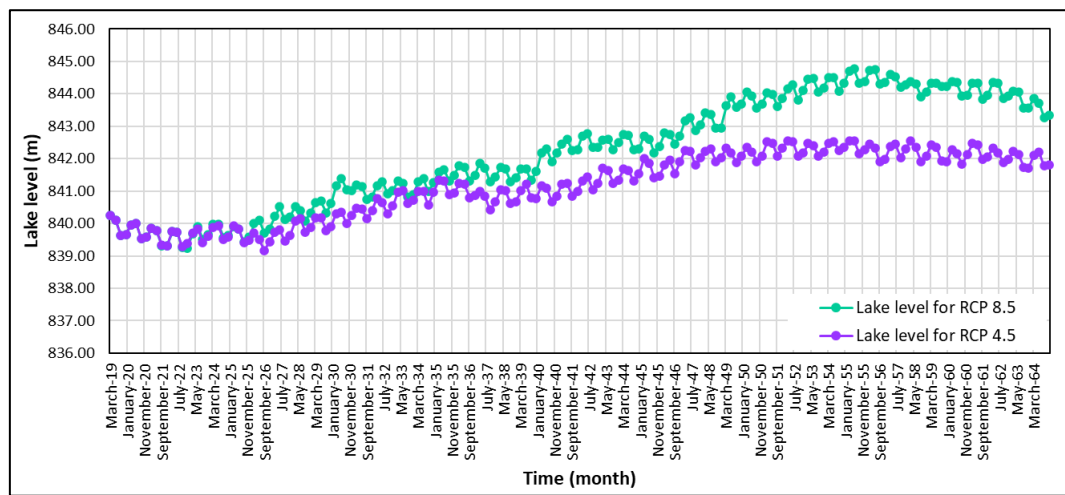


Figure 7.8. Burdur Lake level change for scenario no.3

Unlike other scenarios, an increase in lake levels was observed in this case. The lake levels were predicted to reach 841.8 for RCP 4.5 and 843.3 m for RCP 8.5 in December 2064. These values are 2-3 m higher than the lake level, measured as 840.1 in December 2018. However, considering that the effect of only climate variation during the simulation time decreased the lake level by 5-6 m in the first scenario, it can be interpreted that with the release of surface waters feeding the lake as in this scenario, the lake level is maintained and even increased. These increases correspond to a reserve change of 0.4-0.75 hm³, as seen from the calculated lake budget in Table

7.4. The runoff component of the lake budget is almost twice the value calculated in other scenarios due to the release of runoffs from reservoirs (Tables 7.2-7.4).

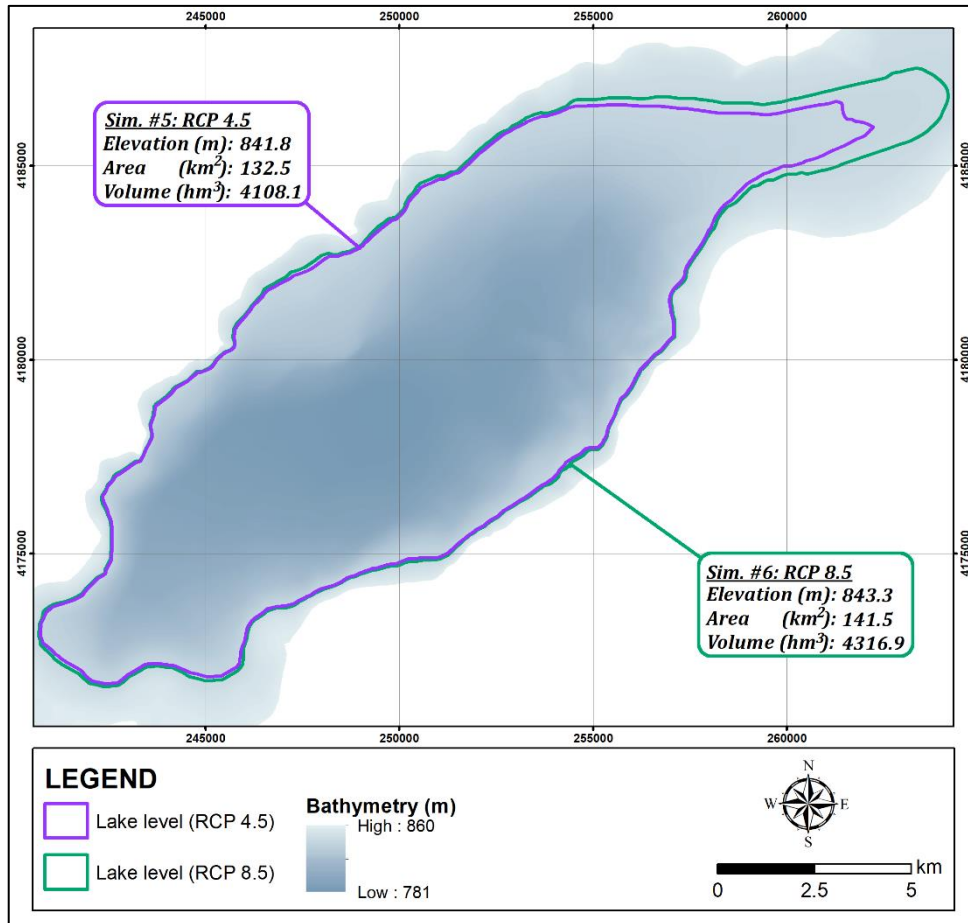


Figure 7.9. The predicted lake surface area in December 2064 for scenario no.3

Table 7.4. Calculated average monthly lake budget for simulations 5 and 6 of scenario no. 3

(hm ³ /month)		Prec.	Runoff	GW inflow	Total lake recharge	Evap.	GW outflow	Total lake discharge	Reserve Change
Scenario 3	Sim. # 5 (RCP 4.5)	4.11	3.97	7.52	15.60	15.19	0.001	15.20	0.40
	Sim. # 6 (RCP 8.5)	4.39	4.26	7.68	16.33	15.58	0.001	15.58	0.75

CHAPTER 8

DISCUSSIONS

A successful groundwater-lake model application requires hydrological and hydrogeological data characterization with insight into the modeling process. In order to conduct site observation and data collection, a field trip to the study area was conducted on August 2020. During this trip, it was deduced that there was no water usage from the lake. The streams were observed in situ to calculate the surface water inflow component to the lake during the conceptualizing of the lake budget. Local people were interviewed about agricultural activities and water usage in the study area, and information about the study area and data collection procedures were taken from the authorities. Although it is necessary to collect the data from the field and update them with observations during the study period, the data generation for a basin of this scale can be possible within the framework of a multidisciplinary team effort at a high cost. Therefore, all required topographical, climatic, meteorological, geological, hydrological, and hydrogeological data were provided by previous studies of governmental institutions. However, since some of the databases in Turkey are still not digitized or are confidential and QA/QC procedures have not been implemented during the development of these databases, the data collection and evaluation procedures from various sources at the beginning of this study were quite challenging.

Setting up detailed conceptual models of the lake and groundwater is another necessity to develop a successful model. In this study, calculations of the lake budget components were elaborated to be a research topic on its own to decrease the uncertainties. All budget components were calculated separately with the analytic methods. Also, the numerical 2D surface water flow model was developed to

calculate the surface water inflow to the lake since there are only three flow gauging stations on two main streams with discontinuous measurements. However, a conceptual groundwater model can not be developed in the basin because of a lack of data on groundwater usage.

Determining the optimal grid spacing and model geometry plays a critical role in model studies. More realistic results can be obtained with finer grid sizes. The study area was discretized into variable size grids from 100 m x 100 m around Burdur Lake to 400 m x 400 m towards the boundaries of the study area. This gridding system creates 159900 cells for each layer. A total of 1119300 cells were obtained as the model was also discretized as seven layers vertically from the surface to 500 m, the top of the impervious basement rocks. Since the computational time increases with the refinement of the grids and MODFLOW has limitations for the number of cells, selected grid sizes were specified as optimum. Although this discretization is fine enough to simulate the lake level successfully with low error limits (NRMSE=0.12, RMSE= 0.24 for 1969-1971 lake levels and NRMSE=0.20, RMSE= 0.12 for 2014-2015 lake levels), the success in calibrating groundwater levels is not within the high limits in a basin of this size (R^2 between 0.07 to 0.77). However, refinement of the grids created problems in simulating boundary conditions since a maximum of 1 GB of data can be imported into the model. It may also be possible to reduce the vertical thickness of the model. In this study, the bottom of the first layer (780 m) coincides with the bottom of the lake. The second was discretized until 750 m to focus on the interaction between the lake and groundwater. Then, the model area was divided into five layers of equal thickness of 50 m along the Pliocene unit until impervious basement rocks (500 m) due to the simulation of vertical lake recharge from the groundwater. The distribution of Pliocene units, including conglomerate, sandstone, claystone, siltstone, marl, and limestone, is unknown in the study area and distinguishing 650 m thickness Pliocene and Plio-Quaternary aged tuff-tuffite, travertine units is difficult. Also, the hydraulic conductivity values of these units, which are expected to be different, has not been specified by the pumping tests. Therefore, this discretization methodology was applied in the first stage of model

development. However, after calibration, it can be concluded that the last three layers (650 m to 500 m) can be ignored since there is no deep recharge into the lake. Considering that the groundwater model should be dynamic, the model could be recalibrated for smaller thickness in future studies to focus on lake-groundwater interaction.

For the simulation period of the study, there are several uncertainties. Unpermitted groundwater and surface water usage in the basin could not be recorded. Therefore, simulating a continuous model from 1969 to 2018 was not possible. This constraint was overcome by separating the model simulation period into two; the natural initial (1969-1971) and human-intervented current conditions (2014-2016). However, assessing the causes of lake level decrease quantitatively for the whole period (1969-2018) with fewer assumptions could be possible only by simulating the model throughout the entire period.

The model is calibrated with acceptable error limits for the years 1969-1971 and 2014-2016, indicating that it was capable of simulating the lake and groundwater relationship quantitatively. The success of the calibration of numerical modeling depends on the quality of the observed data. The Burdur Lake level measurement was taken monthly from January 1969 to December 2018. However, the levels were measured as the same even for the different seasons (841.8 m in November 2015-June 2016, 841.2 m in November 2016-June 2017, and 840.5-840.6 m in October 2017-July 2018). Between November 2015 and June 2016, the lake level was extracted from satellite images and compared with measurements of the lake levels for confirmation. However, since the extracted lake levels did not match the measurements, the period between October 2015-December 2016 was excluded from the calibration error calculations. Calibrating the model successfully with lower error rates may be possible with only more precise measurements.

The calibrated model was simulated under three different scenarios. Since future simulations can not be conducted without a climate dataset, daily CORDEX-based projected precipitation and air temperature data series were generated based on the

RCP 4.5 and RCP 8.5 scenarios. A wide range of climate models is available to provide projections of future climate change. The fourth and most recent Intergovernmental Panel on Climate Change (IPCC) assessment provides twenty-four global climate models under three major greenhouse gas emission scenarios (IPCC, 2007). Although selecting an appropriate climate model to produce the projections is challenging, the previous studies that evaluate the 12 CORDEX models for seven regions in Turkey have been utilized (Aziz and Yücel, 2021 & Aziz et al., 2020). Daily CORDEX-based projected precipitation and temperature data series were generated based on the RCP 4.5 and RCP 8.5 scenarios between 2006-2098. However, model scenario simulations can be conducted only 46 years of data between 2019 and 2064 quarterly since the model can not allow the bigger input data size. Furthermore, the biases of these datasets were corrected after converting them to the mean monthly temperature and precipitation data for the Burdur Lake basin. The bias-corrected annual mean temperatures for the simulation period between 2022-2064 are 15.2 °C and 15.6 °C, while total annual precipitations are 401.8 mm and 431 mm for the RCP 4.5 and RCP 8.5, respectively. Although higher temperature and lower precipitation values are expected based on the worst greenhouse gas (GHG) emission scenario RCP 8.5, and it is correct for the raw data between 2006-2098, the higher precipitation values were extracted in the simulation period corresponding to 2022-2064. To overcome this problem, using ensemble climate models as in climate change studies can be considered in future studies. In all three scenario simulations, precipitation and temperature data of RCP 4.5 and 8.5 were used as the predicted climate series. According to the simulation results of the scenarios, climate change causes the lake level to decrease by 5-6 m at the end of 46 years. The decrease in lake level is expected to decline by up to 7 m with the combined impact of climate variations and excessive pumping. With the release of surface waters from the reservoirs, it is predicted that the lake will return to its natural fluctuation levels or maintain its level and even increase by 3 m despite the impact of climate change within 46 years.

Burdur Lake is a RAMSAR site with international importance. Despite all these challenges, the motivation for this study is to reveal the causes and consequences of the surface area decline which has surpassed a critical level of such an important wetland for nature. For this purpose, the conceptual lake budget was developed in detail, and then this budget was conformed with the 3-D numerical groundwater-lake modeling approach. The impact assessment studies were conducted by simulating scenarios of the effects of climate and anthropogenic factors. In that sense, this is a novel study that supports decision-makers in developing the lake and watershed management plans.

CHAPTER 9

CONCLUSIONS AND RECOMMENDATIONS

The aim of this study is to assess the impacts of future climate variations and human activities on the Burdur Lake level variations to reveal the causes of the lake level decrease and characterize the gain/loss relations of lake and groundwater in a quantitative way for providing essential support for lake and watershed management planning. For this purpose, the topographical, meteorological, geological, hydrological, and hydrogeological properties of the lake basin were gathered and analyzed. The development of the conceptual budget for the lake was the following step of the study after data collection. In order to simulate the groundwater and lake contributions to each other, a 3D numerical groundwater flow model with lake boundary conditions was developed using the MODFLOW. The model was calibrated under steady-state conditions with an NRMSE of 4.03 % and 3.49 % for 1969 and 2014, respectively. The transient calibrated model simulated the lake stages with an NRMSE of 0.12 % for 1969-1971 and 0.20 % for 2014-2015. Then, the simulations were conducted to analyze the effect of climate variabilities, groundwater pumping, and surface water inflow over a period of 46 years.

The following conclusions are made from this study:

- The Burdur Lake level has decreased by 17 m from the beginning of 1969 to the end of 2018. This decrease corresponds to the 95 km² area and 2989 hm³ volume lost, equal to approximately 40 % of the volume of the lake.
- Based on the annual conceptual lake budget, evaporation is the main outflow component of the lake. The surface water and groundwater inflows have a higher contribution to the lake than precipitation as inflow components.

While surface water contribution was higher until 2005, groundwater exceeded it between 2005 and 2018.

- The calculated lake budgets for the simulation periods 1969-1971 and 2014-2016 are summarized in Table 9.1. Evaporation is also the major outflow component based on the calculated lake budget. As in the conceptual budget, the main contributions to the lake are runoff for the model simulated in 1969-1971 and groundwater in 2014-2016. The main reason for this shift is the reduction of the surface water reaching the lake by the construction of several dams and ponds after the 2000s. Groundwater inflow and outflow rates are the same for the calculated groundwater budget showing the equilibrium between the lake-groundwater budgets. The results of the calculated lake budget conform to the conceptual budget for both simulation periods.

Table 9.1. Calculated monthly average lake budget components

Monthly average lake budget components		Prec.	Runoff	GW inflow	Total lake recharge	Evap.	GW outflow	Total lake discharge	Reserve Change
1969-1971	(hm ³ /month)	7.16	15.53	7.84	30.53	22.05	0.01	22.06	8.47
	(%)	23	51	26	100	99.96	0.04	100	-
2014-2016	(hm ³ /month)	3.61	4.90	6.38	14.89	15.35	0.002	15.35	-0.46
	(%)	24	33	43	100	99.99	0.01	100	-

- The impact of climate change and anthropogenic activities on Burdur Lake levels are simulated by considering three case scenarios. Daily climate data were extracted from CORDEX Regional Climate Models of the RCP 4.5 and RCP 8.5 scenarios and converted to bias-corrected monthly precipitation and temperature data for 46 years of simulations between January 2019 and December 2064. In scenario no. 1, the climate change impact on Burdur Lake was evaluated according to the climate series of RCP 4.5 and RCP 8.5 in simulations 1 and 2, respectively. In simulations 3 and 4 of scenario no. 2, the effects of climate change and groundwater pumping based on RCP 4.5

and RCP 8.5 were assessed, while the impacts of climate change and surface water inflow were evaluated in simulations 5 and 6 of scenario no. 3 for the same RCPs. The predicted lake surface areas in December 2064 based on the changed lake levels are presented in Figure 9.1 for all simulations. The lake level, area, and volume change estimations at the end of the simulation period in December 2064 are also summarized in Table 9.2.

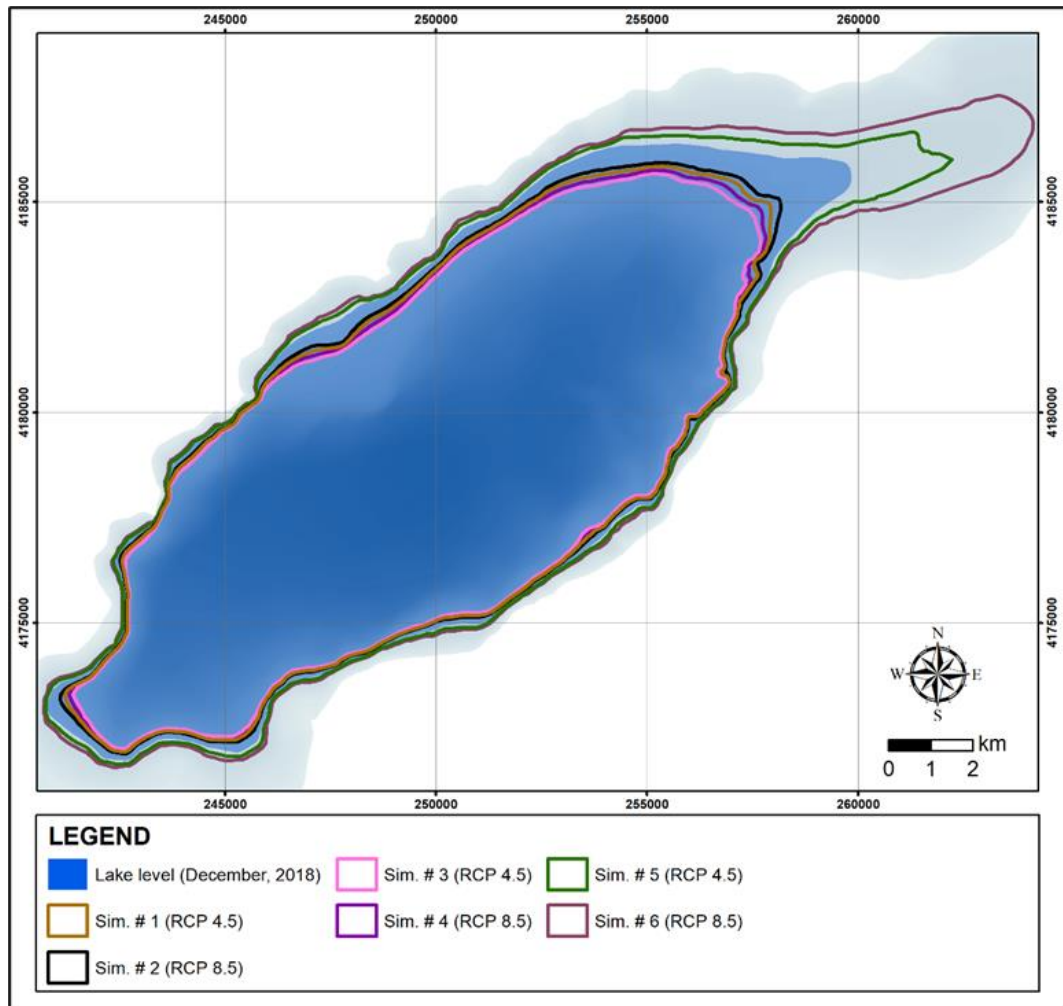


Figure 9.1. The predicted lake surface areas in December 2064

Table 9.2. The predicted lake level, area, and volume changes between December 2018-December 2064

Scenario	Simulation	RCP	Changes in the lake btw. December 2018-December 2064		
			Level (m)	Area (km ²)	Volume (hm ³)
December 2018	-	-	840.1	125.8	3887.4
Scenario 1 - Climate change	Sim. # 1	4.5	5.2 ↓	13.8 ↓	615.2 ↓
	Sim. # 2	8.5	4.1 ↓	11.2 ↓	494.0 ↓
Scenario 2 - Climate change + Pumping rate	Sim. # 3	4.5	7.3 ↓	18.7 ↓	844.2 ↓
	Sim. # 4	8.5	6.2 ↓	16.3 ↓	732.6 ↓
Scenario 3 - Climate change + Surface water inflow	Sim. # 5	4.5	1.7 ↑	6.7 ↑	220.6 ↑
	Sim. # 6	8.5	3.2 ↑	15.7 ↑	429.4 ↑

- Climate change was not the primary force behind the lake level drop until the end of 2018. However, it may cause the lake level to decrease in the future. Also, it can increase the negative effect of anthropogenic activities by imposing stress on Burdur Lake.
- Although the increase in pumping rates with the population growth causes the lake level to drop, it is expected that this component will not be as dominant as the surface water inflow in the shrinkage of the lake. This finding shows that the driving force of the lake level decrease was cutting the natural flow of streams by constructing reservoirs rather than groundwater pumpage in the basin.
- Since the northern part of Burdur Lake is shallower than the other parts, the desiccation will occur from this region firstly in case of future lake level decrease as in the past.

Simulation of lake levels incorporating the potential impacts of climate change is a challenging task because the results of previous studies (Clark et al., 2016) demonstrate large uncertainties in climate change models. The effects of two climate change scenarios were simulated for consideration of this uncertainty. These simulations provided different lake levels making them difficult in applying for lake management. Another source of uncertainty is the lack of sufficient or correct data,

which produced difficulties in comparing simulated lake levels with their field counterparts. The authorities should try to minimize these uncertainties using modern tools and several measurements, such as using water level recorders. The lack of distribution and continuity of the meteorological data in the basin having a large watershed area (1630 km²) produced some uncertainty in the input data used in this study. In this regard, evaporation and precipitation data of only two stations (i.e., Burdur and Yazıköy) were used, with evaporation estimated for the period from October to April, during which measurements were unavailable. Last but not least, the source of uncertainty is the lack of streamflow data from the watersheds surrounding the lake, which forced the simulation of the streamflows using the HEC-HMS model. The predicted streamflows underestimated the peak flows in the wet season, causing uncertainty in simulations of future scenarios. This uncertainty may affect the simulated lake levels being lower than the expected levels. To minimize all these uncertainties, a set of recommendations are made:

- In an internationally important area such as the Burdur Lake basin, data collection, information processing, and interpretation should be based on using technically and scientifically sound methods. In this sense, the monitoring of the lake levels using data loggers is recommended to derive a continuous data set.
- Since the streamflow inflow is the driving force for the feeding of the lake and is controlled by reservoirs, flow gauging stations should be constructed, at least on the main streams, and monitoring should be continued from the existing stations.
- Another uncertainty in the basin is the hydraulic conductivity of the geological units. Since the model is sensitive to this parameter, further studies should be conducted to obtain the hydraulic conductivity of the units.
- In the study area, there is a dynamic relationship between Burdur Lake and groundwater. Therefore, continuous groundwater level measurements should be taken nearby the lake area to investigate the lake water and groundwater interaction.

- In the lake basin, groundwater pumpage and surface water usage for irrigation became high. The usage amounts should be monitored by metering the amounts used. Innovative technologies and management practices should be adopted for irrigation methods to assess water-saving strategies in the basin.
- As can be understood from this preliminary study, climate change is a significant stress factor for Burdur Lake. In order to assess the impact of climate change on Burdur Lake in more detail, ensemble climate models can be used with a more extended simulation period as the concept of future studies.
- Burdur Lake is a wildlife protection area (Ramsar site no. 658). A dynamic lake and watershed management plan should be identified to protect, create and maintain desired conditions in a lake and its watershed. Within this scope, geological, hydrological, hydrogeological, hydrogeochemical, and limnological studies should be taken into consideration under a multidisciplinary approach.

REFERENCES

- Abbo, H., Shavit, U., Markel, D., Rimmer, A. (2003). A numerical study on the influence of fractured regions on lake/groundwater interaction; the Lake Kinneret (Sea of Galilee) case. *Journal of Hydrology*, 283, 225-243.
- Adrian, R., O'Reilly, C.M., Zagarese, H., Baines, S.B., Hessen, D.O., Keller, W., Winder, M. (2009). Lakes as sentinels of climate change. *Limnology and Oceanography*, 54 (6part2), 2283–2297.
- Ala-aho, P., Rossi, P.M., Isokangas, E., Kløve, B. (2015). Fully integrated surface–subsurface flow modelling of groundwater–lake interaction in an esker aquifer: Model verification with stable isotopes and airborne thermal imaging. *Journal of Hydrology*, 522, 391-406.
- Allen, R.G., Pereira, L.S., Raes, D., Smith, D.M. (1998). Crop evapotranspiration, guidelines for computing crop water requirements. FAO Irrig. and Drain. Paper 56, Food and Agric. Orgn. of the United Nations, Rome, Italy. 300 pp.
- Anderson, M.P., and Woessner, W.W. (1991). *Applied Groundwater Modeling: Simulation of Flow and Advective Transport*. Academic Press.
- Anderson, M.P., Hunt, R.J., Krohelski, J.T., Chung, K. (2002). Using High Hydraulic Conductivity Nodes to Simulate Seepage Lakes. *Groundwater*, 40.
- Ataol, M. (2010). The water level changings in Burdur Lake. *Journal of Geographical Sciences*, 8 (1), 77-92
- Aynew, T., and Tilahun, N. (2008). Assessment of lake–groundwater interactions and anthropogenic stresses, using numerical groundwater flow model, for a Rift lake catchment in central Ethiopia. *Lakes and Reservoirs: Research and Management*, 13, 325-343.

- Aziz, R., and Yucel, İ. (2021). Assessing nonstationarity impacts for historical and projected extreme precipitation in Turkey. *Theoretical and Applied Climatology*, pp. 0–0, 2021.
- Aziz, R., Yücel, İ., Yozgatlıgil, C. (2020). Nonstationarity impacts on frequency analysis of yearly and seasonal extreme temperature in Turkey. *Atmospheric Research*, 238, 104875.
- Barcikowska, M.J., Kapnick, S.B., Krishnamurty, L., Russo, S., Cherchi, A., Folland, C.K. (2020). Changes in the Future Summer Mediterranean Climate: Contribution of Teleconnections and Local Factors. *Earth Syst. Dyn.*, 11, 161–181.
- Bennet, T. (1998). Development and application of a continuous soil moisture accounting algorithm for the Hydrologic Engineering Center Hydrologic Modeling System HEC-HMS, MS thesis, Dept. of Civil and Environmental Engineering, Univ. of California, Davis, California.
- Beyhan, M., Şahin, Ş., Keskin, M.E., Harman, B.İ. (2007). Effects of long period water level changing to water quality and heavy metals in Lake Burdur. *Süleyman Demirel University Journal of Natural and Applied Sciences*, 11(2), 173.
- Bozcu, M., Yağmurlu, F., Şentürk, M. (2007). Some Neotectonic and Paleoseismological features of the Fethiye-Burdur Fault zone, SW Anatolia, *Geological Engineering*, 31(1), 25-48.
- Campodonico, V.A., Dapeña, C., Pasquini, A.I., Lecomte, K.L., Piovano, E.L. (2019). Hydrogeochemistry of a small saline lake: Assessing the groundwater inflow using environmental isotopic tracers (Laguna del Plata, Mar Chiquita system, Argentina). *Journal of South American Earth Sciences*.
- Candela, L., Elorza, F.J., Tamoh, K., Jiménez-Martínez, J., Aureli, A. (2014). Groundwater modelling with limited data sets: the Chari–Logone area (Lake Chad Basin, Chad). *Hydrological Processes*, 28.

- Chaudhari, S., Felfelani, F., Shin, S., Pokhrel, Y. (2018). Climate and Anthropogenic Contributions to the Desiccation of the Second Largest Saline Lake in the Twentieth Century. *Journal of Hydrology*. 560.
- Chebud, Y.A., and Melesse, A.M. (2009). Numerical modeling of the groundwater flow system of the Gumera sub-basin in Lake Tana basin, Ethiopia. *Hydrological Processes*, 23.
- Chen, W., Panahi, M., Pourghasemi, H.R. (2017). Performance evaluation of GIS-based new ensemble data mining techniques of adaptive neuro-fuzzy inference system (ANFIS) with genetic algorithm (GA), differential evolution (DE), and particle swarm optimization (PSO) for landslide spatial modelling. *Catena*, 157, 310-324.
- Cheng, X., and Anderson, M.P. (1993). Numerical Simulation of Ground-Water Interaction with Lakes Allowing for Fluctuating Lake Levels. *Ground Water*, 31, 929-933.
- Clark, M.P., Wilby, R.L., Gutmann, E.D., Vano, J.A., Gangopadhyay, S., Wood, A.W., Fowler, H.J., Prudhomme, C., Arnold, J.R., Brekke, L.D. (2016). Characterizing Uncertainty of the Hydrologic Impacts of Climate Change. *Current Climate Change Reports*. 2.
- Corine. (2018). European Environment Agency Corine Land Cover. Retrieved from eea.europa.eu/data-and-maps/data/external/corine-land-cover-2018.
- Council, G. W. (1998). A lake package for MODFLOW. In *Proceedings of the 3rd International Conference of the International Groundwater Modeling Center, Colorado, USA* (pp. 675-682).
- Çolak, M.A., Öztaş, B., Özgencil, İ.K., Soyluer, M., Korkmaz, M., Ramírez-García, A., Metin, M., Yılmaz, G., Ertuğrul, S., Tavşanoğlu, Ü.N., Amorim, C.A., Özen, C., Apaydın Yağcı, M., Yağcı, A., Pacheco, J.P., Özkan, K., Beklioğlu, M., Jeppesen, E., Akyürek, Z. (2022). Increased Water Abstraction and Climate Change Have Substantial Effect on Morphometry, Salinity, and Biotic Communities in Lakes: Examples from the Semi-Arid Burdur Basin (Turkey). *Water*. 14. 1241.

- Dai, L., Liu, H., Li, W., Tang, Z. (2020). Trend and abrupt analysis of Dongting Lake water level and its driving forces using Mann-Kendall approach. IOP Conference Series: Earth and Environmental Science, 467.
- Davraz, A., Karaguzel, R., Soyaslan, I. I. (2003). The importance of hydrogeological and hydrological investigations in the residential area: A case study in Burdur, Turkey. *Environmental Geology*, 44(7), 852-861.
- Deng, B., Lai, S.H., Jiang, C., Kumar, P., El-Shafie, A., Chin, R.J. (2021). Advanced water level prediction for a large-scale river-lake system using hybrid soft computing approach: a case study in Dongting Lake, China. *Earth Science Informatics*, 14, 1987 - 2001.
- Dervişoğlu, A., Yağmur, N., Fıratlı, E., Musaoğlu, N., Tanık, A. (2022). Spatio-temporal assessment of the shrinking Lake Burdur, Turkey. *Int. J. Environ. Geoinf.* 2022, 9, 169–176.
- Dimova, N., Burnett, W.C., Chanton, J.P., Corbett, J.E. (2013). Application of radon-222 to investigate groundwater discharge into small shallow lakes. *Journal of Hydrology*, 486, 112-122.
- DSI (1975). Hydrogeological Investigation Report for Erli, Irla, and Yazı Plains, Ankara.
- DSI (2016-a). Burdur Lake Basin Hydrogeological Investigation Report, Ankara.
- DSI (2016-b). Burdur Basin Master Plan Final Report, Vol I-II, Ankara.
- El-Zehairy, A., Lubczynski, M.W., Gurwin, J. (2018). Interactions of artificial lakes with groundwater applying an integrated MODFLOW solution. *Hydrogeology Journal*, 26, 109-132.
- Erinç, S. (1969). *Climatology and Methods*. İÜ Geo. Inst. Press. 2nd ed. No:35, İstanbul.

- Gibson, J.J., Prowse, T.D., Peters, D.L. (2006). Hydroclimatic controls on water balance and water level variability in Great Slave Lake. *Hydrological Processes*, 20.
- Gülle, İ., Turna, İ.İ., Güçlü, S.S., Küçük, F., Gülle, P., Güçlü, Z. (2008). Vertical Variation of Temperature, Dissolved Oxygen, pH and Electrical Conductivity Values in Burdur Lake. *Ege Journal of Fisheries and Aquatic Sciences*, 25 (4), 283-287.
- Harbaugh, W.A. (2005). MODFLOW-2005, the U. S. Geological survey modular groundwater model — the groundwater flow process MODFLOW-2005, the U. S. Geological survey modular groundwater model — the groundwater flow process: vol. TM 6-A16, (U.S. Geolo). U.S. Geol. Surv. Techniq. Methods 6-A16.
- Hunt, R. (2005). Ground water-lake interaction modeling using the LAK3 package for MODFLOW 2000. *Ground Water*. 41. 114 - 118.
- Hunt, R., Lin, Y., Krohelski, J., Juckem, P.P. (2010). Geological Survey Simulation of the Shallow Hydrologic System in the Vicinity of Middle Genesee Lake, Wisconsin, Using Analytic Elements and Parameter Estimation.
- Hunt, R.J., Haitjema, H.M., Krohelski, J.T., Feinstein, D.T. (2003). Simulating Ground Water-Lake Interactions: Approaches and Insights. *Groundwater*, 41.
- Ines, A.V.M., and Hansen, J.W. (2006). Bias Correction of Daily GCM Rainfall for Crop Simulation Studies. *Agric. For. Meteorol.*, 138, 44–53.
- IPCC (2007). *Climate Change 2007: The Physical Science Basis. Contribution of Working Group I to the Fourth Assessment Report of the Intergovernmental Panel on Climate Change*. Cambridge University Press, Cambridge.
- Jaafar, H.H., Ahmad, F.A., El-Beyrouthy, N. (2019). GCN250, new global gridded curve numbers for hydrologic modeling and design. *Scientific Data*, 6 (145).

- Khazaei, B., Khatami, S., Alemohammad, H., Rashidi, L., Wu, C., Madani, K., Kalantari, Z., Destouni, G., AghaKouchak, A. (2019). Climatic or regionally induced by humans? Tracing hydro-climatic and land-use changes to better understand the Lake Urmia tragedy. *Journal of Hydrology*. 569.
- Kidmose, J., Engesgaard, P., Nilsson, B., Laier, T., Looms, M.C. (2011). Spatial Distribution of Seepage at a Flow-Through Lake: Lake Hampen, Western Denmark. *Vadose Zone Journal*, 10, 110 - 124.
- Kidmose, J., Engesgaard, P., Ommen, D.O., Nilsson, B., Flindt, M.R., Andersen, F.Ø. (2015). The Role of Groundwater for Lake-Water Quality and Quantification of N Seepage. *Groundwater*, 53.
- Lerman A., Imboden D.M., Gat J.R. (1995). *Physics and Chemistry of Lakes*. Press. 2nd ed. Springer Verlag, Berlin.
- Lin, Y., Hong, N., Wu, P., Lin, C. (2007). Modeling and assessing land-use and hydrological processes to future land-use and climate change scenarios in watershed land-use planning. *Environmental Geology*, 53, 623-634.
- Lu, C., He, X., Zhang, B., Wang, J., Kidmose, J., Jarsjö, J. (2022). Comparison of Numerical Methods in Simulating Lake–Groundwater Interactions: Lake Hampen, Western Denmark. *Water*.
- Lu, C., Zhang, B., He, X., Cao, G., Sun, Q., Yan, L., Qin, T., Li, T., Li, Z. (2020). Simulation of Lake-Groundwater Interaction under Steady-State Flow. *Ground Water*, 59, 90 - 99.
- Mahmood, R., Jia, S., Wenbin, Z. (2019). Analysis of climate variability, trends, and prediction in the most active parts of the Lake Chad basin, Africa. *Scientific Reports*. 9. 6317.
- Meng, Q. (2019). Climate Change and Extreme Weather Drive the Declines of Saline Lakes: A Showcase of the Great Salt Lake. *Climate*

- Merritt, M.L., and Konikow, L.F. (2000). Documentation of a Computer Program to Simulate Lake-Aquifer Interaction Using the MODFLOW Ground-Water Flow Model and the MOC3D Solute-Transport Model: U.S. Geological Survey Water-Resources Investigations Report 00-4167, 146 p.
- Meyer, A.F. (1915). Computing runoff from rainfall and other physical data, Paper 1348, presented at the American Society of Civil Engineers Meeting, April 21, 1915.
- Milanović, P.T. (1981). Karst Hydrogeology, Water Resources Publication, Littleton, Colorado, USA, 434 pp.
- ModaresiRad, A., Kreitler, J., Abatzoglou, J., Fallon, K. Roche, K., Sadegh, M. (2022). Anthropogenic stressors compound climate impacts on inland lake dynamics: The case of Hamun Lakes. *Science of The Total Environment*. 829. 154419.
- Moriasi, D.N., Gitau, M.W., Pai, N., Daggupati, P. (2015). Hydrologic and Water Quality Models: Performance Measures and Evaluation Criteria. *American Society of Agricultural and Biological Engineers*, 58(6), 1763–1785.
- MTA (2010). 1:100000 Scaled Turkey Geological Maps Series: Isparta M24 Sheet, 2. Ed., MTA (General Directorate of Mineral Research and Exploration).
- Mylopoulos, N., Mylopoulos, Y., Tolikas, D., Veranis, N. (2007). Groundwater modeling and management in a complex lake-aquifer system. *Water Resources Management*, 21, 469-494.
- Nilsson, C., and Grelsson, G. (1995). *Journal of Applied Ecology* Vol. 32, No. 4, pp. 677-692.
- Nistor, M.M. (2020) Groundwater Vulnerability in the Piedmont Region under Climate Change, *Atmosphere*, 11(779).

- Nourani, V., Danandeh Mehr, A., Azad, N. (2018). Trend analysis of hydroclimatological variables in Urmia lake basin using hybrid wavelet Mann–Kendall and Şen tests. *Environmental Earth Sciences*, 77, 1-18.
- NRSC (1997). Time of Concentration. Design manual. Chapter 2-stormwater. 2B-Urban Hydrology and Runoff, National Resource Conservation Service.
- Nsubuga, F., Botai, J.O., Olwoch, J.M., Rautenbach, C., Kalumba, A.M., Tsela, P.L., Adeola, A.M., Sentongo, A.A., Mearns, K.F. (2015). Detecting changes in surface water area of Lake Kyoga sub-basin using remotely sensed imagery in a changing climate. *Theoretical and Applied Climatology*, 127, 327-337.
- Özkaptan, M., Kaymakçı, N., Langereis, C.G., Gülyüz, E., Özacar, A.A., Uzel, B., Sözbilir, H. (2018). Age and kinematics of the Burdur Basin: Inferences for the existence of the Fethiye Burdur Fault Zone in SW Anatolia (Turkey). *Tectonophysics*.
- Price, S.P., and Scott B. (1991) Pliocene Burdur basin, SW Turkey: tectonics, seismicity, and sedimentation, *Journal of Geology Society*. 148:345-354.
- Reis, S., and Yılmaz, H.M. (2008). Temporal monitoring of water level changes in Seyfe Lake using remote sensing. *Hydrological Processes*, 22.
- Rossmann, N.R., Zlotnik, V.A., Rowe, C.M. (2019). Simulating lake and wetland areal coverage under future groundwater recharge projections: The Nebraska Sand Hills system. *Journal of Hydrology*.
- Saini, J., and Pandey, S. (2022). Environmental threat and change detection in saline lakes from 1960 to 2021: background, present, and future. *Environmental Science and Pollution Research*. 30. 1-12.
- Sattari, M.T., Mirabbasi, R., Jarhan, S., Shaker Suredh, F., Ahmad, S. (2020). Trend and abrupt change analysis in water quality of Urmia Lake in comparison with changes in lake water level. *Environmental Monitoring and Assessment*, 192.

- Schneider, R.L., Negley, T.L., Wafer, C.C. (2005). Factors influencing groundwater seepage in a large, mesotrophic lake in New York. *Journal of Hydrology*, 310, 1-16.
- SCS (1964). SCS (Soil Conservation Service) National Engineering Handbook, Section 4: Hydrology, Updated 1972, U.S. Department of Agriculture, Washington D.C.
- Semiz, G.D., and Akşit, C. (2013). Water quality, surface area, evaporation and precipitation of Lake Burdur. *International journal of food, agriculture and environment*, 11, 751-753.
- Smerdon, B.D., Mendoza, C.A., Devito, K.J. (2007). Simulations of fully coupled lake-groundwater exchange in a subhumid climate with an integrated hydrologic model. *Water Resources Research*, 43.
- Song, C., Huang, B., Ke, L., Richards, K.S. (2014). Remote sensing of alpine lake water environment changes on the Tibetan Plateau and surroundings: A review. *Isprs Journal of Photogrammetry and Remote Sensing*, 92, 26-37.
- Soriano, E., Mediero, L., Garijo, C. (2019). Selection of Bias Correction Methods to Assess the Impact of Climate Change on Flood Frequency Curves. *Water*, 11, 2266.
- Swenson, S.C., and Wahr, J.M. (2009). Monitoring the water balance of Lake Victoria, East Africa, from space. *Journal of Hydrology*, 370, 163-176.
- Şener, E., Davraz, A., Özçelik, M., (2015). An integration of GIS and remote sensing in groundwater investigations: A case study in Burdur, Turkey. *Hydrogeology Journal* 13. 826–834.
- Şener, Ş., Şener, E., Davraz, A., Varol, S. (2020) Hydrogeological and hydrochemical investigation in the Burdur Saline Lake Basin, Southwest Turkey. *Geochemistry*, 125592.

- Taşdelen, S. (2018). Hydrodynamic Relationship Between Dry Lakes of Insuyu Cave and Cine Ovası Aquifer (Burdur, Turkey). *OHU J. Eng. Sci.*, 7(2), 795-807.
- Thornthwaite, C.W. (1948). An approach towards a rational classification of climate. *Geographical Review*, 38(1):55–94.
- Toth, J. (1999). Groundwater as a geologic agent: an overview of the causes, processes, and manifestations. *Hydrogeol J*; 7:1–14.
- USACE (2013). Geospatial Hydrological Modeling Extension (HEC-GeoHMS) User's Manual: Version 10.1. CA, USA: Hydrologic Engineering Center: Davis.
- USACE (2018). Hydrologic Modeling System (HEC-HMS) User's Manual: Version 4.3.0. CA, USA: Hydrologic Engineering Center: Davis.
- Virdi, M.L., Lee, T.M., Swancar, A., Niswonger, R.G. (2012). Simulating the Effect of Climate Extremes on Groundwater Flow Through a Lakebed. *Groundwater*, 51.
- Voulanas, D., Theodosiou, N., Hatzigiannakis E. (2021). Assessment of potential hydrological climate change impacts in Kastoria basin (Western Macedonia, Greece) using EUROCORDEX regional climate models. *Global NEST: the international Journal*.
- Wei, H., Wang, J., Cheng, K., Li, G., Ochir, A., Davaadorj, D., Sonomdagva, C. (2018). Desertification Information Extraction Based on Feature Space Combinations on the Mongolian Plateau. *Remote Sensing*. 10
- Williams, W.D. (1996). The largest, highest and lowest lakes of the world: Saline lakes. *Verh. Internat. Verein. Limnol.* 26:61-79.

- Wollschläger, U., Ilmberger, J., Isenbeck-Schröter, M., Kreuzer, A.M., Rohden, C.V., Roth, K., Schäfer, W. (2007). Coupling of groundwater and surface water at Lake Willersinnweiher: Groundwater modeling and tracer studies. *Aquatic Sciences*, 69, 138-152.
- Wu, Y., Zheng, H., Zhang, B., Chen, D., Lei, L. (2014). Long-Term Changes of Lake Level and Water Budget in the Nam Co Lake Basin, Central Tibetan Plateau. *Journal of Hydrometeorology*, 15, 1312-1322.
- Yağbasan, Ö., and Yazıcıgil, H. (2009). Sustainable management of Mogan and Eymir Lakes in Central Turkey. *Environmental Geology*, 56, 1029-1040.
- Yağbasan, Ö., and Yazıcıgil, H. (2012). Assessing the impact of climate change on Mogan and Eymir Lakes' levels in Central Turkey. *Environmental Earth Sciences*, 66, 83-96.
- Yağbasan, Ö., Demir, V., Yazıcıgil, H. (2020). Trend Analyses of Meteorological Variables and Lake Levels for Two Shallow Lakes in Central Turkey. *Water*, 12, 414.
- Yapiyev, V., Sagin, J., Inglezakis, V., Samarkhanov, K., Verhoef, A. (2017). Essentials of Endorheic Basins and Lakes: A Review in the Context of Current and Future Water Resource Management and Mitigation Activities in Central Asia. *Water* 2017, Vol. 9, Page 798. 9. 798.
- Yarar, A., Onüçyıldız, M., Coptý, N.K. (2009). Modelling level change in lakes using neuro-fuzzy and artificial neural networks. *Journal of Hydrology*, 365, 329-334.
- Yihdego, D., and Becht, R. (2013). Simulation of lake–aquifer interaction at Lake Naivasha, Kenya using a three-dimensional flow model with the high conductivity technique and a DEM with bathymetry. *Journal of Hydrology*, 503, 111-122.

- Yihdego, D., Reta, G., Becht, R. (2016). Human impact assessment through a transient numerical modeling on the UNESCO World Heritage Site, Lake Naivasha, Kenya. *Environmental Earth Sciences*, 76, 1-16.
- Yücel, A.G., Marković, M., Atılgan, A., Rolbiecki, R., Ertop, H., Jagosz, B., Ptach, W., Łangowski, A., Jakubowski, T. (2022). Investigation of Annual Lake Water Levels and Water Volumes with Şen Innovation and Mann-Kendall Rank Correlation Trend Tests: Example of Lake Eğirdir, Turkey. *Water*.
- Zhang, G., Chen, W., Xie, H. (2019). Tibetan Plateau's lake level and volume changes from NASA's ICESat/ICESat-2 and Landsat Missions. *Geophysical Research Letters*, 46, 13,107–13,118.
- Zhou, S., Kang, S., Chen, F., Joswiak, D.R. (2013). Water balance observations reveal significant subsurface water seepage from Lake Nam Co, south-central Tibetan Plateau. *Journal of Hydrology*, 491, 89-99.

APPENDICES

A. DSI Wells

Well No.	Location	Purpose	Year	Elevation (m)	Depth (m)	Static Level (m)	Dynamic Level (m)	Well Yield (L/s)	Specific Capacity (L/s/m)	Screen Level (m)		Aquifer Lithology	Formation
										Top	Bottom		
DSI001	Düğer	Investigation	1963	913	250	15	21.55	1	6.550	6	22	16	Quaternary
DSI002	Yazköy	Investigation	1964	867	250	3.3	12.18	9.5	0.935	21	29	8	Quaternary
DSI003	Yazköy	Investigation	1964	861	250	-1.25	-	1.5	-	71	89	18	-
DSI004	Akariye	Investigation	1965	879	250	-1.4	16.1	2	0.795	73	90	17	Quaternary
DSI005	Cerçin	Investigation	1965	880	215	-3.1	25.24	10.5	2.699	34	46	12	Quaternary
DSI006	Cerçin	Investigation	1965	880	30	4.4	8.72	20.8	0.208	10	24	14	Quaternary
DSI007	İnsuyu	Investigation	1965	1185	24	-2.12	-6.55	20	0.222	7	20	13	Pliocene
DSI008	İnsuyu	Investigation	1965	1185	92	2.05	17.3	10	1.525	30	88	31	Pliocene
DSI009	Kılıç	Investigation	1968	929	101	-0.06	40	0.5	6.790	35	90	24	Pliocene
DSI010	Senir	Operation	1968	871	201.8	2.81	35.37	19.23	1.693	72	200	104	Pliocene
DSI011	Kılıç	Operation	1969	912	200	5.79	32.06	20	1.314	35	135	72	Pliocene
DSI012	Kılıç	Operation	1969	915	180	0.69	24.84	24	1.006	40	136	64	Pliocene
DSI013	Senir	Operation	1969	882	118	26.87	31.12	35.32	0.120	48	118	34	Pliocene, Oligocene
DSI014	Senir	Operation	1969	883	170	27.31	32.26	33	0.150	58	170	74	Pliocene, Oligocene
DSI015	Senir	Operation	1969	890	169	27.54	42.13	26	0.561	56	169	81	Pliocene, Oligocene
DSI016	Senir	Operation	1971	882	168	21.5	30.2	54	0.161	42	168	44	Pliocene, Oligocene
DSI017	Senir	Operation	1971	881	160	21.23	35.86	33.1	0.442	46	156	67	Pliocene, Oligocene
DSI018	Senir	Operation	1971	880	160	14.1	31.48	50.4	0.345	48	160	76	Pliocene, Oligocene
DSI019	Senir	Operation	1973	896	208	39.8	47.15	31.22	0.235	48	176	72	Pliocene, Oligocene
DSI020	Senir	Operation	1973	877	90	25.5	28.5	61.06	0.049	-	-	-	Pliocene, Oligocene
DSI021	Senir	Operation	1973	874	183.6	22.1	34.7	31	0.406	70	180	68	Oligocene
DSI022	Senir	Operation	1974	901	90	30.7	33.55	60.24	0.047	-	-	-	Pliocene, Oligocene
DSI023	Senir	Operation	1974	895	265	29.5	43.78	40.62	0.352	120	228	50	Oligocene
DSI024	Senir	Operation	1974	872	145	21.5	26.25	60.62	0.078	90	104	8	Oligocene
DSI025	Senir	Operation	1974	874	80	19.35	20.44	63.32	0.017	-	-	-	Pliocene, Oligocene
DSI026	Gölbasi	Operation	1977	875	60	0.6	2.9	63.2	0.036	16	56	36	Jurassic-Triassic
DSI027	Düğer	Operation	1977	915	93	3.08	6.12	63.2	0.048	-	-	-	Pliocene, Paleocene
DSI028	Düğer	Operation	1977	915	103	2.9	5.21	63.8	0.036	-	-	-	Pliocene, Paleocene
DSI029	Düğer	Operation	1977	926	140	2.3	20.27	41.38	0.434	28	98	52	Pliocene
DSI030	Yassıgüne	Operation	1977	909	38	21.9	25.47	29.33	0.122	12	32	20	Quaternary, Pliocene
DSI031	Düğer	Operation	1977	914	118	2.2	7.27	40.62	0.125	38	58	16	Pliocene
DSI032	Yassıgüne	Operation	1977	904	40	16.85	30.72	10.1	1.373	12	36	24	Pliocene
DSI033	Düğer	Operation	1977	918	65	2.62	3.26	63.2	0.010	28	48	20	Pliocene
DSI034	Düğer	Operation	1977	915	124.5	2.9	6.3	63.2	0.054	24	92	40	Pliocene
DSI035	Akariye	Operation	1978	885	152	32.28	35.64	36.83	0.091	36	144	80	Pliocene
DSI036	Karakent	Investigation	1979	909	158	39.08	62.93	19.24	1.240	26	148	80	Pliocene, Jurassic-Triassic
DSI037	Düğer	Operation	1983	915	45	1.2	6.55	63.2	0.085	22	24	2	Paleocene
DSI038	Düğer	Operation	1983	913	30	2	4.82	63.2	0.045	-	-	-	Pliocene, Paleocene

Well No.	Location	Purpose	Year	Elevation (m)	Depth (m)	Static Level (m)	Dynamic Level (m)	Well Yield (L/s)	Specific Capacity (L/s/m)	Screen Level (m)		Aquifer Lithology	Formation
										Top	Bottom		
DSI039	Gökçebağ	Operation	1984	888	150	8.26	41.96	32.17	1.048	40	144	64	Pliocene
DSI040	Kılıç	Operation	1985	893	203	4.95	23.31	51.1	0.359	34	192	108	Pliocene
DSI041	Kılıç	Operation	1985	897	202	12.8	18.32	59.42	0.093	30	192	104	Pliocene
DSI042	Kılıç	Operation	1985	900	200	9.42	27.08	52.8	0.334	22	190	108	Quaternary, Pliocene
DSI043	Kılıç	Operation	1985	891	202	1.6	21.53	49.83	0.400	36	196	104	Pliocene
DSI044	Hacılar	Operation	1986	941	60	13	19.69	63.2	0.106	-	-	-	Pliocene, Cretaceous
DSI045	Karakent	Operation	1986	869	130	14.3	48.15	30.28	1.118	14	122	80	Pliocene
DSI046	Hacılar	Operation	1986	941	46	7.3	25.57	30.02	0.609	14	43	20	Pliocene, Cretaceous
DSI047	Yassıgüne	Operation	1986	951	120	27	49.39	10.1	2.217	24	114	64	Pliocene, Cretaceous
DSI048	Karakent	Operation	1986	878	120	28.98	34.06	37.59	0.135	26	116	60	Pliocene
DSI049	Hacılar	Operation	1986	921	78	39	46.74	60.24	0.128	22	74	34	Pliocene, Cretaceous
DSI050	Yassıgüne	Operation	1986	958	75	14	46.19	2	16.095	20	69	38	Pliocene, Cretaceous
DSI051	Bağarası	Operation	1986	919	120	15.65	42	52.23	0.504	36	112	48	Pliocene
DSI052	Karakent	Operation	1986	881	120	28.67	30.15	44.34	0.033	26	114	62	Pliocene
DSI053	Bağarası	Operation	1986	920	122	19.5	43	38.35	0.613	26	116	56	Pliocene
DSI054	Karakent	Operation	1986	872	120	17.05	18.82	46.49	0.038	28	116	58	Pliocene
DSI055	Bağarası	Operation	1986	899	120	8.57	36.54	43.65	0.641	28	116	68	Pliocene
DSI056	Bağarası	Operation	1986	928	120	25	38.71	42.13	0.325	32	113	52	Pliocene
DSI057	Senir	Investigation	1987	863	100	9.65	25.23	60.46	0.258	40	96	40	Oligocene
DSI058	Merkez	Operation	1990	969	130	43.94	60.81	20.69	0.815	52	126	44	Pliocene
DSI059	Gümsüğü	Operation	1991	876	130	8.9	21.47	40.62	0.309	24	126	52	Pliocene
DSI060	Koçtepe	Investigation	1991	932	149	18.65	23.45	40.62	0.118	30	143	60	Cretaceous
DSI061	Askeriye	Operation	1992	897	150	36.13	53.97	36.08	0.494	36	140	68	Pliocene
DSI062	Bağarası	Operation	1992	913	120	28	52.5	38.35	0.639	28	114	48	Pliocene
DSI063	Bağarası	Operation	1992	916	120	28.87	48.72	47.87	0.415	32	114	40	Pliocene
DSI064	Senir	Investigation	1992	868	61	10.6	39.7	45	0.647	26	56	20	Oligocene
DSI065	Bağarası	Operation	1992	916	120	23.6	44.62	53.93	0.390	28	116	48	Pliocene
DSI066	Bağarası	Operation	1992	930	120	10.52	39.48	50.46	0.574	28	108	40	Pliocene
DSI067	Kılıç	Investigation	1992	940	157	29.61	48.49	40.62	0.465	28	148	68	Pliocene
DSI068	Güneykent	Operation	1992	891	197	9.12	40.36	29.33	1.065	24	192	94	Pliocene, Cretaceous
DSI069	Güneykent	Operation	1992	902	196	10.14	39.2	31.22	0.931	36	192	80	Pliocene, Cretaceous
DSI070	Kışla	Operation	1992	857	150	45	78.8	2	16.900	26	138	56	Quaternary, Pliocene

Well No.	Location	Purpose	Year	Elevation (m)	Depth (m)	Static Level (m)	Dynamic Level (m)	Well Yield (L/s)	Specific Capacity (L/s/m)	Screen Level (m)		Aquifer Lithology	Formation
										Top	Bottom		
DSI071	Güneykent	Operation	1992	900	139	21.14	50.46	4	7.330	36	132	56	Pliocene, Cretaceous
DSI072	Güneykent	Operation	1992	904	190	37.1	48.42	33.05	0.343	40	180	84	Pliocene, Cretaceous
DSI073	Gökçebağ	Operation	1992	872	150	4.12	38.47	33.05	1.039	32	146	60	Pliocene
DSI074	Gökçebağ	Operation	1993	893	150	23.23	49.7	35.32	0.749	44	144	64	Cretaceous
DSI075	Güneykent	Operation	1993	900	184	30.97	69.18	4.78	7.994	40	176	84	Pliocene, Cretaceous
DSI076	Kışla	Operation	1993	901	150	26.6	84.4	30.27	1.909	28	146	60	Pliocene
DSI077	Koçtepe	Operation	1993	938	151	22.27	61.9	23.46	1.689	40	140	52	Cretaceous
DSI078	Gökçebağ	Operation	1993	873	153	16.57	32.1	43.65	0.356	36	148	60	Pliocene
DSI079	Karakent	Operation	1993	873	110	28	40.15	40.62	0.299	32	104	40	Pliocene, Cretaceous
DSI080	Karakent	Operation	1993	870	110	25.24	39.68	33.81	0.427	36	106	36	Cretaceous
DSI081	Gölbasi	Operation	1993	895	100	35.2	38.87	62.32	0.059	-	-	-	Jurassic-Triassic
DSI082	Güneykent	Operation	1993	902	200	18.3	56.86	24.79	1.555	44	196	88	Pliocene, Cretaceous
DSI083	Kışla	Operation	1993	924	147	24.66	70	7.3	6.211	36	140	60	Pliocene
DSI084	Güneykent	Operation	1993	891	200	13.21	44.82	37.59	0.841	48	196	88	Pliocene
DSI085	Gökçebağ	Operation	1993	888	150	24.83	35.5	36.83	0.290	28	144	72	Quaternary, Pliocene
DSI086	Aşağımslülmer	Operation	1994	897	125	13	28.7	35.32	0.445	48	120	32	Pliocene
DSI087	Kılıç	Operation	1995	898	210	14.83	26.64	54.43	0.217	32	206	108	Pliocene
DSI088	Merkez	Operation	1995	939	127	17.12	61.78	5	8.932	32	124	56	Pliocene
DSI089	Merkez	Operation	1995	959	121	14.21	58.45	11.67	3.791	32	116	52	Pliocene
DSI090	Merkez	Operation	1995	963	139	6	60.58	19.24	2.837	24	118	56	Pliocene
DSI091	Merkez	Operation	1995	958	181	7.23	52.8	14.19	3.211	36	176	80	Pliocene
DSI092	Merkez	Operation	1995	950	148	42.12	74.88	8.8	3.723	36	142	64	Pliocene
DSI093	Koçtepe	Operation	1995	932	180	18	43.62	45.1	0.568	40	172	76	Cretaceous, Jurassic-Triassic
DSI094	Güneykent	Operation	1995	902	186	21.45	44.75	15.32	1.521	56	180	80	Pliocene, Cretaceous
DSI095	Güneykent	Operation	1995	900	156	32.5	81.75	10.85	4.539	60	152	48	Quaternary, Pliocene, Cretaceous
DSI096	Çendik	Operation	1995	897	101	18.7	39.1	20.37	1.001	28	96	36	Quaternary, Pliocene
DSI097	Çendik	Operation	1996	902	103	18.2	28.76	25.3	0.417	28	100	36	Quaternary, Pliocene
DSI098	Çendik	Operation	1996	901	103	18.7	32.1	20.37	0.658	28	100	24	Quaternary, Pliocene
DSI099	Kılıç	Operation	1996	895	202	11	34.15	45.1	0.513	84	196	36	Pliocene
DSI100	Bayındır	Operation	1996	1137	133	3	59.58	14.19	3.987	28	132	52	Pliocene
DSI101	Bayındır	Operation	1996	1132	152	3	61.22	25.08	2.321	20	148	72	Pliocene
DSI102	Ilyas	Operation	1996	872	96	38	54.69	22.14	0.754	40	94	32	Pliocene, Oligocene

Well No.	Location	Purpose	Year	Elevation (m)	Depth (m)	Static Level (m)	Dynamic Level (m)	Well Yield (L/s)	Specific Capacity (L/s/m)	Screen Level (m)		Aquifer Lithology	Formation
										Top	Bottom		
DSI103	Ilyas	Operation	1996	861	94	27	66.47	30.28	1.304	32	90	36	Oligocene
DSI104	Gökçebağ	Operation	1997	872	163	16	38.67	21.44	1.057	-	-	-	-
DSI105	Senir	Operation	1997	896	130	50.25	55.25	63.2	0.079	-	-	-	Pliocene, Oligocene
DSI106	Senir	Operation	1997	893	130	42.75	50.25	63.2	0.119	-	-	-	Pliocene, Oligocene
DSI107	Merkez	Operation	1997	976	163	30.15	66.25	20.69	1.745	32	156	60	Pliocene
DSI108	Aşağımsümler	Operation	1997	960	125	11.01	38.25	22.07	1.234	-	-	-	Jurassic-Triassic
DSI109	Yassigüme	Operation	1997	902	50	kuru	kuru	kuru	-	12	44	20	Quaternary, Pliocene
DSI110	Kılıç	Operation	1998	914	170	23.5	75.25	21.13	2.449	36	162	72	Pliocene
DSI111	Kılıç	Operation	1998	911	170	26.65	74.15	11.67	4.070	36	162	72	Pliocene, Cretaceous
DSI112	Çerçin	Operation	1998	889	150	31	55	36.082	0.665	36	148	72	Pliocene, Cretaceous
DSI113	İğdecik	Investigation	1998	954	120	29.66	40.15	63.2	0.166	36	98	40	Cretaceous, Jurassic-Triassic
DSI114	Bağarası	Operation	1998	887	120	35	68.71	20	1.686	24	112	44	Quaternary, Pliocene
DSI115	Bağarası	Operation	1998	895	120	26	53.76	25.3	1.097	36	116	40	Quaternary, Pliocene
DSI116	Büğdüz	Operation	1998	1119	100	5.43	36.91	24.28	1.297	16	98	40	Pliocene
DSI117	Aşağımsümler	Operation	1998	898	182	10.55	22.3	40.62	0.289	-	-	-	Jurassic-Triassic
DSI118	Bağarası	Operation	1998	895	120	25.36	44.73	32.36	0.599	32	116	44	Pliocene
DSI119	Bağarası	Operation	1998	898	120	24.67	46.32	20.37	1.063	32	116	40	Pliocene
DSI120	Kayaaltı	Investigation	1999	1157	170	12	57.95	18.4	2.497	28	164	72	Pliocene
DSI121	Yassigüme	Operation	1999	903	68	24.52	34.75	25.98	0.394	16	64	28	Quaternary, Pliocene
DSI122	Büğdüz	Operation	1999	1130	100	19	46.38	24.6	1.113	16	98	36	Pliocene
DSI123	Kılıç	Operation	2000	891	200	26.8	41.4	50.46	0.289	28	192	120	Quaternary, Pliocene
DSI124	Bağarası	Operation	2001	904	153	27.88	52.25	33.05	0.737	44	148	56	Pliocene
DSI125	Senir	Operation	2001	874	154	62	87.2	30.27	0.833	44	148	56	Oligocene
DSI126	Askeriye	Operation	2002	890	150	25.72	40.58	40.62	0.366	40	148	56	Pliocene
DSI127	Askeriye	Operation	2002	877	149	54	68	40.62	0.345	48	144	52	Pliocene
DSI128	İğdecik	Operation	2002	956	141	18.65	82	0.5	126.700	36	136	52	Cretaceous
DSI129	Gelmelik	Investigation	2002	1281	170	40.95	66	15.32	1.635	36	164	64	Pliocene
DSI130	Kılıç	Operation	2002	897	212	20	40.44	46.49	0.440	44	204	80	Pliocene
DSI131	Senir	Operation	2003	875	155	23	61.7	15.77	2.454	44	148	52	Pliocene-Oligocene
DSI132	Aşağımsümler	Operation	2003	907	119	28.6	59.45	30.27	1.019	16	114	44	Jurassic-Triassic
DSI133	Akyaka	Operation	2003	908	75	9.31	47.14	12.3	3.076	20	72	28	Pliocene
DSI134	Kılıç	Renewal	2003	893	205	7	25.2	25.98	0.701	52	200	64	Pliocene
DSI135	Akyaka	Operation	2003	912	75	15.09	55.83	6.56	6.210	20	74	32	Pliocene
DSI136	Kumluca	Investigation	2003	871	110	7.86	32.1	43.63	0.556	28	104	36	Pliocene, Cretaceous
DSI137	Karakent	Renewal	2003	877	130	24.3	38.35	40.62	0.346	40	124	40	Pliocene
DSI138	Kayaaltı	Operation	2003	1181	170	27	80.69	7.2	7.457	36	164	64	Pliocene
DSI139	Kayaaltı	Operation	2004	1151	170	4	46.9	30.27	1.417	40	164	60	Pliocene

Well No.	Location	Purpose	Year	Elevation (m)	Depth (m)	Static Level (m)	Dynamic Level (m)	Well Yield (L/s)	Specific Capacity (L/s/m)		Screen Level (m)		Aquifer Lithology	Formation
									Top	Bottom	Top	Bottom		
DSI140	Merkez	Renewal	2004	890	176	30.1	54	43.65	0.548	48	172	68	Clay, Clayey gravel, Gravel, Gravel clay, Ophiolitic melange, Claystone-marl intercalation	Pliocene, Cretaceous
DSI141	Senir	Operation	2005	893	132	47.25	57.56	50.46	0.204	54	126	36	Conglomerate	Oligocene
DSI142	Aşağımüslümler	Renewal	2006	891	141	11	26.15	32.6	0.465	64	136	36	Gravel, Claystone-marl, Limestone	Pliocene, Cretaceous
DSI143	Bağarası	Renewal	2006	892	142	27.36	58.17	20.69	1.489	40	128	40	Gravel, Gravel clay, Clay	Pliocene
DSI144	Düğer	Operation	2006	934	120	15.52	39.47	31.28	0.766	36	116	40	Gravel clay, Clayey gravel, Ophiolitic melange	Pliocene, Cretaceous
DSI145	Düğer	Operation	2006	932	120	9	34.61	32.1	0.798	36	116	40	Gravel, Clay, Clayey gravel, Limestone	Pliocene, Jurassic-Triassic
DSI146	Düğer	Operation	2006	926	120	11	38.14	30.59	0.887	36	116	40	Clay, Clayey gravel, Gravel, Ophiolitic melange	Pliocene, Cretaceous
DSI147	Çendik	Renewal	2006	900	120	14	45.6	37.59	0.841	24	116	40	Gravel, Clay, Gravel clay	Quaternary, Pliocene
DSI148	Kışla	Renewal	2007	909	154	54.54	95	15.32	2.641	44	148	52	Gravel, Clayey gravel, Conglomerate	Pliocene
DSI149	Askeriye	Renewal	2007	890	150	37	60.28	38.35	0.607	60	146	44	Gravel, Clayey gravel, Clay, Gravel clay	Pliocene
DSI150	Aşağımüslümler	Renewal	2007	905	122	32	45.21	38.35	0.344	36	116	40	Limestone	Jurassic-Triassic
DSI151	Aşağımüslümler	Renewal	2007	899	126	27	52	34.58	0.723	44	120	40	Limestone, Ophiolitic melange	Cretaceous, Jurassic-Triassic
DSI152	Gökçebağ	Renewal	2008	892	160	48	75.49	18.4	1.494	48	156	52	Silty sandy clay, Claystone-marl intercalation, Conglomerate	Pliocene
DSI153	Karakent	Renewal	2009	879	130	22	90	2.5	27.200	31	125	48	Clayey sand, Clayey sandy gravel, Clayey sand, Sandy gravel, Gravel, Gravel clay	Pliocene
DSI154	Askeriye	Renewal	2009	876	122	36	50	39.84	0.351	24	116	44	Gravel sand, Clayey sandy gravel, Clayey sand, Clay	Quaternary, Pliocene
DSI155	Koçtepe	Operation	2009	930	170	24.19	63.91	30.28	1.312	44	164	60	Ophiolitic melange, Limestone	Cretaceous, Jurassic-Triassic
DSI156	Koçtepe	Operation	2009	937	170	26.09	64.37	32.1	1.193	48	164	60	Gravel clay, Ophiolitic melange, Limestone	Cretaceous, Jurassic-Triassic
DSI157	Kışla	Operation	2010	932	160	22.43	65.46	18.7	2.301	36	152	60	Clay-marl-limestone intercalation	Pliocene
DSI158	Çendik	Renewal	2010	904	115	16.91	41.83	25.1	0.993	32	112	40	Gravel, Gravel clay, Clayey gravel, Clay, Gravel-clay intercalation	Pliocene
DSI159	Bağarası	Renewal	2010	890	130	32.14	46.78	30.02	0.488	28	124	48	Gravel, Clayey gravel, Gravel clay	Pliocene
DSI160	Kumlucu	Operation	2010	875	90	11.56	16.09	55	0.082	16	82	40	Limestone	Jurassic-Triassic
DSI161	Gökçebağ	Renewal	2011	921	180	20	106	1	86.000	44	172	64	Limestone-Marl-Claystone intercalation	Pliocene
DSI162	Ardıçlı	Operation	2011	899	160	49.3	55	33.08	0.172	32	152	60	Gravel, Clay, Conglomerate	Pliocene, Oligocene
DSI163	Ardıçlı	Operation	2011	931	160	52	68.5	22.5	0.733	32	152	56	Clay, Gravel, Conglomerate	Pliocene, Oligocene
DSI164	Ardıçlı	Operation	2013	920	200	70.3	84.15	33.85	0.409	44	196	80	Conglomerate	Oligocene
DSI165	Güneyyayla	Investigation	2013	1430	275	85.3	162	1	76.700	36	264	128	Limestone, Ophiolitic melange	Cretaceous
DSI166	Suludere	Investigation	2013	902	168	17.8	32.65	35.22	0.422	28	164	72	Clay, Gravel, Limestone	Pliocene, Cretaceous
DSI167	Çendik	Renewal	2013	902	136	19.3	38.5	20.69	0.928	32	134	54	Clay, Gravel	Pliocene
DSI168	Askeriye	Renewal	2014	898	170	35	75	29.33	1.364	40	164	64	Clay, Gravel, Conglomerate	Pliocene

B. DSI water level recorder installed wells

Well No.	Location	Purpose	Year	Elevation (m)	Depth (m)	Static Level (m)	Dynamic Level (m)	Well Yield (L/s)	Specific Capacity (L/s/m)	Screen Level (m)			Aquifer Lithology	Formation
										Top	Bottom	Length		
6980-1	İnsuyu	Investigation	1965	1185	141	3	29.5	2.5	10.600	127	141	14	Limestone	Cretaceous
10840	Kılıç	Operation	1969	948	189.4	7	50	3	14.333	40	187	103	Clay, Clayey gravel, Gravel, Gravel clay	Pliocene
10849	Kılıç	Operation	1969	947	180.6	3.03	29.57	10	2.654	36	176	96	Gravel, Clay, Clayey gravel, Sandy clay	Pliocene
15024	Merkez	Operation	1971	931	41	4.43	26.82	12.2	1.835	17	37	12	Conglomerate	Pliocene
18705	Senir	Operation	1974	880	253	13.5	40.1	4	6.650	45	242	66	Sand, Clay, Gravel, Conglomerate	Pliocene, Oligocene
47209	Günalan	Investigation	1994	1224	193	35.7	79.8	1.5	29.400	32	188	84	Gravel, Clayey gravel, Clay, Gravel clay	Pliocene
49269	Askeriye	Operation	1995	887	141	36.12	48.54	50.46	0.246	36	136	56	Clay, Sandy clay, Gravel, Clayey gravel, Gravel clay	Pliocene
60580	Aşağımsütlüler	Renewal	2010	902	151	30	75	5.2	8.654	36	144	56	Limestone, Ophiolitic melange	Cretaceous, Jurassic-Triassic
63524	Kılıç	Operation	2015	946	189	11.15		-	-	-	-	-	-	-
63283	Düğer	Operation	2015	921	120	6.6	9.7	3.32	0.934	-	-	-	-	-
63287	Yassıgüne	Operation	2015	921	80	8.3		-	-	-	-	-	-	-
63293	İlyas	Operation	2015	887	120	36.6	40.83	5.88	0.719	-	-	-	-	-
63297	Gökçeboğ	Investigation	2015	879	100	6.27	8.06	7.15	0.250	28	96	36	Gravel clay, Gravel	Pliocene
63298	Merkez	Investigation	2015	933	80	12.42	14.93	6.41	0.392	24	76	28	Clayey gravel, Gravel clay, Clay	Pliocene
63374	Günalan	Investigation	2015	1222	200	110.74	114.65	2.65	1.475	44	196	76	Gravel clay, Clay, Gravel, Clayey gravel	Pliocene
63284	Çineovası	Investigation	2015	1192	80	8.66	57.83	0.12	409.750	28	76	28	Gravel clay, Clay	Pliocene

CURRICULUM VITAE

PERSONAL INFORMATION

Surname, Name : Kılıç Germeç, Hatice

Nationality : Turkish (TC)

EDUCATION

Degree	Institution	Year of Graduation
MSc.	METU Geological Engineering	2016
B.S.	METU Geological Engineering	2012
High School	İncirli High School, Ankara	2006

WORK EXPERIENCE

Year	Place	Enrollment
2014-2023	METU Geological Engineering	Research Assistant
2012-2014	Çınar Engineering Consulting Inc.,	Hydrogeologist, GIS Expert

FOREIGN LANGUAGES

Advanced English

ABSTRACTS / CONFERENCE PROCEEDINGS

1. Yazıcıgil H. and Kılıç H. “Prediction of Groundwater Inflow Rates to Longwall Coal Panels in Central Turkey”, 46th IAH Congress, Malaga, Spain, Sept 22-27, 2019 (oral presentation).
2. Yazıcıgil H., Güney Y.C., and Kılıç H. “Hydrogeological Characterization for Mining and Environmental Impact Assessment in Alpu Coal Basin, Eskişehir-Turkey”, GRECPIMA, Muğla - Turkey, May 8-10, 2019 (oral presentation).
3. Yazıcıgil H., Peksezer Sayıt A., Yağbasan Ö., Argunhan Atalay Ç., and Kılıç H. “Madencilikte Hidrojeolojinin Önemi ve Problemleri”, Hidro’2018 Hidrojeoloji ve Su Kaynakları Sempozyumu, Ankara – Turkey, September 27-29, 2018 (oral presentation).

HOBBIES

Reading, Watercolor painting, Hiking